Understanding the Retinoid-x-receptor biology and manipulating it as a novel strategy to protect the retina

Yogita Dheer

B.Pharm, M.Pharm
Faculty of Medicine and Health Sciences
Macquarie University

January 2018

Supervisors

Prof. Stuart L Graham
Faculty of Medicine and Health Sciences
Department of Clinical Medicine
Macquarie University

Dr. Vivek K Gupta
Faculty of Medicine and Health Sciences
Department of Clinical Medicine
Macquarie University

MACQUARIE University
SYDNEY·AUSTRALIA

Copyright statement

Yogita Dheer

January 2018

Authenticity statement

'I certify that the Library deposit digital copy is a direct equivalent of the final officially approved version of my thesis. No emendation of content has occurred and if there are any minor variations in formatting, they are the result of the conversion to digital format.'

Yogita Dheer

January 2018

I would like to dedicate this thesis to my mother and in the loving memory of my late father Sh.Ravinder Kumar Dalla.

Originality statement

`I hereby declare that this thesis entitled "*Understanding the retinoid-x-receptor biology and manipulating it as a novel strategy to protect the retina.*" is my own work and to the best of my insight it contains no materials beforehand published or written by someone else, or generous extents of material which have been acknowledge for the award of some other degree or certificate at Macquarie University or if any other educational organization, with the exception of where due affirmation is made in the thesis. I additionally proclaim that the intellectual content of this thesis is the result of my own work, except to the extent that help from others in the project's outline and origination or in style, presentation and semantic expression is acknowledged.'

Yogita Dheer

January 2018

Acknowledgements

"I believe that anything is possible when you have the right people there to support you"

First and foremost, I would like to express my gratitude to my supervisor Professor Stuart L Graham. The opportunity to share space in his lab and contribute towards an important research project has been an honour. He introduced me to the field of ophthalmologic research and has provided me his valuable guidance throughout this project. I am thankful for his scientific suggestions, always nudging me right direction and encouragement to present research work at global front. I am fortunate to work under the supervision of such illustrious person who has played a significant role in shaping me a confident scientific research.

I convey my sincerest appreciation to my associate supervisor Dr. Vivek K. Gupta without whom none of this would be possible. Dr. Gupta has been the brains and hard work behind designing this project. I appreciate his help in guiding me towards the successful progress of this project with thorough and thoughtful approach to experimental methods and realistic goals. With my close interaction with him, I have learnt a lot in past three years and would always be thankful to him.

In addition, I would like to extend my thanks to dedicated group of staff members; especially Dr. Nitin Chitranshi for being a constant resource for scientific input. He has been first point of contact for day to day issues, relating to experimental/scientific discussions, administrative jobs or any software related matters.

I recognize and thank my fellow researchers Samridhi Sharma, Mojdeh Abbassi, Roshana Vander Wall, Shabarni Gupta, Rashi, Chitra and Abu who have contributed in successful transformation of research project into this thesis.

Last, this work would not have been possible without the constant support from my family. I thank my mom, Manjula Kumari for her unwavering care and firm support. She is my greatest inspiration and driving force in this extraordinary journey. My gratitude also goes to my father-in-law Satpal and mother-in-law Kanta, both of whom have always given me their unconditional support. My sincerest appreciation to my sister Bhavana, brother Lovedeep, and brother-in-law Ravi Kumar, who always provide constant motivation. I express my special thanks to Mr. Sunil Hargunani for last moment support. My deepest adoration goes to my husband, Sandeep. His passion, guidance, encouragement, sacrifices, patience and confidence in my abilities allowed me to victoriously complete this journey. He is the shining star that relentlessly guided me through every obstacle in my triumphs and tribulations. My constant source of enthusiasm, happiness, and love are my children, Jahnavi and Divija.

Finally, completing my PhD degree is the most significant educational achievement of my life.

I would like to dedicate this work to my father Late Sh.Ravinder Kumar Dalla.

This study was supported by:

Australian Postgraduate Award scholarship (**APA**) Macquarie University

Postgraduate Research Fund (**PGRF**)

Skipper Postgraduate / Early Career Researcher Travel Award

Publications

Manuscript under preparation/ submitted from the thesis

1. **Yogita Dheer**, Nitin Chitranshi, Veer Gupta, Samridhi Sharma, Mojdeh Abbasi, Mehdi Mirzaei, Yuyi You, Stuart L Graham, Vivek Gupta. Retinoid x receptor modulation protects against ER stress response and rescues glaucoma phenotype in adult mice Manuscript submitted to Journal of Cell Death and Disease. (Manuscript under revision in Journal of Cell Death and Disease).
2. Nitin Chitranshi, Yogita Dheer, Sanjay Kumar, Stuart L Graham, Vivek Gupta. Molecular docking, dynamics and pharmacology studies on Bexarotene as a retinoid X receptor agonist, nuclear receptor expressed in retina and brain. (Manuscript submitted to Journal of Cellular Biochemistry).

Other accepted/ published journal articles

1. **Yogita Dheer**, Nitin Chitranshi, Veer Gupta, Mojdeh Abbasi, Mehdi Mirzaei, Yuyi You, Roger Chung, Stuart L Graham, Vivek Gupta. Bexarotene Modulates Retinoid-X-Receptor Expression and is Protective against Neurotoxic Endoplasmic Reticulum Stress Response and Apoptotic Pathway Activation. Mol Neurobiol. 2018 Apr 10. doi: 10.1007/s12035-018-1041-9.
2. Nitin Chitranshi, **Yogita Dheer**, Veer Gupta, Mojdeh Abbasi, Mehdi Mirzaei, Yuyi You, Roger Chung, Stuart L.Graham,Vivek Gupta (2017) PTPN11 upregulation in SH-SY5Y cells induces endoplasmic stress and apoptosis through its negative modulatory effects on TrkB phosphorylation. Neuroscience. doi.org/10.1016/j.neuroscience.2017.09.028.
3. Vivek Gupta, Mehdi Mirzaei, Veer Bala Gupta, Nitin Chitranshi, **Yogita Dheer**, Roshana VanderWall, Mojdeh Abbasi, Yuyi You, Roger Chung, Stuart Graham (2017) Glaucoma is associated with plasmin proteolytic activation mediated through oxidative inactivation of neuroserpin. Scientific Reports 7, 842, doi:10.1038/s41598-017-08688-2
4. Mehdi Mirzaei, Veer Gupta, Joel chick, Todd Greco, Yunqi Wu, Nitin Chitranshi, Roshana Vander Wall, Eugene Hone, Liting Deng, **Yogita Dheer**, Mojdeh Abbasi, Mahdie Rezaeian, Nady Braidy, Yuyi You, Ghasem Hosseini Salekdeh, Paul A.Haynes, Mark P. Molloy, Ralph Martins, Ileana M. Cristea, Steven P. Gygi, Stuart L.Graham, Vivek K. Gupta (2017) Age-related neurodegenerative disease associated pathways identified in retinal and vitreous proteome from human glaucoma eyes. Scientific Reports 7, 12685, doi:10.1038/s41598-017-12858-7
5. Nitin Chitranshi, **Yogita Dheer**, Roshana Vander Wall, Veer Gupta, Mojdeh Abbasi, Stuart L Graham, Vivek Gupta (2016) Computational analysis unravels novel destructive single nucleotide polymorphisms in the non-synonymous region of human caveolin gene. Gene Reports. doi.org/10.1016/j.genrep.2016.08.008
6. Vivek Gupta, Veer B Gupta, Nitin Chitranshi, Sumudu Gangoda, Roshana Vander Wall, Mojtaba Golzan, **Yogita Dheer**, Tejal Shah, Alberto Avolio, Roger Chung, Ralph Martins, Stuart L Graham (2016) One protein, multiple pathologies: Multifaceted involment of amyloid β in neurodegenerative disorders of the brain and retina. Cell Moll. Life Sci doi: 10.1007/s00018-016-2295-x
7. Vivek Gupta, Nitin Chitranshi, Veer B Gupta, Mojtaba Golzan, **Yogita Dheer**, Anna E King, James C Vickers, Roger Chung, Stuart L Graham (2016) Amyloid β accumulation

and inner retinal degenerative changes in Alzheimer's disease transgenic mouse. Neurosci Lett, Apr 28; 623:52-56

8. Nitin Chitranshi, Vivek Gupta, **Yogita Dheer**, Veer Gupta, Roshana Vander Wall, Stuart Graham (2016) Molecular determinants and interaction data of cyclic peptide inhibitor with the extracellular domain of TrkB receptor. Data in Brief Mar; 6:776-782

Conference Presentations

1. **Yogita Dheer**, Nitin Chitranshi, Vivek K Gupta, Stuart L Graham (2018) Bexarotene suppresses the retinal expression of ER stress marker proteins p-PERK and GADD153 in experimental model of glaucoma. ARVO 2018
2. Nitin Chitranshi, **Yogita Dheer,** Vivek K Gupta, Stuart L Graham (2018) Shp2 knockdown reduces ocular specific endoplasmic reticulum stress in experimental glaucoma. ARVO 2018
3. **Yogita Dheer,** Nitin Chitranshi, Vivek K Gupta, Stuart L Graham, (2017) Retinoid-X-receptor (RXR) targeting can rescue inner retinal structural and functional deficits in mouse model of glaucoma. SOE 2017
4. Mojdeh Abbasi, Vivek Gupta, **Yogita Dheer**, Chitra Joseph, Roshana Vanderwall, Stuart L Graham (2017) Effects of Caveolin-1 ablation in the inner retina under healthy and experimental glaucoma conditions. EVER 2017
5. Nitin Chitranshi, Vivek K Gupta, **Yogita Dheer**, Stuart L Graham (2017) AAV mediated PTPN11 knockdown stimulates TrkB activity in neuronal cells in culture and in rat retina. 12th Gottingen Meeting of the German Neuroscience Society 2017
6. **Yogita Dheer**, Nitin Chitranshi, Roshana Vander Wall, Vivek K Gupta, Stuart L Graham (2017) Retinoid-X-receptor agonist Bexarotene treatment provides retinal functional protection in acute and chronic model of glaucoma. ASIA-ARVO 2017
7. Nitin Chitranshi, Vivek K Gupta, **Yogita Dheer**, Stuart L Graham (2017) Adeno-associated virus knockdown of Shp2 phosphatase protect inner retinal structure and function in experimental glaucoma. ASIA-ARVO 2017
8. Mojdeh Abbasi, Vivek K Gupta, Nitin Chitranshi, **Yogita Dheer**, Anita Turner, Roshana Vander Wall, Stuart L. Graham (2016) Cav-1 ablation protects against loss of inner retinal function caused by PTPN11 overexpression. ANS2016
9. Nitin Chitranshi, Roshana Vander Wall, **Yogita Dheer**, Stuart L. Graham, Vivek K Gupta. (2016) AAV Mediated Gene Therapy to Modulate Neurotropic Factors in the Retina and in Neuronal Cells in Culture. 19th Annual meeting of ASGCT, Mol. Therapy 24: S321-S350; doi : 10.1038/mt.2016.80
10. **Yogita Dheer**, Nitin Chitranshi, Roshana Vander Wall, Stuart L. Graham, Vivek K. Gupta. (2016) Retinoid -X-receptor (RXR) expression in the rodent retina and effects of its modulation in neuronal cells. ARVO 2016, Invest. Ophthalmol. Vis. Sci. 2016; 57(12):1725
11. Nitin Chitranshi, Vivek K. Gupta, Roshana Vander Wall, **Yogita Dheer**, Stuart L. Graham. (2016) SHP2 (PTPN11) over-expression by AAV gene delivery impairs neuronal cell growth in SH-SY5Y cells and induces neurodegeneration of SD rat retinal ganglion cells. ARVO 2016, Invest. Ophthalmol. Vis. Sci. 2016; 57(12):3997

Abstract

Glaucoma is a degenerative optic neuropathy affecting nearly 80 million individuals by 2020 worldwide. Glaucoma is mainly manifested as alterations of the optic disc with progressive degeneration of retinal ganglion cells (RGCs) contributing to visual field loss. High intraocular pressure (IOP) is considered as the main risk factor of glaucoma. Unfortunately, a significant number of patients show disease progression despite treating with IOP lowering drugs. So, RGC degeneration cannot be prevented only by reducing eye pressure. There is need for development of more novel strategies targeting retinal neuroprotection. Within this context, this PhD project aimed to assess the potential neuroprotective effect of RXR activation by its agonist bexarotene both *in vitro* studies as well as *in vivo* acute and chronic glaucoma models.

Retinoid X receptors (RXRs) are ligand-dependent transcription factors that belong to the nuclear receptor (NR) superfamily. RXRs have three different isoforms (α, β, and γ) and can form both homo- and heterodimers with other nuclear receptors. Numerous studies have linked RXR modulation with neuroprotection. This thesis was mainly focused to elucidate the role of bexarotene as RXR modulator in glaucoma pathology.

In first part of this study I demonstrated the expression and regulation of RXR receptors in SH-SY5Y cells using different concentrations of bexarotene. I also studied the role of TrkB signalling with RXR pathway in regulating endoplasmic reticulum stress response and apoptotic pathway activation. The results obtained from *in vitro* studies demonstrated that optimum concentrations of bexarotene upregulated the expression of all the three isoforms of RXRs. Also my studies revealed that higher concentrations of bexarotene upregulates ER stress proteins and BAD which can be prevented by pharmacological targeting of the TrkB receptor.

I further extended my studies to assess the neuroprotective effects of RXR activation in mice in preventing loss of retinal ganglion cells (RGCs) under experimental glaucoma conditions. Two models i.e increased excitotoxicity mediated glutamate model (acute model) and microbead induced increased intraocular pressure model (chronic 2 months model) of RGC degeneration were used for *in vivo* studies. Bexarotene treatment showed enhanced expression of RXRs as compared to control and glaucoma mice retinal sections. Furthermore it was seen that bexarotene maintained inner retinal functional and structural integrity confirmed by electroretinography, H and E staining and Bieschowlsky silver staining of optic nerve sections. Moreover, docking studies also validated binding of bexarotene to RXR receptors.

This thesis represents an integration of three different methodologies i.e *in vitro, in vivo, in silico.* The results from this thesis provide evidence to the hypothesis that RXR activation can be neuroprotective to RGCs in preventing apoptosis and cell death. Bexarotene or other RXR agonists may have potential for future therapeutic management of glaucoma.

TABLE OF CONTENTS

List of Figures and Tables

Figures

List of abbreviations

Aβ	amyloid beta
AD	Alzheimer's disease
AIF	apoptosis inducing factor
AMD	age related macular degeneration
AR	androgen receptor
ALS	amyotrophic lateral sclerosis
AMPA	α-amino-3-hydroxy-5-methyl-4 isoxazolepropionic acid
APP	amyloid precursor protein
AM1	austin model-1
ATF 6	activating transcription factor 6
BCA	bicinchoninic acid assay
BAD	Bcl-2-associated death promoter
BDNF	brain-derived neurotrophic factor
BiP	binding immunoglobulin protein
CaMK	calpain and calcium/calmodulin-dependent kinase 2
CHOP	C/EBP-homologous protein
CNS	central nervous system
CNTF	ciliary neurotrophic factor
CTCL	cutaneous T-cell lymphoma
CTX-B	cyclotraxin-B
DAPI	4', 6-diamidino-2-phenylindole
DBD	DNA-binding domain
DHA	docosahexaenoic acid

DMEM	dulbecco modified eagle medium
DMSO	dimethyl sulfoxide
EDTA	ethylenediaminetetraacetic acid
ET1	endothelin-1
ER	endoplasmic reticulum
ERG	electroretinography
FXR	farnesoid X receptor
FBS	fetal bovine serum
GCL	ganglion cell layer
GADD153	growth arrest and BDA-damage-inducible protein 153
GR	glucocorticoid receptor
GSH	glutathione
GRP78	glucose-regulated protein 78
HSP	heat shock protein
HRP	horse radish peroxidase
HD	huntington's disease
HEPES	4-(2-hydroxyethyl)-1-piperazineethanesulfonic acid
IHC	immunohistochemistry
IOP	intraocular pressure
IPL	inner plexiform layer
INL	inner nuclear layer
IRE1	inositol-requiring protein-1
JNK	c-Jun N-terminal kinases
KA	kainite
LBD	ligand binding domain

LGA	lamarckian genetic algorithm
LGN	lateral geniculate nucleus
LXRs	liver X receptors
BDNF	brain-derive neurotrophic factor
MOPAC	molecular orbital package
MR	mineralocorticoid receptor
MS	multiple sclerosis
MYOC	myocilin
NeuN	neuronal nuclei
NGF	nerve growth factor
NMDA	N-methyl-D-aspartate
NO	nitric oxide
NR	nuclear receptor
NT-3	neurotrophin-3 Neurotrophin (NT) neurotrophic factor (NF)
NT-4	neurotrophin-4
OCT	optimal cutting temperature
OHT	ocular hypertension
ON	optic nerve
ONH	optic nerve head
ONL	outer nuclear layer
PACG	primary angle-closure glaucoma
PBS	phosphate-buffered saline
PCG	primary congenital glaucoma
PD	Parkinson's disease

P-PERK	phospho-protein kinase RNA
PFA	paraformaldehyde
POAG	primary open angle glaucoma
PPARs	peroxisome proliferator-activated receptors
PR	progesterone receptor
pSTR	positive scotopic threshold response
PXR	pregnane X receptor
PVDF	polyvinylidene difluoride
RA	retinoic acid
RAR	retinoic acid receptor
RAREs	retinoic acid response elements
RGC	retinal ganglion cell
RMS	root mean square
ROCK	rho kinase
ROS	reactive oxygen species
RPE	retinal pigment epithelium
RXR	retinoid X receptor
TR	thyroid hormone receptor
TrkB	tropomyosin receptor kinase B
TTBS	tri Tris-buffered saline
UPR	unfolded protein response
VDR	vitamin D3 receptor
7,8-DHF	7,8-di-hydroxyflavone

CHAPTER 1

GENERAL INTRODUCTION

1.1 Glaucoma

1.1.1 Definition

Glaucoma is a widespread challenging chronic neurodegenerative disease and is the second leading cause of irreversible blindness (Kingman, 2004). The term "glaucoma" refers to a group of conditions that includes retinal ganglion cell death and optic nerve fiber loss. Elevated intraocular pressure (IOP) is the commonest cause of vision loss in most types of glaucoma with subsequent injury to the optic nerve. IOP is maintained by aqueous humour which is a clear fluid filling both the anterior and posterior chambers of the eye. The aqueous humour leaves the eye at the anterior chamber angle, then through the trabecular meshwork, across the inner wall of Schlemm's canal, drained into its lumen (Tamm, 2009). IOP ranging between 10 and 21 mm Hg are considered to be normal. Equilibrium exists between the production and outflow of aqueous humour to maintain normal range IOP. Disruption in aqueous humour draining leads to rise in IOP, which is a major risk factor for glaucomatous damage (Leske et al., 2004). There are no warning symptoms at the onset of the disease since the gradual elevation of IOP is not painful, and the peripheral visual loss is not detected by the patient until late. It has been reported that in 50% cases people remain unaware with this disease (Bourne, 2006). Chronic glaucoma gradually leads to permanent loss of vision without treatment and thus it is described as a silent disease or "the sneak thief of sight" (Abdull et al., 2016).

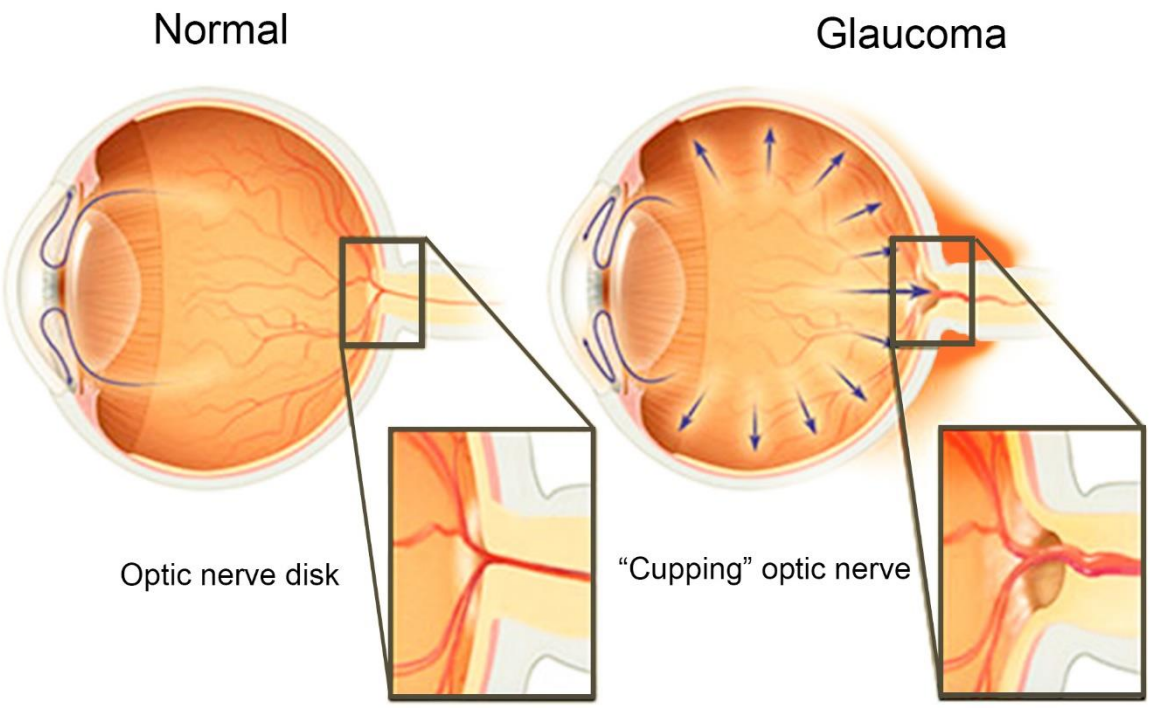

Figure 1.1 Schematic representation of glaucoma and optic nerve cupping.The blockage in aqueous humor drainage results in an increase in intraocular pressure (shown by blue arrows) leading to increase in optic cup to disk ratio which ultimately damages the optic nerve. Image used with permission of Mayo Foundation for Medical Education and Research.

1.1.2 Classification

Glaucoma can be classified in a number of ways based on: level of IOP, anatomy of the drainage angle, age of onset and absence or presence of causative factors (Foster et al., 2002). There are different kinds of glaucoma. Primary open angle and angle closure are the two main types of glaucoma both of which are manifested by increase in IOP.

(i) Primary open-angle glaucoma (POAG) or chronic glaucoma: It is commonest form of glaucoma. The underlying cause of POAG in most cases is due to the obstruction of the drainage canals, resulting in increased IOP. As IOP increases, the pressure builds up which pushes on the fibers of the optic nerve, causing irreversible nerve damage and vision loss. In POAG, the peripheral vision loss usually occurs first followed by central vision loss.

(ii) Normal-tension glaucoma (low-tension or normal-pressure glaucoma): It is a chronic optic neuropathy that parallels POAG (usually classified as a subset of POAG), showing characteristic feature optic nerve head cupping and functional visual-field loss, excluding but no measured elevation of the IOP.

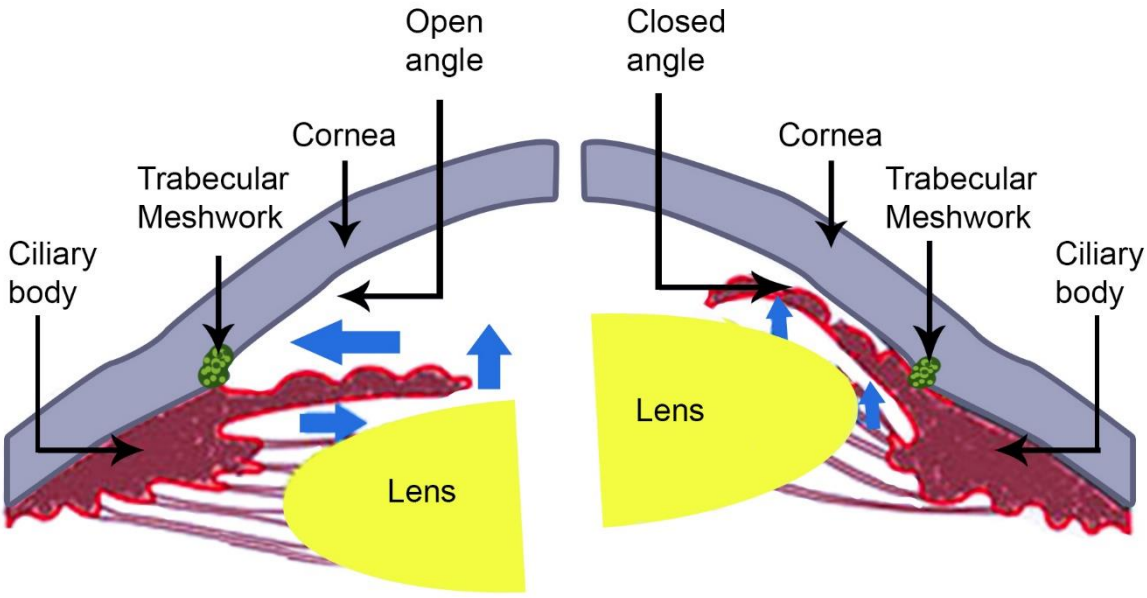

Figure 1.2 Open angle and closed angle pathways.Schematic representation demonstrating the difference between open angle (left) and angle closure (right).Blue arrows showing direction of flow of aqueous humor.Image adapted from: B B Eye Foundation (with permisssion).
http://www.sagarbhargava.com/yag-peripheral-iridotmoy/

(iii) Primary angle-closure glaucoma (PACG) or acute glaucoma: Angle closure is caused due to blocking of fluid access to the trabecular meshwork by iris, resulting in a sudden rise in IOP, and this form is usually painful with rapid loss of vision. It is comparatively a less common form of glaucoma but represents an ophthalmologic emergency.

(iv) Primary congenital glaucoma (PCG) (also called as childhood/paediatric/infantile/ juvenile glaucoma): Represents a primary cause of childhood visual disability affecting

children between birth and 3 years and is due to a hereditary defect presenting at birth or abnormal development in childhood. It is characterized by improper development of the eye's anterior chamber, leading to reduced aqueous outflow and elevation in IOP. The increased IOP consequently resulting in damage to optic nerve, and vision loss.

(v) Secondary glaucoma: This may be caused by either genetic or physical conditions such as an eye injury, inflammation, tumour, certain drugs such as steroids and advanced cases of cataract or diabetes and ischemia. Following are the common secondary types of glaucoma:

(a) Pigmentary glaucoma: It occurs due to the disruption of cells (lining back of iris) containing pigment and dispersing into the anterior chamber leading to blockage and causes secondary raised IOP.

(b) Pseudoexfoliative glaucoma: Glaucoma that results when there is an abnormal accumulation of fibrillar material produced by cells within ocular tissues. The tiny clumps of fibrillar material obstruct the trabecular meshwork, causing raised IOP.

(c) Neovascular glaucoma: Neovascular glaucoma results from the formation of new blood vessels in the retina in response to ischemia, with associated proliferation in the anterior chamber angle, causing a secondary angle closure glaucoma. It is always associated with other abnormalities such as diabetic neuropathy or central retinal artery or vein occlusions.

(d)Traumatic glaucoma: Traumatic glaucoma refers to cases in which direct injury to the eye occurs e.g. by a punch, car accident or head injury. The injury can cause damage to the drainage mechanism in the eye with secondary raised IOP. It can occur immediately or years later after an injury to the eye.

(e) Steroid-induced glaucoma: It is associated with long term use of topical steroids, but it may also develop with the use of oral, inhalational, nasal corticosteroids as well as with intravenous or intravitreal steroid implantation. A persistent rise in IOP occurs with the use of these medications.

(f) Inflammatory glaucoma (also called uveitic glaucoma): This type of glaucoma is caused by internal ocular inflammation or uveitis. Such inflammation will usually increase IOP, but can sometimes lower IOP through ciliary body inflammation. The inflammatory cells collect in the aqueous humour and obstructs the trabecular meshwork preventing aqueous outflow from the eye.

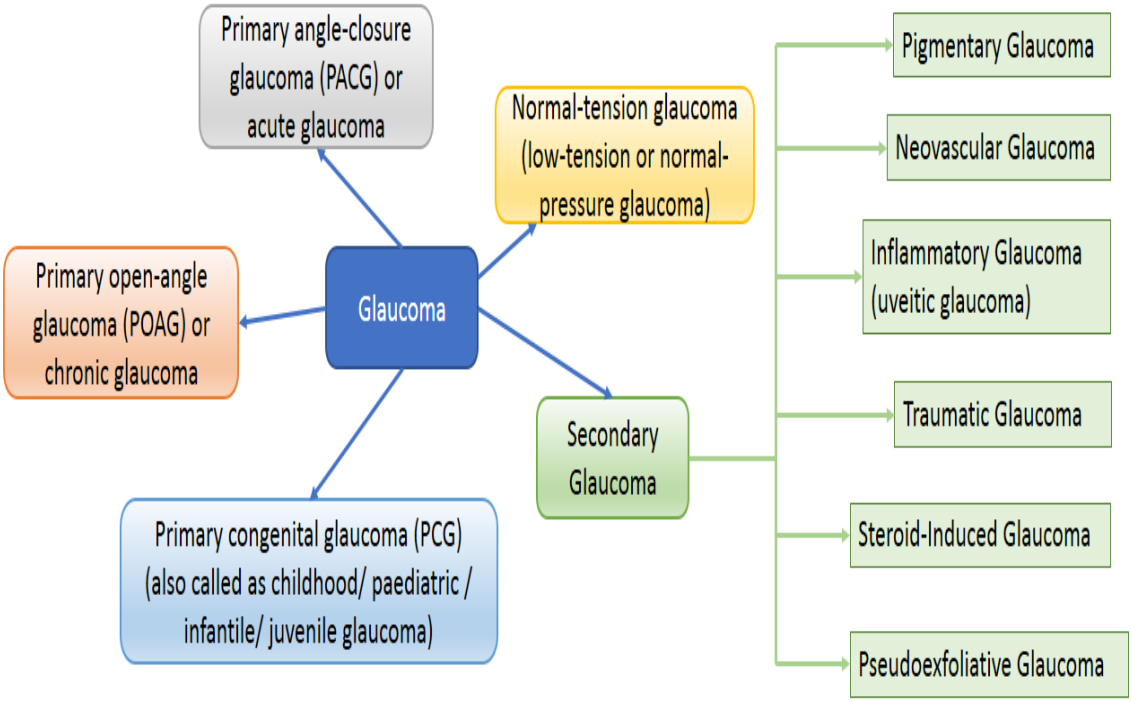

Figure 1.3 Graphical representation of different types of glaucoma.

1.1.3 History of Glaucoma

From the Hippocratic period till now, debate on glaucoma definition has persisted and has not reached conclusion. During the era of Hippocrates, glaucoma was described as elderly blinding disease without any difference from cataract. The disorder now defined as glaucoma originated from the Greek term "glaukos" which implies blue, green, or light gray colour of the pupil (Leffler et al., 2015). In 1622, Dr Richard Bannister described glaucoma with four characteristics - eye tension, prolonged disease condition, fixed pupil and the lack of perception of light. It was Dr Antoine-Pierre Demours who gave the concept of increased ocular tension for glaucoma in 1818. Later in 1823 glaucoma was recognized as hardness of the eye by Dr G.J. Guthrie. Thereafter, Sir William Lawrence in 1832 used the terms "glaucoma" and "acute glaucoma" in his book "A Treatise on Diseases of the Eye". The modern era began in 1835 when Dr. William McKenzie distinguished the acute and chronic glaucomas. Von Helmholtz in 1850 invented the ophthalmoscope which further helped to diagnose glaucomatous changes in the fundus. In 1862, Donders discovered the concept of high intraocular pressure leading to blindness. In the mid to late 1900's the definition of glaucoma was gradually changed to be a disease of the optic nerve, with or without raised IOP. According to current concepts, glaucoma is now considered to be a multifactorial group of heterogeneous diseases with characteristic morphological changes of the optic disc and irreversible retinal ganglion cell (RGC) loss (Agarwal et al., 2009).

1.1.4 Epidemiology

The global prevalence of glaucoma is estimated 111.8 million in 2040 (Tham et al., 2014). People with advancing age (40-80years) are at higher risk: 1 in 200 at the age of 40 and 1

in 8 people at the age of 80 suffered from glaucoma. Glaucoma varies depending upon ethnicity. Glaucoma burden is found to be highest in Africans (Rudnicka et al., 2006). In US more than 520,000 of African–Americans suffered from glaucoma according to data analyzed in 2012. Data showed that the glaucoma prevalence in African Americans aged between 50-59 years was 4 percent while it was 13 percent in ages between 80-89 years. Tham *et al* found that men are at higher risk to glaucoma as compared to women. People having a family history of glaucoma are more likely to have POAG due to similarity in genes related to IOP or optic nerve anatomy. Increased IOP, greater cup-to-disk ratio, older age, African ethnicity, family history are main risk factors contributing to glaucoma. The major problem with glaucoma is that people remain unaware of the disease. There is need to develop educational programs to alert patients with glaucoma especially of African ethnicity. In Australia, presently around 300,000 people are affected by glaucoma and due to increasing old age population, this will increase to 400,000 people by 2025. From these statistics, it is clear that there is an urgent need of developing potential therapeutic agents aiming towards elimination of glaucoma blindness.

1.1.5 Impact of glaucoma on quality of life

Visual disability due to eye diseases e.g. glaucoma is a global concern which significantly affects quality of life. Various questionnaires regarding glaucoma and general health related were designed to collect information about the impact of glaucoma on quality of life which clearly indicates that eye sight has been revealed to be one of the most determining factor on quality of life (Spaeth et al., 2006). Several tools have been devised to estimate of the impact of glaucoma on quality of life of the patients which indicates poor visual function leading to poorer quality of life (Altangerel et al., 2003). Visual

impairment due to glaucoma affects not only daily activities of life but also leads to serious consequences like injuries related to fall or automobile accidents (Coleman et al., 2004, McGwin et al., 1998). Studies have shown that glaucoma patients are at higher risk of a motor vehicle collision (Haymes et al., 2007). For safe driving performance, detection of glaucoma is necessary (Wood et al., 2016). Glaucoma affects mental health like anxiety and depression in many patients (Owsley and McGwin, 2004). Higher prevalence of disturbed sleep remains another clinical problem among glaucoma patients (Agorastos et al., 2013). These factors increase psychological burden among glaucoma individuals. Apart from all this, glaucoma patients also suffer from financial burden (Varma et al., 2011).

1.1.6 Mechanism of retinal ganglion cell (RGC) death in glaucoma

Glaucoma management is a challenge as several mechanisms seem to be involved in RGC death. While IOP and reduced vascular perfusion may be the primary factors, the mechanisms that are associated with the loss of RGCs include glutamate induced excitotoxicity (Sucher et al., 1997), neurotrophin insufficiency (Ginty and Segal, 2002), apoptosis (Das et al., 2006), increased nitric oxide (Cheon et al., 2003), oxidative stress (Yildirim et al., 2005), protein misfolding (Tzekov et al., 2011), Aβ aggregation (Guo et al., 2007), and ER stress (Peters et al., 2015).

Glutamate induced excitotoxicity: Excitotoxicity is proposed as one of the causes of RGC death in glaucoma. The reason for excitotoxicity has been attributed either due to increased glutamate synthesis or decreased glutamate clearance (Osborne et al., 2006).

There are three types of glutamate receptors: i) NMDA (N-methyl-D-aspartate) ii) kainate iii) AMPA (α-amino-3-hydroxy-5-methyl-4-isoxazolepropionic acid) (Casson, 2006). Over stimulation of NMDA receptors leads to increase in intracellular Ca^{2+} influx (Laabich et al., 2001). Excessive intracellular Ca^{2+} activates calpain and calcium/calmodulin-dependent kinase 2 (CaMK). Ca^{2+} overload also initiates a cascade of events that leads to several apoptotic pathways such as disrupted mitochondrial activity, increased release of cytochrome c, apoptosis inducing factor (AIF), and reactive oxygen species (ROS) (Chiu et al., 2005, Takeda et al., 2007). AIF triggers caspase-independent apoptotic pathway and initiates nuclear chromatin condensation and DNA fragmentation. On the other hand release of mitochondrial cytochrome c activates caspase-9 and subsequently caspase-3 (Zhang et al., 2002). Studies have confirmed glutamate-mediated RGC death is one of the contributing factors for glaucoma (Guo et al., 2006).

Neurotrophin (NT) withdrawal: NT have an indispensable role in promoting neuronal survival and regeneration. Neurotrophin deprivation decreases the survival of neurons in rodent models. In glaucoma, lack of neurotrophic factors (NF) is associated with impaired axonal transport in the optic nerve (Oppenheim, 1991). NFs include brain-derived neurotrophic factor (BDNF), ciliary neurotrophic factor (CNTF), nerve growth factor (NGF), neurotrophin-4 and 5 (NT4 and NT5). NT signaling is activated through Trk receptors and leads to two cascades i) Ras/Raf/MEK/ERK1/2 MAP kinase pathway ii) PI3-K/Akt/mTOR pathway. Erk1/2 pathway activation plays a key role in RGC survival in glaucoma (Cheng et al., 2002, Zhou et al., 2005).

Oxidative stress: Various human and animal studies have shown the involvement of oxidative stress in glaucoma pathology (Tanito et al., 2012, Tanito et al., 2015). Excessive

reactive oxygen species (ROS) production, decreased ROS scavenging, impaired mitochondrial function and antioxidant defence mechanisms are underlying factors for oxidative stress. Under conditions of ocular hypertension or hypoxia, there is increased ROS production which progressively leads to RGC death by apoptotic and autophagic pathways (Nita and Grzybowski, 2016). Also overwhelming ROS production augments nitric oxide (NO) production which further produces NO mediated cytotoxic effects on the RGCs (Neufeld and Liu, 2003). Additionally mitochondria are the principal site of ROS production. Under glaucoma conditions, there is increased accumulation of Ca^{+2} within mitochondria which further leads to enhanced ROS production (Kristian and Siesjo, 1998). Also mitochondrial dysfunction triggers release of cytochrome c (apoptosis inducing protein) (Nickells, 1999).

Amyloid beta (Aβ) deposition: Aβ plaques have been implicated in various neurodegenerative disorders including Alzheimer's disease (Murphy and LeVine, 2010), Parkinson's disease (Dugger et al., 2012) and multiple sclerosis (Matías-Guiu et al., 2016). Recently Aβ deposition has also been characterised in the pathogenesis of glaucoma (McKinnon et al., 2002, Goldblum et al., 2007). Abnormal APP (amyloid precursor protein) processing results in formation of Aβ plaques. There are three APP processing enzymes α- secretase, β- secretase and γ-secretase (Epis et al., 2012). Among these three proteases, β-secretase serves as main enzyme for insoluble Aβ formation causing APP cleavage followed by γ-secretase (Na et al., 2007). On the other hand, α-secretase is responsible for non-amyloidogenic processing of APP that serves to perform various essential biological functions (Lichtenthaler, 2012). The exact mechanisms by which Aβ induces neurotoxicity is unclear. Activation of JNK-c-Jun-Fas ligand-Fas pathway (Morishima et al., 2001), TNF receptor signaling cascade (Li et al., 2004), involvement of

multiple caspases (Allen et al., 2001) are found to be responsible for Aβ mediated neuronal apoptosis.

Loss of heat shock protein (HSP) activity: These proteins belong to a group of molecular chaperones that are supposed to protect cell viability under various stressful conditions like high temperatures (Lindquist and Craig, 1988), ischemia (Li et al., 2003), osmotic stress (Dasgupta et al., 1992) and oxidative stress (Omar and Pappolla, 1993). Under stressful conditions, heat shock factors (HSFs) enter the nucleus, binds to heat shock elements (HSEs), induce transcription of HSPs and provide a cytoprotective action (Morimoto, 1998). These shock proteins are expressed in various ocular tissues and are believed to play a unique role in glaucoma injury due to IOP elevation (Li et al., 2004). Recent studies have shown that HSPs, mainly HSP70 and small HSPs (alpha A and alpha B crystallins) are found to enhance the survival of retinal ganglion cells (RGCs) in glaucoma (Piri et al., 2016).

Endoplasmic reticulum (ER) stress: ER has been recognized as the central, primary intracellular organelle responsible for biosynthesis, folding, maturation and trafficking of proteins (Ron and Walter, 2007, Todd et al., 2008). ER allows release of only properly folded competent proteins to the Golgi apparatus. The ER also serves to maintain intracellular calcium homeostasis (Gorlach et al., 2006). In addition, other major functions of the ER include synthesis of phospholipids and sterols, carbohydrate metabolism, and drug detoxification. Perturbations in ER function, termed ER stress trigger an unfolded protein response (UPR), which further coordinates signalling pathways and modulates cell function to protect the cells. The UPR is mediated by the action of three signalling proteins

located on the ER membrane: protein kinase RNA (PKR)-like ER kinase (PERK) (Harding et al., 1999), inositol-requiring enzyme 1 (IRE1) (Calfon et al., 2002) and activating transcription factor 6 (ATF6) (Ron and Walter, 2007). Under normal physiological conditions, all ER stress transducers i.e. PERK, ATF6 and IRE1α proteins remain in an inactive state by binding to the ER resident chaperone- Binding Immunoglobulin Protein (Bip), also known as glucose-regulated protein 78 (GRP78) (Bertolotti et al., 2000, Ng et al., 1992). Upon ER stress, GRP78 dissociates from the ER membrane proteins due to accumulation of excessive unfolded proteins in the ER lumen (Haze et al., 2001). After dissociating from the luminal domains of PERK, ATF6 and IRE1α proteins, GRP78 binds to misfolded proteins and facilitates their ATP-dependent protein folding. During ER stress, UPR is an adaptive cellular response which decreases the accumulation of unfolded or misfolded proteins and promotes cell survival (Schroder and Kaufman, 2005b). However, when the ER function is severely impaired, UPR fails to restore the normal function of the ER and apoptosis occurs (Paschen and Frandsen, 2001, Rao et al., 2004). It has been reported that RGCs are very sensitive to ER stress (Shimazawa et al., 2007). In the experimental glaucoma conditions, ER stress has been found to play a pivotal role in RGC apoptosis associated with ER stress indicating that targeting ER stress might be a good therapeutic potential to protect RGCs (Doh et al., 2010).

1.1.7 Glaucoma and other Neurodegenerative disorders

Neurodegenerative or degenerative nerve disorders are common diseases that have a tremendous impact on our society with medical, social and financial burdens. The term "neurodegeneration" indicates loss of nerve structure and function. Alzheimer's disease (AD), Parkinson's disease (PD), Huntington's disease (HD), amyotrophic lateral sclerosis

(ALS), and glaucoma are some of the best known neurodegenerative diseases. These diseases share common molecular and cellular pathologies affecting elderly population, progress slowly and carry a genetic predisposition (Hung et al., 2010). This indicates that potential treatments available for treating neurodegenerative disorders could be used for glaucoma and vice-versa. A characteristic feature of glaucoma is death of the RGCs and glaucomatous damage extends secondarily from RGCs to the visual cortex (Yücel et al., 2003). Recent research has linked glaucoma-associated neurodegeneration in the intracranial optic nerves, lateral geniculate nucleus (LGN) and visual cortex of primates and humans (Gupta et al., 2006). Studies have shown that various neurochemical, metabolic and degenerative changes of the CNS occur in glaucoma (Vickers et al., 1997, Crawford et al., 2000, Yucel et al., 2000).

Glaucoma and Alzheimer's disease (AD): Recent findings showed that glaucoma and AD share some basic apoptotic cell death mechanisms. Formation of Aβ oligomers aggregates known as amyloid plaques is associated with neuronal and vascular degeneration in AD brains (Roth et al., 2005). It has been seen that caspase activation creates Aβ production by sequential amyloid precursor protein (APP) proteolysis in cultured hippocampal neurons as well as in brains of Alzheimer's patients (Gervais et al., 1999). This same mechanism of upregulation of Aβ and activation of caspase-3 has been seen in RGCs after optic nerve transection in an ocular hypertensive rat model of glaucoma (McKinnon, 2003). In addition, it has been reported that AD patients show higher incidence of glaucoma as compared to their age- and sex-matched control subjects (Bayer et al., 2002, Tamura et al., 2006, Helmer et al., 2013). Moreover, glaucoma and AD are characterized by common features such as synaptic dysfunction and neuronal cell death (Sartucci et al., 2010, Sivak, 2013).

Glaucoma and Parkinson's disease (PD): PD is characterised by deficiency of dopamine. PD patients have been reported to have an increased risk of glaucoma. Dopamine plays an important role in the eye by acting on dopaminergic receptors, regulating IOP (Scheife et al., 2000) and preventing apoptosis due to excessive oxidative stress (Linden, 2000). Lack of dopamine correlates with oxidative stress and hypersensitizes the ganglion cells. Another potential factor for an increased risk of glaucoma in PD is decreased levels of reduced glutathione (GSH) which is one of the prominent antioxidants found in the eye (Costarides et al., 1991, Perry et al., 1982) and provides protection against oxidative stress (Njie-Mbye et al., 2013). A further similarity between glaucoma and PD is the pathophysiological role of synucleins. These are small proteins, expressed in neurons, which occur in three isoforms i.e. α, β and γ-synuclein and posseses chaperone like activity (Souza et al., 2000). α-synuclein is predominantly found in PD patients (Polymeropoulos et al., 1997) while γ-synuclein is selectively and abundantly expressed in retinal ganglion cells (Surgucheva et al., 2008).

Glaucoma and multiple sclerosis (MS): MS is characterised by a chronic inflammation and demyelinating lesions in the central nervous system (Trapp and Nave, 2008) including the optic nerve - the latter producing optic neuritis (Arnold, 2005). Following the inflammatory process, RGC loss occurs from optic neuritis (Shindler et al., 2006). However to date there is little overlap described between glaucoma and MS pathology other than retinal axonal dropout.

1.1.8 Glaucoma models

Glaucoma is a complex, heterogeneous disease that can be caused by different biological processes and affected by both environmental and genetic factors. Although glaucoma has complicated pathogenesis the loss of RGCs is a common finding. The brainstem, visual cortex and the visual pathway are also affected in the disease. The investigation of glaucoma has been associated with the development of animal models as these models help in understanding the pathophysiology of the disease. Moreover animal models are required for facilitating development of therapeutic strategies. A wide variety of animal models including rodents, monkeys, cats, dogs, and several other species have been used to study glaucoma. These models provide valuable information and bring a unique perspective to understand the disease process. For pre-clinical studies, careful selection of an animal model should be based on experimental needs, neuroprotective strategy and considering the benefits and limitations in order to halt or slow the progression of disease. Among all animal models, primate models are most relevant to study human glaucoma but they have limited scope due to their availability and high cost. Rodents are the most popular species to study glaucoma as they have similar ocular anatomy, a high degree of availability, are inexpensive, have a short life-span (relatively fast disease progression), small size, reproduce easily, mature rapidly and can be readily subjected to experimental and genetic manipulation. A wide range of rodent models for glaucoma are available and they are categorized depending on the pathogenesis whether it is genetic or experimentally induced.

A) Genetic rodent models of glaucoma: There are numerous inherited rodent models with different genetic causes and distinct genetic backgrounds that show glaucomatous

pathology. Additionally one can investigate the molecular mechanisms of glaucoma by specific genetic mutations in rodents. A wide variety rodent models of glaucoma have been developed using mutations in the genes e.g. Myocilin (MYOC) (Stone et al., 1997), Optineurin (OPTN) (Rezaie et al., 2002) and WDR36 (Monemi et al., 2005). Knockout mice of the genes OXC1, FOXC2, FOXE3, PITX2, PITX3, LMX1B, PAX6, MAF (Cvekl and Tamm, 2004, Gould et al., 2004, Sowden, 2007, Liu and Allingham, 2011), Glast and Eaac1 have also been considered as genetic mouse models of glaucoma (Harada et al., 2007). The DBA/2J mouse strain carrying recessive mutations in the Gpnmb and Tyrp1 genes provides a secondary pigment dispersion and angle closure model of glaucoma (Libby et al., 2005) and has been widely used.

B) Experimentally induced rodent models of glaucoma:

Laser-induced ocular hypertension: This is simple and reliable method to induce glaucoma in rodents in which a laser beam is applied on the corneal limbus to increase resistance of aqueous outflow pathways (Feng et al., 2013). This method of laser photocoagulation needs expensive equipment and specialized trained personnel. Sometimes laser treatment induces inflammation which is another major concern (Aihara et al., 2003).

Episcleral vein saline injection: In this method episcleral veins of rats are injected with hypertonic saline to induce chronic IOP elevation (Morrison et al., 1997). The resistance to aqueous outflow is increased by inserting a microneedle into the episcleral vein. The

main drawback of this model is the technique for which training and experience is required. Another disadvantage is that IOP elevation is only for short period of time and repetition of hypertonic saline injections are needed to maintain elevated IOP changes (Marcelo and Saragovi, 2005).

Episcleral vein cauterization: The procedure of cauterization of two or more extraocular veins also induces significant IOP elevation in rodent eyes (Ruiz-Ederra and Verkman, 2006). Occlusion of episcleral veins produces long-lasting IOP elevation and this method has been used in experimental glaucoma. This method is highly reproducible (Yu et al., 2006). Major drawback of episcleral vein cauterization includes damage to ocular surface and sclera and it may also cause intraocular inflammation.

Intracameral injection: Intracameral injection of inert substances into the anterior chamber of rodent eyes to produce sustained IOP elevation has also been frequently used. The inert substances include sodium hyaluronate, viscoelastic substances (Moreno et al., 2005), polystyrene microbeads (Sappington et al., 2010) and paramagnetic polystyrene microspheres (Samsel et al., 2011). This model of intracameral injection is inexpensive, technically easy to perform and can provide a gradual elevation with sustained IOP. However sequential treatments are required to maintain elevated IOP in this model making this technique more laborious. It has been suggested that combining microbeads with a viscoelastic substance may provide IOP elevation for at least 3 months following a single co-injection (Frankfort et al., 2013).

Optic nerve crush or transection: This is an acute model of injury and thus not as typical of chronic human glaucoma. Optic nerve axotomy in mice will always induce RGC loss. This is an invasive surgical technique and care must be taken not to interfere with ocular blood flow. Optic nerve transection in rodents can be done in different ways e.g. physically transecting the nerve (Sun et al., 2011) or by using clips (Feng et al., 2010) or forceps (Ohlsson et al., 2004) to crush the nerve.

Excitotoxic agent administration: Intravitreal administration of NMDA, glutamate or kainic acid are the most common excitotoxic agents that trigger RGC death. Glutamate-mediated excitotoxicity is extensively associated in the pathophysiology of RGC apoptosis in glaucoma as glutamate is a major excitatory neurotransmitter in retina (Lucas and Newhouse, 1957, Thoreson and Witkovsky, 1999). Glutamate acts on N-methyl-D-aspartate (NMDA), α-amino-3-hydroxy-5-methyl-4-isoxazolepropionic acid (AMPA), and kainate (KA) receptors (Yu and Miller, 1996). If excessive amounts of glutamate are released then it induces excitotoxicity. This model is widely used due to its reproducibility, low technical difficulty and cost effectiveness.

Retinal Ischemia/reperfusion: This model produces acute elevation of IOP to high levels (>60mmHg) and produces a short-term ocular ischemia. It is achieved by cannulating the anterior chamber and connecting it to an elevated saline infusion. The subsequent retinal reperfusion insult leads to RGCs death which serves as an acute glaucoma model. Injecting

endothelin-1 (ET1) also produces retinal ischemia (Yorio et al., 2002). This model results in damage to many layers of the retina so this model denotes total retinal degeneration not glaucoma alone. Moreover, by this method it is difficult to quantify histopathological changes (Buchi et al., 1994).

C) Cell culture models to study glaucomatous optic neuropathy: Retinal ganglion cell loss is the main pathological process of glaucoma so isolating pure RGC culture from retina is the best cell culture model for studying glaucomatous optic neuropathy (Hong et al., 2012). However some labs also use mixed retinal cultures but the major drawback of it is that this culture is not characteristic of RGCs. This disadvantage also parallels organotypic retinal explant cultures, in which entire pieces of retina are cultured. Some researchers also use primary cultures or cell lines derived from neurons as ischemia, apoptosis and growth factor deprivation can also be induced in neuronal culture (Kortuem et al., 2000).

Briefly, several glaucoma models are available yet there is no ideal model due to complicated pathophysiology of the disease which has hampered progress in glaucoma research.

There are a wide variety of *in vitro* as well as *in vivo* models for experimental glaucoma and it remains difficult to decide which model is best for studying glaucoma. To obtain valid preclinical data, preferences for the choice of model will initially be for simpler techniques that can rapidly and reproducibly show some neuroprotection, then moving to more complex models that more closely represent human glaucoma pathological processes.

S.No	Models of glaucoma	Advantages	Disadvantages
1	Genetic rodent models	-These animals produce more uniform increase in IOP as well as retinal damage as compared to surgically induced models. -Animals having specific mutations at particular gene that have been identified in human glaucoma can be produced. -It is easier to obtain a large number of animals with genetic modification. -These animals do not require specialized induction techniques and that are readily available.	-The course of glaucomatous pathology in genetic rodent models necessitates a significant time commitment for experimentation
2	Experimentally induced rodent models		
	Laser-induced ocular hypertension	-Simple and reliable method	-Needs expensive equipment and specialized trained personnel. -Sometimes laser treatment induces inflammation.
	Episcleral vein saline injection	-Relatively cheaper method to produce glaucoma as it requires less specialized equipment.	-Extensive training and experience is required. -IOP elevation is only for short period of time and repetition of hypertonic saline injections are needed to maintain elevated IOP changes.
	Episcleral vein cauterization	-Produces long-lasting IOP elevation and highly reproducible.	Risk of damage to ocular surface and sclera that may also cause intraocular inflammation.
	Intracameral injection	-Provide a gradual elevation with sustained IOP. -Inexpensive and technically easy to perform.	-Sequential treatments are required to maintain elevated IOP in this model making this technique more laborious.
	Optic nerve crush or transection	-Relatively simple to perform in both rats and mice.	-It is only an acute model of injury.

	Excitotoxic agent administration	-Quick onset of pathology as RGC degeneration begins quickly following the procedure. -Highly reproducible -low technical difficulty and cost effectiveness.	-Does not fully represent glaucoma. It is hypothesized that any neurological disease can be associated with changed state of excitatory amino acid.
	Retinal Ischemia/reperfusion	-Relatively easy method and reproducible.	-This model results in damage to many layers of the retina so this model denotes total retinal degeneration not glaucoma alone.
3	RGC culture and retinal explant organ culture	-Convenient system that has been used to assess many aspects of RGC biology, pharmacology, and electrophysiology and extremely simple	-The major drawback of *in vitro* systems is that they are not characteristic of RGCs e.g. in organotypic retinal explant cultures, the entire pieces of retina are cultured.

Table 1.1 Table showing the advantages and disadvantages of glaucoma models.

1.1.9 Current available treatments for glaucoma

The main aim for glaucoma treatment is to prevent patient's vision loss and providing them safe, cheap and non-invasive treatment methods which can improve their quality of life. POAG is one of the commonest forms of glaucoma caused by intraocular hypertension (Ang and Eke, 2007). Current treatment modalities are based on lowering the IOP that includes medications, surgery and laser therapy. Treatment with medications can be categorized into topical and systemic forms. The five main classes of topical ocular hypotensive drugs currently in clinical use are: beta-blockers (timolol, betaxolol), cholinergic agents (pilocarpine), carbonic anhydrase inhibitors (dorzolamide, acetazolamide and brinzolamide), alpha-2 agonists (brimonidine and iopidine), and prostaglandin analogues (latanoprost, bimatoprost, travoprost and tafluprost). Rho kinase

(ROCK) inhibitors are novel emerging compounds for glaucoma treatment. These agents are currently in Phase II and III US Food and Drug Administration trials (Wang and Chang, 2014). Netarsudil has recently received an FDA approval as the first Rho Kinase inhibitor for the treatment of glaucoma. The major drawback of long-term medication is non-compliance in many patients. These drugs are mainly aimed at lowering IOP and are the first line of treatment in the developed world. On the other hand, surgery is often favoured as the first-line of treatment in developing countries (Kim et al., 2008) due to costs and problems with supply of medications as well as issues with follow up. Glaucoma can also be treated by using laser procedures termed trabeculoplasty, which directly treats the trabecular meshwork (Brancato et al., 1991). The most common type of surgery is called trabeculectomy and it consists of removal of a small portion of the trabecular meshwork to provide a drainage route for aqueous humour to the sub-conjunctival space. Other non-penetrating surgeries like deep sclerectomy (Fedorov et al., 1982), viscocanalostomy (Stegmann et al., 1999) and canaloplasty (Lewis et al., 2007, Grieshaber et al., 2010) for glaucoma are also available. Apart from conventional therapies, use of Ologen® implant have been introduced for the management of glaucoma (Radhakrishnan et al., 2014, Sarkisian, 2009) . Other surgical devices and stents are also now available and in clinical trial phase which may improve the fluid outflow into the Schlemm's canal like trabectome (Francis et al., 2006), Glaukos istent (Nichamin, 2009) and EyeOP1 (Giannaccare et al., 2016).

Current treatment options for glaucoma are mainly focused on lowering the IOP. However, studies have shown that despite reducing IOP, glaucoma continues to progress in many patients (Heijl et al., 2002, Wu et al., 2017). Extensive research has been conducted to find out the newer possible strategies for treating glaucoma. Mainly RGC loss is considered to be involved in the pathophysiology of all forms of glaucoma.

New approaches to hamper RGC loss have been recognized as beneficial to this incapacitating disease. Various pharmacological approaches have been developed over a period of time that provide neuroprotection e.g. NMDA receptor antagonists (Vorwerk et al., 1996), neurotrophic factors (Fu et al., 2009), anti-apoptotic agents (Osborne, 2008), Nitric oxide synthase antagonists (Neufeld et al., 2002), antioxidants (Dilsiz et al., 2006). Gene therapy and stem cell therapies are also promising modalities providing neuroprotection.

1.2 Nuclear receptors

From the past decade, research on therapies targeting nuclear receptors have gained substantial interest to treat neurodegenerative diseases. Yan *et al* published effects of a nuclear receptor agonist in an animal model of AD for the first time in 2003 (Yan et al., 2003). Nuclear receptors belong to a large superfamily of ligand-regulated transcription factors that mediate numerous biological processes. All nuclear receptors exhibit a common structure comprised of 5 domains, designated as A/B, C, D, E, and F domain. A/B domain is also denoted as AF-1 which is highly variable NH2-terminal region and is capable of ligand-independent functioning. Region C or conserved DNA-binding domain (DBD) functions to recognise specific DNA sequences. Linker region D connects DBD to the conserved E region that in turn contains the ligand binding domain (LBD). Some receptors also possess a COOH-terminal region or F domain with unknown functions (Aranda and Pascual, 2001).

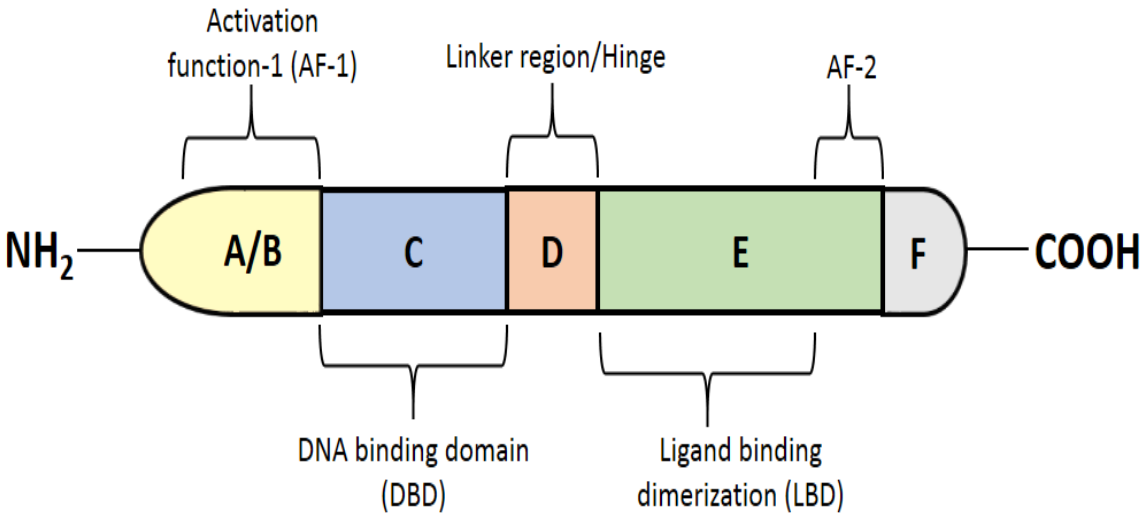

Figure 1.4 Schematic representation of a nuclear receptor.

There two main types of NRs: Type I receptors which includes mineralocorticoid receptor (MR), androgen receptor (AR), progesterone receptor (PR), glucocorticoid receptor (GR), and estrogen receptor (ER) and Type II which includes vitamin D3 receptor (VDR), thyroid hormone receptor (TR), retinoid X receptor (RXR) and retinoic acid receptor (RAR) (Liu et al., 2017). Among all the nuclear receptors available, retinoid X receptor (RXR) are highly diverse owing to the ability to activate multiple nuclear receptors (Ahuja et al., 2003). Growing amount of compelling data indicates that RXR activation represents important targets for new therapeutic approaches for various neurodegenerative disorders.

1.2.1 Retinoid-x-receptors (RXRs)

In 1990, Mangelsdorf *et al* isolated a novel nuclear receptor, referred to as hRXRα (Mangelsdorf et al., 1990). Later on, three RXR isotypes encoded by distinct genes were identified i.e. RXRα (NR2B1), RXRβ (NR2B2) and RXRγ (NR2B3) (Chiba et al., 1997). Expression of RXRs can be found in every tissue of the body: RXRα is mainly expressed

in skin, liver, lung, muscle, spleen kidney, intestine, epidermis, placenta and a variety of visceral tissues and, RXRβ can be found ubiquitously while RXRγ is mainly restricted in brain, cardiac and skeletal muscles (Germain et al., 2006). The understanding of pattern expression of all three RXRs revealed that they exhibit vital functions throughout the course of development as well as in adult life (Mangelsdorf et al., 1992). RXR is an intriguing and essential member of nuclear receptor (NR) superfamily of ligand-dependent transcription factors (Lefebvre et al., 2010, Dawson and Xia, 2012). RXRs control target genes by directly binding to DNA at specific sequences called as RA response elements (RAREs) (Mangelsdorf et al., 1995). RXRs functions as both homodimer (dimer with either itself) and heterodimer (dimer with another NR). RXR heterodimers are further categorized into permissive that can be activated by agonist of either RXR or heterodimeric partner or non-permissive in which RXR acts as a "silent partner and are activated only by ligands specific for the other NR. Examples of permissive heterodimers are liver X receptors (LXRs), peroxisome proliferator-activated receptors (PPARs), farnesoid X receptor (FXR), pregnane X receptor (PXR) (Aranda and Pascual, 2001) and the orphan receptor nur77/NGFB-1. Non-permissive heterodimers include retinoic acid receptors (RARs), thyroid receptors (TRs), and vitamin D receptor (VDR) (Berrodin et al., 1992, Kliewer et al., 1992). Due to this versatility, RXRs exert pleiotropic roles in reproduction, cellular differentiation, bone development, haematopoiesis and pattern formation during embryogenesis (Chung and Cooney, 2003). From an initial evolution of a nuclear hormone receptor, RXR homologues are the most ancient members which give rise to many other receptors (Wiens et al., 2003). Several studies showed that the RXR signal pathway is independent of other nuclear receptors (e.g RAR) suggesting existence of RXR-specific signaling which may serve as independent target for new pharmacologic activities (Szanto et al., 2004). Despite tremendous work to find out the specific functions

of RXRs, it is still on the crossroad of different metabolic biological pathways. Knockout studies were carried out in order to find out the significance of RXR and its subtypes in adult animals. RXRα -/- mice cause embryonic death due to cardiac deformities and RXRα ablation showed ocular defects (Kastner et al., 1994). On the other hand, mice having RXRβ and RXRγ mutations are phenotypically normal but show male sterility in RXR beta mutant mice (Kastner et al., 1996) and null mutation of RXRγ lead to memory deficits in mice (Wietrzych et al., 2005). More interestingly, RXR alpha +/-/RXR beta -/-/RXR gamma -/- triple mutants were viable but showed abnormal spermatogenesis due to loss of RXR beta indicating that RXR alpha is the most important RXR subtype (Krezel et al., 1996).

1.2.2 RXR ligand binding domain

There are several crystal structures of the C-terminal ligand binding domain (LBD) of nucleic receptors from different organism has been studied (Rastinejad et al., 2015). RXR receptors consists of 11 α helices (H1-H11) and 2 small β strands (Figure 1.5). Within the ligand binding pocket (LBP), most of the H11 helix residues are hydrophobic and polar that impart the stable confirmation to the RXR protein. There is a large conformational change observed previously in ligand bound RXR structures at H3, and H10 helix region in comparison to naïve RXR structure (Bourguet et al., 1995). It was suggested that ligand induced the transition at H11 helix, followed by change in position of H3 and H4, all together this repositioning causes H11 helix to expose from hydrophobic cleft to the surface of the LBD. H11 helix has a major role in forming dimerization with other proteins inside the hydrophobic cleft formed by H3 and H4 helix residues and initiate the process of transcriptional activation (Gampe et al., 2000). RXRα (PDB ID: 1FM9, Homo sapiens) LBD

consists of 238 amino acid complexed with 9-cis-retinoic acid (9cRA). LBD of RXRα form a coil along H10 helix to have additional interaction with additional nuclear receptors to form heterodimer (Figure 1.5 A). Crystal structure of RXRβ LBD constitute similar structural geometry to that of RXRα but it has shorter length of amino acid, 236 amino acids (PDB ID: 1UHL, chain A, Homo sapiens) and has methoprenic acid bound ligand (Figure 1.5 B).The binding of methoprenic acid in LBD of RXRβ make it to adopt L-shaped structure like that of 9cRA but this complex showed narrower LBP in comparison to 9cRA-RXRβ LBD complex (Svensson et al., 2003, Egea et al., 2002). LBD of RXRγ was taken from protein data bank (Figure 1.5 C) (www.rcsb.org) (PDB ID: 2GL8, Homo sapiens). Not much information is available about the structure of RXR γ LBD.

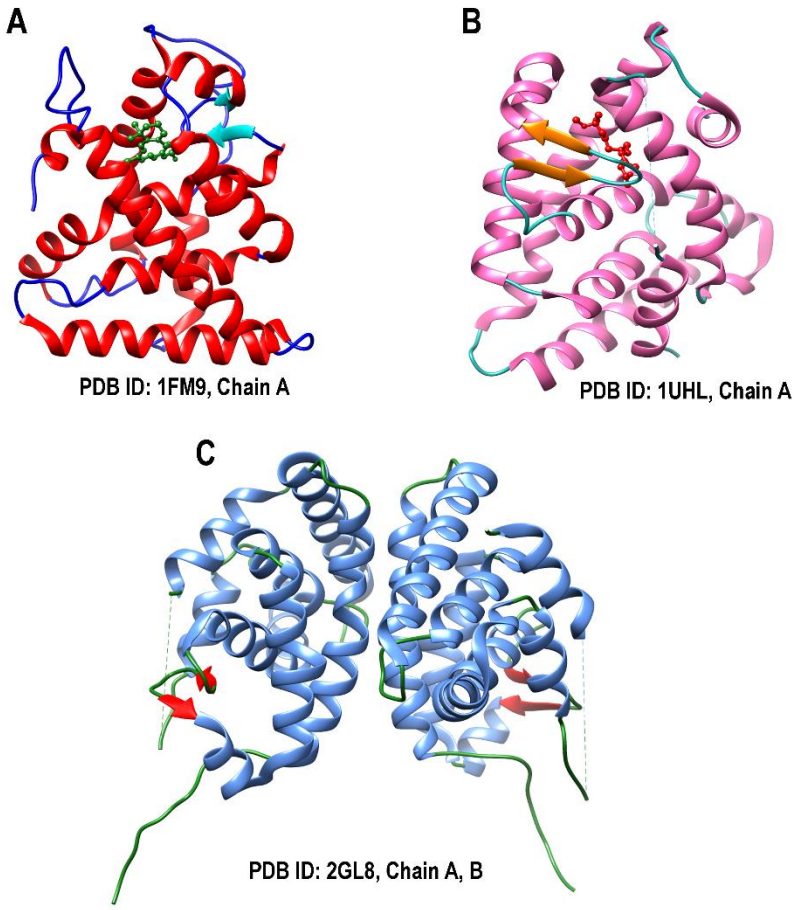

Figure 1.5 Ribbon-diagram overviews of A) RXRα (red) with ligand (green), B) RXRβ (pink) with ligand (red) and C) RXRγ (blue) (downloaded from protein data bank).

1.2.3 Role of RXRs in eye development

The localization of RXRs has been extensively studied in mouse ocular tissues (Mori et al., 2001). In developing and adult mouse retina, RXR α and γ were reported to localize to specific tissues or cells while RXR β showed ubiquitous distribution. Studies have shown that retinoic acid (RA) which is active metabolite of vitamin A (retinol) promotes proper functioning of the retina. RA signalling pathways and RA activated nuclear receptors play

specific roles during embryonic eye development. RA activity is regulated by interaction of retinoid receptors i.e. retinoic acid receptors (RARs) and retinoid X receptors (RXRs). RAR subtypes bind both 9-cis retinoic acid (9cRA) and all-trans retinoic acid (atRA) while 9 cis RA is the ligand for RXRs (Allenby et al., 1993). The exact mechanism of action of the RAR/RXR in ligand-mediated gene transcription is still a matter of debate. Genetic ablation studies have revealed a more direct approach to find out the specific functions of different retinoid receptors involved in retinoid signalling After reviewing results of single or double RAR or RXR mutants, it has been seen that out of all receptor knockouts only RXRα null-mutants died *in utero*. RXRα null-mutants showed severe myocardial and ocular malformations that relate to the fetal vitamin A deficiency. Based on these facts it was concluded that RXRα is the most important receptor involved in retinoid signalling (Janssen et al., 1999). Further immunohistochemistry was performed to find out the retinoid receptor expression patterns. RXRβ was expressed ubiquitously in mouse retina. RXRγ is found to be expressed in neuroretina and RXRα found in neuroretina, RPE (retinal pigment epithelium), iris/ciliarybody, cornea, conjunctiva (Mori et al., 2001, Cvekl and Wang, 2009).

1.2.4 Retinoid X receptor (RXR) and Histone proteins

Histones are the main protein components of chromatin that play a role in gene regulation. These histone proteins undergo various post-translational modifications such as acetylation, methylation, phosphorylation, ubiquitination, and sumoylation (Cosgrove et al., 2004). These modifications regulates various physiological and pathologicalconditions. The acetylation and deacetylation of histone have been identified as an important step in regulating gene expression (Hsieh et al., 2004, Kuo and Allis,

1998). In general, histone acetylation activates gene expression, and histone deacetylation suppresses gene expression (Barneda-Zahonero and Parra, 2012). This regulation is controlled by two important enzymes (a) histone acetyltransferases (HAT) and, (b) histone deacetylases (HDAC). HAT enzymes are the catalytic subunit of large multisubunit HAT complexes that acetylate the ε-amino group of specific lysine residues on histone tails to promote transcriptional activation whereas HDAC are a class of enzymes that remove acetyl groups (O=CCH3) from an ε-N-acetyl lysine amino acid on a histone, allowing the histones to wrap the DNA more tightly. Studies have shown that in the absence of ligands for RXRs, the receptors' target genes are repressed (Altucci and Gronemeyer, 2001).The unliganded RXRs are associated with corepressor like NCoR (nuclear receptor corepressor) and SMRT (silencing mediator of retinoic acid and thyroid hormone receptor), both of these repress transcription below basal levels. These corepressors leads to the recruitment of histone deacetylase (HDAC) which results in histone deacetylation and chromatin condensation. Several *in vitro* and *in vivo* studies have demonstrated that the combination of RXR agonists alongwith a HDAC inhibitor enhances the effects of RXR activation and gene transcription (Epping et al., 2007, Ferrara et al., 2001). In the retina, recent evidence shows that epigenetic modification of histones mainly deacetylation plays an important role in loss of RGCs after optic nerve injury (Schmitt et al., 2016).

1.2.5 Ligands for RXR

9-cis-retinoic acid (vitamin A derivative) was first identified as natural RXR ligand with high affinity (Mangelsdorf et al., 1990), but its status as an endogenous agonist is still a matter of debate (Wolf, 2006). Some polyunsaturated fatty acids such as docosahexaenoic acid (DHA), arachidonic acid, linoleic, linolenic acid and a metabolite of chlorophyll, phytanic acid were also recognized as specific RXR ligands but with low affinity (Lengqvist et al., 2004, Rühl et al., 2015, Dawson and Xia, 2012). Recently, honokiol which is extract of the bark of *Magnolia obovata*, has been characterized as another natural RXR ligand having higher potency than phytanic acid and docosahexaenoic acid , but lower than 9-*cis*-retinoic acid (Kotani et al., 2010). Numerous synthetic RXR-specific ligands (rexinoids), have also been identified and synthesised (Pérez et al., 2012) e.g. bexarotene (Targretin), which is chemopreventive agent in cancer therapy (Qu and Tang, 2010). Apart from these agents, other RXR ligands are also known like organotin compounds that are used as anti-fouling agents in marine structures (le Maire et al., 2009). Non-steroidal anti-inflammatory agents like R-enantiomer of etodolac (Kolluri et al., 2005) and sulindac sulphide (Zhou et al., 2010) exert their anti-cancer effects by binding to RXRα. Regardless of their abundant advantageous effects, most of the RXR ligands induce hepatomegaly, increase in triglyceride and cholesterol levels and dysregulation of the thyroid hormone axis, which limits their use (Pérez et al., 2012). For that reason, bexarotene is the only FDA approved RXR agonist.

1.2.6 RXR agonist: Bexarotene

Bexarotene[4-[1-(5,6,7,8-tetrahydro-3,5,5,8,8-pentamethyl-2-naphtalenyl)ethenyl] benzoic acid] also known as LG10269 or Targretin, is a synthetic rexinoid with specific affinity for RXRs (Farol and Hymes, 2004). Bexarotene treatment induces gene expression by selectively binding and activating RXRs.

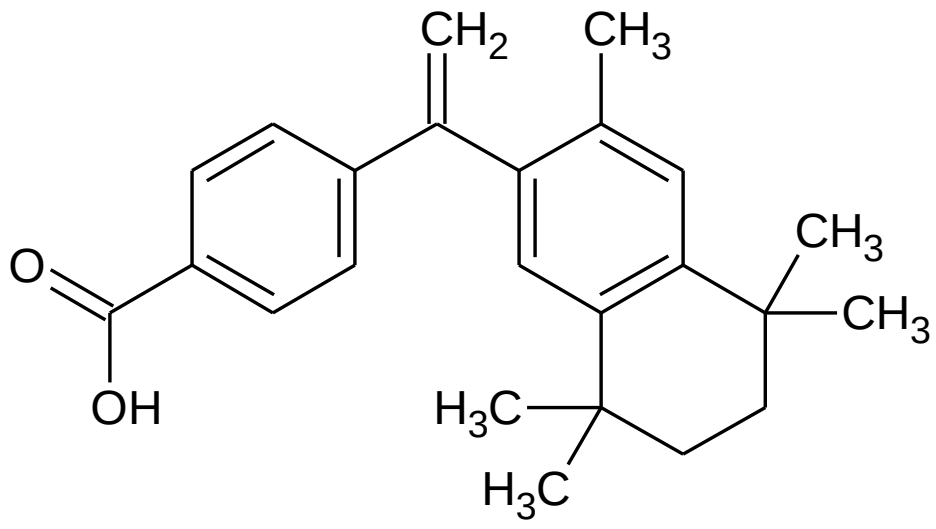

Figure 1.6 Chemical structure of Bexarotene.

Pharmacological actions of Bexarotene: Bexarotene is approved for treatment of cutaneous T-cell lymphoma (CTCL) by US Food and Drug Administration in 1999 (Gniadecki et al., 2007). Bexarotene also shows chemopreventing activity on lung cancer (Zhang et al., 2011, Yen and Lamph, 2005). From the past decade, it has become evident that targeting RXRs reach far beyond its use as anti-cancer agent. RXR agonists e.g. bexarotene have been shown to regulate gene expression in the brain (Boehm-Cagan and

Michaelson, 2014, Mounier et al., 2015). It has been reported that RXR ligands serve as potential therapeutic agents providing neuroprotection. Bexarotene has been reported to improve a wide range of neurodegenerative diseases including AD (Cramer et al., 2012), aging-related synapse loss (Tachibana et al., 2016), parkinsonism (McFarland et al., 2013), multiple sclerosis (Natrajan et al., 2015), amylotrophic lateral sclerosis (Riancho et al., 2015) and ischemic stroke (Certo et al., 2015). Apart from anti tumour activity and as neuroprotective agent, bexarotene also has beneficial actions in other metabolic pathologies like preventing atherosclerotic lesion by lowering circulating atherogenic cholesterol-containing lipoproteins (Lalloyer et al., 2006).

Pharmacokinetics of Bexarotene: Bioavailabilty of bexarotene was confirmed after oral administration by pharmacokinetic studies in rats and dogs. The maximum plasma concentration of bexarotene was reached after 2-4 hrs of drug administration. The half life of bexarotene was 2 hr to 3 hr in rats and 3 hr to 6 hr in dogs after intravenous administration. The oral bioavailability of bexarotene was found to vary with different formulations. The reduction in particle size of bexarotene enhance bioavailability as dissolution rate is one of the rate limiting factors for drug absorption. Studies have demonstrated that bexarotene is distributed throughout the body after oral administration. It is more than 99.9% plasma protein bound drug. Oxidation and glucuronidation are the major routes of metabolism of bexarotene (Howell et al., 2001). More than 90% of drug is excreted through faecal matter after oral administration.

1.2.7 Role of Bexarotene in Alzheimer's disease

In 2012,Cramer *et al* reported that oral administration of bexarotene leads to Aβ clearance from the brain in AD mouse which resulted in rapid reversed behavioural and olfactory deficits (Cramer et al., 2012). Later on other follow up studies confirmed no change in soluble Aβ levels with bexarotene treatment (Tesseur et al., 2013, Price et al., 2013). All these findings highlighted that Aβ clearance and improved cognitive deficits by bexarotene is still under debate. A more recent pilot study has claimed that bexarotene causes improved cognitive function in AD by reducing network excitability (Bomben et al., 2014). This study showed that there are other possible mechanisms of bexarotene apart from amyloid cascade responsible for its effects on AD. Not only in AD but strong evidence has been found showing involvement of Aβ in glaucoma (McKinnon et al., 2002, Guo et al., 2007). Additionally, there are specific mechanisms which overlap between AD and glaucoma. Both are neurodegenerative disorders affecting mainly people with old age. Moreover, optic nerve degeneration and RGC loss has also been studied in AD patients (Hinton et al., 1986, Sadun and Bassi, 1990, Tsai et al., 1991).

As RXRs involve in regulating gene expression in the brain and activation of these receptors play important roles in neuroprotection (Boehm-Cagan and Michaelson, 2014, Bomben et al., 2014, McFarland et al., 2013, Riancho et al., 2015, Tai et al., 2014). Based on its potential role in various neurodegenerative disorders we further exploit RXR modulation in disease conditions with a main focus on glaucoma, which is a major neurodegenerative disease of the RGCs. We investigated them in the retina by targeting pharmacologically with the RXR agonist bexarotene.

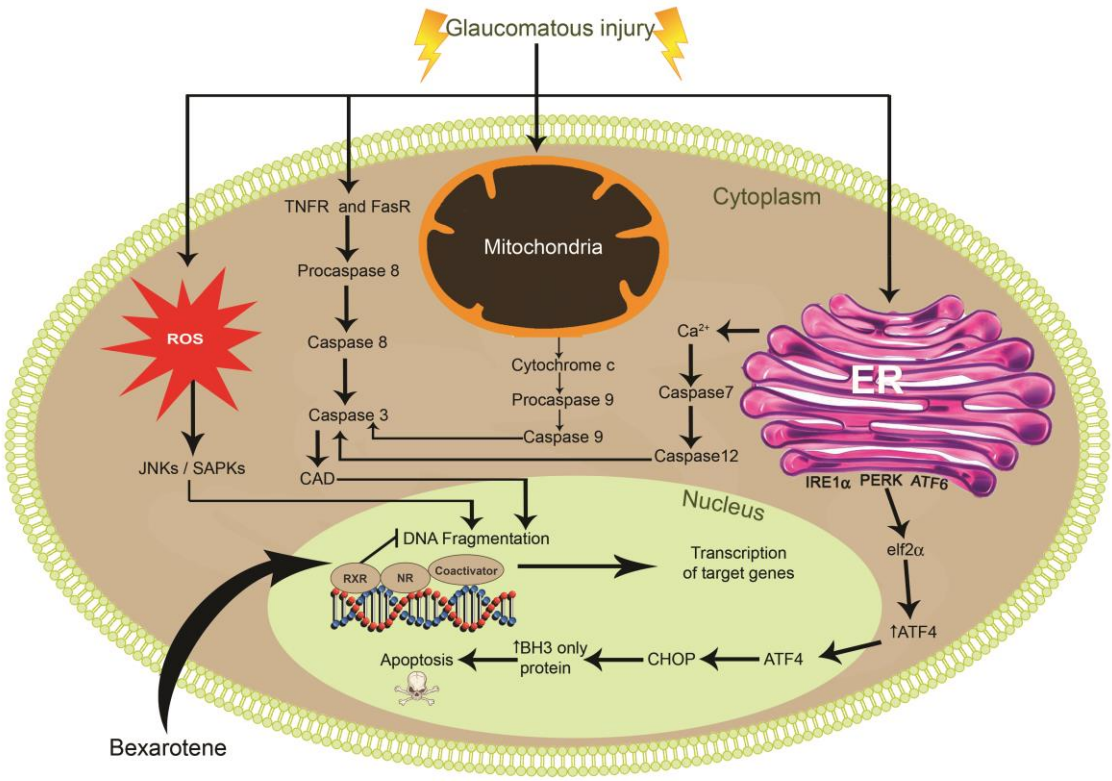

Figure 1.7 Schematic representation showing activation of RXR by bexarotene regulating gene transcription. TNFR: tumor necrosis factor receptor; FasR: first apoptosis signal receptor;JNKs: c-Jun N-terminal kinases;SAPKs: stress-activated protein kinases;ROS: Reactive oxygen species;CAD: Caspase-activated DNase;IRE1α: Inositol-requiring kinase 1α;PERK: protein kinase R (PKR)-like endoplasmic reticulum kinase;ATF6: Activating transcription factor 6;elf2α: eukaryotic translation initiation factor;ATF4: Activating transcription factor 4;CHOP: CCAAT/-enhancer-binding protein homologous protein;BH3: (Bcl-2 (B-cell lymphoma-2) homologous 3);RXR;retinoid x receptor;NR:nuclear receptor.

Hypothesis

Retinoid-X-Receptors (RXR) belong to the family of nuclear receptors comprising RXR α, β and γ isoforms. RXRs regulate the transcriptional activity of multiple genes, are involved in wide range of cellular pathways and are essential for normal eye development. RXR activation has proven to be beneficial in neurodegenerative models affecting the brain. Also RXR activation protects retinal neurons from oxidative stress induced apoptosis. Activation of RXRs has also been demonstrated to promote photoreceptor survival by impeding apoptosis. However neuroprotective effects of RXR activation on the inner retina particularly RGCs have not been investigated. Based on the known neuroprotective effects of RXR upregulation in the neuronal cells in brain and retina, we hypothesised that RXR activation could exert protective effects in the retina under glaucoma conditions.

Aims

The aims of this thesis are:

1. To determine the effects of bexarotene on RXR (α, β and γ) expression in neuronal cells.

2. To investigate the *in vivo* effect of RXR activation under acute as well as chronic glaucoma stress conditions.

3. To study the binding pattern and stability of different RXRs with their agonist(s) using molecular modelling approach.

CHAPTER 2

MATERIALS AND METHODS

2.1 Animals and Ethics

Male C57BL/6 mice (7-8 weeks) were purchased from the animal research centre, Perth and APP-PS1 mice tissues were obtained from University of Tasmania, Australia. All experimental procedures and conditions involving animals were conducted in accordance with the Australian Code of Practice for the Care and Use of Animals for Scientific Purposes and with the approved guidelines of the ARVO statement for the Use of Animals in Ophthalmic and Vision Research. All animals used for glaucoma studies were cared according to guidelines approved by the Animal Ethics Committee of Macquarie University, NSW, Australia (ARA: 2015/012). Animals were housed in a 12 hours light /dark cycle and provided with standard rodent diet and water.

2.2 Bexarotene treatment

Mice were weighed at the beginning of the treatment period and the necessary volume of solubilized bexarotene was calculated to produce a concentration of 100 mg/kg for each animal. Bexarotene was suspended in 10% DMSO in saline and 200 µl was administered. Bexarotene (100 mg/kg) was administered orally by syringe feeding to C57BL/6 mice once daily in drug treatment groups and continued for seven days in glutamate model and for fourteen days in the microbead model of glaucoma.

2.3 Development of glaucoma models

2.3.1 Glutamate injection: A single intravitreal injection of glutamate was performed into the vitreous chamber behind the pupil using a 10 µl Hamilton syringe with a 33 gauge needle under the surgical microscope. Mice were injected intravitreally with a volume of 1 µl solution containing 200 nmol concentrations of glutamate dissolved in saline.

2.3.2 Microbead Injection: Intracameral injections of microbeads (Fluospheres, Molecular Probes, 10 μm) were made into the anterior chamber of the eye using a 10 μl Hamilton syringe with a 33 gauge needle under microscope avoiding needle contact with the iris or lens. The microbead injection was repeated every week for up to 2 months to maintain a high IOP. Prior to all injections, animals were anesthetized with combination of ketamine (75mg/kg) and medetomidine (0.5 mg/kg). After the animal was anaesthetised, a single drop of 0.5% proparacaine hydrochloride (Alcaine, Alcon) (for topical anesthesia) and 1% tropicamide (Mydriacyl, Alcon) (for mydriasis) was applied on the cornea. After the injection was performed, the needle was allowed to remain in the eye for further 30sec to minimise risk of loss of injected drug when the needle was withdrawn. Dexamethasone and 2% povidone-iodine were applied topically post injection to prevent any ocular inflammation and infection. Also carprofen (2.5mg/kg s.c) as pain killer and cephazolin (20mg/kg i.v) as antibiotic were administered. Lacri-lube (Allergan, NSW, Australia), an ointment to prevent drying of cornea was also applied. After the procedure, atipamazole (1mg/kg s.c) was given to reverse the effect of anaesthesia and animals were allowed to recover on a heating pad maintained at 37°C. The animals were closely watched and returned to the animal facility post injection when they started moving freely with full recovery and then monitored for two consecutive days after the injection.

IOP was measured by using a handheld electronic tonometer (Icare Tonovet, Helsinki, Finland) prior to each injection. The IOP was the mean of six consecutive measurements as displayed on the tonometer. A total of three consecutive IOP readings were obtained from each eye and the average number was taken as the IOP.

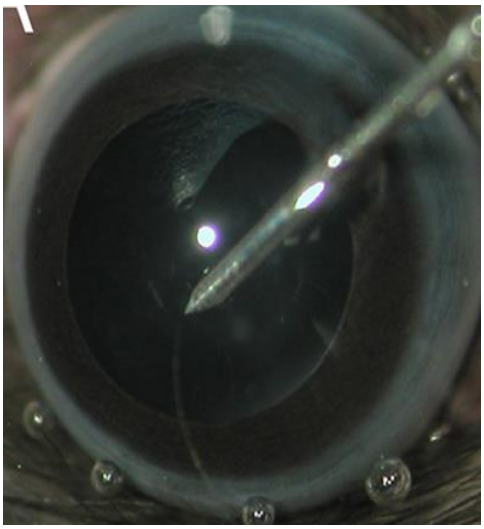

Figure 2.1 Image showing Intracameral microbead injection (Bogner et al., 2015) (reproduced with permission).

2.4 Drugs, reagents and equipment list

2.4.1 Drugs and instruments for animal experiments and electrophysiology: Ketamine 100 mg/ml (Ketamil, Troy Laboratories); Medetomidine 1 mg/ml (Domitor, Pfizer); Atipamazole hydrochlorine 5 mg/ml (Antisedan, Pfizer); Cephazolin sodium (Hospira); Carprofen 50mg/ml (Norbrook); Tropicamide 1.0% (Mydriacyl, Alcon); Proparacaine hydrochloride 0.5% (Alcaine, Alcon); Dexamethasone 0.1% (Maxidex, Alcon); Ciprofloxacin hydrochloride 0.3% (Ciloxan, Alcon Laboratories, NSW, Australia); 0.3% Tobramycin (3mg/ml, Tobrex, Alcon); glutamate, bexarotene and retinoic acid (Sigma); $A\beta_{1\text{-}42}$ (Life Technologies, Australia); fluorescent polystyrene microspheres (FluoSpheres,Invitrogen); DMSO (Sigma)**;** Homoeothermic blanket system (Harvard Apparatus); Goldring corneal electrode (3103RC, Roland Consult, Brandenburg, Germany); Hand-held multi-species electroretinograph (HMsERG) (OcuScience); ERG

viewer software (OcuScience); Hamilton syringe (Hamilton); TonoLab tonometer (Icare Tonovet, Helsinki, Finland).

2.4.2 Reagents and equipments for histological studies: Paraformaldehyde (Sigma); Automatic tissue processor (ASP200S, Leica); Rotary microtome (Microm); Tissue Tek TEC tissue embedding console (Sakura Finetek); Cryostat (CM1950, Leica); Tissue Tek OCT cryostat embedding medium (Sakura Finetek); Hematoxylin (Sigma); eosin (Sigma); Silver nitrate (Sigma); Normal horse serum (Sigma); Vectashield HardSet mounting medium (Vector Laboratories); Axio Imager Z1 fluorescence microscope (Zeiss).

2.4.3 Antibodies: Primary antibodies anti-RXR α (5388S), anti-RXR β (8715S) and anti-RXR γ (5629S) antibodies were purchased from cell signalling technology. Anti-TrkB (sc20542), anti-GADD-153 (sc-7351), anti-p-PERK (sc-3257) antibodies were obtained from Santa Cruz Biotechnology, CA, USA. Anti-pTrkBY^{515} (ab51187), anti-beta III tubulin (ab78078), anti-NeuN (ab104225) were obtained from Abcam, VIC, Australia. β-actin antibody (AC-40), bexarotene (SML0282) and retinoic acid (R2625) were obtained from Sigma, USA. Alexa-Fluor 488 goat anti-rabbit IgG, Alexa-Fluor 555 goat anti-mouse IgG, Alexa-Fluor 594 goat anti-mouse IgG and $A\beta_{1-42}$ were used from Life Technologies, Australia.

2.4.4 Cell culture: The SH-SY5Y neuronal cells was obtained from American type culture collection (ATCC, VA, USA). Neurobasal-A media (Life Technologies); B-27 supplement (Life Technologies); 7,8-Dihydroxyflavone (7,8 DHF) was purchased from

Tocris Bioscience, UK. Cyclotraxin-B (CTX-B) was procured from Life Research Ltd, Australia. Dulbecco's modified Eagle's medium (DMEM) and Fetal bovine serum (FBS) from Life Technologies. Poly-D-lysine, Trypan blue dye, Neubauer micro-chamber were purchased from Sigma-Aldrich, St. Louis, MO, USA. Dapi from Molecular Probes and cell counter from Wertheim, Germany. All other analytical grade chemicals and reagents purchased from either from Sigma (St. Louis, MO, USA) or Invitrogen (Carlsbad, CA, USA).

2.5 Electroretinographic recordings

To assess the functional changes of RGCs, ERG recordings were done at the initial point to get the baseline and at the final time point after 7 days in glutamate model and after 2 months in microbead model. Animals were dark-adapted overnight and anaesthetized as described earlier. The body temperature of animals were maintained at 37°C from the start of experiment till complete recovery of the animal. A total of three electrodes were used for ERG recordings: 1) Reference electrode-placed in the forehead of the animal 2) Ground electrode-placed in the tail of the animal. Both these electrodes were placed subcutaneously. 3) Recording electrode (solid gold ring) - placed on the surface of each eye contacting cornea. All ERGs recordings were done using a flash intensity of 3 log cd·s/m^2 (Ocusciences, Xenotec, Inc., MO, USA. The measurements were done from baseline to the a-wave trough and from the a-wave trough to the peak of b-wave for a-wave and b-wave amplitudes respectively. On the other hand, for positive scotopic threshold responses (pSTRs) dim stimulation (–3.4 log cd·s/m^2) was delivered 30 times

(frequency of 0.5 Hz). For all positive STR responses, measurements were done from baseline to the positive peak observed around 120 ms.

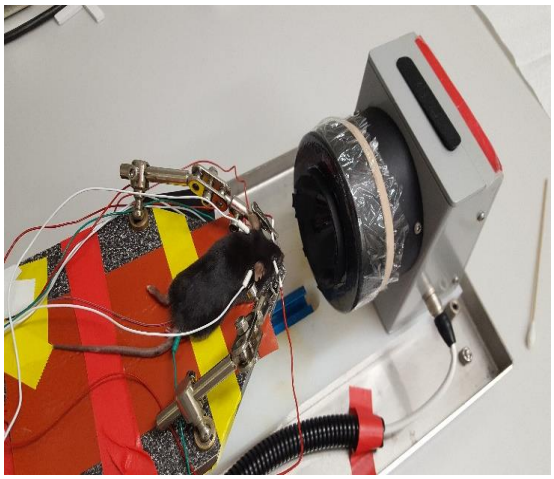

Figure 2.2 Instrument used for visual electrophysiology.

2.6 Tissue fixation, embedding and sectioning

Animals were euthanized with an overdose of intra-peritoneal injection of sodium pentobarbitone (100 mg/kg Lethabarb, Virbac Pty, Australia) and then perfused transcardially with 4% paraformaldehyde (PFA, Sigma). Tissues (eyes, optic nerve and brain) were harvested for morphometric and immunofluorescent studies. For morphometric analysis, the eyes were fixed for 2 hours in 4% PFA and then incubated in 70% ethanol overnight at 4°C. Eyeballs were placed in embedding cassette and processed *via* automatic tissue processor (ASP200S, Leica). Eyes were subsequently embedded in molten paraffin wax. Using a rotator microtome, 7 µm thick paraffin embedded sections involving the whole retina as well as the optic disc, were cut from the vertical meridian of each eye and mounted onto Superfrost Plus slides (Menzel-Glaser Lomb). For immunofluorescent study, eye, optic nerve and brain tissues were kept in 4% PFA for 1-2 hours at room temperature, followed by three subsequent washings with 1X- PBS. Tissues

were cryopreserved in 30% sucrose solution (in 1x PBS with 0.01% sodium azide) in 4°C until the tissue sank completely. Then after the samples was embedded in OCT cryostat embedding medium and cryosections were made using the cryostat.

2.7 Hematoxylin and Eosin (H&E) staining

H&E staining was performed on paraffin embedded sections after standard procedures of deparaffinization (xylene) and dehydration (graded ethanol, 100%, 95%, 75%, 50%). Sections were then incubated in 0.005% hematoxylin solution for 4 min, followed by 0.1% eosin solution for 1 min.

2.8 Bielschowsky's silver staining

Bielschowsky's silver staining was carried out to evaluate axonal density in the optic nerve. Slides were pre-treated in 10% silver nitrate at 40°C for 15 min, and then incubated in ammonium silver solution for 30 min. Next, sections were placed directly into the developer working solution (0.08% formaldehyde, 0.005% citric acid, 0.005% nitric acid and 1% concentrated ammonium hydroxide) for 30 sec, followed by incubation in 5% sodium thiosulfate solution for 5 min.

2.9 Immunofluorescence

Then after the samples were embedded in OCT cryostat embedding medium and cryosections were made using a cryostat (Gupta et al., 2016). Tissue sections were permeabilized in 0.1 % Triton X-100 in PBS (You et al., 2014). This was followed by incubating the sections with the appropriate primary antibodies overnight at 4°C. Further, slides were incubated with either of the secondary antibodies for 1 h at room temperature

followed by extensive washing and mounting using anti-fade mounting media with DAPI. Cells were similarly fixed for 10 min, permeabilised and treated with respective primary and secondary antibodies. Images were acquired using a Zeiss fluorescence microscope (Rajala et al., 2013).

2.10 Protein extraction

The cells or tissues were washed with cold phosphate buffered saline (PBS). After washing with PBS the cells or tissues were lysed in cell lysis buffer (20Mm HEPES, pH 7.4, 1%Triton-x-100, 2mM EDTA) containing protease inhibitor cocktail and sonicated. Following incubation for 30 minutes on ice the lysates were clarified by spinning for 10 minutes at 12,000 RPM at 4°C.The supernatant containing protein mix was transferred to fresh tube and stored at -80°C. The protein concentration was determined using the BCA protein assay kit.

2.11 Western blotting

The tissues or cell lysates were resolved by 10% SDS–PAGE and transferred to PVDF (polyvinylidene difluoride membrane). Following protein transfer, the membrane was washed with TTBS [20 mM Tris–HCl (pH 7.4), 100 mM NaCl, and 0.1% Tween 20] and blocked in 5% skimmed milk in TTBS for 1 h at 25°C. The membranes were then incubated with primary antibody solution anti-RXRα (1:1000), anti-RXRβ (1:1000), anti-RXRγ (1:1000), anti-GADD 153 (1:1200), anti-p-PERK (1:200), anti-TrkB (1:1000), anti-pTrkB Y515 (1:1000) and anti-β-actin (1:5000) at 4°C overnight and next day after three washes (10 min each) in TBST, immunoblots were further incubated with horseradish peroxidase (HRP)-labelled secondary antibodies for 1 hour at room temperature. The

antibody detection was accomplished with Super signal West Pico Chemiluminescent substrate (Pierce). Signals were detected using an automated luminescent image analyser (ImageQuant LAS 4000; GE Healthcare, UK). The densitometric analysis of the band intensities was performed using the Image J software (NIH, USA). β-actin was used as loading control and relative density of the peaks were calculated in excel spreadsheet after normalizing with β-actin.

Statistical Analysis

Data including fluorescence changes were analysed and graphed using excel and graph Pad Prism software (Graph Pad Software, CA). All values with error bars are presented as mean ±SD for given *n* sizes and compared using one way ANOVA followed by Bonferroni post-hoc test for multiple-comparison and student's *t* test for unpaired data. The significance was set at $p<0.05$.

CHAPTER 3

NEUROPROTECTIVE EFFECTS OF RXR MODULATION IN SH-SY5Y CELLS AGAINST ER STRESS

Data presented in this chapter have been accepted for publication

Yogita Dheer, Nitin Chitranshi, Veer Gupta, Mojdeh Abbasi, Mehdi Mirzaei, Yuyi You, Roger Chung, Stuart L Graham, Vivek Gupta. Bexarotene Modulates Retinoid-X-Receptor Expression and is Protective against Neurotoxic Endoplasmic Reticulum Stress Response and Apoptotic Pathway Activation.

Mol Neurobiol. 2018 Apr 10. doi: 10.1007/s12035-018-1041-9.

Part of this chapter was also presented in ARVO 2016, Seattle, USA

Abstract

Retinoid-x-receptors (RXRs) are the ligand-dependent transcription factors that belong to the family of nuclear receptors that have gained recent research focus as potential targets for neurodegenerative disorders. Bexarotene is an RXR pharmacological agonist that is shown to be neuroprotective through its effects in promoting amyloid beta (Aβ) uptake by the glial cells in the brain. This study aimed to evaluate the dose dependent effects of bexarotene on RXR expression in SH-SY5Y neuroblastoma cells and validate the drug effects in the brain *in vivo*. The protein expression studies were carried out using a combination of various drug treatment paradigms followed by expression analysis using western blotting and immunofluorescence. Our study demonstrated that bexarotene promoted the expression of RXR α, β and γ isoforms at optimal concentrations in the cells and in the mice brain. Interestingly, a decreased RXR expression was identified in Alzheimer's disease mouse model and in the cells that were treated with Aβ. Bexarotene treatment not only rescued the RXR expression loss caused by Aβ treatment ($p<0.05$) but also protected the cells against Aβ induced ER stress ($p<0.05$) and pro-apoptotic BAD protein activation ($p<0.05$). In contrast, higher concentrations of bexarotene upregulated the ER stress proteins and led

to BAD activation. Our study revealed that these downstream neurotoxic effects of higher drug concentrations could be prevented by pharmacological targeting of the TrkB receptor. The ER stress and BAD activation induced by high concentrations of bexarotene was rescued by the TrkB agonist, 7,8 dihydroxyflavone ($p<0.05$) while TrkB inhibitor CTX-B treatment further exacerbated these effects. Together these findings suggest a cross-talk of TrkB signalling with downstream effects of bexarotene toxicity and indicate that therapeutic targeting of RXRs could prevent the Aβ induced molecular neurotoxic effects.

3.1 Introduction

Identifying the novel neurodegenerative disease-modifying pathways remains a primary objective of neurodegeneration research. Alzheimer disease (AD) is one of the prominent neurodegenerative disorders of the central nervous system that has a multifactorial etiology. The disease is associated with aberrant Aβ aggregation and plaque formation along with abnormal tau phosphorylation changes (Goldsworthy and Vallence, 2013). The vast variety of therapeutic approaches that have been developed to treat AD and reduce Aβ levels in the brain have met with little success in the clinical setting (Holmes et al., 2008, Mangialasche et al., 2010, Rosenblum, 2014). Recent research has also highlighted Aβ accumulation in the retina in various neurodegenerative disorders of the eye such as glaucoma and age related macular degeneration (Gupta et al., 2016). Aβ deposition has also been observed in the retina in AD mouse models and human retinal tissues from AD subjects (Gupta et al., 2016, Koronyo-Hamaoui et al., 2011).

ApoE gene polymorphisms and plasma apolipoprotein levels are strongly shown to correlate with the risk associated with development of the sporadic form of AD and as a potential disease biomarker (Gupta et al., 2011). ApoE expression is transcriptionally regulated by heterodimer formation of the retinoid X receptors (RXR) with liver X receptors (LXR) and

peroxisome proliferator-activated receptor gamma (PPARγ) (Lefebvre et al., 2010). RXR also forms heterodimers with vitamin D receptors (VDR) that are critical for the physiological and biochemical actions of vitamin D (Barsony and Prufer, 2002). Vitamin D deficiency has been suggested as a risk factor for late onset AD and its receptor (VDR) as a susceptibility gene for the sporadic form of AD (Wang et al., 2012). RXR heterodimerizes with retinoic acid receptors (RAR) and defects in spatial learning and memory have been identified in mice with mutated RAR/ RXR receptors (Chiang et al., 1998, Wietrzych et al., 2005). Similar to the retinoic acid receptors, three different isotypes of RXRs, RXRα (NR2B1), RXRβ (NR2B2), and RXRγ (NR2B3) have been identified with different tissue-specific expression (Mangelsdorf et al., 1992). Retinoic acid administration was shown to attenuate amyloid accumulation and protect against the memory loss in animal model of AD (Goodman, 2006, Ding et al., 2008, Etchamendy et al., 2003). Therapeutic targeting of RXR as well as its interacting partners LXR and PPARγ using pharmacological ligands was effective in modulating Aβ levels and improved the cognitive function in various experimental models of AD (Mandrekar-Colucci and Landreth, 2011, Cramer et al., 2012). Similarly, upregulation of VDR expression resulted in reduced amyloid precursor protein (APP) transcription in neuroblastoma cells (Wang et al., 2012). Unsaturated fatty acids such as linoleic, linolenic, arachidonic acid and docosahexaenoic acids along with 9-cis retinoic acid are reported as natural ligands for RXRs (Heyman et al., 1992, LaClair et al., 2013).

Retinoid signalling (RA) plays a critical role in synaptic network formation and in the learning and memory development (Lane and Bailey, 2005, Chiang et al., 1998, Mingaud et al., 2008). RXR receptors can stimulate neurotrophin production in cells (Price et al., 2007) and RA treatment of neuroblastoma cells has been shown to induce functional expression of the TrkB receptor (Edsjo et al., 2003, Matsumoto et al., 1995, Lucarelli et al., 1995). TrkB

is essential for neuronal development, protection and plasticity in both central and peripheral nervous system and is known to be a key mediator of learning and memory processes in the brain (Minichiello, 2009). Aβ treatment is shown to induce dysregulation of TrkB receptor expression in neuronal cells (Jeronimo-Santos et al., 2015). Further, TrkB signalling is impaired in AD brains (Peng et al., 2005) and its chronic activation using pharmacological compounds protected against memory loss and BACE1 elevation in a mouse model of AD (Devi and Ohno, 2012, Zhang et al., 2014).

RXR activation using bexarotene which is a synthetic agonist of the RXRs enhanced glial uptake of soluble Aβ in animal brains and decreased its concentrations (Cramer et al., 2012). Other follow up studies on bexarotene effects argued against the level of therapeutic protection conferred by the drug treatment on memory preservation, changes in Aβ levels and cognitive aspects in animal models (LaClair et al., 2013, Ulrich et al., 2013). Bexarotene is essentially an anti-neoplastic agent (Boehm et al., 1995) which was primarily approved as a drug for cutaneous T-cell lymphoma management (Gniadecki et al., 2007). Recent findings however indicate that apart from its effects on Aβ clearance as mentioned above, bexarotene also exhibits beneficial effects in Parkinson's disease (McFarland et al., 2013) and in Amyotrophic lateral sclerosis mice models (Riancho et al., 2015).

The present study investigated the differential effects of bexarotene on various RXRs in neuroblastoma SH-SY5Y cells and in the brain. The molecular effects of drug treatment on endoplasmic reticulum (ER) stress response elucidation and its cross talk with TrkB modulation were also studied, with a view to determining potential therapeutic effects of modulating RXRs.

3.2 Materials and Methods

3.2.1 Chemicals

SH-SY5Y cell line was obtained from American type culture collection (ATCC, VA, USA). 7,8 Dihydroxyflavone (7,8 DHF) was purchased from Tocris Bioscience, UK. Primary antibodies RXR (α, β, γ) antibodies were purchased from Cell Signalling Technology. TrkB antibody, ER stress antibodies (GADD 153 and p-PERK) were obtained from Santa Cruz, Biotechnology. pTrkB Y^{515} antibody was obtained from Abcam. β-actin antibody, bexarotene and retinoic acid were obtained from Sigma, USA. Cyclotraxin-B (CTX-B) was procured from Life Research Ltd, Australia. Alexa Fluor 488 secondary antibody, $A\beta_{1-42,}$ Dulbecco's modified Eagle's medium (DMEM) and Foetal bovine Serum (FBS) were obtained from Life Technologies, Australia. DAPI, Bicinchoninic acid assay (BCA) protein detection kit and Super signal West Pico Chemiluminescent substrate were obtained from Pierce, Rockford, USA. All other reagents were of analytical grade purchased from Sigma or Invitrogen.

3.2.2 Animals

Male C57BL/6 mice were purchased from Animal research centre, Perth and APP-PS1 mice tissues were obtained from University of Tasmania, Australia. All animal experiments were approved by the Institutional Animal Ethics Committee (AEC) of Macquarie University and followed the Australian code of practice for the care and use of laboratory animals. All animals were housed in cages under standard conditions, 12 h light/dark cycle, 22 °C, 35% relative humidity with *ad libitum* access to water and food. Bexarotene was administered 100 mg/kg per os to C57BL/6 mice for seven days daily in drug treatment groups.

3.2.3 Cell culture and treatment

The human neuroblastoma SH-SY5Y cell line were cultured in DMEM supplemented with 1% (v/v) penicillin/streptomycin (antibiotics, Invitrogen) and 10% (v/v) foetal bovine serum in a humidified atmosphere containing 5% (v/v) CO2 at 37°C. Cells were plated 2.0 × 10^5/cm^2cells into 6-well plates and maintained in growing medium. Briefly, SH-SY5Y cells were grown to 80% confluency. Cells were pre-differentiated with 10 μM *all-trans* retinoic acid for 2 days. Medium was changed into retinoic acid medium without antibiotics for 48 h. Following 48 h of retinoic acid treatment, cells were exposed to different concentrations of bexarotene (0.001, 0.01, 0.1,1, 5 and 10 μM) for 12 h to study the effect of drug. The pre-differentiation of the neuroblastoma SH-SY5Y cells with retinoic acid was done in both control and experimental group.Therefore the corresponding change in bexarotene treated group was not due to the effect of retinoic acid. Bexarotene was dissolved in dimethylsulfoxide (DMSO), which was used as control/ vehicle with final concentration below 0.05%. Treated cells were studied using cell survival assay, immunoblotting, and immunofluorescence measurement. For another set of experiments, the cells were treated with TrkB receptor agonist, 7,8DHF (100nM, 12h) and a cyclic peptide CTX-B, which is a TrkB antagonist (5 μM, 12 h) while for treatment group, cells were treated with bexarotene (5 and 10 μM) along with TrkB receptor agonist and antagonist. Subsequently, cells were harvested, lysed and the cell lysates subjected to western blotting. For the amyloid beta treatment experiments, the cells were pre-treated with 5 μM $A\beta_{1\text{-}42}$ oligomer for 4h and then with optimal concentrations of bexarotene (0.1 and 1 μM) for 12 h while control cells were treated with 5μM $A\beta_{1\text{-}42}$ peptide for 4h alone.

3.2.4 Measurement of *in vitro* cell viability

Cell viability was measured using trypan blue vital dye exclusion assay (Strober, 2015). After 12 h drug treatment, the cells were harvested from plate using PBS washing followed by trypsinization. Then 10 µL of trypsinized and re-suspended cells were mixed with 10 µL of 0.4% solution of Trypan blue dye (Sigma-Aldrich) for 1 min. Cell counter (Wertheim, Germany) was used to evaluate cell density using a Neubauer micro-chamber (Sigma-Aldrich).

3.2.5 Protein extraction

The method of protein extraction was described previously in chapter 2, section 2.10.

3.2.6 Western blotting

Cell lysates containing 40 µg of protein were resolved by 10% SDS–PAGE and transferred to PVDF (polyvinylidene difluoride membrane). Following protein transfer, the membrane was washed with TTBS and blocked in 5% skimmed milk in TTBS for 1 h at 25°C. The membranes were then incubated with primary antibody solution anti-RXRα (1:1000), anti-RXRβ (1:1000), anti-RXRγ (1:1000), anti-GADD 153 (1:1200), anti-p-PERK (1:200), anti-TrkB (1:1000), anti-pTrkB Y^{515} (1:1000) and anti-β-actin (1:5000) at 4°C overnight. Further detailed procedure was discussed already in chapter 2, section 2.11.

3.2.7 Immunofluorescence

The SH-SY5Y cells were treated with different concentrations of drugs for various time points as indicated. Afterwards the cells were fixed with 4% formaldehyde for 15 min, rinsed three times in 1x PBS for 5 minutes each. For brain sections, animals were euthanized with an overdose of anaesthetics and then perfused transcardially with 4% PFA. Brains were harvested and fixed in 4% PFA overnight. Following fixation in 4% PFA, the brains were washed with PBS, incubated in 30% sucrose and embedded in OCT cryostat embedding medium. Brain sections were prepared using a cryostat. Then cells /brain sections were incubated with blocking buffer (1x PBS / 5% normal serum / 0.3% Triton X-100) for 60 min and incubated with appropriate primary antibodies anti- RXR α, anti-RXR β and anti-RXRγ at 4 °C overnight. Primary antibodies were diluted in antibody dilution buffer (1x PBS/ 1% BSA/ 0.3% Triton X-100). Cells were washed in PBS and then incubated with fluoro chrome-conjugated secondary antibody: Alexa Fluor-488 conjugated anti-rabbit (1:400) diluted in antibody dilution buffer for 2 h at room temperature in the dark. Finally, slides were mounted using prolong diamond antifade reagent containing DAPI. The images were captured with a Zeiss microscope. The level of fluorescence in a given region (e.g. nucleus) was measured using Image J. The values were then spread into excel work sheet and plotted.

3.2.8 Statistical Analysis

Data including fluorescence changes were analysed and graphed using excel and graph Pad Prism software (Graph Pad Software, CA). All values with error bars are presented as mean ±SD for given n sizes and compared using one way ANOVA followed by Bonferroni post-hoc test for multiple-comparison and student's t test for unpaired data.. The significance was set at $p<0.05$.

3.3 Results

3.3.1 Bexarotene induced modulation of RXR expression

The effects of different concentrations of bexarotene on cell viability of SH-SY5Y neuroblastoma cells was investigated by treating the cells with increasing concentrations of drug from 0.001 to 10 µM. Drug induced cytotoxicity and cell death was observed at higher concentrations of 5 (98.64±7.61 to 80.08±7.69 %) and 10µM (98.64±7.61% to 76.89.29±8.79 % (Figure 3.1). The effects of bexarotene treatment (12 h) on RXR expression modulation was evaluated across different concentrations ranging from 0.001-10µM using western blotting and immunofluorescence approaches. RXRα and γ isoform expression was significantly elevated at 0.1 µM while RXRβ isoform also demonstrated an enhanced expression in this range with peak expression levels at 1µM bexarotene concentration. β-actin was used as an internal control and the expression changes were evaluated using densitometric quantification for comparison (*$p<0.05$) (Figure 3.2 A-D). Effects of bexarotene treatment (0-10µM) on RXR expression and protein localisation were further evaluated using immunofluorescence staining in the cells. Expression of all the three RXR isoforms was found to be upregulated in response to drug treatment showing maximum expression of RXRα and γ isoform at 0.1 µM and RXRβ isoform at 1 µM (Figure 3.3). The effects of bexarotene on RXR expression were further investigated *in vivo* in the mice brains that were administered the drug orally for 7 days and compared with the control animal tissues. In accordance with our observations in neuroblastoma cells, an increased expression of the RXR isoforms was also identified in the mice brain (Figure 3.4 A-C). These results indicated that the bexarotene which is an RXR agonist induced expression changes in various isoforms of the receptor in the neuronal cells in culture as well as the brain *in vivo* (Figure 3.3 and 3.4).

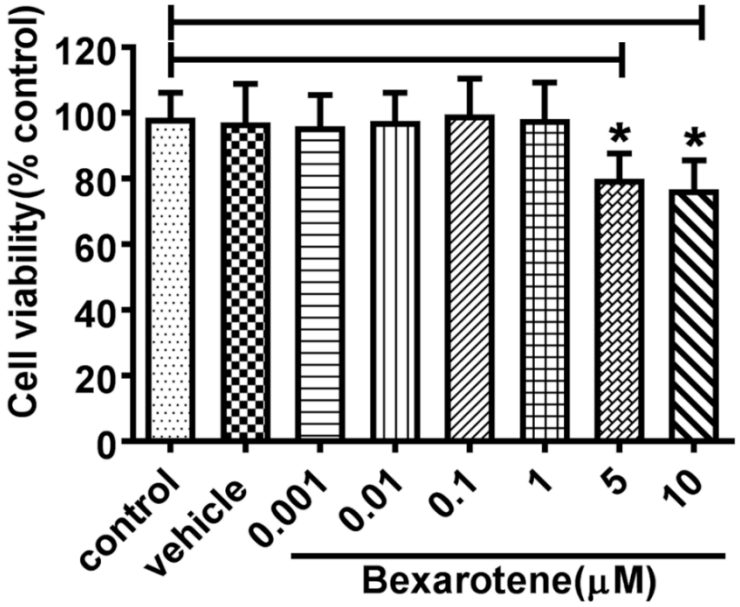

Figure 3.1 Dose-dependent effects of bexarotene on SH-SY5Y cell-viability. SH-SY5Y cells were treated with (or without) varying concentrations of bexarotene starting from 0.001 to 10 μM for 12 h. Cell viability after bexarotene treatment was measured by Trypan blue exclusion assay. Values are the means ± SD of of three independent experiments; *$p<0.05$ versus control as indicated by Student-t test.

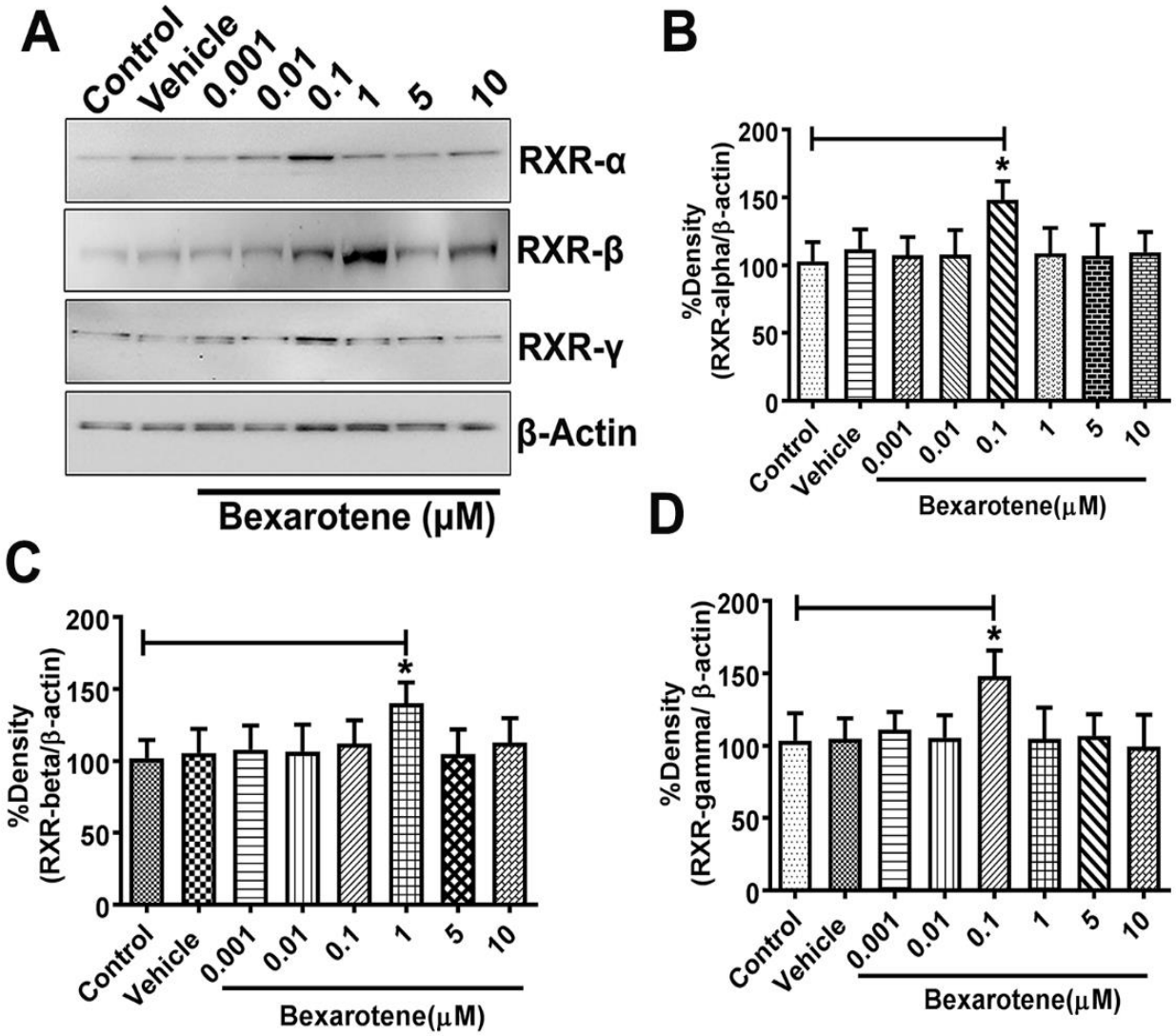

Figure 3.2 Immunoblot analysis of RXR (α, β and γ) protein expression in SH-SY5Y cells following bexarotene treatment. A) SH-SY5Y cells were treated with bexarotene (0.001-10 μM) for 12h. After exposure to different concentrations of bexarotene, the expression of RXRs (α, β and γ) was detected by western blotting. The equivalent loading of proteins in each well was confirmed by probing with β-actin antibody. B-D) Densitometric quantification of immunoblots relative to β-actin shows significant changes at 0.1 μM for RXR α and γ isoforms while for RXR β, significant changes were observed at 1 μM concentration. Data represent mean ±SD; n=3; (*$p<0.05$, student's t test) (*$p< 0.05$, one way ANOVA followed by Bonferroni post-hoc test).

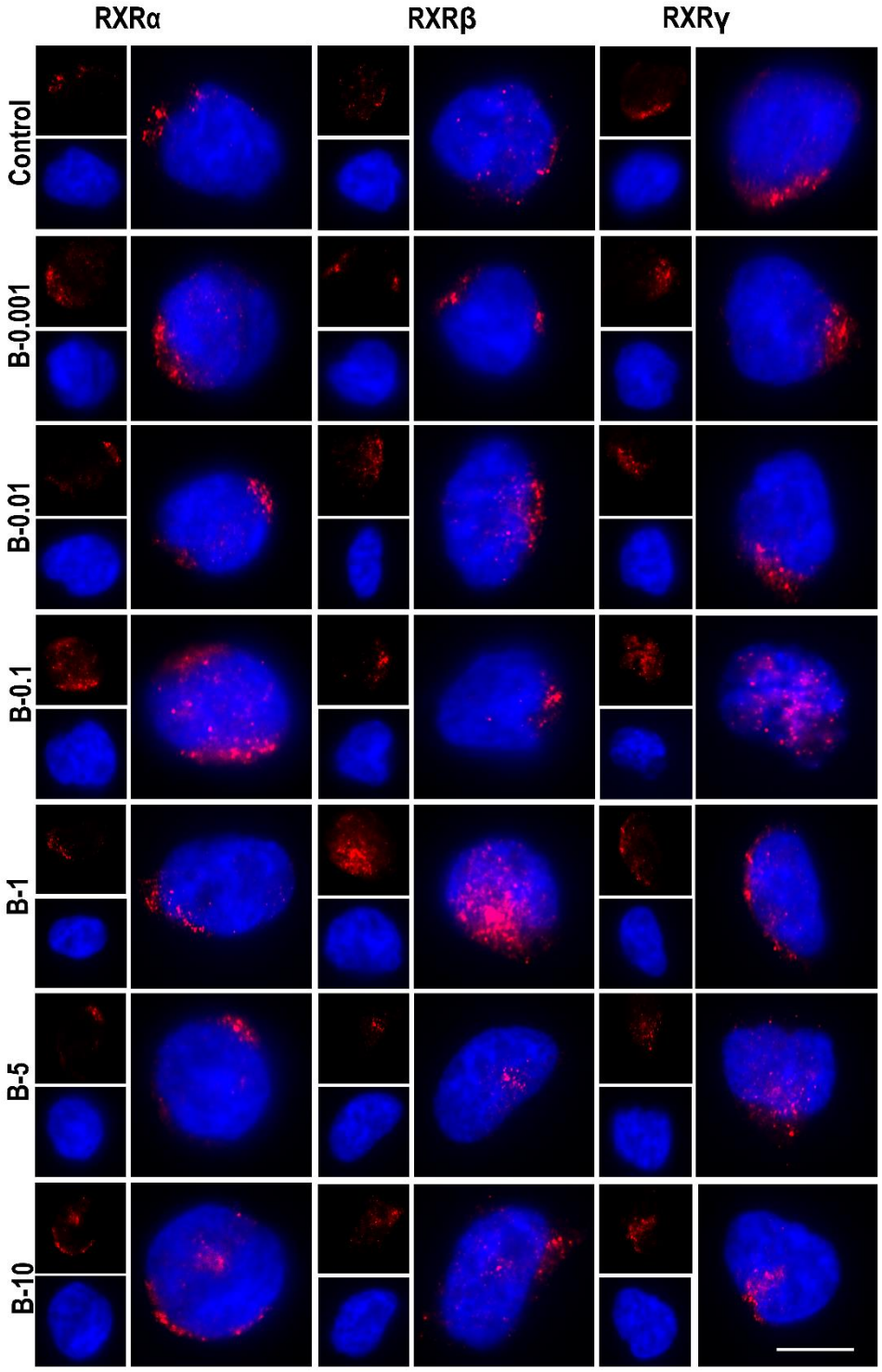

Figure 3.3 Immunofluorescence staining of Bexarotene treated SH-SY5Y cells for RXR (α, β and γ) expression. SH-SY5Y cells were grown on coverslips and treated with different concentrations of bexarotene ranging from 0.001 to10 μM for 12 h as indicated. After 12 h, the cells were fixed and immunostained with

anti-RXR (α, β and γ) followed by Alexa Flour 488 secondary antibody to detect RXR α, β and γ expression (red) (pseudo coloured). Nuclei were stained with DAPI (blue). Scale bar =10µm.

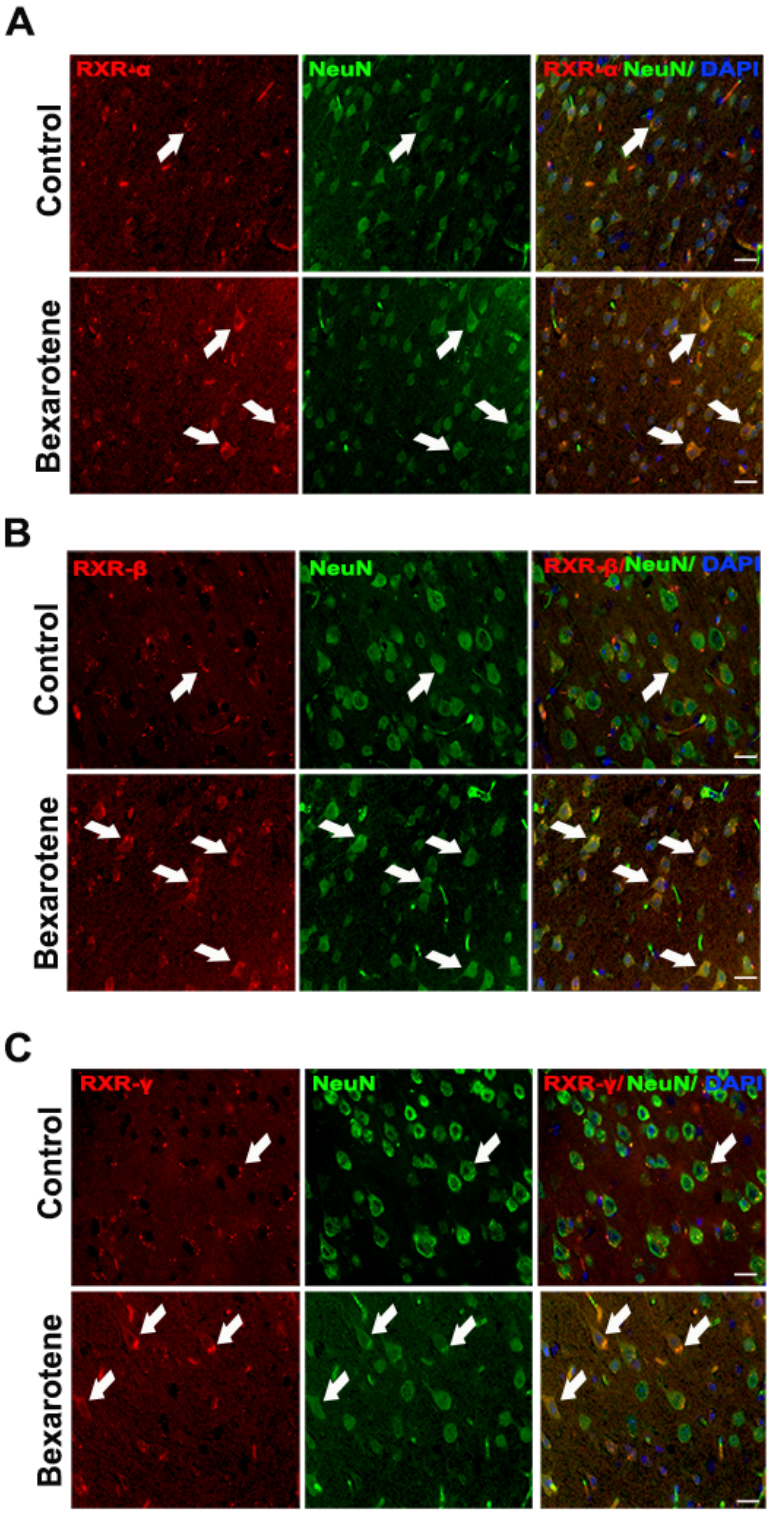

Figure 3.4 Bexarotene treatment upregulates RXR(α, β and γ) expression in the brain. The mice brain sections were fixed and immunostained with anti-RXR (α, β and γ) antibodies followed by Alexa Flour 488 secondary antibody to detect RXR α, β and γ (red) (pseudo coloured). Nuclei were stained with DAPI (blue). Scale bar=50μm. Brain sections from bexarotene treated mice showed enhanced expression of RXR receptors as compared to control mice brains as indicated by white arrows.

3.3.2 Reduced RXR expression in the brain of mouse model of Alzheimer's disease

Bexarotene has previously been shown to modulate the AD pathology in mouse models in various studies. However, whether the drug induces any changes in the expression of its pharmacological target RXR receptors is not known. In this study, we investigated RXR expression changes in the brains of aged APP/PS1 mouse model. The expression of all the three isoforms of RXR was found to be much reduced in the brain tissue lysates as demonstrated by immunoblotting using isoform specific antibodies (Figure 3.5A-D). Actin was used as internal control. The results were also evaluated using immunofluorescence staining in the APP/PS1 mice brain sections using RXR α, β and γ specific antibodies and the results demonstrate a reduced expression of each of these isoforms in the brain in the AD mouse model (Figure 3.6).

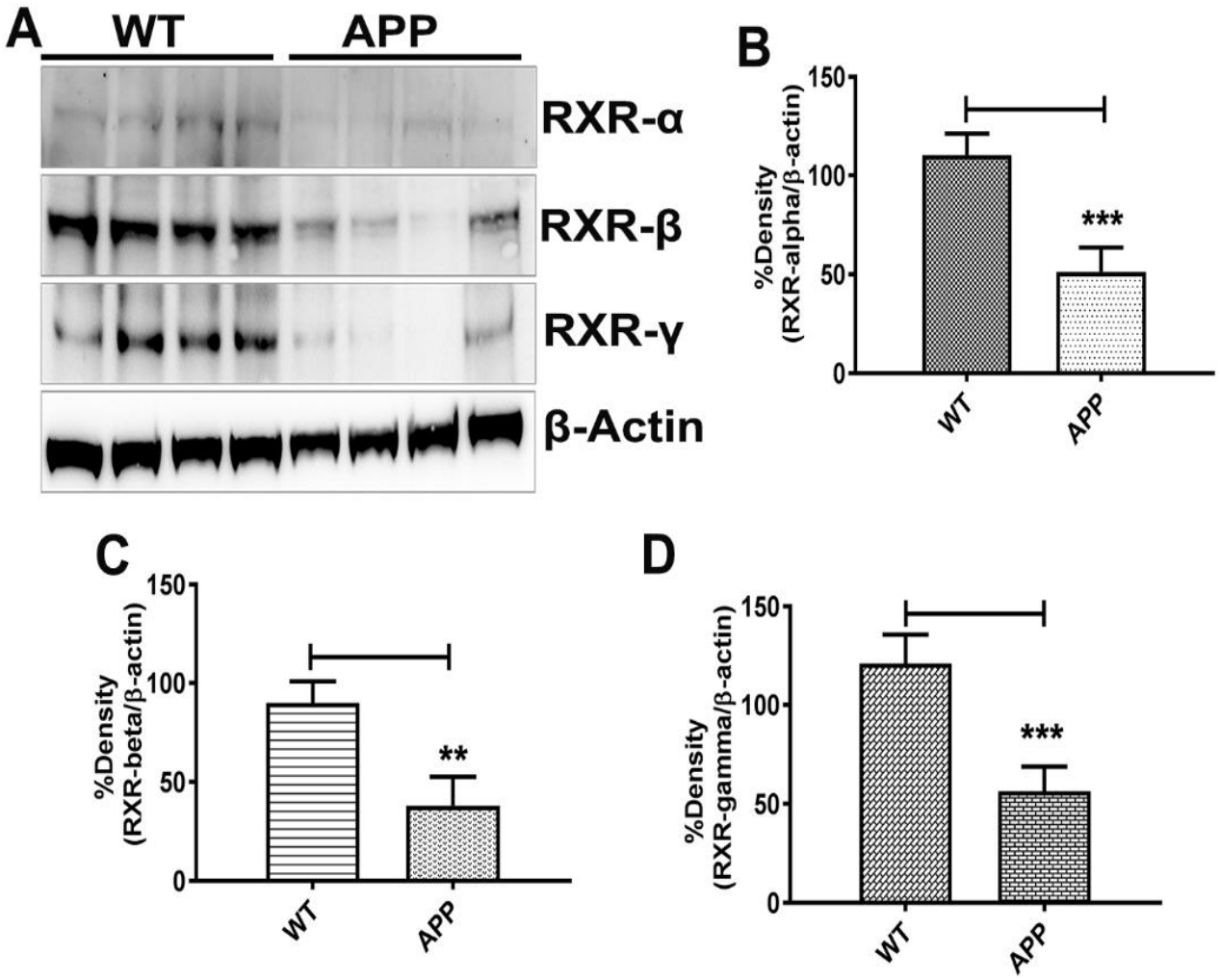

Figure 3.5 Immunoblotting analysis of RXR (α, β and γ) expression in APP/PS1 mice brains. A) The expression of RXRs (α, β and γ) in WT type and APP/PS1 mice brain lysates was investigated by western blotting. The equivalent loading of proteins in each well was confirmed by probing with β-actin. B-D) Densitometric quantification of immunoblots relative to β-actin shows significantly higher expression of RXRs in WT type mouse brain lysates as compared to APP/PS1 mice brain samples. Data represent mean ±SD ; n=3; (**p<0.05, ***p<0.001, student's t test)

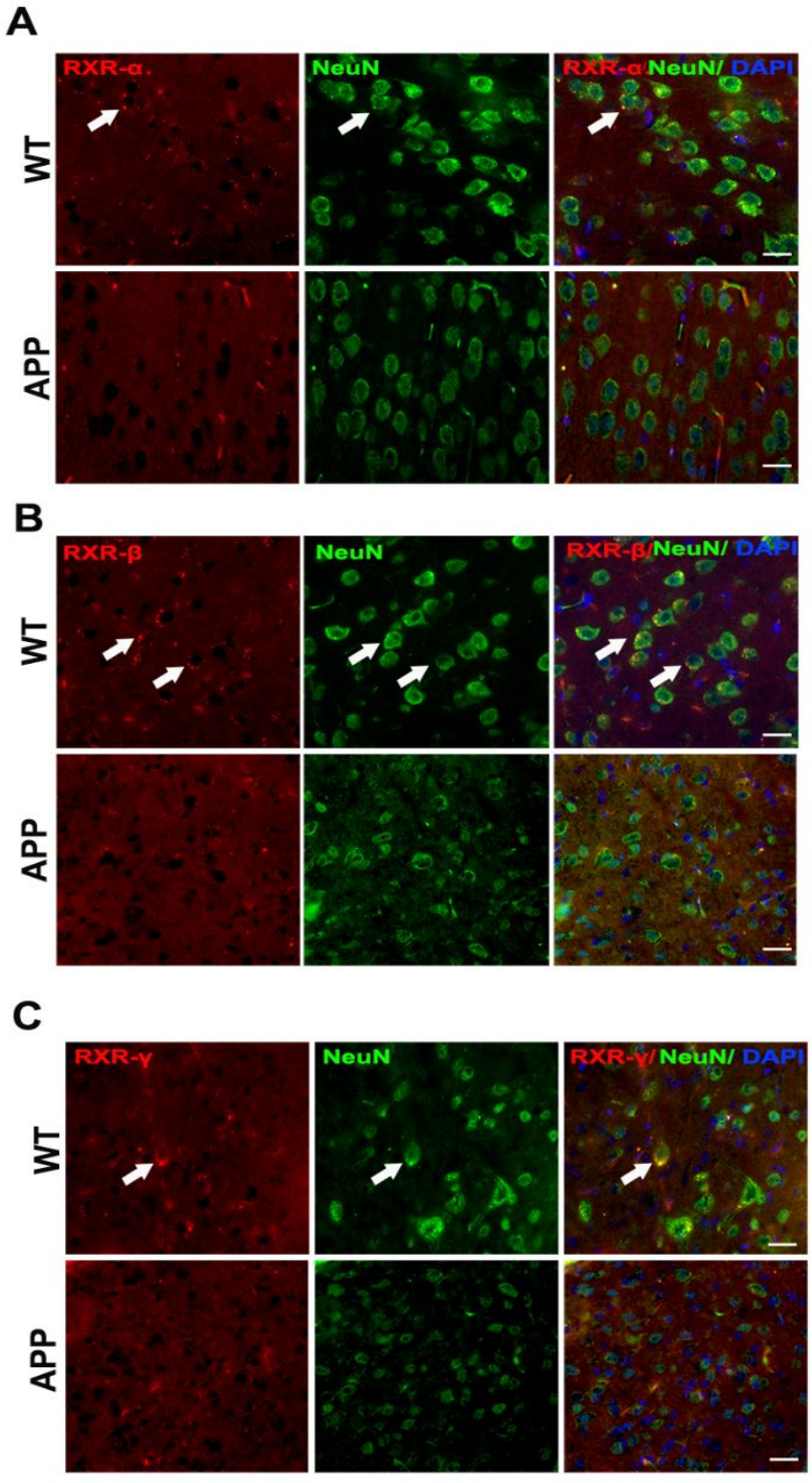

Figure 3.6 Immunofluorescence staining revealed reduced RXR (α, β and γ) staining in APP/PS1 mice brains. The WT and APP/PS1 mice brain sections were fixed and immunostained with anti-RXR (α, β and γ) antibodies followed by incubating with Alexa Flour 488 secondary antibody to detect RXR A) α B) β and C) γ expression. Nuclei were stained with DAPI (blue). Scale bar =50µm. APP/PS1 mice brain sections showed relatively less RXR immunoreactivity when compared to WT mice as indicated by white arrows.

3.3.3 Aβ induced RXR suppression is rescued by bexarotene treatment

We sought to understand whether the loss of RXR expression in brains of APP/PS1 mice was associated with increased Aβ levels and tested this hypothesis using Aβ treated SH-SY5Y cells in culture. Briefly, the cells were treated with $A\beta_{1-42}$ (5μM) for 4 hours and the effects on RXR expression evaluated using immunoblotting for α, β, and γ isoforms of RXR expression using specific antibodies. Densitometric quantification of the westerns revealed a significant reduction in the RXR expression upon Aβ treatment (RXRα: *$p<0.05$; RXRβ: *$p<0.05$) (Figure 3.7A-F)

As bexarotene was observed to upregulate the RXR expression (Figure 3.2), we investigated whether the drug could modulate Aβ induced effects on RXR expression changes. The cells were treated with optimal concentrations of bexarotene (0.1 and 1μM) after they were pre-treated with $A\beta_{1-42}$ peptide and it was observed that the loss of RXR expression caused by Aβ treatment was significantly alleviated upon drug treatment. Densitometric quantification of immunoblots was carried out for expression comparison and actin was used as the loading control in each case (RXRα, RXRβ and RXRγ: $p<0.05$) (Figure 3.7A-F).

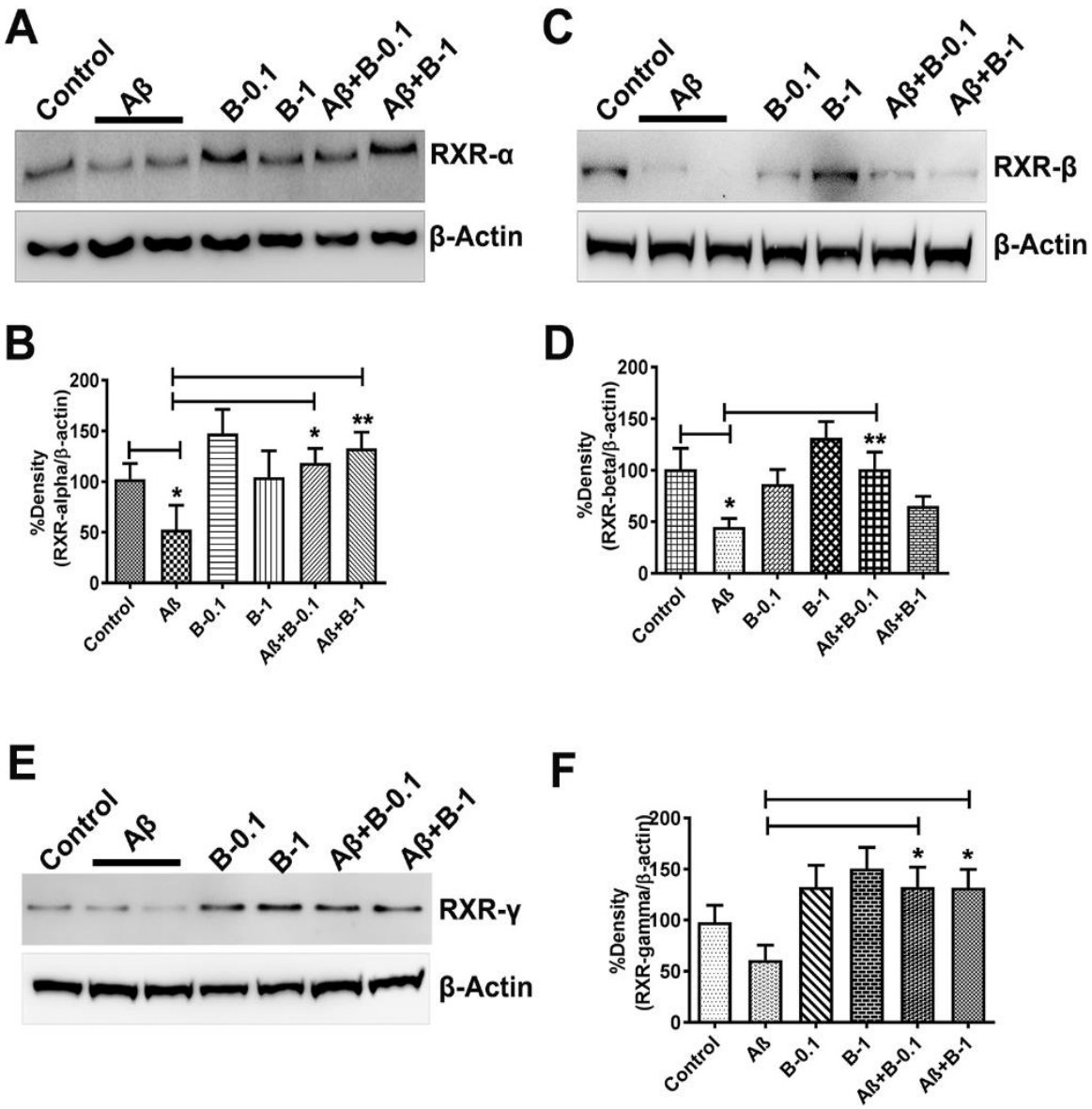

Figure 3.7 Amyloid beta treatment suppressed RXR expression and the impact of bexarotene treatment. SH-SY5Y cells were incubated with amyloid beta peptide for 4 h at concentration of 5μM before addition of RXR receptor agonist bexarotene (0.1 and 1μM). A, C and E) Protein levels of RXR in amyloid beta treated cells were evaluated by Western blotting. The equivalent loading of proteins in each well was confirmed by β-actin. B, D and F) Densitometric quantification indicated that bexarotene treatment significantly protected against RXR expression loss induced by amyloid beta. Data represent mean ± SD from 3 independent experiments; $p<0.05$, student's t test) (**$p< 0.05$ (RXRα), **$p< 0.05$ (RXRβ), *$p< 0.05$(RXRγ) ,one way ANOVA followed by Bonferroni post-hoc test).

3.3.4 Bexarotene protected against Aβ induced ER stress response and BAD activation

Aβ has previously been shown to induce ER stress response in AD (Cornejo and Hetz, 2013, Fonseca et al., 2013). In this study, we identified that Aβ treatment resulted in enhanced GADD153 (***$p<0.001$) and p-PERK (*$p<0.05$) expression in SH-SY5Y cells. PERK is an ER transmembrane protein which undergoes autophosphorylation during early stages of ER stress (Liao et al., 2013) and is a key sensor of unfolded protein response (UPR). GADD153, also known as C/EBP homologous protein (CHOP), has an important role as an ER stress- induced cell death modulator (Oyadomari and Mori, 2003). The effects of bexarotene on Aβ induced ER stress markers GADD153 and p-PERK were investigated using immunoblotting. The cells were treated with bexarotene (12 h) after they were pre-treated with Aβ (5 μM). Significant reduction in both GADD153 and p-PERK expression was observed when the cells were treated with either 0.1 (GADD153: **$p<0.05$; p-PERK: *$p<0.05$) or 1 μM (GADD153: **$p<0.05$; p-PERK: *$p<0.05$) bexarotene. The upregulated expression of pro-apoptotic proteins is one of the major mechanisms for the cell death process. Therefore, expression changes in pro-apoptotic member of the Bcl-2 gene family i.e. Bcl-2-associated death promoter (BAD) protein which is involved in processes that favour apoptosis were studied. Enhanced ER stress caused by Aβ was associated with upregulation of apoptotic protein BAD expression in cells (****$p<0.001$) and bexarotene treatment resulted in significant reduction in BAD protein expression (0.1μM: *$p<0.05$; 1μM: *$p<0.05$). The immunoblots of cellular lysates were quantified and data plotted with actin as internal control (Figure 3.8A-E).

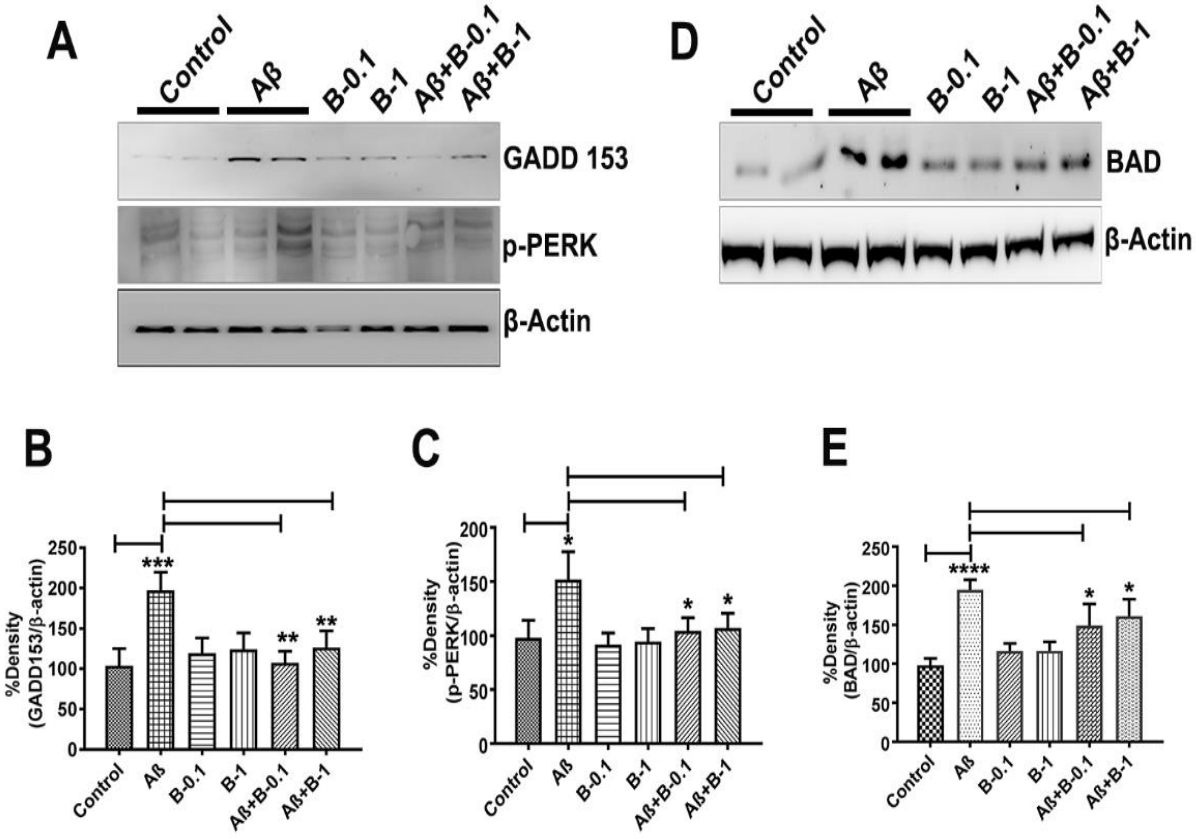

Figure 3.8 Bexarotene protected against amyloid beta induced ER stress induction and BAD upregulation. SH-SY5Y cells were pretreated with amyloid beta peptide for 4 h (5µM) followed by bexarotene treatment. A and D) Levels of GADD 153, p-PERK and BAD proteins were determined by western blot analysis. β-actin was used as an internal control. B,C and E) Densitometry analysis showed that expression of GADD 153, p-PERK and BAD significantly decreased after bexarotene treatment. Data represent mean ± SD; n=3; (*p,**p<0.05, ***p, ****p<0.001, student's t test) (****p< 0.0001 (Aß vs. Aß+B-0.1), *** p< 0.001 (Aß vs. Aß+B-1) (GAD 153), **p< 0.05 (p-PERK), *p< 0.05 (BAD), one way ANOVA followed by Bonferroni post-hoc test).

3.3.5 High concentration of bexarotene mediated ER stress and BAD response in neuroblastoma cells

As bexarotene is an anti-neoplastic agent that exerts cytotoxic effects in a concentration dependent manner (Budgin et al., 2005, Zhang et al., 2002), we sought to investigate the dose dependent effects of bexarotene on the ER stress markers GADD153 and p-PERK expression in neuroblastoma cells. Cell lysates were subjected to immunoblotting and densitometric quantification suggested an increased expression of these markers implying elevated ER stress at higher drug concentrations (5 µM, GADD153: *$p<0.05$; p-PERK: *$p<0.05$) (10µM, GADD153: **$p<0.05$; p-PERK: *$p<0.05$) (Figure 3.9A-C). The band intensities were quantified and plotted (Figure 3.9E). In accordance with ER stress induction at high drug concentrations, an upregulated expression of pro-apoptotic BAD protein was also observed in cellular lysates (5µM, **$p<0.05$) (10µM, **$p<0.05$) (Figure 3.9D).

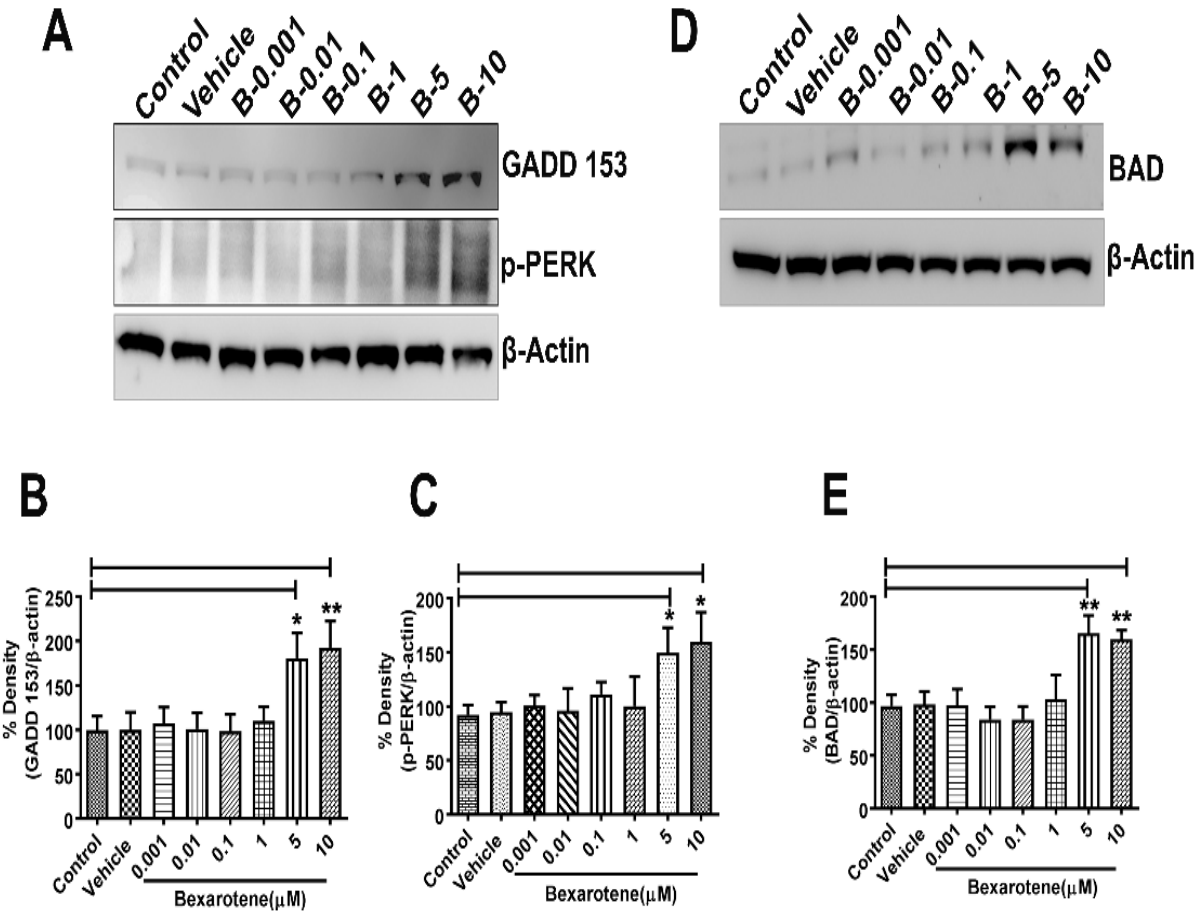

Figure 3.9 Effects of various bexarotene concentrations on ER stress and pro-apoptotic protein BAD expression. A and D) Immunoblotting analysis of SH-SY5Y cells treated with different concentrations of bexarotene against GADD 153, p-PERK (ER stress antibodies) and BAD (pro-apoptotic protein). B,C and E) Densitometry analysis showed that expression of GADD 153, p-PERK and BAD significantly increased at 5 and 10 μM concentrations. Data represent mean ±SD ; n=3; *,**p<0.05, student's t test) (***p< 0.001 (GAD 153), **p< 0.05 (Control vs. 5 μM), *** p< 0.001 (Control vs. 10 μM) (p-PERK), ****p< 0.0001 (Control vs. 5 μM), *** p< 0.001 (Control vs. 10 μM) (BAD), one way ANOVA followed by Bonferroni post-hoc test).

3.3.6 Neurotoxic molecular effects of bexarotene were moderated by pharmacological modulation of TrkB receptor

BDNF/TrkB pathway has previously been shown to suppress ER stress response activation in tunicamycin treated neuroblastoma cells (Chen et al., 2007). TrkB agonist 7,8 dihydroxyflavone was also recently shown to attenuate ER stress activation in HK-2 cells (Ma et al., 2016). We sought to identify whether ER stress induced by high concentrations of bexarotene treatment in SHSY5Y cell is modulated upon pharmacological treatment with TrkB agonist, 7,8 dihydroxyflavone (7,8DHF). Accordingly, the cells pre-treated with bexarotene (5 and 10µM; 12h) were incubated with TrkB agonist 7,8 DHF (100nM; 12 h). Following this treatment paradigm, the cells were harvested, lysed and subjected to immunoblot analysis using specific antibodies against ER stress markers GADD153 and p-PERK. Densitometric quantification indicated that bexarotene treated cells that were also treated with 7,8DHF demonstrated significantly reduced ER stress marker expression compared to the bexarotene treated cells alone (GADD153: bex 5µM, *$p<0.05$; bex 10µM, *$p<0.05$) (p-PERK: bex 5µM, *$p<0.05$; bex 10µM, *$p<0.05$).

Alternatively, we also evaluated potential detrimental effects of TrkB antagonist cyclotraxin-B (CTX-B) on the ER stress response in bexarotene treated cells. An exacerbation of the ER stress markers was identified in the neuroblastoma cells that were treated with CTX-B (5µM, 12 h) subsequent to bexarotene treatment (Figure 3.10 A-C). 7,8 DHF treatment also resulted in reduction in the expression levels of pro-apoptotic protein BAD in neuroblastoma cells after they were treated with high concentrations of bexarotene (bex 5µM, *$p<0.05$; bex 10µM, **$p<0.05$). In contrast, CTX-B treated cells demonstrated elevated BAD protein levels compared to bexarotene treated cells alone (Figure 3.10D-E).

In the control experiments, SHSY5Y cells were treated with 7,8DHF and CTX-B separately. In accordance with previous reports, 7,8DHF resulted in elevated TrkB phosphorylation while CTX-B treatment resulted in significant reduction in pTrkB levels (pTrkB Y^{515} residue) (*$p<0.05$) (Figure 3.11A-B). A significant upregulation of the ER stress protein markers as well as pro-apoptotic protein BAD expression was identifiable upon treatment of the cells with CTX-B. This suggested that loss of TrkB signalling was involved in enhanced ER stress response (GADD 153: **$p<0.05$; p-PERK: ***$p<0.001$) and BAD protein activation (***$p<0.001$) (Figure 3.11C-G). Actin was used as loading control for each sample.

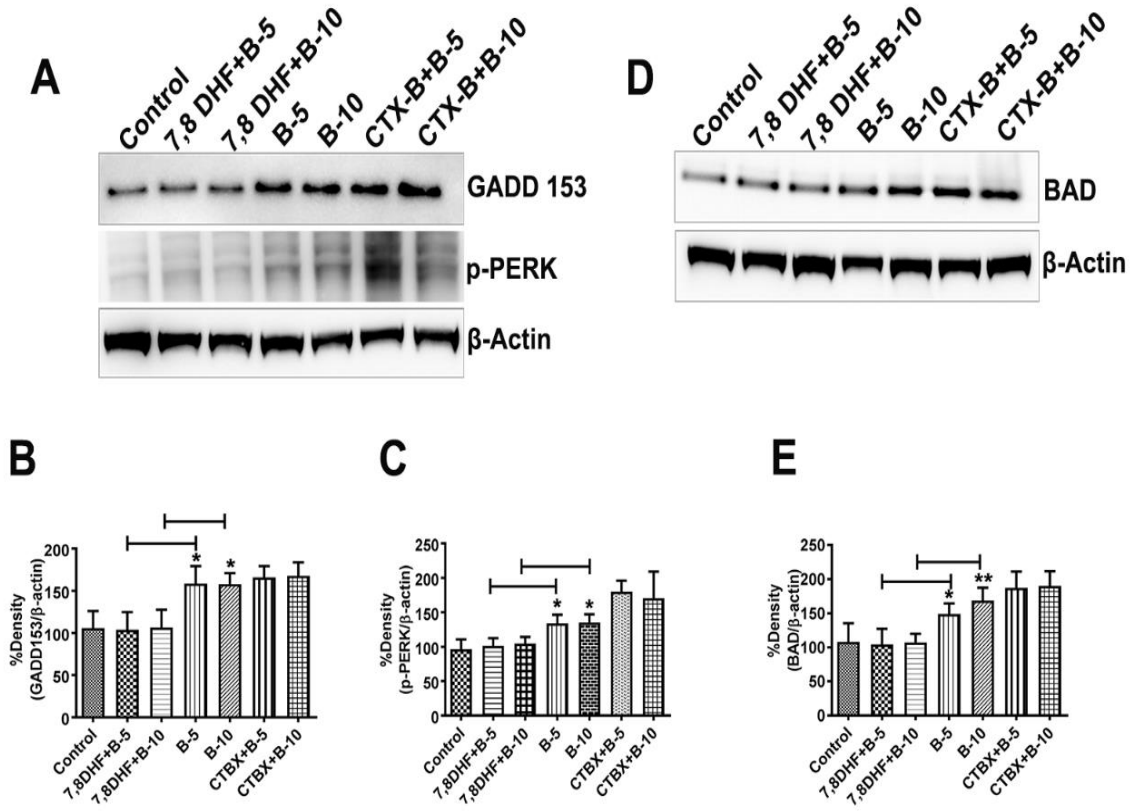

Figure 3.10 ER stress and BAD protein activation caused by bexarotene are moderated by TrkB modulation. A and D) Bexarotene treated cells were subjected to further treatment with either 7,8 DHF or CTX-B and lysates subjected to western blotting. The blots were probed for GADD153, p-PERK and β-actin. B, C and E) Densitometry quantification shows that expression of GADD 153, p-PERK and BAD significantly decreased upon 7,8DHF treatment, while an increasing trend was observed upon CTX-B treatment. Data represent mean ±SD; n=3; $p<0.05$, student's t test) (**$p< 0.05$ (GAD 153), *$p< 0.05$ (p-PERK), *,**$p< 0.05$ (BAD), one way ANOVA followed by Bonferroni post-hoc test).

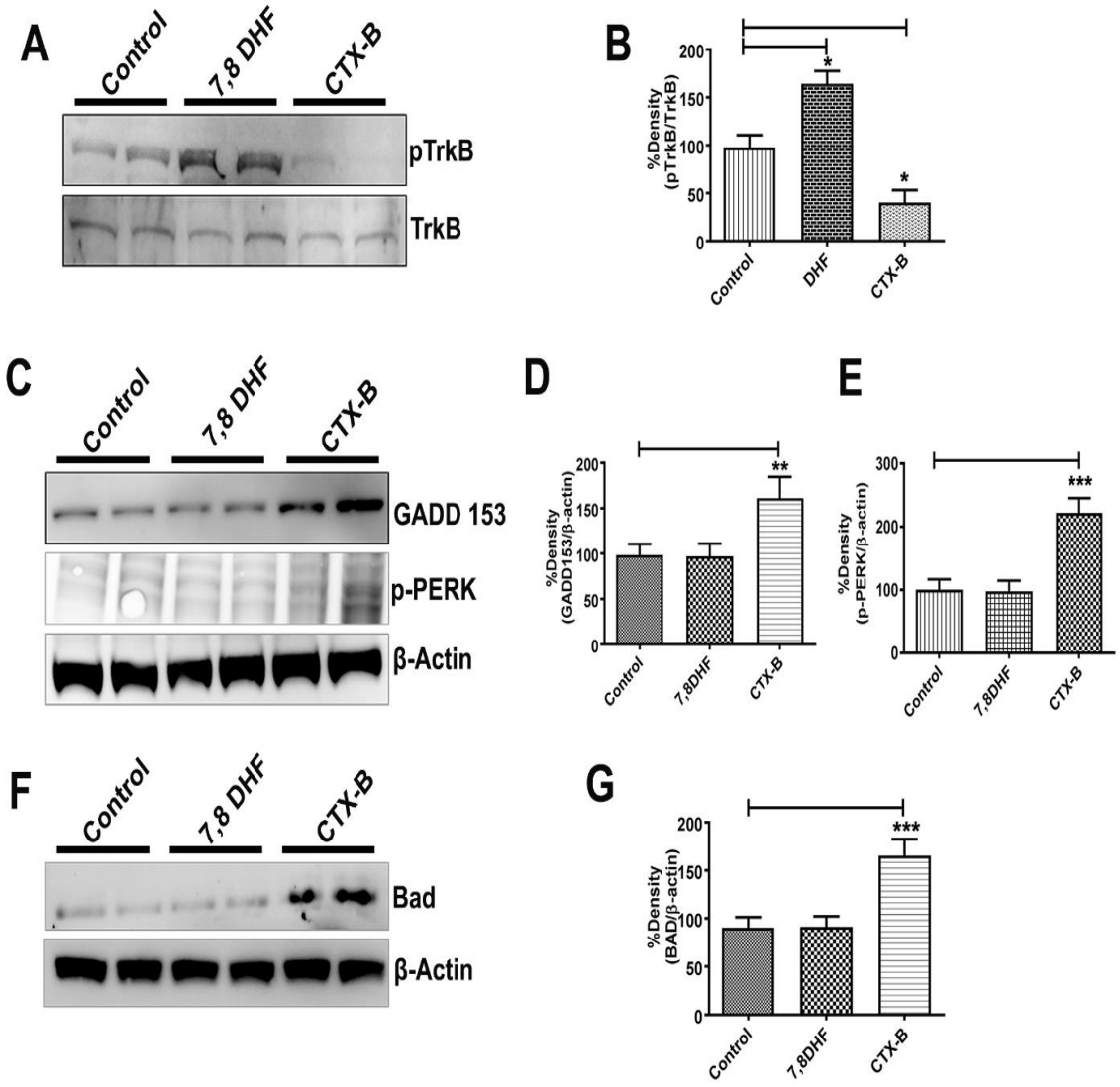

Figure 3.11 Effects of TrkB modulation on ER stress protein and BAD expression. A) Cells were treated with either 7,8 DHF or CTX-B and the effects of the drugs on expression of A) pTrkB, TrkB C) GADD153, p-PERK and F) BAD protein investigated. B) D) G) Densitometric quantification of bands demonstrated significant increase in pTrkBY^{515} in 7,8 DHF treated cells and decrease in in CTX-B treated cells. Data represent mean ± SD; n=3; *p<0.05. Further, GADD 153, p-PERK and BAD expression significantly increased with CTX-B treatment. Data represents mean ± SD ; n=3; **p <0.05, *** p<0.001, student's t test) (**p< 0.05 (GAD 153), ****p< 0.0001 (p-PERK), ****p< 0.0001 (BAD), one way ANOVA followed by Bonferroni post-hoc test).

3.4 Discussion

Recent studies have highlighted mixed and sometimes partly contradictory findings illustrating the effects of the retinoid x receptor agonist bexarotene in mediating glial uptake of Aβ and facilitating its clearance from the brain with cognitively beneficial effects in animal models of AD (Fitz et al., 2013, LaClair et al., 2013, Price et al., 2013, Tesseur et al., 2013, Veeraraghavalu et al., 2013, Cramer et al., 2012). This report provides evidence that bexarotene has a concentration dependent effect on expression of various RXR isoforms in neuroblastoma cells. SH-SY5Y cells were used in the present study as the cultures of SH-SY5Y cells include both adherent and floating cells, both types of which are viable. Also, SH-SY5Y cells are commonly used in studies related to various neurodegenerative diseases like Parkinson's disease, Alzheimer's disease, Amyotrophic Lateral Sclerosis and Huntington's disease. On the other hand, the cultures of hippocampal neurons is particularly challenging since mature neurons do not undergo cell division and show signs of cell death after 2 or 3 weeks. The magnitude of receptor expression changes can vary depending on the drug concentration. However, it is important to note that RXRs being nuclear receptors play critical roles in biological processes such as regulating chromatin condensation, acetylation of histone proteins and transcription regulation (Brazda et al., 2014, Mounier et al., 2015), therefore even relatively modest expression changes may have profound effects over a period of time such as in chronic neurodegenerative conditions like AD. RXR expression analysis in mice brains that were treated with bexarotene corroborated our findings that bexarotene treatment resulted in RXR expression modulation *in vivo* (Figure3.4).

Although bexarotene has previously been shown to act as RXR agonist, this is the most comprehensive investigation to date to evaluate RXR expression changes in response to differential drug concentrations. This study also identified for the first time that the APP/PS1

mouse model of AD has reduced levels of RXR expression in the brain (Figure 3.5 and 3.6). We sought to determine whether these findings could be attributed to altered Aβ levels in these mice brains and tried to recapitulate this experiment in neuroblastoma cells in culture that were treated with Aβ peptide. $A\beta_{1\text{-}42}$ treatment resulted in reduced RXR expression levels in these cells (Figure 3.7). This is the first study to identify that Aβ is associated with a reduction in RXR expression. In addition, we demonstrate that at low concentrations, bexarotene can rescue the loss of RXR expression caused by Aβ administration (Figure 3.7). Previous studies have indicated that amyloid beta pathology may be important in regulating the biological activity of RXR agonists *in vivo* (Tai et al., 2014). Bexarotene treatment in human AD subjects was shown to reduce Aβ levels in brain along with upregulated blood $A\beta_{1\text{–}42}$ concentrations especially in ApoE4 noncarriers but the exact biochemical basis of these observations is unclear (Cummings et al., 2016). Amyloid β induced RXR expression changes and protection conferred by optimal concentrations of bexarotene can be a potential molecular basis of the bexarotene effects in cell culture experiments and in animal models of AD (Kuntz et al., 2015, Mariani et al., 2017, Bachmeier et al., 2013) This report will guide future studies aiming to investigate the role of RXR expression changes in AD and also suggests a molecular mechanism underlying bexarotene induced protective effects observed in some of the recent studies (Bomben et al., 2014, Boehm-Cagan and Michaelson, 2014, Nam et al., 2016).

Aβ has been shown to be associated with enhanced ER stress marker response in brain endothelial cells (Fonseca et al., 2013). Increased ER stress response has also been shown in animal models of AD (Ho et al., 2012, Rozpędek et al., 2016), glaucoma (Zode et al., 2014) and other neurodegenerative disorders like Parkinson's, Huntington's disease and amyotrophic lateral sclerosis (Paschen and Mengesdorf, 2005). Although RXR receptors

have previously been implicated in AD (Kawahara et al., 2014), targeting RXRs using bexarotene and modulating ER stress response expression is a novel area. We observed a significant upregulation of GADD153 and p-PERK expression in cells that were treated with Aβ and identified that these neurotoxic effects of Aβ on ER stress response elucidation were partially suppressed when the cells were subsequently treated with low concentrations of bexarotene (Figure 3.8 A-C). Enhanced ER stress response has been shown to promote pro-apoptotic pathways in neurodegenerative diseases (Tabas and Ron, 2011) as well as cardiovascular diseases (Szegezdi et al., 2006). Ding *et al*. (Ding et al., 2012) demonstrating that sustained ER stress could lead to deleterious effects in epithelial cells triggering cell death. Apoptotic pathway activation has previously been established in Aβ treated cells (Alvarez et al., 2004) and in mouse models of AD (Cancino et al., 2008). Our data substantiated these observations and reported an upregulation of pro-apoptotic protein BAD in the cells upon $A\beta_{1-42}$ treatment (Figure 3.8 D-E). More importantly, treatment with optimal concentrations of bexarotene facilitated partial reduction in BAD protein levels suggesting a molecular protective effect of the drug treatment. Our data thus far indicated that Aβ negatively affected RXR expression, enhanced ER stress response and promoted pro-apoptotic pathways and that pharmacological treatment using optimal concentrations of bexarotene could protect the cells under these conditions.

The role of RXR agonist in moderating ER stress and apoptotic pathway suppression is an important finding; however, bexarotene is also an established anti-neoplastic agent that is known to induce cell apoptosis in cutaneous T-cell lymphoma cells (Zhang et al., 2002). Accordingly, we examined the changes induced by the bexarotene on neuroblastoma cells at relatively higher drug concentrations (5-10 μM). The drug treatment resulted in an upregulation of the ER stress marker proteins, GADD153 and p-PERK. Increased ER stress

response at higher concentrations also corresponded with enhanced BAD protein activation and together these results implicate that the drug has concentration dependent cellular effects in SH-SY5Y cells (Figure 3.9).

The BDNF/TrkB pathway has previously been shown to selectively block both the stress-induced upregulation and intracellular translocation of GADD153 in human neuroblastoma SH-SY5Y cells (Chen et al., 2007). Treatment with 7,8 DHF which is a potent TrkB agonist resulted in GADD153 suppression in HK-2 cells reducing the ER stress response and thereby supporting the evidence of protective effects of TrkB pathway activation on ER stress (Ma et al., 2016). 7,8 DHF binding induces TrkB autophosphorylation and its dimerization and activates the intracellular PI3K/Akt and MAPK/Erk signalling in neuronal cells (Gupta et al., 2013, Gupta et al., 2013c). Furthermore, TrkB activates Akt pathway which is downstream of the receptor tyrosine kinase signalling and blocks the pro-apoptotic Bcl-2 family member BAD (Nguyen et al., 2009). 7,8 DHF treatment was indeed shown to block the BAD protein activation in mouse model of experimental brain injury (Wu et al., 2014). Similarly, cyclotraxin-B is a potent and selective TrkB inhibitor that blocks Tyr^{515} phosphorylation, its downstream Akt activation and associated biochemical signalling pathways (Cazorla et al., 2010, Gupta et al., 2013, Gupta et al., 2014). Pharmacological treatment of neuroblastoma cells with 7,8 DHF and CTX-B resulted in modulation of ER stress response proteins and pro-apoptotic BAD protein expression changes induced by high concentrations of bexarotene (Figure 3.10). Supporting previous literature, our study elucidated that 7,8 DHF treatment resulted in enhanced $pTrkBY^{515}$ phosphorylation while CTX-B treatment lead to significant decline in pTrkB activation (Gupta et al., 2013) (Figure 3.11 A-B). In addition to its effects on TrkB activation, CTX-B treatment upregulated the ER stress markers (GADD153/ p-PERK) and BAD protein expression in

SHSY5Y cells (Figure 3.11 C-G). TrkB agonist treatment on the other hand, resulted in reduced GADD153/ p-PERK and BAD protein expression (Figure 3.11 C-G). While 7,8DHF treatment resulted in reduced expression of ER stress proteins caused by high levels of bexarotene, CTX-B treatment further exacerbated the ER stress protein expression induced by the drug (Figure 3.10). The cross-talk of TrkB signalling with RXR pathway in regulating ER stress proteins GADD-153 and p-PERK, and BAD protein expression is an intriguing finding both mechanistically and because of significant implications in developmental, oncogenic and neurodegenerative processes. These results suggest a mechanistic rationale for TrkB pathway as an additional drug target that may help reduce the side effects associated with high concentrations of bexarotene. Future studies will help validate tissue specific relevance of these findings in humans and in various animal models of disease.

Overall, in addition to its implications in cancer research, such as in neuroblastoma and cutaneous T-cell lymphoma, better therapeutic targeting of RXRs may be useful in AD drug development. These findings are also relevant to retinal degenerative conditions associated with enhanced Aβ levels such as glaucoma, age related macular degeneration and AD pathology (Gupta et al., 2016). BDNF/TrkB signalling has been consistently shown to support the survival of neurons in brain and for the retinal ganglion cells (Gupta et al., 2014, Gupta et al., 2013, Nagahara et al., 2009). Our study raises the possibility of specific biochemical pathway linking RXR expression changes with Aβ accumulation and its cross-talk with TrkB receptor signalling. These findings and potential therapeutic applicability provide rationale to further explore bexarotene pharmacodynamics along with RXR biological cross talk with TrkB receptor signalling.

CHAPTER 4

RETINOID-X-RECEPTOR MODULATION PROTECTS AGAINST ER STRESS RESPONSE AND RESCUES GLAUCOMA PHENOTYPES IN ADULT MICE

Data presented in this chapter have been submitted for publication

Yogita Dheer, Nitin Chitranshi, Veer Gupta, Samridhi Sharma, Mojdeh Abbasi, Mehdi Mirzaei, Yuyi You, Stuart L Graham, Vivek Gupta. Retinoid x receptor modulation protects against ER stress response and rescues glaucoma phenotype in adult mice Manuscript submitted to Journal of Cell Death and Disease.

Part of this chapter was presented in SOE (European Society of Ophthalmology) 2017, Barcelona, Spain

Abstract

Glaucoma is a progressive optic neuropathy associated with loss of retinal ganglion cells (RGCs). Neuroprotective strategies to prevent RGC loss are being extensively explored to rescue vision loss in glaucoma. Mounting evidence suggests that RXR activation may be neuroprotective in the central nervous system. However, its potential neuroprotective role in the retina and specifically in glaucoma remains unexplored. This study investigated changes in RXR expression in the mouse retina under glaucomatous stress conditions and investigated the effect of RXR modulation on the RGCs using pharmacological approaches. RXR protein levels in retina were downregulated in glaucoma while bexarotene treatment resulted in upregulation of RXR expression particularly in the inner retinal layers. Retinal electrophysiological recordings and histological analysis indicated that inner retinal function and retinal laminar structure were preserved upon treatment with RXR agonist, bexarotene. These protective effects were associated with downregulation of ER stress marker response upon bexarotene treatment under glaucoma conditions. Overall, RXR modulation significantly protected RGCs by suppressing ER stress activation and rescuing the inner retinal deficits in glaucoma.

4.1 Introduction

Glaucoma is the second most common cause of vision loss after cataract and it is anticipated that by 2020, 79.6 million people will suffer from this disease globally (Quigley and Broman, 2006, Sappington et al., 2010). The disease is characterised by slow, progressive degeneration of retinal ganglion cells (RGCs) and optic nerve atrophy. Retinoid receptors play an important role in the course of eye development and are localized to specific cell types in the adult retina (Mori et al., 2001). RXR activation has proven to be beneficial in neurodegenerative models affecting the brain. However neuroprotective role of RXR activation on RGC in glaucoma has not been explored. RXR activation was found to protect retina pigment epithelial cells (RPE) from oxidative stress-induced apoptosis suggesting RXR agonists might be protective in the retina (Ayala-Peña et al., 2016). There are also reports indicating that RXR activation may be protective against amyloid beta toxicity (Bachmeier et al., 2013), mitochondrial dysfunction (Lee et al., 2015) and glutamate excitotoxicity (Mariani et al., 2017). All these factors are reported to be involved in RGC death in glaucoma.

RXRs belong to the superfamily of steroid/thyroid receptors, are involved in number of cellular and metabolic processes and are classified into α, β, and γ subtypes (Dawson and Xia, 2012). These can form both homodimer as well as heterodimer with other nuclear receptors making it a unique member of nuclear hormone receptor family that includes peroxisome proliferator-activated receptor (PPAR), liver-X-receptor (LXR), farnesoid X receptor (FXR), pregnane X receptor (PXR), retinoic acid receptor (RAR), vitamin D receptors (VDR), thyroid hormone receptor (TR) etc (Forman et al., 1995, Kurokawa et al., 1994). This versatile role of RXR to serve as a common heterodimer partner for multiple NRs enables this receptor to be involved in several key cellular signalling

pathways. RXRs also regulate gene expression by forming homodimers upon being activated by selective agonists.

The RXR agonist bexarotene is approved for the treatment of cutaneous T-cell lymphoma and more recently, therapeutically beneficial effects of the drug are being explored for metabolic disorders like diabetes and obesity inflammatory disorders, atherosclerosis, and other cardiovascular diseases (Altucci et al., 2007, Claudel et al., 2001). Evidence from recent reports strongly suggests a neuroprotective role of the drug in other neurodegenerative diseases such as Parkinson's disease (McFarland et al., 2013), multiple sclerosis (Natrajan et al., 2015) and Alzheimer's disease (Crunkhorn, 2012). RXR activation by bexarotene is also promising neuroprotective therapy for amyotrophic lateral sclerosis (ALS) as it delays motor neuron degeneration and maintains neuronal survival in transgenic SOD1G93A mice (Riancho et al., 2015). Recently, RXR activation by bexarotene has been found to decrease neuronal hyperexcitability in mouse models of epilepsy (Bomben et al., 2014).

Recent in vitro studies demonstrated that bexarotene treatment protects neurons from glutamate-induced excitotoxicity (Huuskonen et al., 2016). It is a highly selective synthetic retinoid which has high blood brain permeability and activates all the three isoforms of RXRs i.e RXRα, RXRβ and RXRγ (Cramer et al., 2012). Understanding of the role of RXRs in the retina is rather limited and the potential effects of RXR activation in glaucoma have not been previously investigated.

In this study, we sought to investigate the involvement of RXRs in the retina with particular focus under glaucoma conditions. The effects of bexarotene treatment on RXR expression and other biochemical effects in the retina were studied. The effects of RXR modulation in the retina in two different experimental models of RGC injury were studied.

A glutamate mediated increased excitotoxicity model was used to understand relatively acute effects of the RGC injury and a microbead injection model with chronically increased intraocular pressure (IOP) was utilised to study the IOP related effects. Our findings underscore that RXR activation using bexarotene suppresses the ER stress and apoptotic processes and protects the retinal ganglion cells and retinal function in glaucoma, thus providing a novel therapeutic target for the treatment of glaucoma and possibly other neurodegenerative disorders.

4.2 Materials and Methods

Ethics, animals, drug (bexarotene treatment), chemicals, glaucoma models (glutamate and microbead) and equipments used are described in chapter 2 under sections 2.1, 2.2, 2.3 and 2.4

4.2.1 Electroretinographic recordings

Detailed method to perform electroretinogram recordings is discussed in chapter 2, section 2.5.

4.2.2 Histology

Animal tissue (both eye and optic nerve) fixation, embedding and sectioning were done as described in chapter 2, section 2.6.The retinal sections were stained with H and E staining as discussed in chapter 2, section 2.7. The number of cells in the ganglion cell layer was counted over a length of 300 μm (100 μm to 600 μm from the edge of the optic disc) for both superior and inferior retina. For each eye, cell counts were averaged

over three consecutive sections to analyse the number of cells in the retinal ganglion cell layer (GCL). The optic nerve sections were subjected to Bielschowsky silver staining as explained in chapter 2, section 2.8 and axonal density was determined for each optic nerve by counting number of axons.

4.2.3 Western blotting

After retinal enucleation, optic nerve head region of the retina was excised from the retina. The tissue lysate was prepared as described in chapter 2, section 2.10. The protein concentration was determined using the BCA protein assay kit. Western blotting was performed as discussed in chapter 2, section 2.11. Membranes were incubated overnight with anti-RXRα (1:1000), anti-RXRβ (1:1000), anti-RXRγ (1:1000), anti-GADD 153 (1:1200), anti-p-PERK (1:200), and anti-β-actin (1:5000). Further procedure already reported in chapter 2, section 2.11.

4.2.4 Immunofluorescence

Method of immunofluorescence of retinal cryosections was discussed previously in chapter 2, section 2.9.

4.2.5 Statistical Analysis

GraphPad Prism software was used to analyse ERG/pSTR amplitudes, GCL density, axonal density as well as protein expression. All values with error bars are presented as mean ±SD for given *n* sizes and compared using one way ANOVA followed by Bonferroni

post-hoc test for multiple-comparison and student's *t* test for unpaired data.. The significance was set at $p<0.05$.

4.3 Results

4.3.1 Glaucoma downregulates RXR expression in mice retinas

We assessed the expression of RXR receptor isoforms in the mice retinas and evaluated the effects of glaucomatous injury on the RXR expression levels. Immunostaining of the retinal sections revealed that RXR α was observed to be well expressed in all the retinal layers while RXR β staining was predominantly localised in the ganglion cell layer. RXR γ immunoreactivity was also identified in all the retinal layers (Figure 4.1 and 4.2). The expression of various RXR receptors was also studied in the optic nerve head tissue using western blotting in the control and experimental glaucoma groups in glutamate excitotoxicity and microbead induced increased IOP model (Figure 4.3A). Microbead administration resulted in chronic increase in IOP i.e. 20.11±2.63 mmHg (mean± SD) compared to control group with an average IOP of 9.16± 0.43 ($p<0.001$) (Figure 4.4A). No IOP increase was observed in the glutamate treated group (Figure 4.4B). Results from immunofluorescence and densitometric quantification of the immunoblotting indicate that RXR expression was significantly downregulated in both the experimental glaucoma models compared to the control groups (RXR α, control 113 ± 6.699 vs glutamate 53.23±4.657, ***$p<0.001$; microbead 53.21±4.446, ***$p<0.001$; RXR β, control 101.8 ± 5.27 vs glutamate 65.96 ±3.303, **$p< 0.05$; microbead 65.33 ± 3.186, **$p< 0.05$; RXR γ, control 101.7 ±3.258 vs glutamate 51.58±2.982, ****$p< 0.0001$; microbead 49.95±2.373, ****$p< 0.0001$ mean± SD %) (Figure 4.3 B-D).

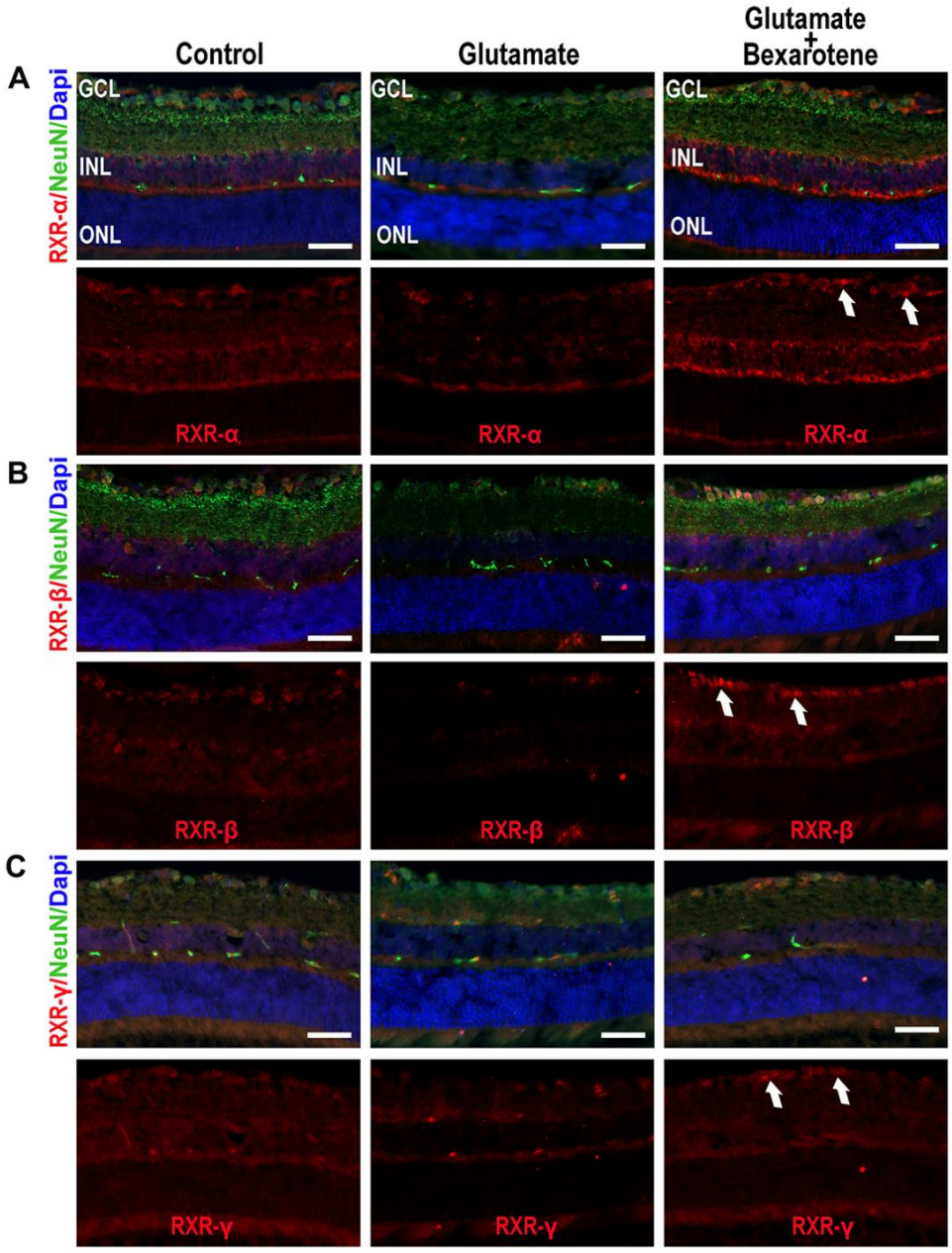

Figure 4.1 Changes in expression of RXR (α, β, and γ) in control, glutamate and glutamate +bexarotene group (A), (B) and (C) represents immunofluorescence of mice retinal cryosections with anti-RXRs (α, β, and γ) and anti NeuN (neuronal marker) from different groups. Red colour and green color indicates staining for RXR and NeuN respectively while blue nuclei is for DAPI; GCL, retinal ganglion cell layer; INL, inner nuclear layer; ONL, outer nuclear layer. Microscopic images after immunostaining revealed that bexarotene treatment in mice exposed to intravitreal glutamate upregulates expression of all the three isoforms of RXR as compared to glutamate group. Scale bar =50 μm.

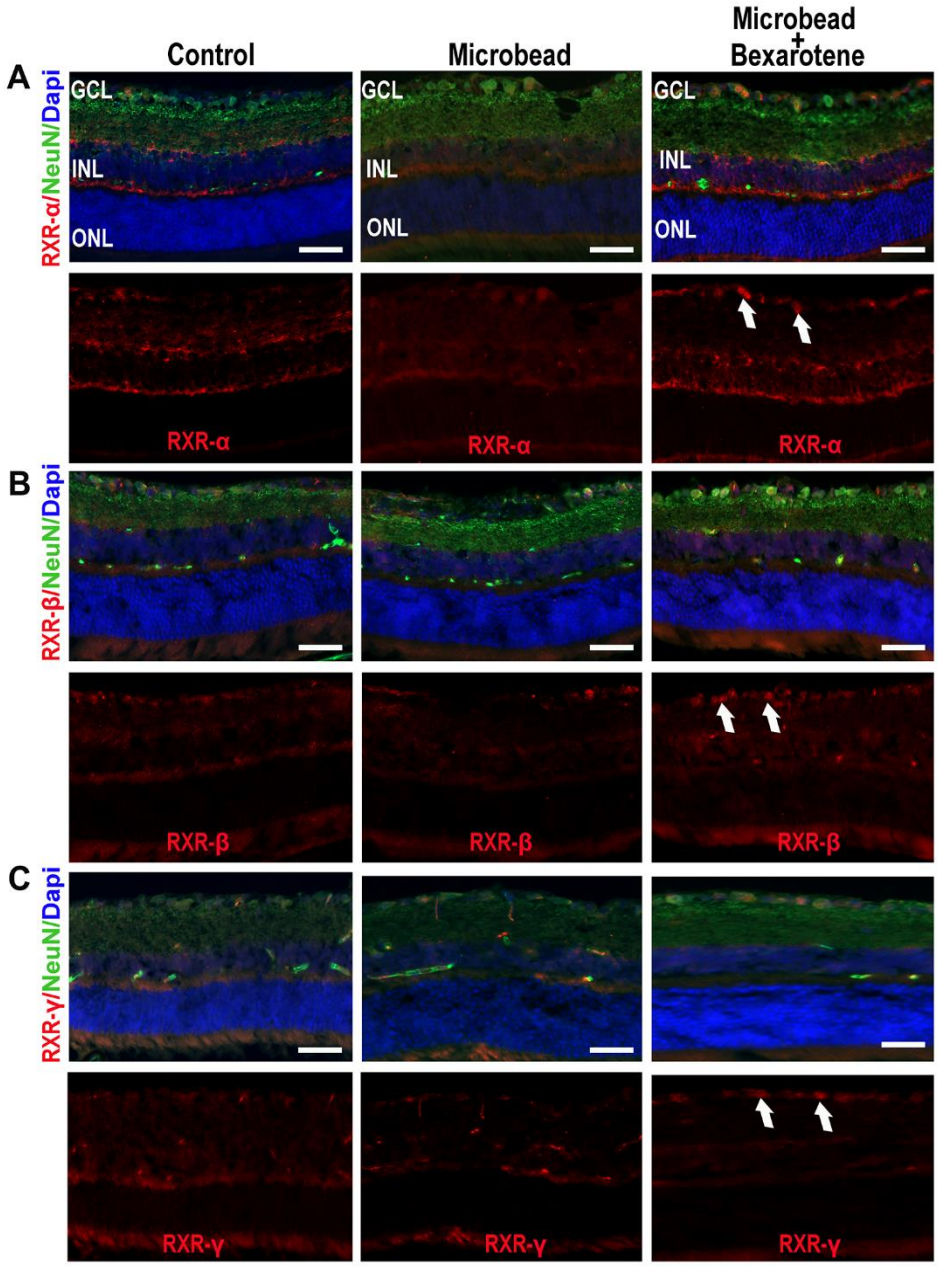

Figure 4.2 Changes in expression of RXR (α, β, and γ) in control, microbead and microbead+bexarotene group (A), (B) and (C) represents immunofluorescence of mice retinal cryosections with anti-RXRs (α, β, and γ) and anti NeuN (neuronal marker) from different groups. Red colour and green color indicates staining for RXR and NeuN respectively while blue nuclei is for DAPI; GCL, retinal ganglion cell layer; INL, inner nuclear layer; ONL, outer nuclear layer. Microscopic images after immunostaining revealed that bexarotene treatment in mice exposed to Intracameral microbeads upregulates expression of all the three isoforms of RXR as compared to microbead group. Scale bar =50 μm.

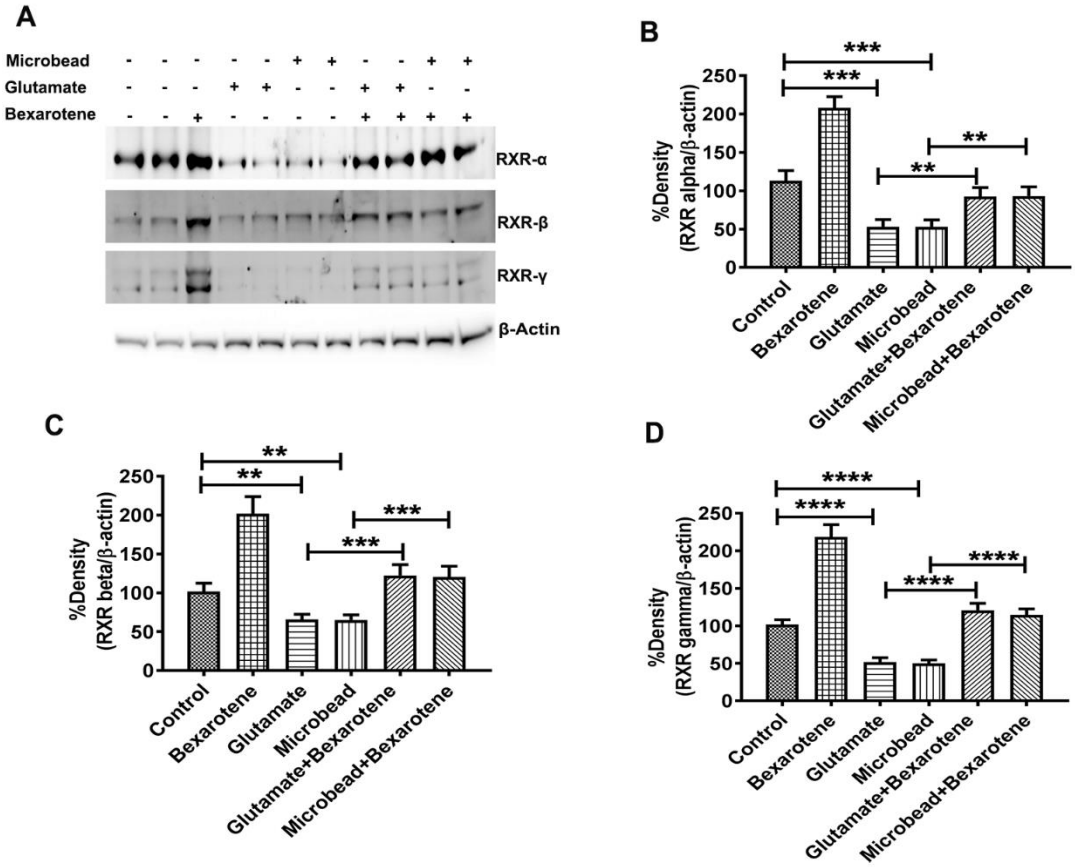

Figure 4.3 Bexarotene mediated upregulation of RXRs (α, β, and γ) in control, glaucoma and glaucoma+bexarotene group (A) represents western blot of RXR (α, β, and γ) expression in optic nerve lysates of control, bexarotene, glaucoma and glaucoma+ bexarotene group. (B), (C) and (D) Densitometric analysis showed a significant upregulation of RXRs in glaucoma+ bexarotene as compared to glaucoma. (**p< 0.05, ***p<0.001, ****p< 0.001, student's t test) (***p<0.001, ****p< 0.0001, one way ANOVA followed by Bonferroni post-hoc test).

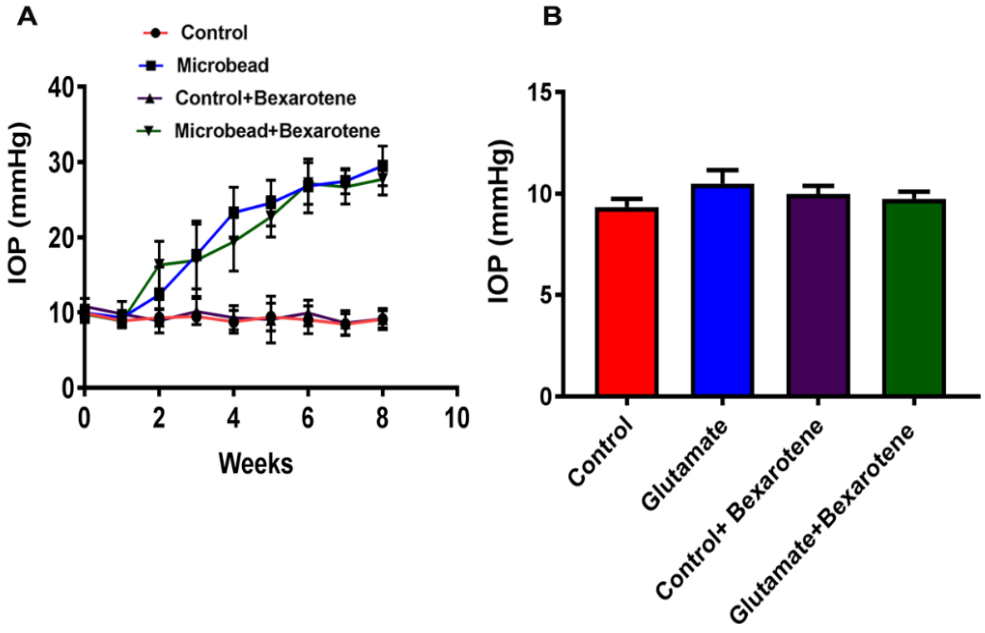

Figure 4.4 Intraocular pressure (IOP) measurements**.** Mean IOP in control, bexarotene, glaucoma (glutamate and microbead) and glaucoma +bexarotene mice eyes were measured. (A) represents sustained increase in IOP observed from 0 week to 8 weeks with microbead injection. (B) represents that there was no significant rise in IOP was observed in control, bexarotene, glutamate, glutamate+ bexarotene groups.

4.3.2 Treatment with RXR agonist bexarotene enhanced retinal RXR expression

To investigate the effects of bexarotene drug treatment on the RXR expression in the retinas under control and experimental glaucoma conditions, optic nerve head lysates were subjected to immunoblotting analysis. Results demonstrated increased expression of RXR α,β, and γ isoforms in the bexarotene treated groups as compared to glaucoma conditions (RXRα, bexarotene 92.51± 5.869, **p< 0.05 (glutamate), 93.23 ± 5.931,**p< 0.05 (microbead); RXRβ, bexarotene 122.4±6.912, ***p< 0.001, (glutamate), 120.6±6.83***p< 0.001 (microbead); RXRγ, bexarotene 120.7±4.722,****p< 0.0001 (glutamate), 114.6±3.96,****p< 0.0001 (microbead) mean± SD %) (Figure 4.3 B-D). Drug treatment as such did not result in any IOP increase or decrease in control or experimental glaucoma groups. The retinal sections from the bexarotene treated animals

were also subjected to immunofluorescence analysis. Results substantiate the WB findings and highlight that bexarotene treatment resulted an increased RXR expression in retinas exposed to glaucomatous injury (Figure 4.1 and 4.2). The increased expression was predominantly associated with the inner retina partcularly GCL and localised with the NeuN postive ganglion cells.

4.3.3 RXR activation reduces ER stress response in experimental glaucoma

Taking into account that ER stress is associated with retinal ganglion cell death, we investigated ER stress associated changes in our acute and chronic mouse model of experimental glaucoma (Doh et al., 2010, Jing et al., 2012, Shimazawa et al., 2007). Expression of ER stress protein markers p-PERK and GADD 153 was evaluated in retinal sections using immunofluorescence and data indicates increased staining in the glaucoma conditions. The reactivity of p-PERK was mainly localised to the GCL, outer plexiform layer and INL while for GADD153 it was mainly localised to the GCL (Figure 4.5). DAPI was used for orientation and to identify various cellular layers in the retina. The effects of the RXR agonist bexarotene on the ER stress protein localisation and protein expression was evaluated in the retinal sections. Drug treatment of the glaucoma animals resulted in reduced expression of both p-PERK and GADD 153 proteins and no remarkable changes were noticed in the localisation of the protein with respect to retinal layers in either glaucoma or tissues from drug treated mice (Figure 4.5 A-B).

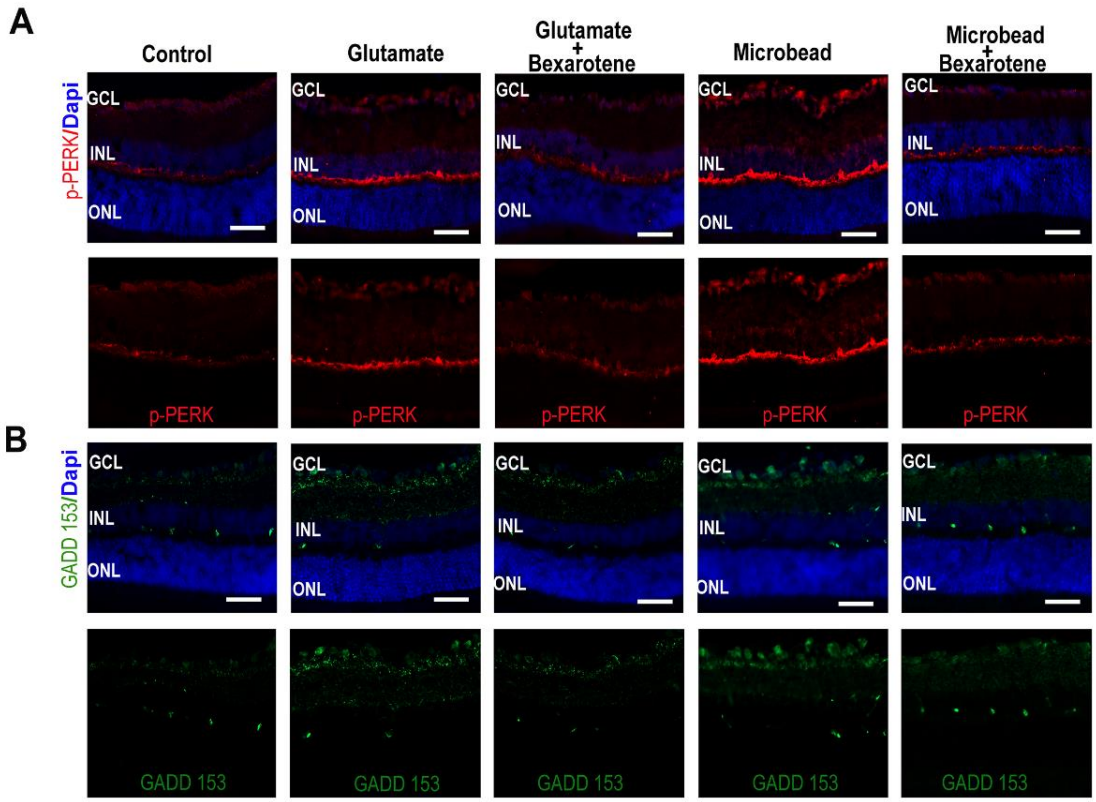

Figure 4.5 Effects of bexarotene on glutamate and microbead injections induced ER stress (A) and (B) Immunohistochemical images of mice retinal sections stained with p-PERK (red) and GADD 153 (green), revealed that there is upregulation of p-PERK and GADD 153 (ER stress markers) in glaucoma (glutamate and microbead). Bexarotene treatment suppressed the expression of ER stress markers. DAPI was used as nucleus marker. Scale bar =50 μm.

The changes in ER stress protein markers p-PERK and GADD 153 was also evaluated in the optic nerve head lysates using western blotting and data quantified using band intensities. A significant increase in the ER stress proteins was identified in both glutamate and microbead models compared to control tissues (p-PERK, control 99.6 ± 6.6 vs glutamate 182.9 ±14.08, **p<0.05; microbead 216±11.13, ***p<0.001; GADD153, control 129 ± 10.38 vs glutamate 204 ±14.09, **p< 0.05; microbead 208 ± 19.02, *p< 0.05; mean± SD %) (Figure 4.6 A-C). Tissue lysates from glaucoma mice treated with the RXR agonist demonstrated a significantly reduced activation of p-PERK and GADD153 proteins compared to the glaucomatous tissues alone (p-PERK, (mean± SD %) 130.5± 5.37,*p< 0.05 (glutamate), 123.6 ±9.94, ***p<0.001 (microbead) ; GADD153, (mean±

SD %) 151± 12.3, *p< 0.05 (glutamate),155.2±10.08, *p< 0.05 (microbead) (%) (Figure 4.6 A-C). Together, these experiments establish that bexarotene can reduce the ER stress activation in the glaucoma models *in vivo*.

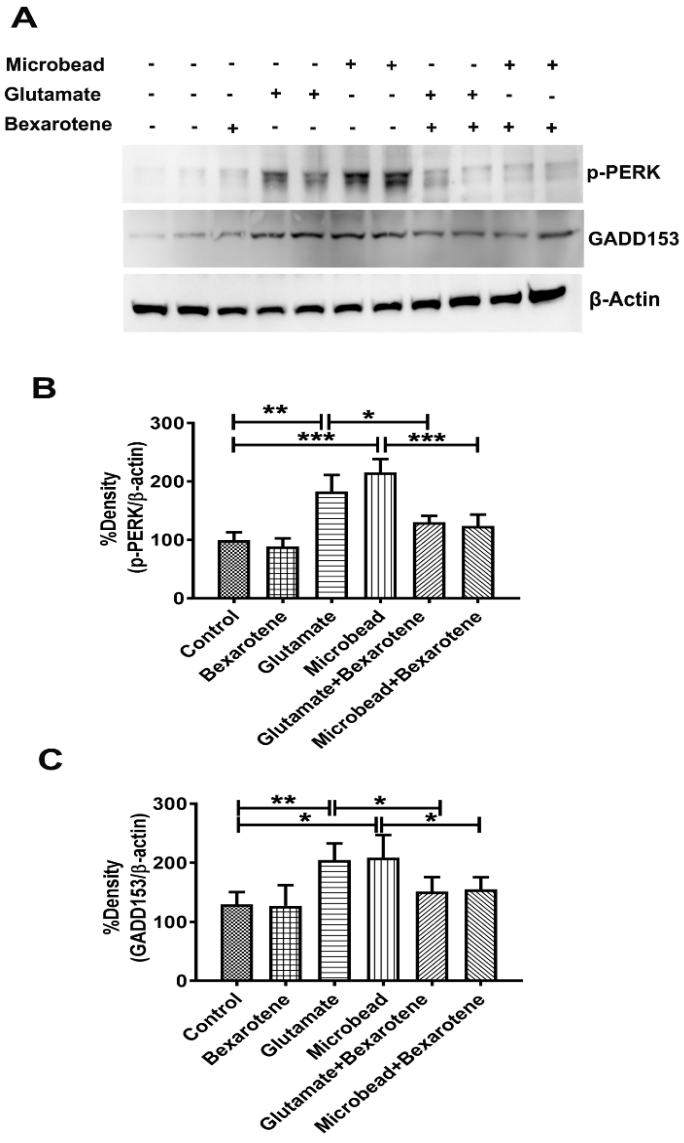

Figure 4.6 Effect of bexarotene on glutamate and microbead injections mediated ER stress marker response (A) Western blot of p-PERK and GADD 153 expression in mice optic nerve lysates. (B) and (C) Statistical analysis of western blot results indicates that the protein level of p-PERK and GADD 153 was significantly decreased with bexarotene treatment as compared to glaucoma group. (*p< 0.05, ***p< 0.001, student's t test) (*,**p< 0.05, ****p< 0.0001, one way ANOVA followed by Bonferroni post-hoc test).

4.3.4 Reduced apoptotic pathway activation in glaucoma upon RXR activation

We evaluated the expression of BAD protein which is an apoptotic marker in both glutamate and microbead induced glaucoma model using immunoblotting. Quantifications showed significant BAD upregulation in glaucoma tissues compared to control tissues (Control 99.26 ± 7.2 (mean± SD %), glutamate 224.4 ± 9.5, ***$p<0.001$; microbead, 227.1 ± 15.1, ****$p< 0.0001$). Bexarotene treatment of the glaucoma mice resulted in BAD suppression *in vivo* as demonstrated by reduced band intensities (glutamate, 144± 10.09, **$p<0.05$; microbead, 127.2 ± 9.78, ** $p<0.05$). Actin was used as loading control in each case. Bexarotene treatment of the control mice did not result in any significant changes in BAD protein expression suggesting that RXR activation was effective in reducing BAD expression once it is activated in experimental glaucoma conditions (Figure 4.7 A-B).

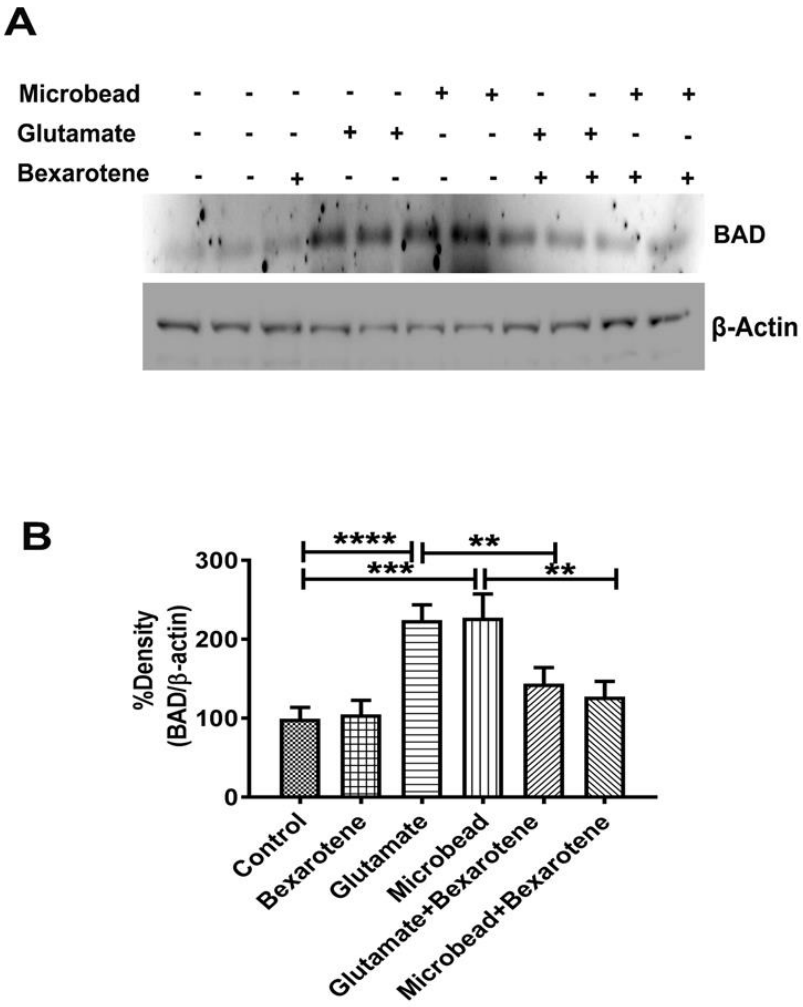

Figure 4.7 Bexarotene mediated suppression of apoptosis (A) Western blot of BAD expression in mice optic nerve lysates. (B) Statistical analysis of western blot results indicates that the protein level of BAD was significantly decreased with bexarotene treatment as compared to glaucoma group. (**p< 0.05, student's t test) (***p< 0.001, ****p< 0.0001, one way ANOVA followed by Bonferroni post-hoc test).

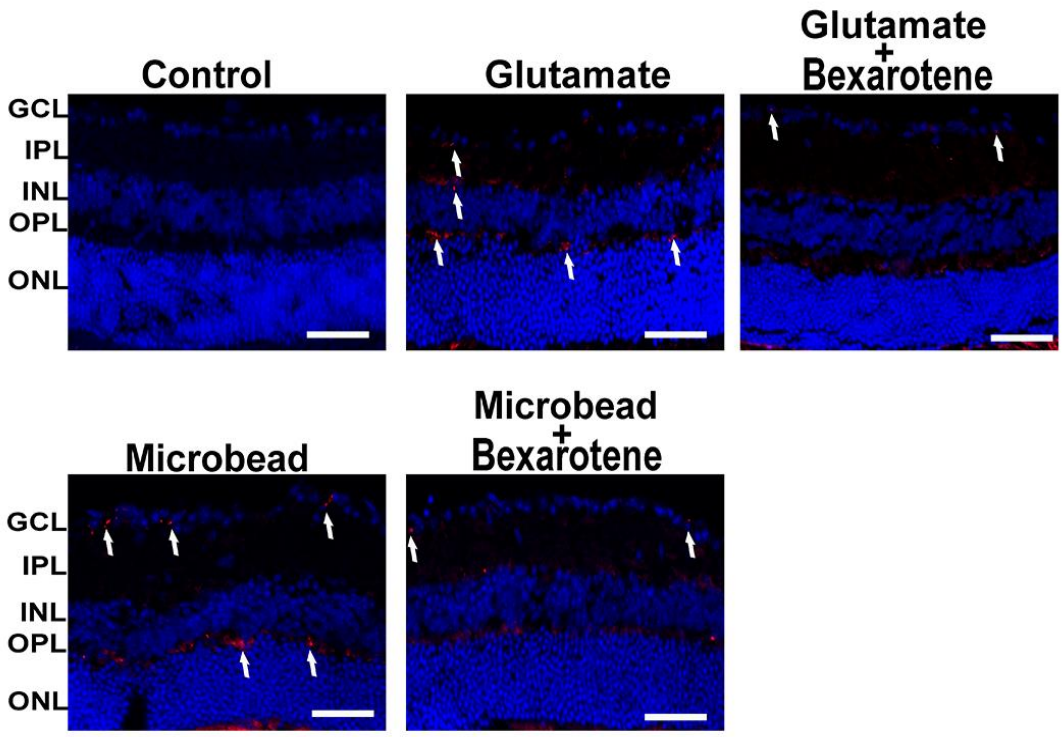

Figure 4.8 Effects of bexarotene on glaucoma induced upregulation of apoptosis. Immunohistochemical images of mice retinal sections stained with TUNEL assay kit for apoptotic changes. Images showing increased TUNEL reactivity (red) in glaucoma. DAPI was used as nucleus marker. Scale bar =50 μm.

Mice retinal sections were also investigated for apoptotic changes using TUNEL staining (Figure 4.8). Glutamate and microbead injected mice revealed more TUNEL-positive retinal cells. Bexarotene treatment reduced the number of TUNEL-positive cells. These results suggest that apoptotic pathway activation associated with ER stress protein upregulation in glaucoma can be suppressed by pharmacological activation of RXR receptors in the retina. We have seen TUNEL staining within the retinal nuclear layers. It is important to highlight that the images were taken at 20X. Images at high resolution ie at 63X or 100X can be taken to further see the single cell staining that co-localizes with the nucleus.

4.3.5 RXR activation deteriorated amyloid β accumulation in the retinas of glaucoma mice

Recent studies have shown increased amyloid beta accumulation in retina of glaucoma mice. In this study, we observed increased amyloid reactivity in the retina in glaucoma animals and this staining was significantly reduced in the tissues of mice that were pretreated with RXR agonist (Figure 4.9 A-C).

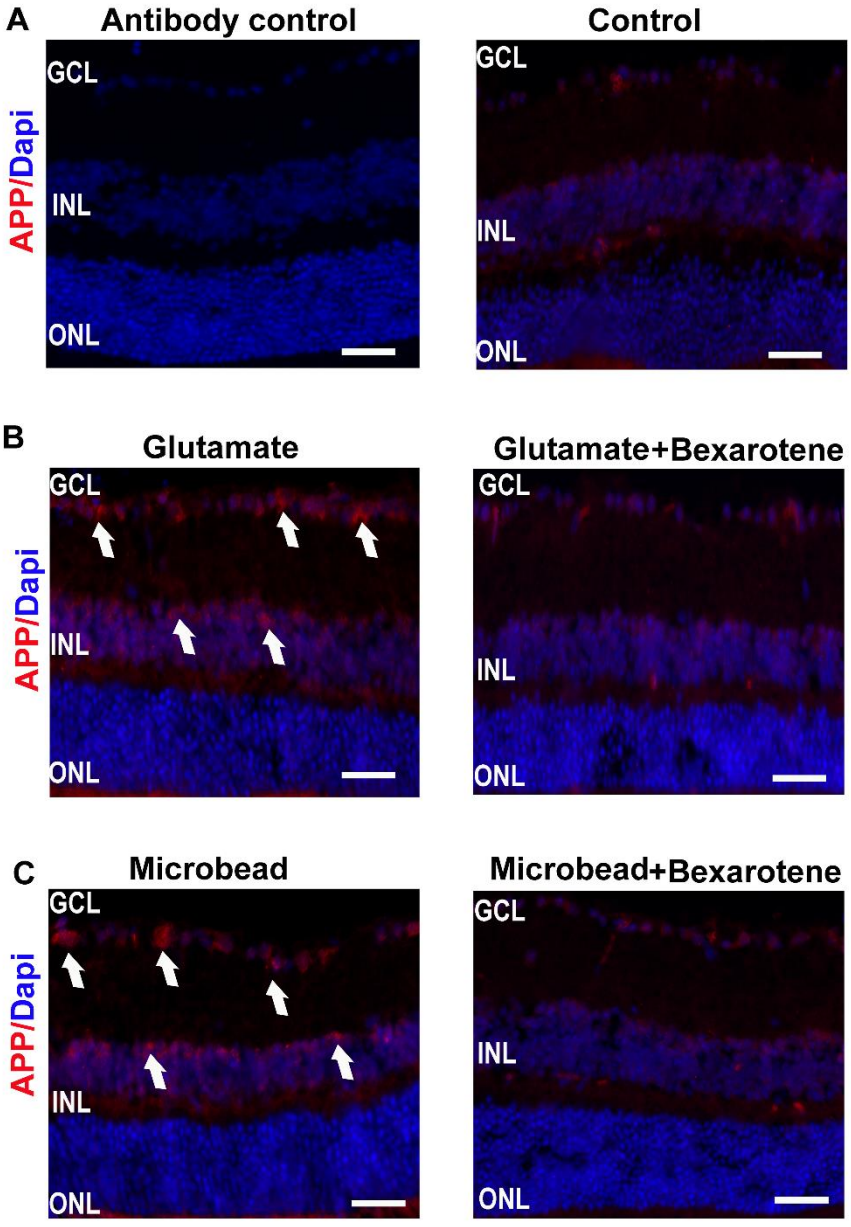

Figure 4.9 Bexarotene treatment reduces amyloid beta accumulation in glaucoma eyes. Representative images of mice retinal sections in control, glaucoma and glaucoma +bexarotene group immunostained with

Aβ specific antibodies (red). The white arrows indicating. Aβ deposition and DAPI (blue colour) was used as nuclear marker. Scale bar= 50 μm.

4.3.6 RXR activation ameliorated inner retinal functional deficits associated with glaucomatous stress

Both glutamate excitotoxicity and experimental glaucoma models are reported to be associated with inner retinal functional deficits characterised by a reduced positive scotopic threshold response (pSTR) (Bui et al., 2009, Della Santina et al., 2013). In this study both intravitreal glutamate injection and microbead administration resulted in reduction of pSTR amplitudes (29.35± 2.71 μV; n=6 in glutamate model and 22.82± 1.80 μV; n=8 in microbead model) as compared to control mice (55.97± 6.92 μV, n=10, mean ± SD) (Figure 4.10 A, B, E and F). We investigated whether treatment with the RXR agonist and resulting increased expression of various RXR isoforms correlated with any effects on the retinal functional recordings. The loss of pSTR amplitude was significantly prevented upon bexarotene treatment in both the glutamate (40.82± 3.14 μV; *p< 0.05; n=9) and microbead (41.28± 3.078 μV; ***p< 0.001; n=9) groups as compared to the corresponding glaucoma groups. The whole retinal scotopic ERG recordings demonstrated no significant changes in a- or b- wave amplitudes in either glaucoma or RXR agonist treatment groups suggesting that effects of glaucoma injury and protective effects of RXR agonist treatment were mainly localised to the inner retina (Figure 4.10 C,D,G and H). These results indicate that RXR upregulation by its pharmacological agonist partially rescues the retinal functional impairment caused by glutamate excitotoxicity and microbead induced increased IOP injury.

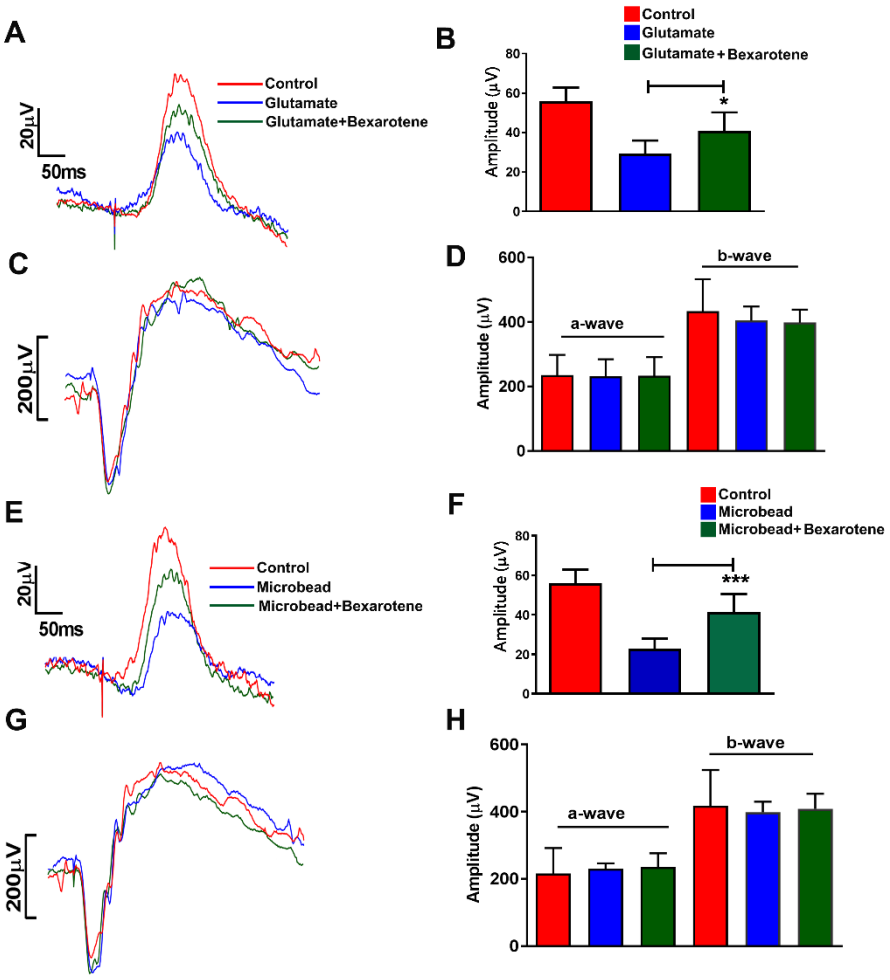

Figure 4.10 Effects of bexarotene on electroretinography (ERG) and positive scotopic threshold response (pSTR) responses (A) and (E) represents positive scotopic threshold responses of all groups (both glutamate and microbead model) (B) and (F) Quantification of pSTR amplitudes indicates a significant elevated amplitude of pSTR in the bexarotene treated mice as compared to the glaucoma mice. *p< 0.05, ***p< 0.001, student's t test) (*p< 0.05, ****p< 0.0001, one way ANOVA followed by Bonferroni post-hoc test). (C) and (G) Representative ERG for the control, glaucoma and glaucoma+bexarotene group (D) and (H) Data analyses of ERG indicates no significant change in a-wave and b-wave.

4.3.7 Effects of RXR agonist on the ganglion cell layer and optic nerve

We investigated whether the protective effects of the drug on electrophysiological recordings was supported by protection of cellular morphology in the retinal laminar structure. Retinal sagittal sections were subjected to immunohistochemical analysis using H and E staining, (Fu and Sretavan, 2010) and analysed using light microscopy (Figure

4.11 A). A significant decrease in the number of cells in GCL was observed in both glutamate and microbead induced glaucoma injury models (79.49 ± 3.42 % cells in control versus 43.83 ± 2.17 cells % in glutamate, ***p< 0.001, and 33.15±1.87 in microbead model, ****p< 0.0001) (Figure 4.11). Interestingly, the RXR agonist significantly prevented the loss of GCL density and increased number of cells were identified in both the experimental glaucoma injury models (58.17 ± 2.66 % cells in glutamate **p< 0.05, and 57.41±2.8 in microbead model, ***p<0.001) (Figure 4.11 B-C) compared to controls.

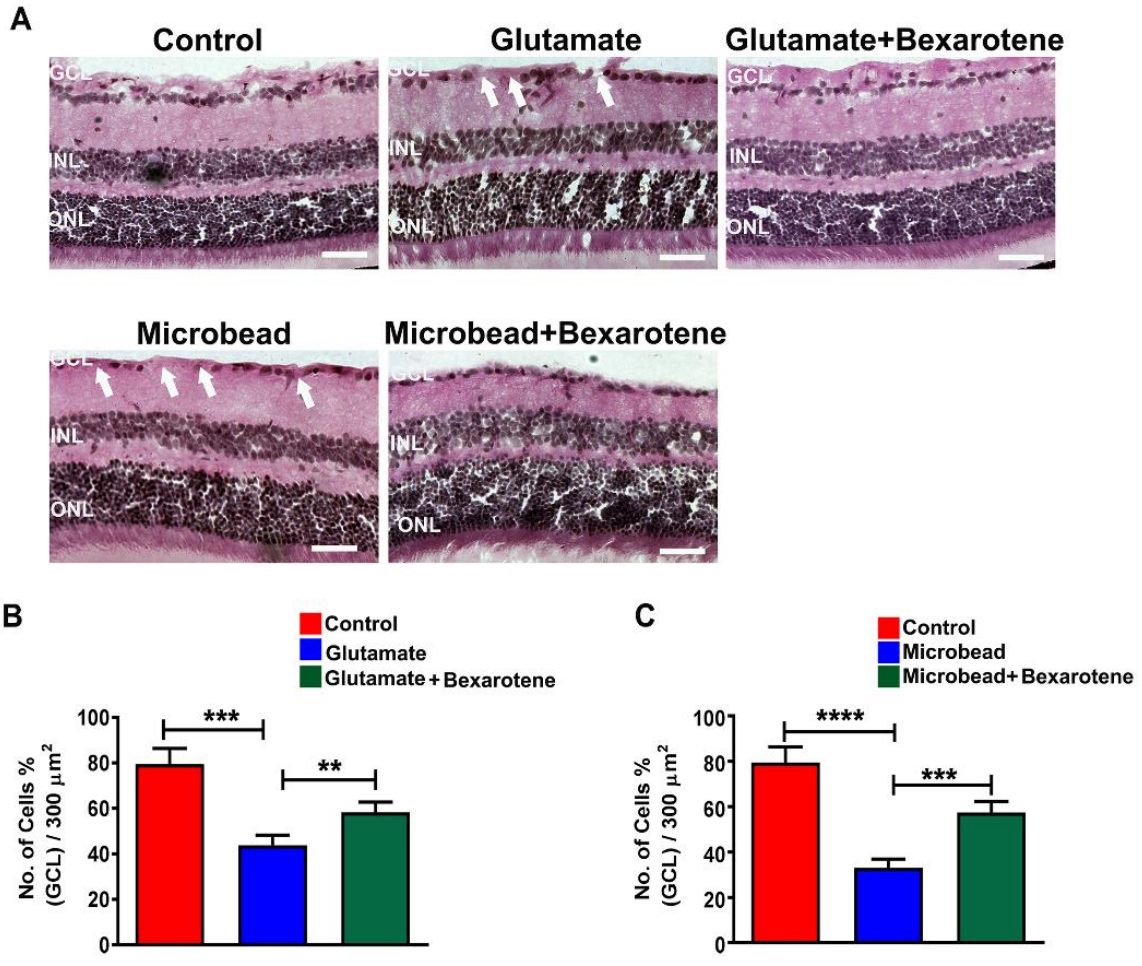

Figure 4.11 Histological changes in control, glaucoma and glaucoma+bexarotene group using H and E staining to reveal retinal morphology (A) Representative images of H and E stained mice retinal sections showing a decline in number of retinal ganglion cells in glaucoma (both glutamate and microbead) (B) and (C) Quantification indicating significant preservation of GCL with bexarotene treatment as compared to glaucoma in mice retinal sections (**p< 0.05, ***p< 0.001, student's t test) (*p< 0.05, ***p< 0.001, one way ANOVA followed by Bonferroni post-hoc test). Scale bar= 50 µm.

The retinal sections were also subjected to immunofluorescence staining using beta-III tubulin which is a ganglion cell specific marker in the retina (Figure 4.12A) (Jiang et al., 2015). These results corroborate H and E staining observations and demonstrate significantly reduced βIII tubulin positive ganglion cells in the retinas of glutamate and microbead models ($p<0.001$). An increased number of βIII tubulin positive cells were observed in the bexarotene treated mice groups indicating that the drug has a protective effect on the RGCs in experimental glaucoma conditions ($p<0.05$) (Figure 4.12 B-C).

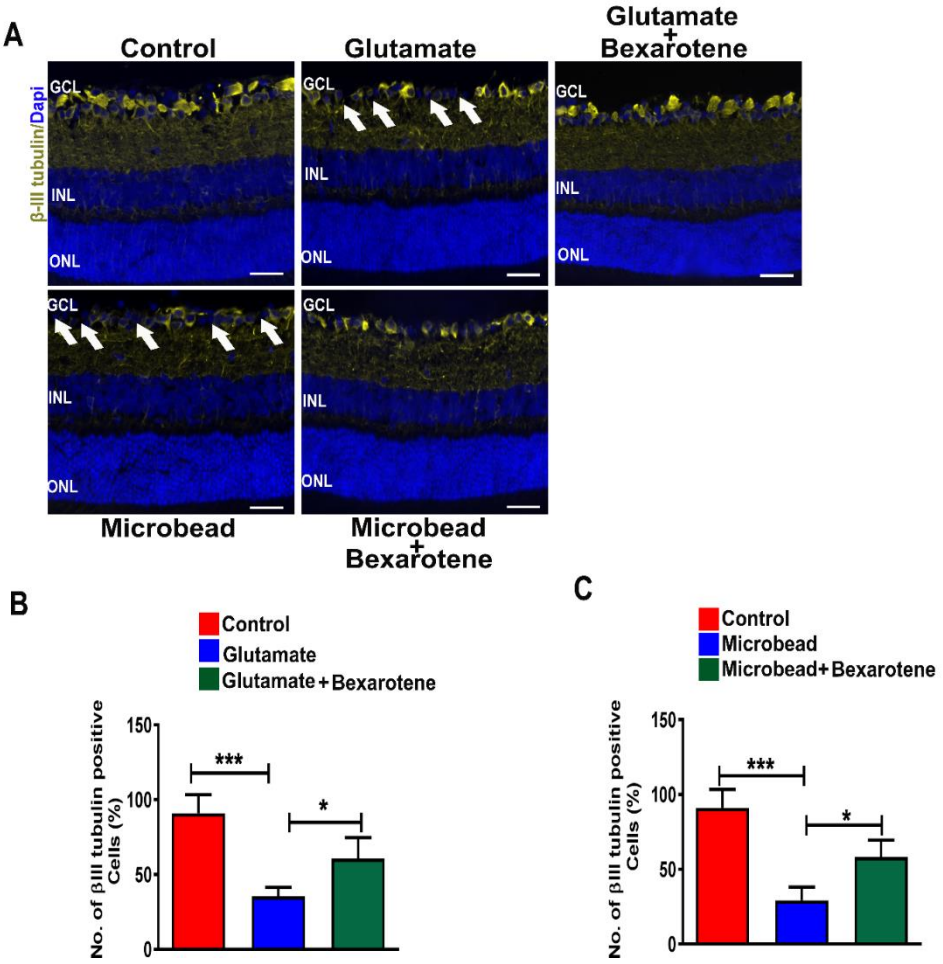

Figure 4.12 Immunostaining with β-III-tubulin to study RGC loss (A) Microscopic images of retinal sections that were immunostained by anti–β-III-tubulin (*green colour)* in control, glaucoma and glaucoma + bexarotene group. The white arrows indicating loss of RGCs caused by glutamate and microbead injections. DAPI (blue colour) was used as nuclear marker. (B) and (C) Quantification indicating significant changes in GCL density with bexarotene treatment (*$p< 0.05$, student's t test) (*$p< 0.05$, one way ANOVA followed by Bonferroni post-hoc test). Scale bar= 50 µm.

Axons of the RGCs converge to the optic nerve through which signals from retina are transmitted to higher visual centres in the brain. The protective effect of the RXR agonist on the RGCs was evaluated by monitoring axonal density of the optic nerve sections in experimental glaucoma and drug treated groups. Optic nerve sections were stained using Bielschowsky's silver staining and axonal density analysed using light microscopy (Figure 4.13A) (You et al., 2011). Whereas both the experimental glaucomatous injury models showed a loss of axonal density in the optic nerve (control 85.12 ± 6.27, glutamate 58.95 ± 5.22%, ****p< 0.0001, microbead 42.2±4.78 % (mean ± SD), ****p< 0.0001), the amount of loss was much reduced in the mice that were being pharmacologically treated with RXR agonist (glutamate 71.82± 5.88%;**p< 0.05, microbead 60.4± 4.29 %;**** p <0.0001, n=6 each) (Figure 4.13 B-C).

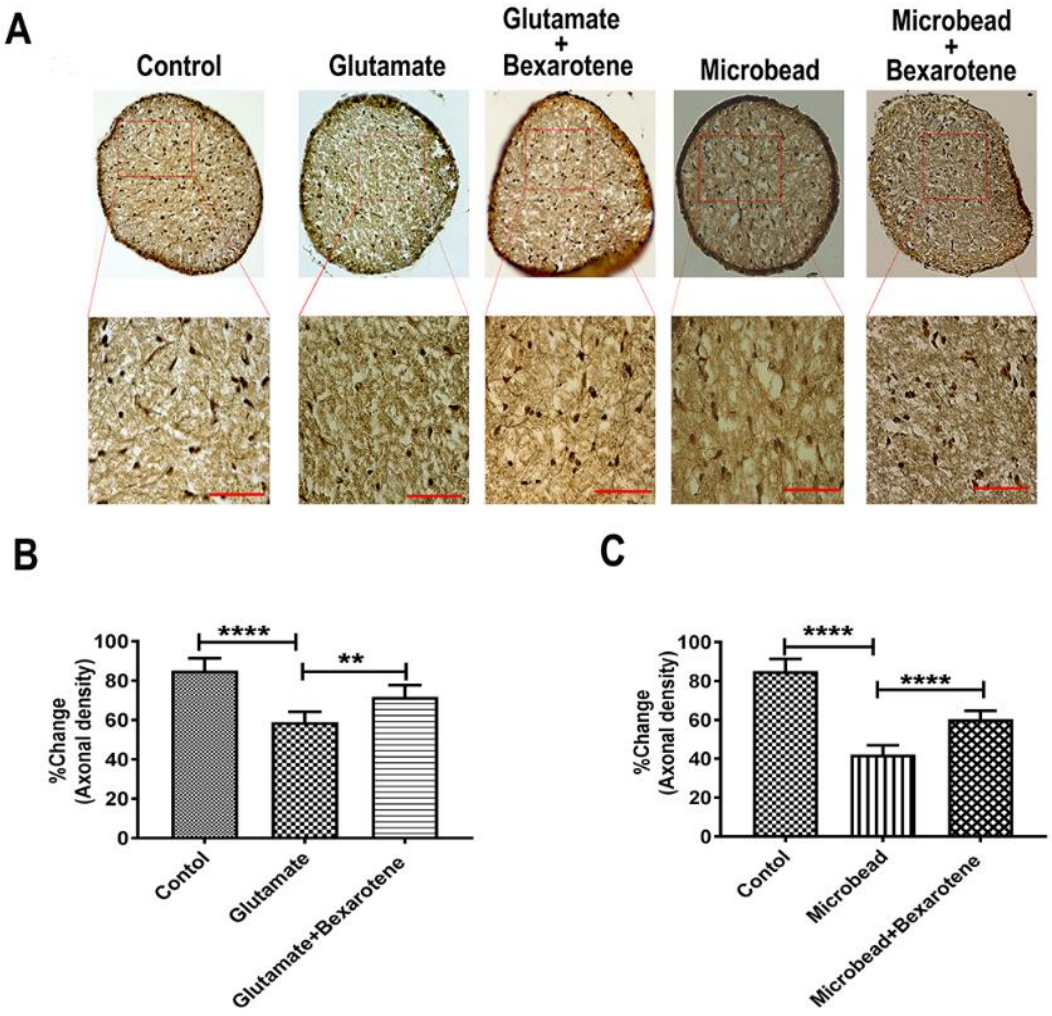

Figure 4.13 Prevention of axonal loss in optic nerve by bexarotene treatment (A) Representative images of Bielschowsky's silver staining of optic nerve sections in control, glaucoma and glaucoma +bexarotene group. (B) and (C) Quantification revealed that bexarotene significantly rescued axonal loss caused by glaucoma. **p< 0.05, **** p <0.0001, student's t test) (**p<0.05, ****p <0.0001, one way ANOVA followed by Bonferroni post-hoc test). Scale bar= 10 µm.

Results indicate that treatment with RXR agonist helps prevent RGC and optic nerve axonal loss in glaucoma conditions that also correlate with retinal electrophysiological protection conferred by the drug (Figures 4.10-4.13).

4.4 Discussion

This study examined the role of RXR activation in the retina in glaucoma using its pharmacological agonist bexarotene. Emerging evidence indicates that bexarotene plays a neuroprotective role in the CNS and has particularly been shown to reverse cognitive and behavioural deficits in AD models, although the extent of protection conferred by the drug requires further investigations (Certo et al., 2015, Riancho et al., 2015, Tousi, 2015, Bachmeier et al., 2013). Glaucoma has been shown to exhibit biochemical similarities in cellular neurodegenerative pathways with AD (Ghiso et al., 2013) and we and others have shown increased accumulation of amyloid β species in the retina in glaucoma conditions (Gupta et al., 2016). The objective of this study was to examine various biochemical pathways affected by the drug in the retina to enhance our understanding of the role of RXR in the retina in healthy and glaucoma conditions.

RXR are well expressed in the retina (Mori et al., 2001) and recent studies indicate that activation of these receptors promotes photoreceptor survival and suppresses apoptosis (German et al., 2013). This study demonstrated that glaucoma leads to a decrease in the expression of various RXRs in the retina, particularly in the inner retinal layers. Treatment with bexarotene during initial stages of the glaucomatous injury is effective in inducing an increased expression of the various RXRs in the retina. Further, RXR activation reduced the ER stress marker proteins in the inner retina in both of these models and suppressed the apoptotic pathway activation. Pharmacological upregulation of RXRs was demonstrated to be effective in protecting against the inner retinal functional and anatomical deficits induced by glaucoma in both of these experimental models.

Our results indicating loss of RXR expression in the inner retina in glaucoma are novel and RXR activation caused by bexarotene treatment is in agreement with previous reports

(Janakiram et al., 2012, Mounier et al., 2015, Riancho et al., 2015). RXR expression was decreased in both the mouse models of RGC injury indicating that effects on RXR expression are independent of IOP changes are associated with converging pathways associated with RGC degeneration. In addition, we also identified that RXR expression was downregulated in human glaucoma retinal tissues. We observed increased expression of RXR α, β and γ isoforms in the inner retina in bexarotene treated mice tissues using both western blotting and immunofluorescence approaches.

As in other neurodegenerative diseases, many studies have shown that ER (endoplasmic reticulum) stress pathway gets activated in the retina of glaucoma mice model and plays a key role in RGC death (Yasuda et al., 2014, Yang et al., 2016). Drugs showing anti-ER stress properties have been shown to prevent RGC death (Tsuruma et al., 2012, Nakamura et al., 2017). Bexarotene has been demonstrated to reduce protein aggregation and inhibit accumulation of cytoplasmic inclusion bodies and maintaining neuronal proteostasis (Riancho et al., 2015). Any disturbances in homoeostasis results in improper protein processing leading to ER stress with subsequent accumulation of structurally abnormal or unfolded proteins in the ER lumen (Zhang and Kaufman, 2006). Unfolded protein response eliminates misfolded proteins and decreases translocation of protein into the ER lumen (Schroder and Kaufman, 2005a). PERK (protein kinase RNA (PKR)-like ER kinase), is a major ER stress sensor (Harding et al., 1999, Yoshida et al., 1998, Mori et al., 1993) and previous studies found that the CHOP (transcriptional factor C/EBP homologous protein, also known as GADD 153) signal pathway plays a role in RGC death associated with ER stress (Doh et al., 2010). Activation of the p-PERK and GADD153 during chronic ER stress promotes pro-apoptotic pathways (Zinszner et al., 1998, Wang et al., 1996). Our studies found that bexarotene treatment diminished the expression of p-PERK and GADD 153 in both the models of experimental glaucoma. We also observed

reduced BAD (Bcl-2-associated death promoter) activation in the retina in drug treated animals. Increased endoplasmic reticulum (ER) stress has been demonstrated to contribute to the glaucoma pathology (Zode et al., 2014, Zode et al., 2011) and prolonged ER stress has been shown to play a key role in retinal apoptosis and cell death (Jing et al., 2012, Anholt and Carbone, 2013, Doh et al., 2010, Shimazawa et al., 2007, Yang et al., 2011, Anholt and Carbone, 2013). ER stress and unfolded protein response (UPR) has been implicated in both in the experimental acute (Awai et al., 2006) and chronic glaucoma models (Doh et al., 2010).

Previous studies have shown that amyloid precursor protein (APP) mediates ER stress-induced apoptosis through CHOP activation (Takahashi et al., 2009). Increased amyloid beta levels in the inner retina in glaucoma has been reported by us and other groups. We have seen that bexarotene reduces Aβ deposition in the mice retina under glaucomatous conditions. This observation supports the previous studies that have highlighted decreased amyloid levels in the brains of AD mice models that were treated with bexarotene (Mariani et al., 2017).

In order to understand, whether these biochemical changes were associated with any effects on retinal function, we tested the control and drug treated animals with electrophysiological recordings and then examined retinal structure histologically. Our *in vivo* retinal functional and ex-vivo structural analyses demonstrated that RXR targeting is effective in ameliorating inner retinal dysfunction caused by both acute and chronic models of experimental glaucoma.

The functional protection identified in the drug treated animals corresponded with protective effects on retinal laminar structure. Histological analysis indicated significant loss of the GCL in both of these glaucoma models and RXR activation lead to significant

protection against this loss in both of these models. Consequently, these results suggest that RXR activation protects the RGCs against both excitotoxic and IOP induced injury and can protect the retina under both acute and chronic glaucoma conditions. Immunological staining of the retinal sections by β III tubulin also indicated reduced numbers of RGCs in the glaucoma which were partially protected in RXR activated conditions. Furthermore, optic nerve axonal density evaluation using Bielschowsky's silver staining substantiated the fact that the drug was effective in significantly protecting the RGC axons in glaucoma conditions.

In summary, these findings support our conclusion that activation of RXR receptors, demonstrated in this case by bexarotene, offers a potential treatment for glaucoma, and that this may be via its anti-ER stress role. The results obtained from functional and structural data supports that bexarotene exerts neuroprotective effects on retina and optic nerve in normal as well as increased IOP models in mice. To this extent, RXR activation could be a novel strategy to manage glaucoma as a complementary therapy, possibly in combination with surgical intervention and IOP lowering therapies.

CHAPTER 5

PHARMACOLOGICAL TARGETING OF RXR RECEPTORS: *IN SILICO* STUDIES

Data presented in this chapter have been submitted for publication

Nitin Chitranshi, **Yogita Dheer**, Sanjay Kumar, Stuart L Graham, Vivek Gupta. Molecular docking, dynamics and pharmacology studies on Bexarotene as a retinoid X receptor agonist, nuclear receptor expressed in retina and brain. Manuscript submitted to Journal of Cellular Biochemistry.

Contribution to this manuscript: Experimental design, analyse data and contributed to writing the manuscript.

Abstract

Retinoid-x-receptors (RXR) are the nuclear receptors which upon binding with ligands undergo heterodimerisation in association with other nuclear receptors and regulate gene transcription. There are three different forms of RXR i.e α, β and γ and these isoforms are known to express in brain and retina. Retinoic acid, a RXR agonist, is the naturally occurring ligand and is believed to transactivate RXRs. Due to low concentration of endogenous retinoic acid, it is important to find other agonists of RXR receptors. We have computationally studied natural (retinoic acid and calcitriol) and synthetic (bexarotene, acitertin, tamibarotene and tazarotene) origin retinoids using the integrated approach of docking and molecular simulation to assess the binding affinities of these retinoids to RXR α, β and γ receptors. Docking and simulation studies suggest strong binding affinities of bexarotene with RXR α and β but not with γ isoform in comparison to retinoic acid. The hydrogen bonding and hydrophobic interactions predominantly contribute to the stability of bexarotene in RXR α and β complexes. Therefore, bexarotene can further be exploited for their potential to serve in treatment of brain and retinal disorders.

5.1 Introduction

Retinoid- X -receptors (RXRs) are characterized as ligand dependent transcription factors and are important member of the nuclear receptor superfamily (Dawson and Xia, 2012). There are three known RXR isotypes i.e RXRα, RXRβ and RXRγ, each of these RXR subtypes showed distinct tissue patterns (Lefebvre et al., 2010). RXRα is mainly expressed in liver, lung, muscle, kidney, epidermis, and intestine, RXRβ is found to be expressed ubiquitously and RXRγ is found in brain, cardiac and skeletal muscle (Germain et al., 2006). 9-cis-retinoic acid (9-cis-RA) was the first proposed natural ligand of RXR, but many researchers found it to be controversial. Later on, unsaturated fatty acids, particularly linoleic, linolenic, and docosahexaenoic acids were found to be natural RXR ligands which selectively bind and activate RXR but with poor affinities (Wolf, 2006). RXRs are master regulators of gene expression because of their ability to form both homodimers as well as heterodimers making RXRs to exert diverse pleiotropic functions in various biological processes, including cell development, differentiation, homeostasis and various aspects of metabolic signaling pathways (lipid and glucose metabolism) (Ahuja et al., 2003). They serve as promising target for cancer therapy. Not only in cancer but RXRs also play an important role as pharmacological interventions in various metabolic, autoimmune, and neurodegenerative disorders (Vaz and de Lera, 2012, Yamada and Kakuta, 2014, Thomas et al., 2012). RXR serve as common partner for many other nuclear receptors and activates various nuclear receptors complexes which prompted the search for novel RXR selective ligands. In this context, much effort has been focused on the development of synthetic retinoids or retinoids with more affinity and stability as compared to natural ligands.

The detailed studies to understand the retinoid actions in the development and functions of the eye can be utilized to understand the mechanistic insight of this important receptor that are involved in numerous cell process which are essential for normal eye development (Mori

et al., 2001). Mori *et al*, reported ocular abnormalities in RXRα null mutant's mice including dysfunction of the photoreceptors cells (Mori et al., 2004). The functional roles of RXR receptors are still unknown in inner part of retina, particular in retinal ganglion cells (RGCs) and it is of great importance to determine whether RXRs activation by its agonist provide retinal neuroprotection. Naturally occurring ligand (retinoic acid), has high binding affinity to all the three isoforms of RXRs receptors (Tsuji et al., 2015). There is little known about the binding affinity of other agonists to the RXRs.

To understand the structural information of RXRs protein, the X-ray crystal structures of ligand binding domain (LBD) was utilised to study the binding interaction affinity of natural and synthetic retinoids using computer-aided simulation approach of docking and molecular dynamics to predict the binding pattern and stability of the protein-ligand complex. Although crystal structure of RXR α and β share structure similarities but the computational studies presented here showed different binding competences of retinoids to the RXRs protein. This study will provide deep understanding of retinoids agonist role of RXRs proteins for emergence of drug target in various neurodegenerative diseases.

5.2 Methods

5.2.1 Macromolecule selection and its preparation

Crystal structure of the RXR α, β and γ ligand binding domain (LBD) was selected from protein data bank (PDB) (https://www.rcsb.org/). RXRα LBD only chain A was selected as it was bound to retinoic acid (PDB: 1FM9) (Gampe et al., 2000), RXRβ LBD (PDB:1UHL) (Svensson et al., 2003) and RXRγ (PDB:2GL8) (Renaud et al., 1995) from human. The selection of three isoform of RXR proteins were carried out based on resolution. 2.1 Å, 2.9 Å and 2.4 Å were the resolution for RXR α, β and γ LBD respectively. Surflex Dock v2.1 in

SYBYL-X v2.0 (Jain, 2007, Guette-Fernandez et al., 2017) was utilized for the proteins optimization. Binding pocket was determined from the bounded ligand for RXR α and β LBD using the active site residues whereas Castp server (Dundas et al., 2006) for the RXRγ LBD.

5.2.2 Ligand structure optimization

The 3D structures of the naturally occurring retinoids (i.e., retinoic acid and calcitriol) and synthetic retinoids Bexarotene, Acitertin, Tamibarotene and Tazarotene were downloaded from PubChem Chemical database (https://pubchem.ncbi.nlm.nih.gov/). All 6 compounds were optimized by Chemoffice 2004 (http://www.cambridgesoft.com/) with the default parameters and saved into protein databank format. Austin Model-1 (AM1) module in ChemOffice 2004 package was utilized to performed energy minimization (Chitranshi et al., 2016). The energy minimization step was continued till the root mean square (RMS) gradient value became smaller than 0.100 kcal/mol Å and later MOPAC (Molecular Orbital Package) of ChemOffice was used to re-optimization of AM1 energy minimized molecules till the RMS gradient attained a value lesser than 0.0001 kcal/mol Å (Menikarachchi et al., 2013).

5.2.3 Molecular docking of retinoids in RXRα, RXRβ and RXRγ binding domain

We employed AutoDock v.4.2 (Chitranshi et al., 2013) and Surflex-Dock, available in SYBYL-X v2.1, for the docking of natural and synthetic retinoids into the ligand binding site of RXRα, β and γ. Water molecules in the crystal structures were first cleaned and other ligands GI262570 from RXRα, N-(2,2,2-trifluoroethyl)-N-{4-[2,2,2-trifluoro-1-hydroxy-1-(trifluoromethyl) ethyl] phenyl} benzene sulphonamide and methoprenic acid from RXR β

were excluded for the better comparison and docking score (Jee et al., 2017). In order to compare the results from docking protocols, water molecules and other ligands GI262570 (RXRα),N-(2,2,2-trifluoroethyl)-N-{4-[2,2,2-trifluoro-1-hydroxy-1-(trifluoromethyl) ethyl] phenyl} benzene sulphonamide and methoprenic acid from RXR β were excluded for the better docking score (Jee et al., 2017). Macromolecule was treated as rigid body whereas rotatable bonds of the retinoid ligands were allowed to be free (Moitessier et al., 2004). Protein–ligand interactions was studied using rigid docking via AutoDock Tools. Rigid docking procedure was followed as describe previously (Chitranshi et al., 2015). Briefly, the macromolecules, atom and bond types were first assigned. The polar hydrogen atoms, Gasteiger charges and solvation parameters were added on macromolecules but the non-polar hydrogen atom was merged. Gasteiger charges were assigned and non-polar hydrogen atoms were merged in all retinoid ligands. Autogrid program was used to generate grid maps for each atom type in all the ligands and include the active site of RXR(s) proteins. Manually adjusted parameters was used for grid box dimension (60 x 60 x 60 A˚) and grid spacing (0.375 A˚) because to keep the ligand flexible around the protein active site. Empirical free energy function along with the Lamarckian genetic algorithm (LGA) was used to perform docking (Guan et al., 2017). Default parameters of LGA protocol like population size, energy evaluations, mutation rate, crossover and elitism were kept 150 individuals, 250,000, 0.02, 0.8 and 1.0 was kept respectively. Twenty different confirmations were generated for each ligand and has association with the binding free energy. Binding energies were determined using estimated inhibition constant (Ki) and were ranked according to the scores (Morris et al., 2013, Morris et al., 2008). Maestro v11 (Schrödinger Release 2017-4), Discovery Studio Visualizer v2.5 (Pettersen et al., 2004) and UCSF Chimera v1.11.2 (Chitranshi et al., 2015) software's were used for ligand-protein interactions and visualization.

5.2.4 Molecular dynamics simulation studies

Molecular dynamics was performed on the top hit compound screened from docking algorithm to study the binding stability of RXR-ligand complex. Due to strong binding affinity of bexarotene to the RXR protein, RXR-bexarotene complex was selected for MD studies. GROMACS v4.5.0 was used for MD studies applying GROMOS96 43a1 force field (Viet and Li, 2012). Solvated model system was used in a dodecahedron box and water molecules were assigned Simple point charge (SPC). PRODRG server generated Gromos force field topologies for ligand were used in GROMACS (Gharaghani et al., 2013). Gromacs inbuilt steepest descent algorithm was run to do the energy minimization by applying maximum force field of <10.0 kJ/mol/nm that was obtained in maximum 50,000 number of steps. Unfavourable contacts between each molecule were relaxed by using Varlet cut-off scheme. Constant temperature and pressure were maintained during the energy minimization systems till 100 ps. Berendsen thermostat, a modified program, v-rescale was selected for temperature coupling (Basconi and Shirts, 2013) with addition of pressure coupling in Parrinello–Rahman dynamics (Martonak et al., 2003) was applied. MD program was run using leap-frog integrator for 20 ns. Bond lengths constrains was calculated using LINCS (Hess, 2008) algorithm whereas trajectory files were analysed using GROMACS inbuilt scripts.

5.3 Results and Discussion

S.No.	Ligands	RXR Alpha [1FM9] (LEU436, ARG316, ALA327, ILE345, ILE268)		RXR Beta [1UHL] (ILE339, ARG387, ALA398, CYS503, LEU507)		RXR Gamma [2GL8] (K264, E417, E414, R278/Blind)	
		ΔG	Score	ΔG	Score	ΔG	Score
1.	Retinoic acid [CID444795]	-7.73	5.24	-8.70	4.38	-8.82	3.10
2.	Bexarotene [CID82146]	-10.31	0.12	-11.13	3.71	-7.74	4.65
3.	Acitretin [CID5284513]	-6.85	4.68	-6.11	1.11	-8.44	5.37
4.	Calcitriol [CID5280453]	-3.45	-17.99	-6.41	-11.02	-6.97	4.71
5.	Tamibarotene [CID108143]	-7.84	0.19	-6.03	-5.60	-8.50	1.44
6.	Tazarotene [CID5381]	-6.17	-1.15	-7.04	-2.27	-8.30	3.54

Table 5.1 Docking results of retinoids, based on lowest binding energy (ΔG) and scoring function of different RXR's-retinoids complex.

5.3.1 Interaction modes of different retinoids and RXRα

The docking protocol started with a population size of 150 individuals and 20 runs. The binding energy distribution of the natural and synthetic retinoids ligand poses were analysed to identify the best binding pose. The mean binding energy of the RXRα-retinoic acid complex was found to be -7.73kcal mol^{-1}, scoring 5.24. The interaction analysis of the least energy conformation revealed the presence of a conventional hydrogen bond between Arg316 and O2 atom of the retinoic acid (Figure 5.1 A). Bexarotene formed the hydrogen bond with Ala327 and Arg316 and pi-sigma bond with Phe313 and Ala271 residues of RXRα (Figure 5.1 B). The mean binding energy of bexarotene was found to be -10.31 kcal mol^{-1}, scoring 0.12 which was highest among the other retinoids. The mean binding energy

of acitretin was found lower than retinoic acid -6.85kcal mol^{-1}, score 4.68 and pi-sulphur and hydrogen bond interaction with Cys269 and Gln275 respectively were observed (Figure 5.1 C). The least binding energy (-3.45kcal mol^{-1}, score -17.99) was observed in calcitriol docking with RXRα. Arg316 and Ala319 residues formed the hydrogen bond with the hydroxy group of ligand (Figure 5.1 D). Arg316 and Ala327 of RXRα was found to be interacting commonly with tamibarotene and tazrotene retinoids (Figure 5.1 E, F). Tamibarotene has additional hydrogen bonding with Leu309 (Figure 5.1 E). Pi-Pi and amide-pi stacking was also observed in tamibarotene and tazrotene with Phe313 and Ala271 respectively. However, the binding score of last two retinoids was lower than bexarotene (-7.84kcal mol^{-1}, score 0.19 and -6.17kcal mol^{-1}, score-1.15 for tamibarotene and tazarotene respectively) (Table 5.1). Table 5.2 summarizes the different interaction of six retinoids conformations with RXRα.

S.No	Ligands	van der Waals	Hydrogen bond	pi-pi (sigma) bond	Alkyl/pi-Alkyl bond
1	Retinoic acid	None	Arg316	none	Val265, Ile268, Ala272, Leu309, Ile310, Phe313, Ile345, Cys432, His435, Leu436, Phe439
2	Bexarotene	None	Ala327, Arg316	Phe313, Ala271	Val265, Ile268, Ala271, Ala272, Trp305, Leu309, Ile310, Phe313, Ile324, Val349, Cys432, Leu436
3	Acitretin	Leu309	Gln275	None	Val265, Ile268, Ala271, Trp305, Ile310, Phe313, Ala327, Cys432, Leu436, Phe439
4	Calcitriol	None	Arg316, Ala319	None	Pro244, His315, Arg316, Ile318
5	Tamibarotene	Cys432	Arg316, Ala327, Leu309	Phe313	Val265, Ile268, Ala272, Ala271, Phe313, Val342, Ile345, Phe346, His435, Leu436, Phe439
6	Tazrotene	Cys432, Leu309	Arg316, Ala327	Ala271	Val265, Ile268, Ala272, Ala271, Val342, Ile345, His435

Table 5.2 RXRα-retinoids complex interactions analysis based on bond interaction with different amino acid residues.

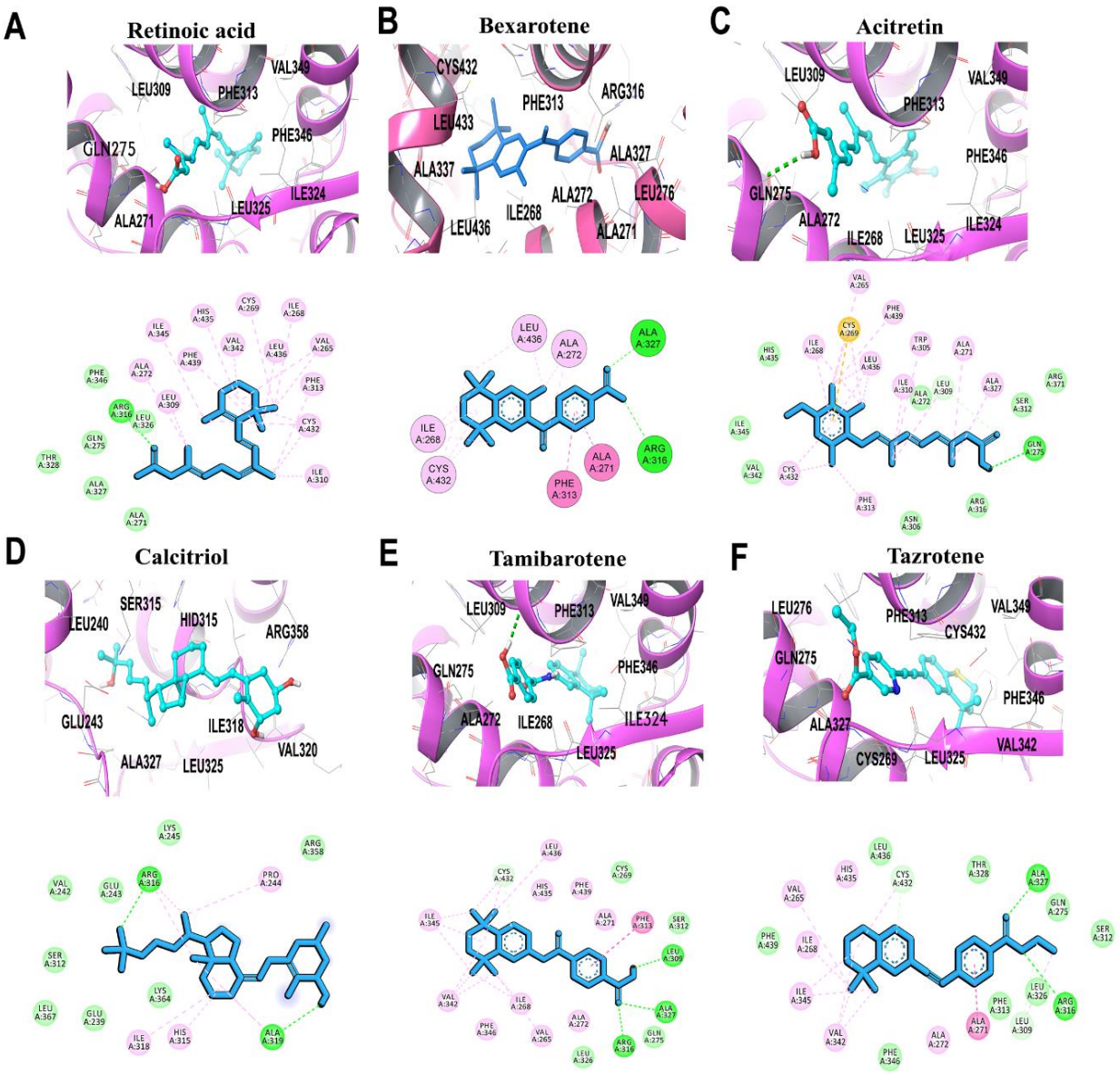

Figure 5.1 Molecular visual representation of different retinoids complexed with RXRα protein in three-dimensional (3D) and two-dimensional (2D) plot of (A) retinoic acid (B) bexarotene (C) acitretin (D) calcitriol (E) tamibarotene and (F) tazrotene. Van der Waals (light green), hydrogen bond (green), pi-pi stacking (dark pink), alkyl stacking (light pink) and pi-sulphur (yellow).

5.3.2 Interaction modes of different retinoids and RXRβ

As seen in Table 5.1, the lowest binding energy of bexarotene is highest than other RXR agonists, including retinoic acid. The lowest binding energy and score of six retinoids docked with RXRβ are tabulated in Table 5.1. Retinoic acid and bexarotene revealed the conservation of residues involved in the interactions with the ligand in majority of the conformations, however, owing to the ligand conformational flexibility, the interactions were formed with Arg387 residues but Gln346 and Leu380 are the additional hydrogen bond in retinoic acid-RXRβ docking complex (Figure 5.2 A). Hydrogen bond (Ala398) and Pi-sigma bond (Ile339) were also observed between bexarotene and RXRβ docking complex (Figure 5.2 B). A pi-cationic interaction (Lys435) was observed in acitretin docking including two hydrogen bonds with Thr349 and Arg442 residues (Figure 5.2 C). His386 form pi-sigma, pi-pi stacking and hydrogen bond with calcitriol (Figure 5.2 D), tamibarotene (Figure 5.2 E) and tazrotene (Figure 5.2 F) retinoids respectively. Gln313 and Ser383 was found to form a hydrogen bond with Calcitriol (Figure 5.2 D). In contrast, pi-cationic (Glu308) and pi-anionic (Arg387) along with Gln313 hydrogen bond was observed in tamibarotene docking (Figure 5.2 E). Similarly, a pi-cationic interaction (Lys435) was also observed in tazrotene and forming Arg387 hydrogen bond in the docking studies (Figure 5.2 F). Table 5.3 summarizes the different interaction of six retinoids conformations with RXRβ.

S.No	Ligands	van der Waals	Hydrogen bond	pi-pi (sigma) bond	Alkyl/pi-Alkyl bond
1	Retinoic acid	None	Gln346, Leu380, Arg387	None	Ile339, Ala342, Ile381, Phe384, Ala398, Val413, Phe417, Cys503, Leu507
2	Bexarotene	None	Ala327, Ala398	Ile339	Ile339, Ala342, Ala343, Leu380, Ile381, Phe384, Ala398, Val413, Phe417, Val420, Cys503, His506, Leu507
3	Acitretin	Leu350, Arg384	Thr349, Arg442	None	Val311, Leu380, His386, Arg387, Lys435
4	Calcitriol	Glu308	Gln313, Ser383, Asp390	His386	His386, Arg387, Ile389, Lys435
5	Tamibarotene	Lys435	Gln313	His386	Arg387, Ile389
6	Tazrotene	Glu312	His386, Arg387	None	Val311, His386, Arg387, Ile389, Arg432

Table 5.3 RXRβ-retinoids complex interactions analysis based on bond interaction with different amino acid residues.

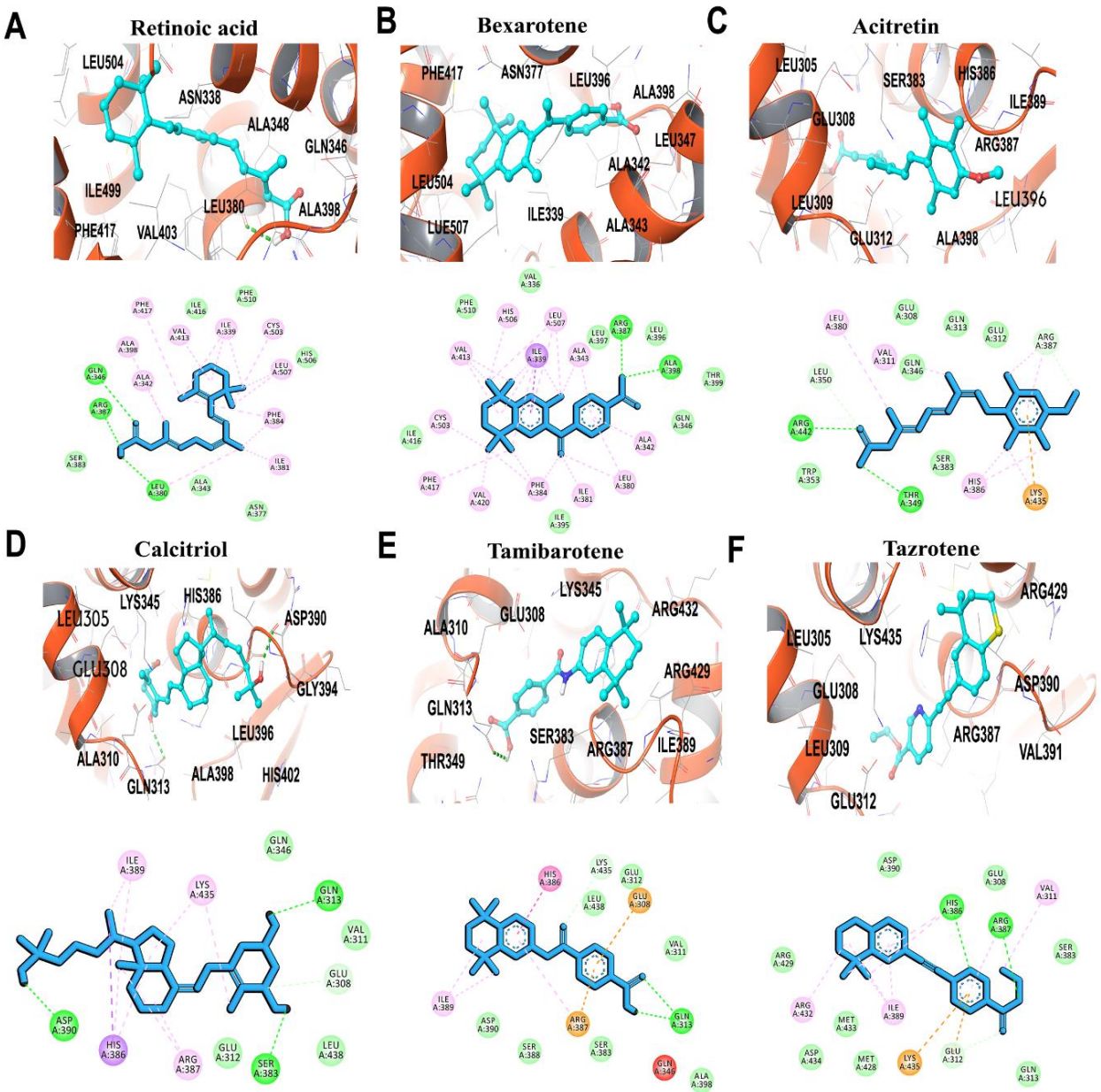

Figure 5.2 Molecular visual representation of different retinoids complexed with RXRβ protein in three-dimensional (3D) and two-dimensional (2D) plot of (A) retinoic acid (B) bexarotene (C) acitretin (D) calcitriol (E) tamibarotene and (F) tazrotene. Van der Waals (light green), hydrogen bond (green), pi-pi stacking (dark pink), alkyl stacking (light pink) and pi-cation/ anion (yellow).

5.3.3 Interaction modes of different retinoids and RXRγ

The binding modes of retinoids agonists with the binding site of RXRγ were identified using LigandFit program (Wang et al., 2016b). Figure 5.3 depicts the binding conformations of the retinoids in the ligand binding pocket of RXRγ. The active site of RXRγ comprises of mostly hydrophobic amino acids Leu55, Thr57, Trp84, Ser91, Leu105, Leu212, Leu215, Phe216 and Phe218. Among which Arg95 and Ala106 forms strong hydrophobic interactions with all the 6 ligands. There was no pi-pi sigma bond observed in retinoic acid binding to RXRγ buy Trp84, Cys211 and Phe216 form the pi-alkyl bond (Figure 5.3 A). Napthalene group of bexarotene formed pi-pi and pi-alkyl bond with Trp84 and Phe216 of RXRγ amino acids (Figure 5.3 B). Acitretin, tambibarotene and tazrotene showed similar pi-pi sigma bond with Trp84 but no pi-pi sigma bond was observed in calcitriol (Figure 5.3 C-F). Whereas Trp84 amino acid was seen to form pi-alkyl bond with calcitriol, tamibarotene and tazrotene (Figure 5.3 D-F). Table 5.1 summarises the docking energies and docking score for all the retinoids.

S.No	Ligands	van der Waals	Hydrogen bond	pi-pi (sigma) bond	Alkyl/pi-Alkyl bond
1	Retinoic acid	None	Leu88, Ser91, Arg95, Ala106	None	Trp84, Ile89, Phe92, Leu105, Cys211, Phe216
2	Bexarotene	None	Arg95, Ala106	Phe92, Leu105, Phe216	Trp84, Leu88, Phe92, Leu215
3	Acitretin	His214	Leu88, Arg95, Ala106	Trp84	Leu55, Leu88, Cys211, His214
4	Calcitriol	None	Ala50, Phe217	None	Leu55, Trp84, Leu88, Phe216
5	Tamibarotene	None	Leu88, Arg95, Ala106	Trp84, Phe92	Trp88, Leu88, Leu212, His214
6	Tazrotene	Leu88, Leu215	Arg95, Ala106	Phe92, Trp84	Leu55, Trp84, Leu88, Leu105 Phe216

Table 5.4 RXRγ-retinoids complex interactions analysis based on bond interaction with different amino acid residues.

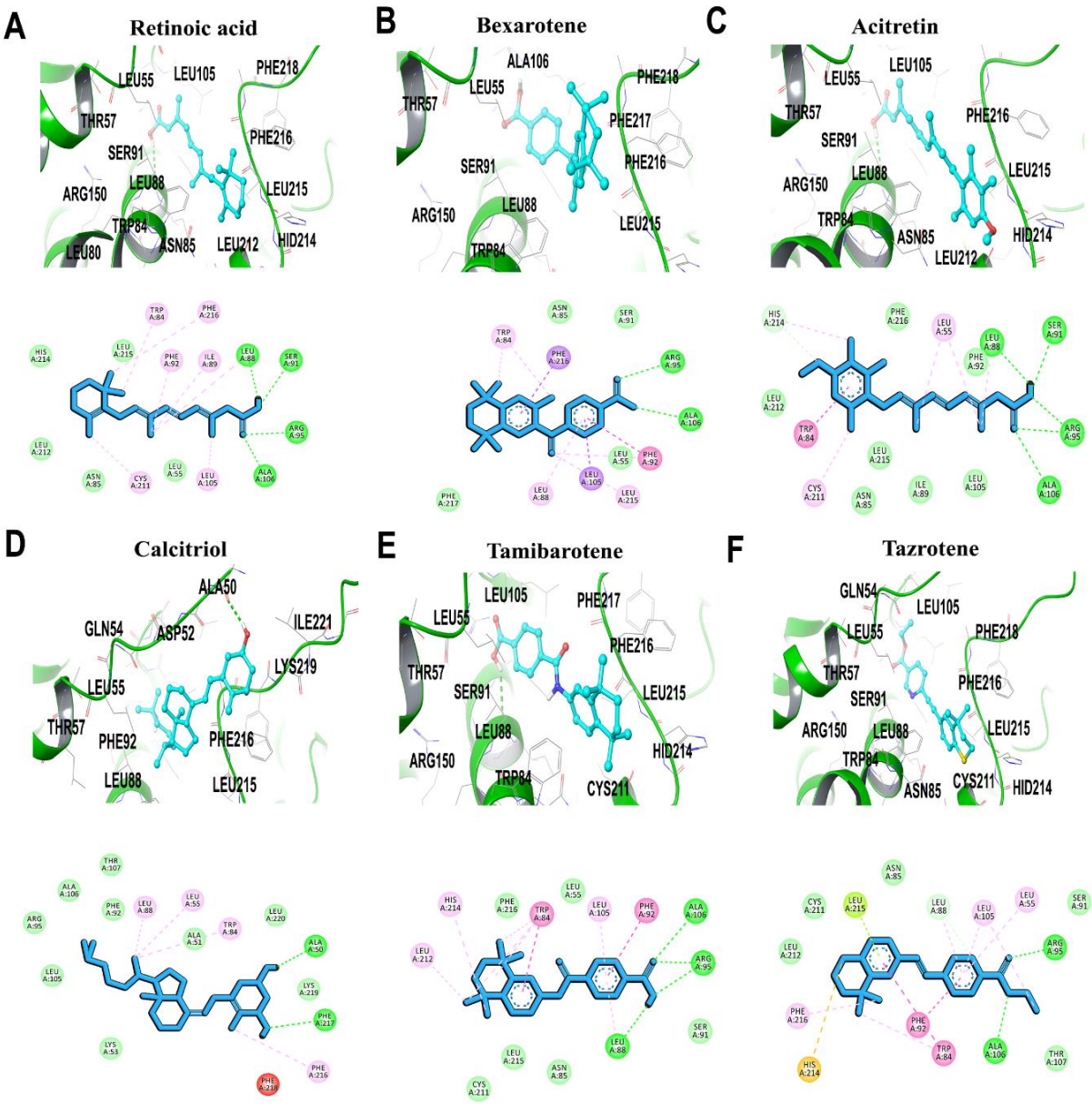

Figure 5.3 Molecular visual representation of different retinoids complexed with RXRγ protein in three-dimensional (3D) and two-dimensional (2D) plot of (A) retinoic acid (B) bexarotene (C) acitretin (D) calcitriol (E) tamibarotene and (F) tazrotene. Van der Waals (light green), hydrogen bond (green), pi-pi stacking (dark pink), alkyl stacking (light pink), pi-sigma (purple) and pi-sulphur (yellow).

5.3.4 Molecular Dynamics (MD) Simulation

Bexarotene complexed with RXR α, β and γ receptors was selected for MD simulation to estimate the stability of the docked complex over a longer timescale. Data from 20 ns MD runs provided important information on the stability and interactions of the retinoid agonist

Bexarotene when docked with the different RXR receptors. The RMSD of the protein backbone with respect to the initial positions of the atoms in the backbone was also evaluated for each RXR. It was found that the RMSD of RXR β was the lowest of those for the RXR: an average between 0.21-0.27 nm (Figure 5.4). This implies that the backbone of RXRβ shows less structural variation than the backbones of the other RXR when bound with bexarotene. The average RMSDs of the protein backbones of RXRα, and RXRγ were found in between 0.25-0.38 nm and 0.39-0.40 nm, respectively. The stable RMSD was found to remain constant between 0.1nm – 0.2nm. RXRα protein backbone atoms RMSD converged and remained stable between 0.2nm – 0.3nm. A constant RMSD suggests that protein has stable conformations with bexarotene in the binding mode (Figure 5.4 A) (Schreiner et al., 2012). Similar constant RMSD was observed in RXRβ between 0.2nm – 0.3nm that depicts same aspect of bexarotene binding and conformational stability (Figure 5.4 B). The fused ring of bexarotene demonstrated higher occupancy in the binding pocket and formed strong hydrogen bond with Arg387 and Ala398 throughout the simulation paradigm. On the other hand, RXRγ showed higher RMSD in comparison to other RXR isoform. RMSD between 0.3nm-0.4nm was observed in RXRγ-bexarotene complex (Figure 5.4 C). The reason for higher RMSD could be the effect of bexarotene binding in N-terminal loop region of LBD of RXRγ (Siddiqui et al., 2003). Overall, bexarotene showed constant RMSD between 0.05nm – 0.15nm in all the RXR forms. Some acceptable fluctuations were seen for bexarotene at 5nsec and 18nsec in RXRα, 4nsec, 7-10nsec in RXRβ and 4 – 5nsec, 10 – 14nsec and 19nsec in RXR γ dynamics complexes. The possible reason for these fluctuations was a distinctive shift of ketone bridgehead in bexarotene forming weak interactions away from the hydrophobic area formed by Phe313 in RXRα, Phe384, Leu380 and ILE381 in RXRβ, Phe92 and Leu105 in RXRγ. The stability of each RXR complex, the RMSD of the ligand with respect to the initial positions of the ligand's atoms was evaluated for each

complex (Figure 5.4). It was found that bexarotene presents the smallest RMSD (0.143 nm on average) when bound to RXRβ; the ligand remained in its original position for most of the simulation when docked to RXRβ. Stability of bexarotene remained constant as it completely fits in the binding pocket of RXRα and β LBD and does not show any interaction with loop regions of the protein. For the other RXR systems, the RMSD of bexarotene was found to be in stable state in the following order: RXRα (~0.173 nm) < RXRγ (~0.146 nm). These results imply that the conformation of bexarotene is stable when it is docked with RXRα, RXRβ and RXRγ. The loop domain from Glu214-Lys219 in RXRγ in the terminal regions showed interactions with bexarotene which make least stable complex of bexarotene-RXRγ.

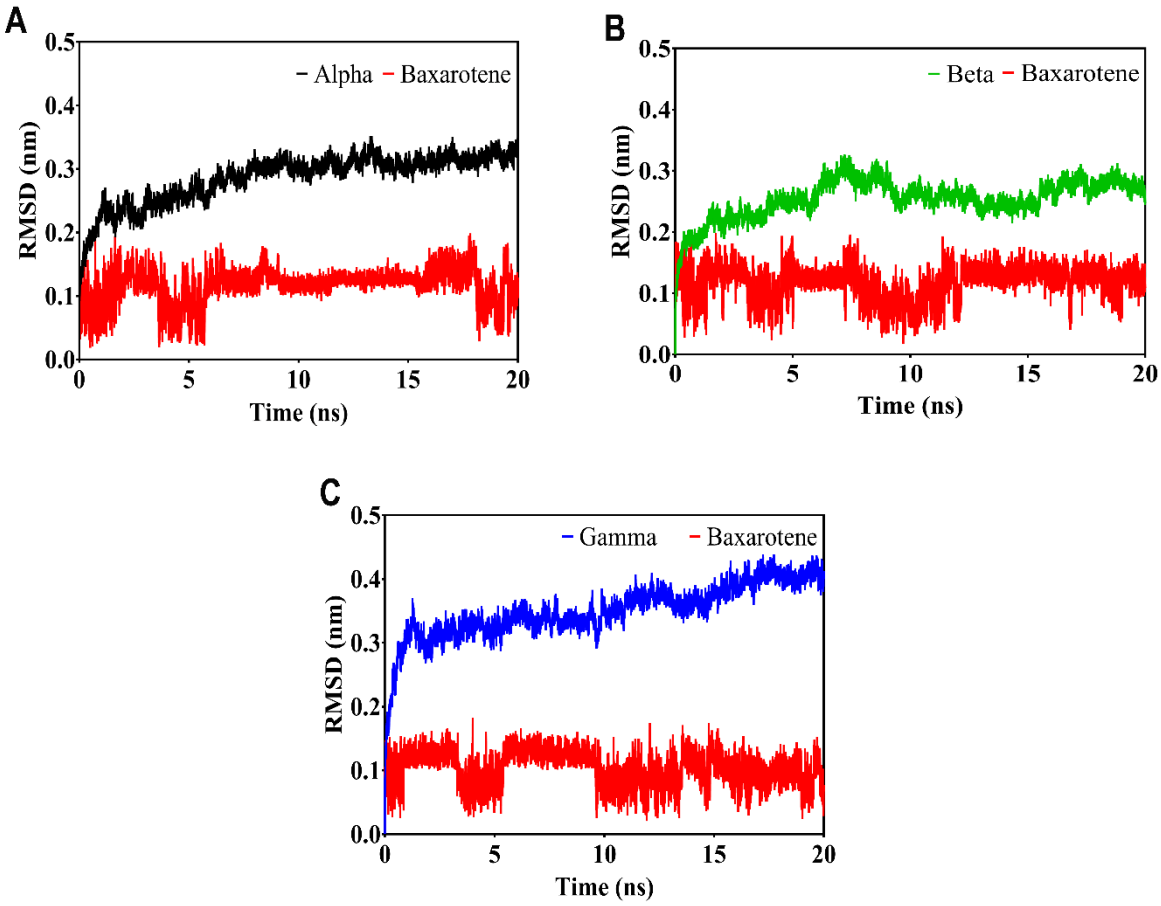

Figure 5.4 RMSD plot of (A) RXRα (B) RXRβ and (C) RXRγ with bexarotene ligand during 20 ns MD simulations. RXRα (black), RXRβ (green), RXRγ (blue) and bexarotene (red).

To elucidate the flexibility in ligand-protein complex, we examined the RMSF analysis (Figure 5.5). RMSF value of ligand-protein complexes gave a maximum value of 0.5nm for RXRα. Initial stable RMSF flexibility was observed between 0.1nm-0.21nm in RXRα protein backbone. Two large peaks of RMSF were seen between residues at 400-415 and 445-447 that comes from alpha helical region and fluctuated between 0.25nm-0.5nm (Figure 5.5 A). This large peak was due to binding of bexarotene that affects the second structure of RXRα. There was no change in secondary structure and any large fluctuations in RMSF was observed in the loop region of RXRβ when bexarotene bind to RXRβ (Figure 5.5 B). Like RXRα, RXRγ backbone atoms from 214-224 showed high fluctuations between 0.21nm-0.52nm RMSF in the loop region (Figure 5.5 C). Based on RMSD and RMSF plots, we can deduce that the RXRβ-bexarotene system is the most stable; in the other systems, the ligand attempts to find a better docking conformation throughout the 20 ns of simulation.

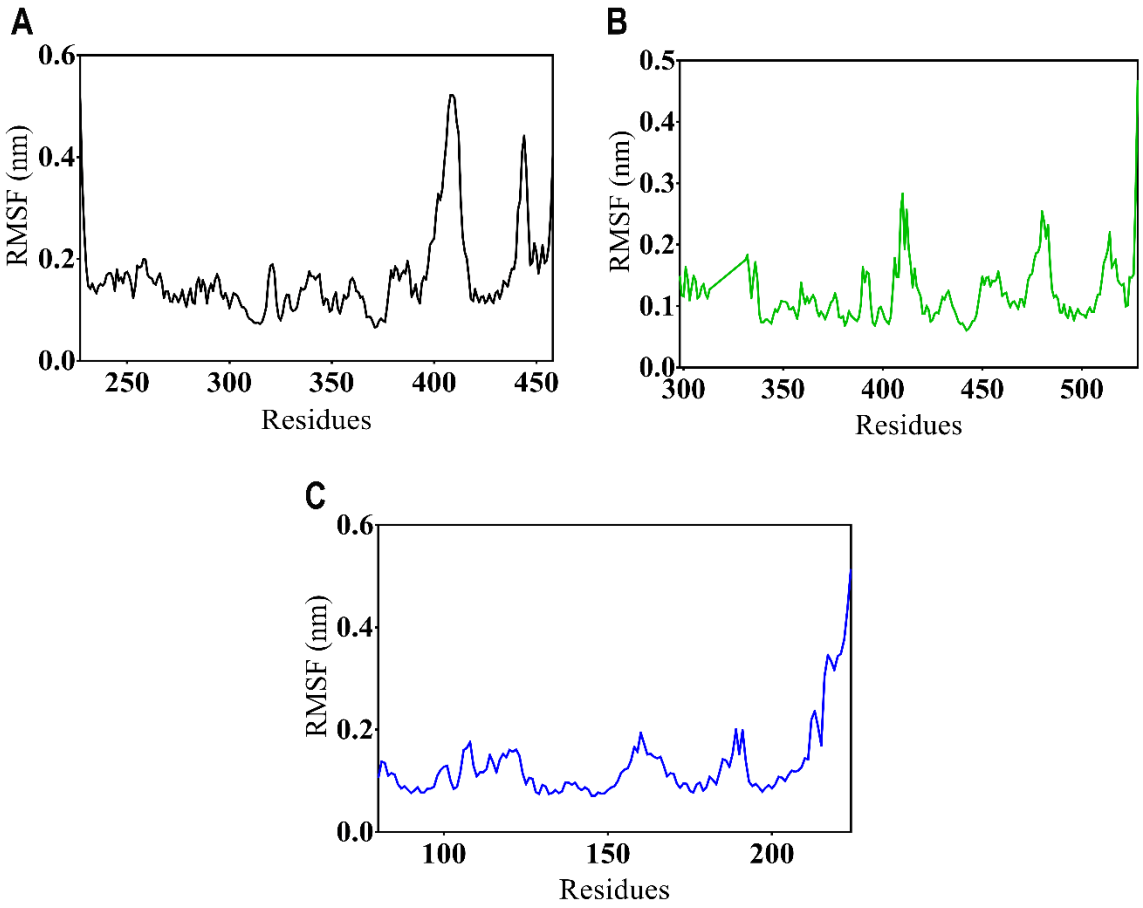

Figure 5.5 Binding effect of bexarotene on ligand binding domain of (A) RXRα (black) (B) RXRβ (green) and (C) RXRγ (blue) during 20 ns MD simulations.

5.3.5 Trajectory motion of RXR's-Bexarotene during different time scale

In order to determine the changes in bexarotene-RXR's complex, the snapshot at different time scales (0ns, 5ns, 10ns, 15ns and 20ns) were captured. We analysed the phenotypic modifications within the bexarotene-RXR's proteins (Figure 5.6). RXRα and β structure start-off with an open confirmation from 0ns time scale and continued till 20ns simulations, on the contrary no major unfolding and structure disintegration was observed in these protein-ligand complex (Figure 5.6 A-D). While bexarotene in RXRγ protein complex broke down within 5 ns and continued for 15 ns simulations (Figure 5.6 E-F). Yellow, cyan and magenta colours are shown to represent the breakdown of bexarotene at 5 ns, 10 ns and 15

ns respectively. This breakdown was not continuous and bexarotene re-arranged its structure in 20 ns (shown in green colour), Figure 5.6 F, in LBD of RXRγ. Simulation studies provided a positive indication of strong binding of bexarotene to RXRα and β but conformational breakdown of bexarotene in RXRγ seems to make the ligand unstable in LBD of RXRγ.

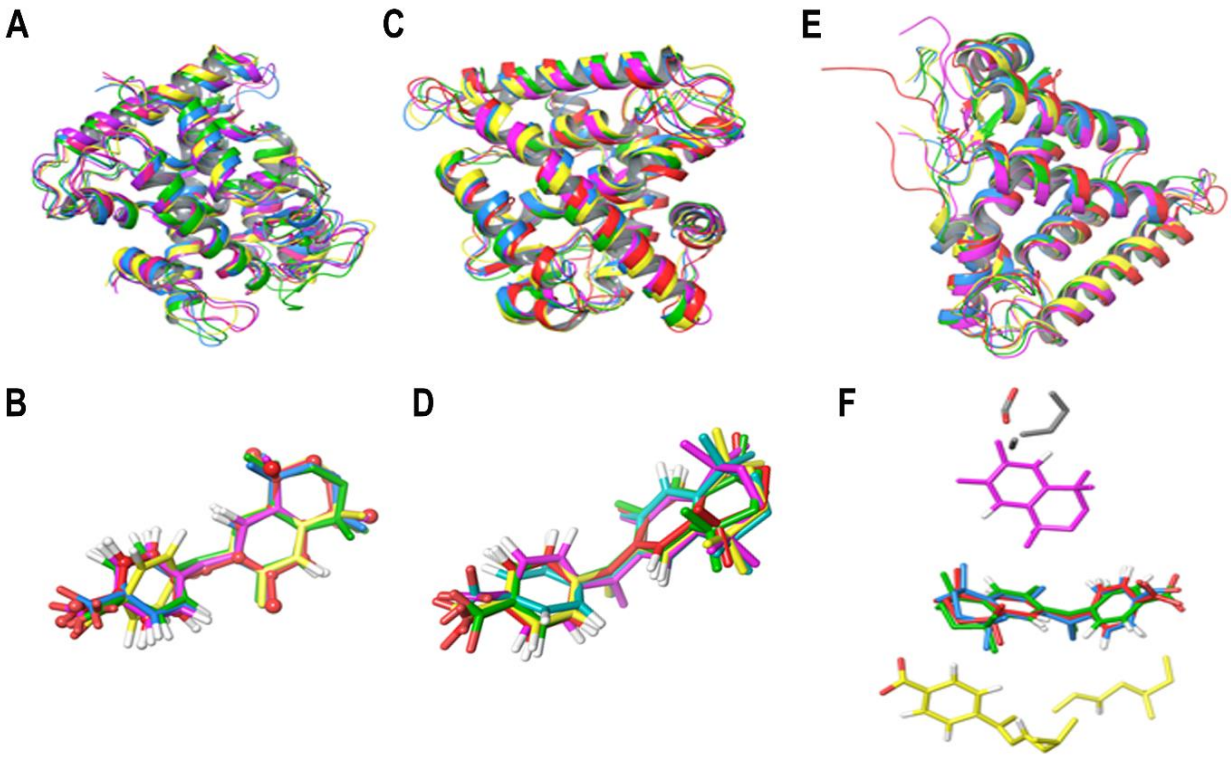

Figure 5.6 Depiction of bexarotene complex with different RXR's at distinctive simulation time executions (A) RXRα trajectory (B) bexarotene binding trajectory in RXRα (C) RXRβ trajectory (D) bexarotene binding trajectory in RXRβ (E) RXRγ trajectory and (F) bexarotene binding trajectory in RXRγ at 0ns (red), 5ns (green), 10ns (cyan), 15ns (magenta) and 20ns (yellow).

5.4 Conclusion

In present study, we aimed to investigate the 6 different retinoids agonists candidates of RXR receptors isoforms (α, β and γ), and predicted the binding affinities of retinoic acid, bexarotene, calcitriol, acitertin, tamibarotene and tazarotene. Bexarotene, had potent binding affinities to LBD of RXR α and β than retinoic acid. However, the binding affinity of bexarotene in RXR γ LBD was weaker than retinoic acid. Bexarotene showed strong hydrogen bond with Ala327 and Arg316 in RXRα LBD, and Arg387, Ala398 in RXRβ LBD. However, a weak hydrogen bond (Arg95 and Ala106) of bexarotene was observed in RXRγ. Molecular dynamic simulation was carried out to evaluate the stability of bexarotene-RXRs complex. RMSD and RMSF analysis demonstrated insights on docked-complex stability over longer period in case of RXR α and β but stability loss was observed in RXR γ-ligand complex after 5 ns of simulation. Thus, the combined docking and dynamic approach could be utilized to study bexarotene as potential RXR agonist and further in vitro/ in vivo experimental methods can be used to confirmed potential of this anti-cancer drug as alternative to other neurodegenerative disorders.

CHAPTER 6

IDENTIFICATION OF AGE-RELATED NEURODEGENERATIVE DISEASE ASSOCIATED PATHWAYS IN RETINAL AND VITREOUS PROTEOME FROM HUMAN GLAUCOMA EYES

LXR/RXR and FXR/RXR pathways activation was confirmed in human retinal and vitreous tissue samples by comparative investigative proteomics analysis. Protein profiles of 10 retinal and vitreous tissue samples obtained from open angle glaucoma patients were compared with age matched controls. Differentially expressed proteins were mapped for biological roles in canonical pathways using Ingenuity Pathway Analysis software.

Data presented in this chapter have been published as:

Mehdi Mirzaei, Veer B Gupta, Joel M Chick, Todd M Greco, Yunqi Wu, Nitin Chitranshi, Roshana Vander Wall, Eugene Hone, Liting Deng, **Yogita Dheer,** Mojdeh Abbasi, Mahdie Rezaeian, Nady Braidy, Yuyi You, Ghasem Hosseini Salekdeh, Paul A Haynes, Mark P Molloy , Ralph Martins, Ileana M Cristea, Steven P Gygi, Stuart L Graham and Vivek K Gupta. Age-related neurodegenerative disease associated pathways identified in retinal and vitreous proteome from human glaucoma eyes. *Scientific Reports*. doi: 10.1038/s41598-017-12858-7.

Contribution to this manuscript: Analyses and interpretation of the data, preparation of retinal and vitreous samples, performed protein estimation as well as western blotting and writing the manuscript.

Abstract

Glaucoma is a chronic disease that shares many similarities with other neurodegenerative disorders of the central nervous system. This study was designed to evaluate the association between glaucoma and other neurodegenerative disorders by investigating glaucoma-

associated protein changes in the retina and vitreous humour. The multiplexed Tandem Mass Tag based proteomics (MS3-TMT) was carried out on retinal tissue and vitreous humour fluid collected from glaucoma patients and age-matched controls followed by functional pathway and protein network interaction analysis. About 5000 proteins were quantified from retinal tissue and vitreous fluid of glaucoma and control eyes. Of the differentially regulated proteins, 122 were found linked with pathophysiology of Alzheimer's disease (AD) and other common neurodegenerative conditions. Pathway analyses of differentially regulated proteins indicate defects in mitochondrial oxidative phosphorylation machinery. The classical complement pathway associated proteins were activated in the glaucoma samples suggesting an innate inflammatory response. Majority of the common differentially regulated proteins in both tissues were members of functional protein networks associated brain changes in AD and other chronic degenerative conditions. Identification of previously reported and novel pathways in glaucoma that overlap with other CNS neurodegenerative disorders promises to provide renewed understanding of the aetiology and pathogenesis of age related neurodegenerative diseases.

6.1 Introduction

Glaucoma represents one of the major causes of irreversible blindness in the elderly. This complex degenerative disorder is characterised by progressive and selective loss of retinal ganglion cells (RGCs) (Guo et al., 2005) in the inner retina. The axons of RGCs form the core component of the optic nerve, relaying visual information detected by the retina to the brain. Therefore, a loss of structural and functional integrity of RGSs plays a major role in the development and progression of visual deficits reported in common optic neuropathies

and particularly in glaucoma (Weinreb et al., 2014). While several risk factors have been identified that are associated with premature loss of RGCs, high intraocular pressure is currently the most significant risk factor in glaucoma (Heijl et al., 2002). The molecular mechanism(s) that result in RGC dysfunction in various optic neuropathies however remain ill-defined. Greater understanding of the underlying neurodegenerative processes is crucial for the development of effective therapeutic strategies for glaucoma.

It is increasingly recognized that glaucoma and AD show overlap of several molecular pathological features including β-amyloid accumulation in the retina (Ghiso et al., 2013, Frost et al., 2010, Gupta et al., 2016). AD is characterized by the presence of extracellular plaques containing abnormal amyloid β (Aβ) aggregates as well as intracellular neurofibrillary tangles composed of hyper-phosphorylated tau, a microtubule-associated protein localised in axons. Clinically, patients exhibit a progressive decline in memory, cognition and learning, which are accompanied by visual and ocular manifestations, similar to glaucoma (Frost et al., 2010, Roberson et al., 2007). These pathological features may explain the impaired contrast sensitivity and motion perception often reported in AD patients. There is evidence for a positive association of glaucoma in patients with AD, and the involvement of Aβ and hyper-phosphorylated tau in ocular degeneration in glaucoma patients (London et al., 2013, Sivak, 2013).

We have previously demonstrated that AD is associated with ocular deficits including inner retinal thinning and impaired retinal electrophysiological response in animal models of AD (Gupta et al., 2016). Similar anatomical and functional deficits predominantly localised to the inner retina have also been reported in clinical studies in AD subjects (Lu et al., 2010). However, the molecular bases of these links remain obscure mainly due to the limited availability of data concerning biochemical and “omics” related retinal changes either in

glaucoma and/or AD. Importantly, the lack of sufficient information about which molecular changes are involved in either glaucoma or AD pathology precludes either an early and accurate disease diagnosis, or the development of critical target-based therapeutic development.

In this study, we investigated the molecular basis of glaucoma pathogenesis by taking a systems level perspective of the retina and vitreous proteome using unbiased quantitative proteomics approaches. Large-scale proteome profiling of human post-mortem tissues were conducted, comparing protein abundances in vitreous and retinal tissues from 'control' and glaucoma eyes. This study provides significant mechanistic advancements into the common molecular pathways implicated in the pathogenesis of glaucoma and other neurological disorders with a particular focus on AD as a representative neurodegenerative condition.

6.2 Materials and Methods

6.2.1 Human eye samples, retina and vitreous extraction

Frozen human post-mortem eye tissues (20 donors) from open angle glaucoma (9 male, 1 female) and age matched control (8 male, 2 female) subjects (Lions NSW Eye Bank), Australia were used in the study. Both the retinal and vitreous tissues were examined (average ages: control 64.5±10, n=10 and glaucoma: 71.5 ±8.5, n=10, respectively). Tissues were obtained within 6 hours after death. None of the subjects had a known history of AD, Parkinson's disease, ocular surgery, macular degeneration or other ocular disorders affecting visual function. Frozen eyes were allowed to thaw and washed with PBS; retina, optic nerve head and vitreous tissues were carefully removed from the eyecups without the retinal pigment epithelium (RPE) layer contamination under the surgical microscope (Carl Zeiss, Oberkochen, Germany).

6.2.2 Preparation of protein samples

Retina and vitreous tissues were lysed in lysis buffer (20 mM HEPES, pH 7.4, 1% Triton X-100, 1 mM EDTA) containing 10 μg/ml aprotinin, 10 μM leupeptin, 1 mM PMSF and 1 mM $NaVO_3$, 100 mM NaF, 1 mM Na_2MoO_4 and 10 mM $Na_4P_2O_7$ and sonicated using a probe sonicator (3 pulses/15s/50 Hz with 20s between each pulse). Insoluble materials were removed by centrifugation at 15,000 g for 10 min at 4°C. Extracted proteins were reduced with 5mM DTT for 15 minutes at room temperature, and then alkylated with 10mM iodoacetamide for 30 minutes in the dark at room at 4°C. The alkylation reaction was then

quenched with addition of 5mM DTT for 15 minutes in the dark. In order to remove the interfering detergents and contaminants, proteins were precipitated using the chloroform methanol precipitation protocol (Wessel and Flügge, 1984). The protein pellet was resuspended in 200 µl 8M Urea in 50mM Tris (pH 8.8). Protein concentration was determined by BCA assay kit (Pierce, Rockford, USA) using bovine serum albumin (BSA) as a standard. Dual digestion was carried out on 150ug protein, initially with Lys-C (Wako, Japan) at a 1:100 enzyme: protein ratio overnight at room temperature, followed by Trypsin (Promega, Madison, WI) at a 1:100 enzyme: protein ratio for at least 4 hours at 37 °C. Samples were then acidified with TFA to a final concentration of 1% (pH 2 to 3) and desalted using SDB-RPS (3M- Empore) Stage Tips (Kulak et al., 2014).

6.2.3 TMT labelling

To accommodate the 40 biological samples (10 control and 10 glaucoma for retina and vitreous tissues each), four separate 10plex TMT experiments were carried out (two TMT experiments for retina and two for vitreous tissues). A detailed experimental design and TMT workflow is illustrated in Figure 6.1. Briefly, dried peptides were resuspended in 200 mM HEPES (pH 8.2) and peptide concentration was measured using the MicroBCA protein assay kit (Thermo Scientific- Rockford, IL). 70 µg of peptides from each sample were subjected to TMT labelling with 0.2 mg of 20µl reagent per labelling reaction. Labelling was carried out at RT for an hour with occasional vortexing. To quench any remaining TMT reagent and reverse tyrosine labelling, 8 µl of 5% hydroxylamine was added to each sample, this was followed by vortexing and incubation for 15 mins at RT. For each of the four 10plex experiments the 10 labelled samples were combined, and then dried down by vacuum centrifugation. Each of the TMT experiments was fractionated by

basic, reversed-phase isocratic step elution using reverse phase spin columns (Pierce). Samples were loaded onto the reverse phase cartridges and elution was performed using 12 fractionation steps with the following acetonitrile concentrations in 10 mM ammonium bicarbonate (5, 10, 12.5, 15, 17.5, 20, 22.5, 25, 27.5, 30, 40, 80% ACN). These fractions were then pooled into 6 subsets (Fraction 1-7, 2-8, 3-9, 4-10, 5-11, 6-12). Each fraction was dried and then desalted using SDB-RPS (3M- Empore) Stage Tips.

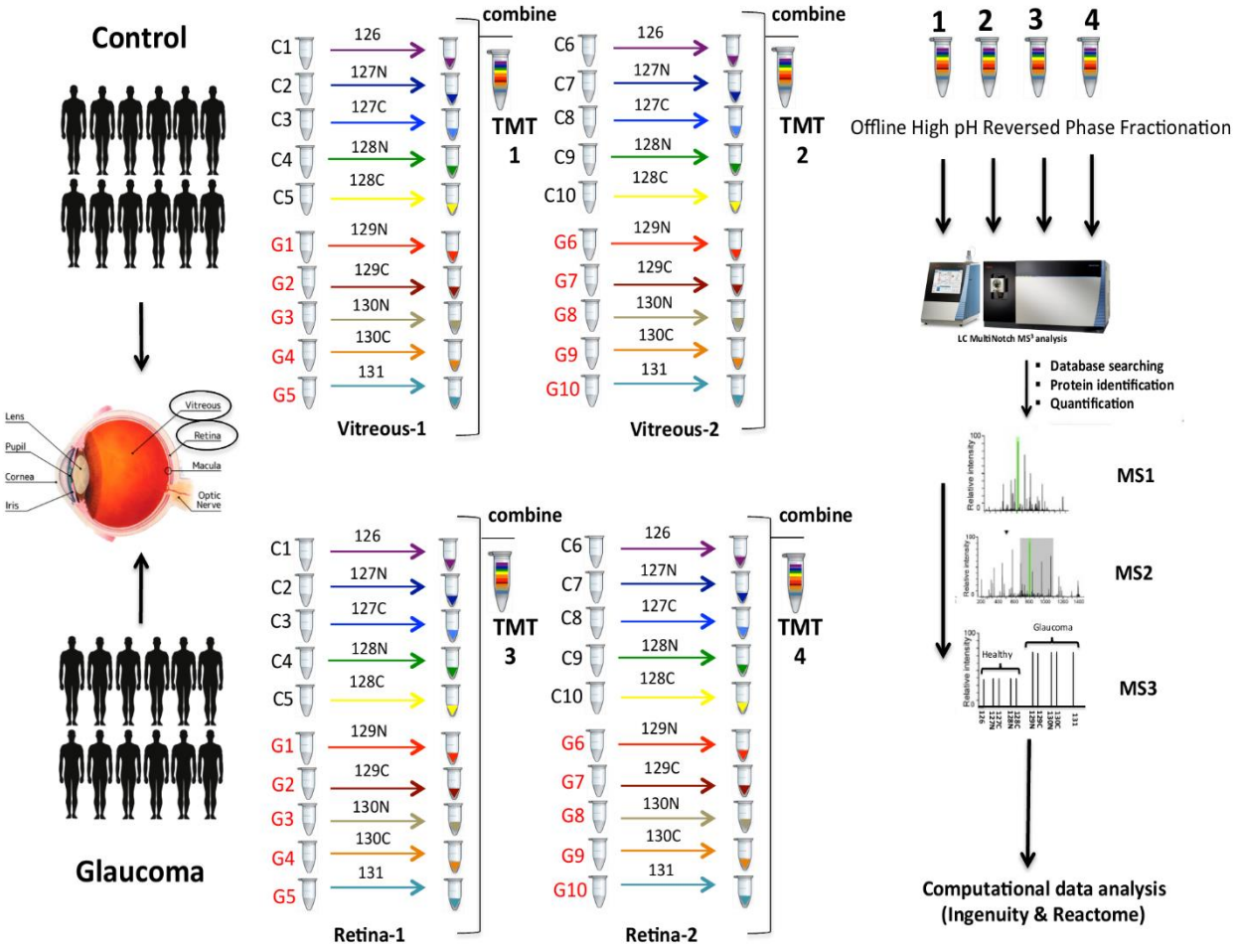

Figure 6.1 Experimental design and TMT labelling workflow of the experiment. Human retinal and vitreous tissues were extracted from postmortem eyes of control (age: control 64.5±10, n=10) and glaucoma subjects (age: 71.5±8.5, n=10). Extracted proteins form 40 samples subjected to reduction, alkylation and subsequent digestion with Trypsin and Lys-C. Extracted peptides were quantified and labeled in a 10 plex TMT reaction. Four TMT experiments were carried out to accommodate all the biological replicates. Briefly, 2 sets of 5 control and 5 glaucoma replicates of retina tissue were used in TMT 1 and 2 experiments, and the same design was used for vitreous samples in TMT3 and TMT4 experiments. Labelled samples within each TMT experiment were pooled together, then were fractionated by basic, reversed-phase isocratic step elution using reverse phase spin columns, and analyzed by LC-ESI-MS/MS on ThermoFisher Orbitrap Fusion mass spectrometer (SPS-MS^3 method). Functional pathway and protein network data analysis was performed using Ingenuity and Reactome pathway analysis.

6.2.4 Liquid chromatography electrospray ionization tandem mass spectrometry (LC-ESI-MS/MS)

Fractionated peptide samples were reconstituted in 30 µl of 0.1% formic acid and 10 µl of samples were analysed using an Orbitrap Fusion Tribrid-MS (Thermo Scientific, USA) equipped with an ultra-high pressure liquid chromatography system (Proxeon). Peptides were separated for 3-hours on a reverse phase column with a gradient of 6-30% acetonitrile in 0.125% formic acid at a flow rate of ~400 nl/min. In each data collection cycle, one full MS scan (400-1400 m/z) was acquired in the Orbitrap (120,000 resolutions at 400 m/*z* and an AGC of 2 x 10^5). MS3 was performed using HCD with 55% collision energy and reporter ion detection in the Orbitrap with an AGC of 150,000 ions, a resolution of 60,000 and a maximum ion accumulation time of 150 ms. Peptide fragmentation and collection of reporter ion spectra were performed using the synchronous precursor selection (SPS)-MS^3 method (McAlister et al., 2014). In this method, first MS2 analysis was conducted using CID fragmentation on the top 10 most intense ions with following settings: normalized collision energy of 35%, AGC $4x10^3$, isolation window 0.5 Da, maximum ion accumulation time 150 ms with 40 seconds of dynamic exclusion. Following each MS2 scan, for the MS3 analyses, precursor isolation was performed using a 2.5 Da window and fragmented in the ion trap using CID as above, except with an AGC setting of 8,000. Multiple fragment ions (SPS ions) were co-isolated and further fragmented by HCD at normalized collision energy (NCE) of 37.5%. Selection of fragment ions was based on the previous MS2 scan and the MS2-MS3 was conducted using recently described sequential precursor selection (SPS) methodology (McAlister et al., 2014).

6.2.5 Database searching/quantification and statistical analysis

In-house software tools were used to convert RAW file to the mzxml format (Chick et al., 2016). Correction of erroneous charge state and monoisotopic m/z values were performed using method detailed in Huttlin et al (Huttlin et al., 2015). Sequence assignment of MS/MS spectra were made with the Sequest algorithm (Eng et al., 1994) using an indexed human Uniprot database prepared with forward and reversed sequences concatenated as per the target-decoy strategy (Elias and Gygi, 2010). Data searches were conducted using cysteine carbamidomethylation and TMT on the peptide N-termini and lysine residues as static modifications, oxidation of methionine as a dynamic modification, precursor ion tolerance of 20 ppm and a fragment ion tolerance of 0.8 Da (for CID). Sequest matches were filtered using linear discriminant analysis to a false discovery rate (FDR) of 1% at the peptide level based on matches to reversed sequences, as previously reported (Elias and Gygi, 2010). The final peptide-level FDR fell well below 1% (~0.2% peptide level). A reductionist model was used for assignment of peptides to protein matches, where all peptides were explained using the least number of proteins. Protein rankings were generated by multiplying peptide probabilities and the dataset was finally filtered to 1% protein FDR.

Quantitation of peptides using TMT reporter ions was performed as previously published (McAlister et al., 2012, Chick et al., 2016). Briefly, a 0.003 Th window centred on the theoretical m/z value of each reporter ion was recorded for each of the 10 reporter ions, and the intensity of the signal closest to the theoretical m/z value was recorded. TMT signals were also corrected for isotope impurities as per manufacturer's documentation. Peptides were only considered quantifiable if the total signal-to-noise (S/N) for all channels

was >200 and a precursor isolation specificity of >0.75. Within each TMT experiment, reporter intensities values were normalized by summing the values across all peptides within each channel and then each channel was corrected so that each channel had the same summed value. Protein quantitation was performed by summing the normalized S/N values for all peptides assigned to a given protein. The protein quantitations from the two TMT experiments for each respective sample type (vitreous and retina) were aggregated into a single report. The proteins were regarded as differentially expressed based on a two sample t-test p-value ($p \leq 0.05$) and a fold change threshold (≥ 1.3 for up-regulation or ≤ 0.76 for down-regulation). The reproducibility of all four TMT experiments output was evaluated by further statistical analysis such as overall data quality, un-supervised analyses such as clustering and PCA analysis, all implemented using our in-house 'TMTPrepPro' software (Mirzaei et al., 2017).

6.2.6 Electrochemiluminescence (ECL) assay

Selected proteins identified by quantitative mass spectrometry as being differentially abundant in glaucoma *versus* control samples and also previously reported to be altered in AD were analysed using a highly sensitive electrochemiluminescence (ECL) based MSD platform. Serum amyloid A (SAA), C-reactive protein (CRP), soluble vascular adhesion molecule 1 (sVCAM1), soluble intercellular adhesion molecule 1 (sICAM1), alpha-2-macroglobulin (A2M), beta-2 microglobulin (B2M), Factor VII (FVII), adiponectin, clusterin and Tenascin (TNC) were quantified in human retinal and vitreous samples from control and glaucoma subjects. Aliquots from tissue lysates were prepared according to the manufacturer's instructions for each panel of assays. Assay plates were washed and blocked using the supplied buffers. Samples and standards were then loaded in duplicate

into each assay plate, sealed and incubated at room temperature for 2 hours. Plates were washed using PBST (pH 7.4), then secondary detection antibodies added and plates were re-sealed and incubated again for 1 hour. Plates were finally washed 3 times with PBST, read solution added according to the assay instructions and read using a Sector Imager 1200 plate reader (MSD, Maryland, USA). The supplied software was used to determine standard curve and sample concentration, according to 5 parameter logistic curve-fitting techniques.

6.2.7 Western blotting

Western blot analyses were carried out on selected proteins (CLU, VTN, CRYBB2 and CRYBB3) to confirm the proteomic data. 25 μg of proteins from each sample was separated by 4–12% SDS-PAGE and transferred to PVDF membrane. Membranes were blocked by Tris-buffered saline containing 5% milk for 1 hour, and primary antibodies added at a final concentration of 1–2 μg/ml. After incubation with the primary antibody overnight at 4 °C, blots were washed with Tris-buffered saline and then incubated with anti-IgG antibody linked to horseradish peroxidase for 2 hours. Signals indicative of protein levels were detected using an enhanced chemiluminescent substrate (Clarity Western ECL Substrate, Bio Rad) and Bio-Rad ChemiDoc MP detection system and band intensities quantified in the linear range of detection.

6.2.8 Bioinformatics and functional pathway analysis

Pathways enrichment analysis was carried out on differentially expressed proteins using Ingenuity Pathway software (Ingenuity® Systems, www.ingenuity.com), Reactome Functional Interaction (FI) network (http://www.reactome.org/) and ClueGO. For Ingenuity, the gene identifiers and their fold change value (glaucoma vs. control) for each tissue were uploaded separately to the software. Identified proteins were correlated to corresponding gene using Ingenuity Pathway Knowledge Base (IPKB). Significant interaction networks ($p < 0.05$) and molecular and cellular functions were identified based on known protein–protein interactions in the published literature (knowledge base). Networks were "named" on the most common functional group(s) present. Canonical pathway analysis allowed us to identify the function-specific genes significantly present within the networks. For specific functional protein ontologies that were differentially regulated, the list of differentially expressed proteins for both retina and vitreous were analysed by the Reactome Functional Interaction (FI) network Cytoscape plug-in. All relevant data are available in the paper and its Supporting Information files.

6.3 Results

6.3.1 Differential protein regulation in glaucoma eye tissues quantified by multiplexed proteomics

We identified 4765 proteins from retinal tissue, and 4987 proteins from vitreous humour, which were quantified by multiple peptides at an initial protein FDR of less than 1%. A series of descriptive statistical analyses were performed to confirm the reproducibility of

the data. The overall distribution of median-normalized and log-transformed protein abundances were visualised in density and box plots. Within each tissue (retina and vitreous), the boxplots showed similar median and 95% confidence intervals. Moreover, comparison of density plots for each individual biological sample showed similar and highly overlapping patterns, with no major asymmetric bias, satisfying the normality assumption for further analysis. Overall, these statistical metrics confirm the similarity in overall protein abundance distributions of individual biological replicates, and demonstrate the reproducibility of measurements within sample groups.

To identify differentially expressed proteins, we used a combination of statistical and empirical thresholds to ensure a high confidence in the reported protein abundance differences. Quantified proteins were retained if their abundances in the glaucoma versus control patients were (1) statistically significant (p-value ≤ 0.05) using a student t-test and (2) differed by at least ±30 %. This two-step differential analysis of glaucoma versus control for retina tissue yielded 252 up regulated proteins (p-value ≤ 0.05 and ≥ 1.3-fold change) and 133 down regulated (p-value ≤ 0.05 and ≤ 0.77-fold change (Figure 6.2B). In comparison, a greater proportion of differentially expressed proteins were identified in vitreous, with 554 and 599 proteins exhibiting increased and decreased abundance, respectively (Figure 6.2C). Hierarchical clustering analysis of proteins with differential abundance illustrated the overall consistency of the up and down regulation within respective control and glaucoma cohorts (Figure 6.2D and E). However, when comparing differential proteins between the vitreous and retinal tissues, we observed only moderate overlap (Figure 6.2F). Given the overall retinal and vitreous proteomes were qualitatively similar (see Figure 6.2A), the differences in these proteins suggested tissue specific dysregulation in glaucoma. It is possible that the cellular pathways dysregulated in glaucoma or their regulation is distinct in these tissues.

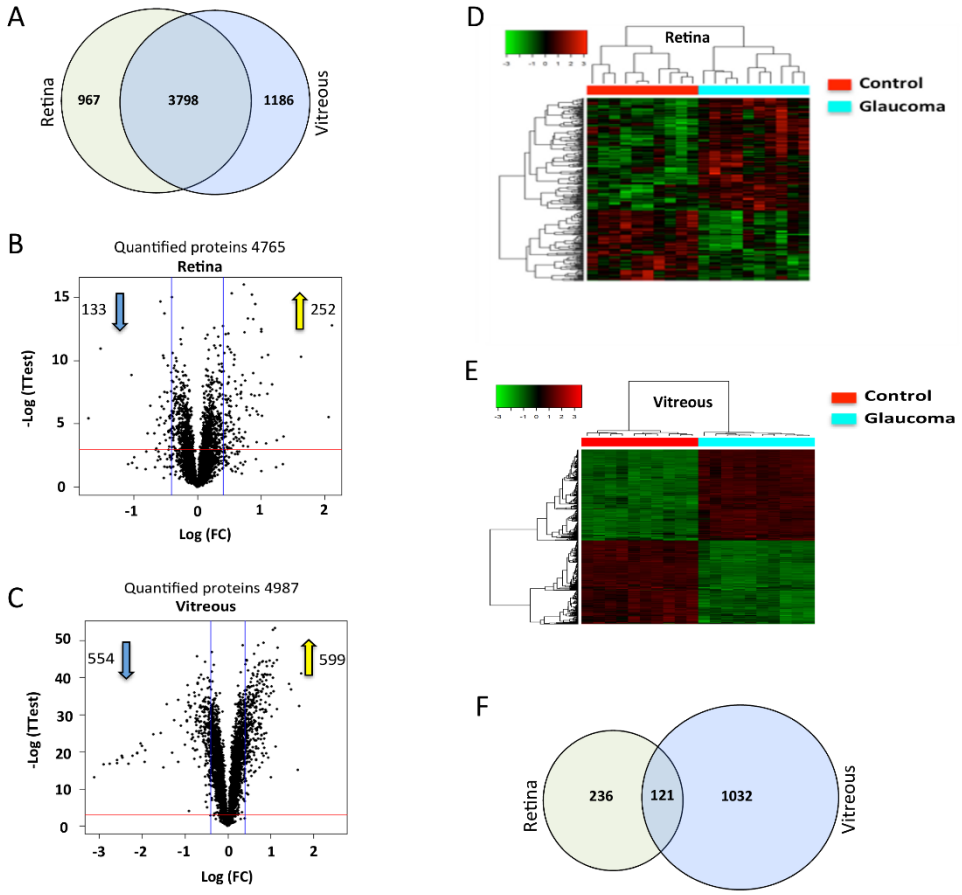

Figure 6.2 Results of proteomics analysis and quality control measurements. A) Venn diagram indicating the overlap between the proteins identified and quantified from vitreous and retinal tissues (1% FDR). (B, C) Volcano plots demonstrating the dual thresholds for differentially regulated proteins. Each data point represents a single quantified protein. The x-axis represents log fold change in abundance (glaucoma/control). Vertical blue lines indicate 1.3 and 0.77 ratio. The -log (p-value) is plotted on the y-axis. Proteins above the red horizontal line indicate significance ≤0.05. Proteins within the upper and outer quadrants meet both the fold change and p-value cut-off, and are therefore considered as differentially regulated. (D, E) Heatmaps (hierarchical clustering) of the log-transformed ratios of differentially expressed proteins (glaucoma vs. control) in retina and vitreous. Column colours indicate treatment type. Red and green color-coding indicate relative increase or decrease in protein abundance, respectively. (F) Venn diagram representing the overlap between the differentially regulated proteins quantified in vitreous and retinal tissues (glaucoma vs. control, p-value ≤ 0.05, ≥ 1.3-fold or ≤ 0.77-fold.

6.3.2 Cellular pathway and protein network analysis reveals functionally coordinated protein abundance changes

To explore these possibilities in greater depth and gain more detailed information about the molecular mechanisms and biological processes that are altered in glaucoma, we performed

cellular pathway enrichment and functional protein network analyses on the differentially expressed proteins of vitreous (1130 proteins) and retinal tissues (355 proteins).

Analysis of the differentially regulated proteins using Ingenuity Pathway Analysis (IPA) revealed that the top canonical pathways associated with immune and inflammatory pathways (e.g. LXR/RXR activation, FXR/RXR activation, acute phase response, and the complement system) were similarly over-represented in the vitreous and retina (Figure 6.3A). In contrast, mitochondria-related pathways, such as, oxidative phosphorylation, NO/ROS production, and mitochondrial dysfunction were more significantly enriched in the retina (Figure 6.3A, orange bars), while the coagulation system, gluconeogenesis I, and G protein and EphrinB signalling pathways were enriched more significantly in the vitreous (Figure 6.3A, blue bars).

To visualize the functional connectivity among these differential proteins, we assembled together retinal and vitreous protein networks using the Reactome analysis tool. A high degree of connectivity, with 136 of the 357 differential proteins in the retina and 568 of the 1153 differential proteins in vitreous, forming interconnected networks (Figure 6.3B) was identified. High network connectivity for the retinal proteins involved in mitochondrial dysfunction, complement pathway, and receptor-mediated endocytosis and retinoid metabolic processes was observed (Figure 6.3B). Within clusters of functionally connected proteins, the relative abundance in glaucoma and control tissues was similar (Figure 6.3C). For example, 13 subunits of the NADH dehydrogenase: ubiquinone oxidoreductase complex I (NDUFA9, NDUFS2, NDUFB3, NDUFB11, etc), four subunits of cytochrome b-c1 complex III (UQCRQ, UQCRC2, UQCR10, UQCRC2), and four subunits of complex IV (COX7B, COX7A2L, NDUFA4, MT-CO2) in the mitochondrial inner membrane were all down regulated, while majority of the functional cluster containing components of the complement signalling cascade (C1QB, C1QC, C1R, etc.) were up regulated. Since the

total number of differential proteins in vitreous was higher compared to that of the retina, significantly higher number of network clusters were identified representing wider array of cellular pathways in vitreous than in the retina. These included complement and coagulation pathways, PI3K-AKT signalling, cholesterol metabolism, apoptotic process, glycolysis, proteasome, RNA processing, mitochondrial ribosomal machinery, glutathione metabolism, oxidative phosphorylation, calcium signalling, synaptic vesicle transport, PPAR signalling, ion trans-membrane transport and receptor-mediated endocytosis. As with the retinal functional protein network (Figure 6.3B), functional clusters were largely co-ordinately regulated, including an upregulated cluster with RNA processing functions, and a ten protein cluster associated with glutathione metabolism, which was down regulated. Overall, the combination of canonical IPA pathway and Reactome-based protein network analysis enabled statistical evaluation and visualization of the most significantly over-represented cellular processes that were impacted in retina and vitreous glaucoma tissues.

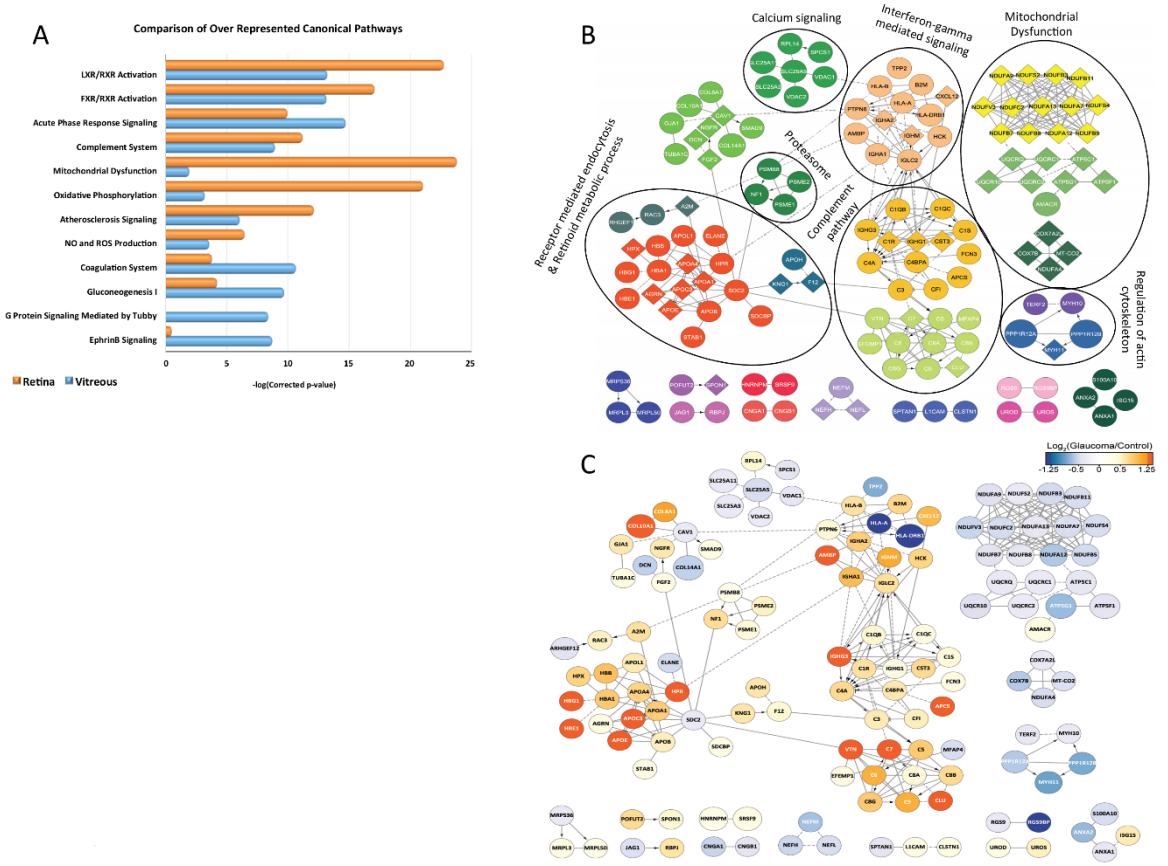

Figure 6.3. Results of functional protein interaction network and pathway analysis (A) Comparison of the top 10 canonical pathways enriched from IPA analysis of differentially regulated proteins (glaucoma vs. control) from vitreous and retina tissues. The significance of functional enrichment is plotted on the y-axis as the -log (p-value). (B) Retinal reactome functional interaction networks analyzed by the Reactome FI Cytoscape plugin. Of 355 retinal differentially expressed proteins, 136 proteins were had at least one other known functional connection. Network nodes are labeled with gene symbols. The Reactome plugin was used to assign functional clusters, which were color-coded and labelled with representative broad functions. (C) Reactome network in (B) color-coded by $\log_2$ (glaucoma/control) relative abundance quantified from TMT analysis.

6.3.3 Functional pathway analysis identifies association with Alzheimer's disease markers in the retina and vitreous

IPA analysis was performed to investigate the top disease-related biological functions commonly associated with the differential proteins in the retina and vitreous. This analysis highlighted networks associated with neuropathological diseases such as amyloidosis, tauopathy, and dementia (Figure 6.4A). Specifically, out of 1510 differentially expressed proteins from retina and vitreous tissues analysed by IPA, 122 were assigned specifically to dementia and AD categories, of which 40 proteins overlapped between the retina and vitreous (Figure 6.4C). While 15 proteins were uniquely expressed in the retina (Figure 6.4B), the remaining 65 proteins were exclusive to vitreous tissue (Figure 6.4D). Majority of these proteins were directly associated with the top IPA canonical pathways (Figure 6.3A), including mitochondrial dysfunction, oxidative phosphorylation, acute phase response signalling, complement signalling, and the coagulation cascade. Based on the bioinformatics evidence linking glaucoma cellular pathology associated with neurodegenerative disorders of the brain, in the following sections, we discuss several examples of pathways and functional protein classes that have common pathophysiology with glaucoma and other CNS disorders particularly AD.

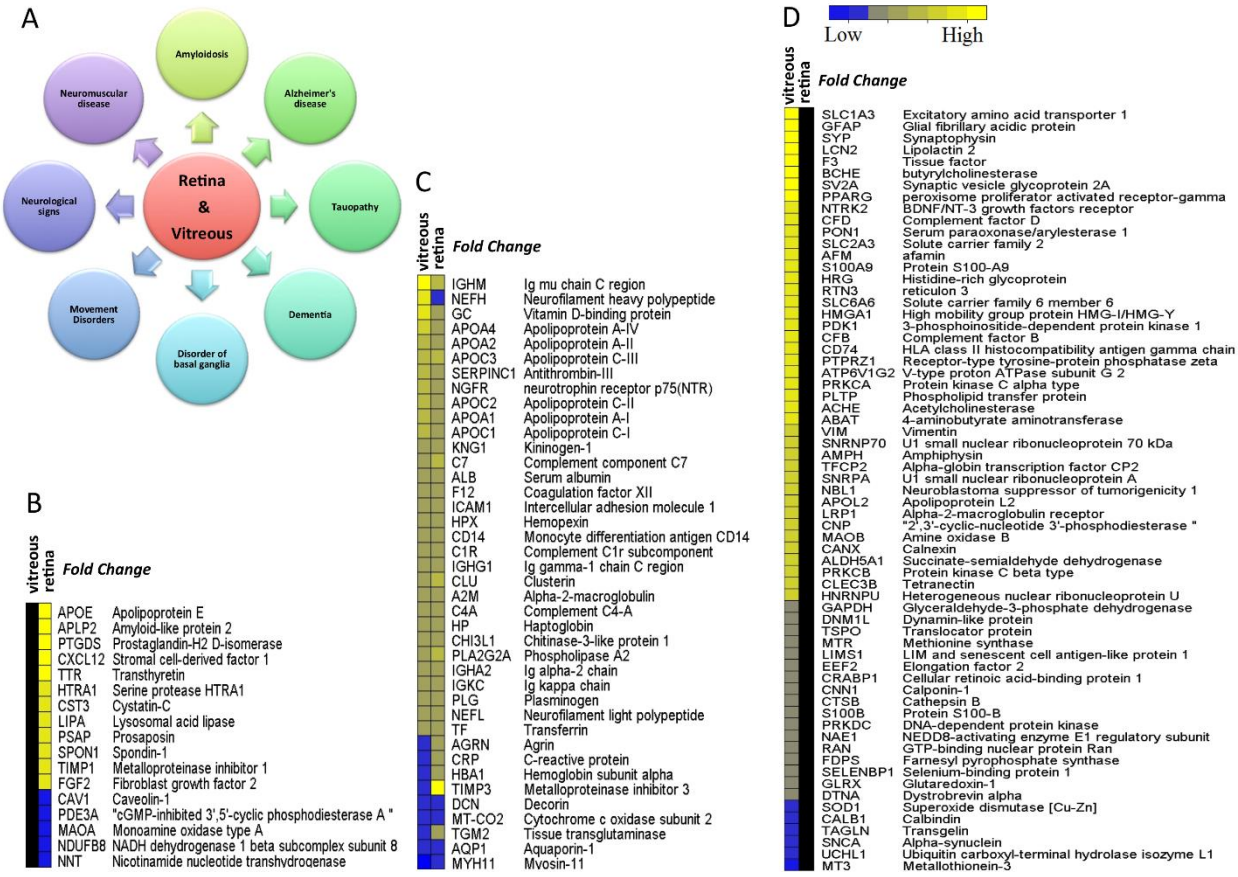

Figure 6.4. Top disease related biological functions and the list of 122 AD associated markers (A) Representation of the top disease-related biological functions, which were commonly enriched in retina and vitreous. (B - D) Heatmaps of the log-transformed abundance ratios (glaucoma vs. control) quantified in retina and vitreous datasets for the 122 AD-associated proteins. Black columns indicate the corresponding protein either was not changed or detected in the dataset, yellow and blue represent up and down regulation, respectively. Relative abundances of (B) 16 AD-associated proteins identified only in the retina, (C) 40 common AD-associated proteins identified both in the retina and vitreous, and (D) 65 AD-associated proteins identified exclusively in the vitreous.

6.3.4 Down-regulation of the mitochondrial electron transport chain proteins

Mitochondria play a central role in regulating neuronal cell survival and its impairment is associated with cell death since it governs both energy metabolism and apoptosis (Bernardi et al., 1999). The energy required for cell growth, development and differentiation is provided by mitochondria in the form of ATP produced *via* oxidative phosphorylation

(OXPHOS) (Green and Reed, 1998). The mitochondrial OXPHOS machinery comprises five key enzyme complexes consisting of 80 proteins, of which 13 are coded by the mitochondrial DNA. The mRNAs for these proteins are translated on mitochondrial ribosomes. The malfunction of ribosomal machinery is associated with decreasing the capacity for protein synthesis, followed by a significant reduction in ribosomal RNA and tRNA levels and subsequently up-regulation of RNA oxidation (Serre et al., 2013). This dysregulation in protein synthesis lead to OXPHOS malfunction affecting all complexes, except the complex II. The electron transport chain is major source of reactive oxygen species (ROS) that accelerates oxidative damage followed by lipid peroxidation that eventually leads to OXPHOS damage that eventually culminates in cell death due to energy restriction (Rötig, 2011). These processes are considered converging features of neurodegenerative diseases, and have been implicated in both glaucoma (Osborne, 2010) and AD (Martin, 2010, Lin and Beal, 2006, Moreira et al., 2010).

In our dataset, we identified 32 retinal and 16 vitreous proteins associated with mitochondrial dysfunction and oxidative phosphorylation, plus seven proteins linked to the mitochondrial ribosomal machinery. Of the 32 retinal proteins, 24 were identified as down regulated, and belonged to outer and inner membranes and ETC complexes I–V, including 13 subunits of complex I (NADH: ubiquinone oxidoreductase), 4 subunits of complex III (Ubiquinol cytochrome c-oxidoreductase), 4 subunits of complex IV (cytochrome c oxidase complex) and 3 subunits of complex V (ATP synthase). In contrast, in the vitreous, proteins in complex III and V were not affected, and 3 subunits of complex I (NDUFV3, NDUFA4L2 and NDUFS5) were up regulated although these were down regulated in the retina1 tissue. Similarly, four subunits of complex IV (COX5B, COX5A, COX6C and COX4I1) were downregulated in the vitreous but not the retina (Figure 6.5A). All seven mitochondrial ribosomal proteins including MRPL13, MRPL39, MRPL47, MRPL20,

MRPL28, MRPL3, MRPL50, MRPS23 were exclusively down regulated in vitreous, but were either not detected or did not change significantly in the retinal tissue (Figure 6.5B).

A

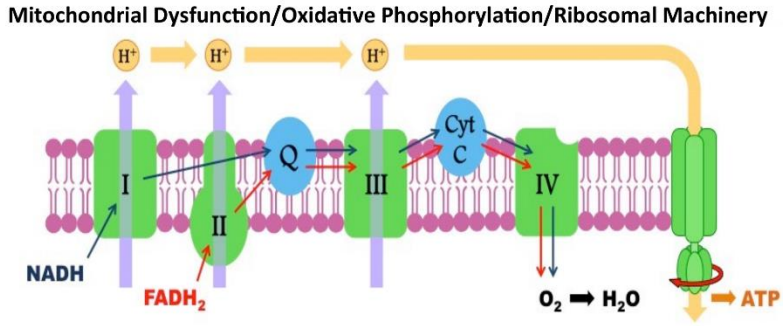

RETINA	Complex I	Complex II	Complex III	Complex IV	Complex V
	NDUFA7		UQCR10	COX7B	ATP5C1
	NDUFA9		UQCRQ	COX7A2L	ATP5F1
	NDUFA12		UQCRC1	MT-CO2	ATP5G1
	NDUFA13		UQCRC2	NDUFA4	
	NDUFB3				
	NDUFB5				
	NDUFB7				
	NDUFB8				
	NDUFB11				
	NDUFS2				
	NDUFS4				
	NDUFV3				
	NDUFC2				
	NDUFA4L2				

Complex I	Complex II	Complex III	Complex IV	Complex V	VITREOUS
NDUFA4L2			COX5B		
NDUFV3			COX5A		
NDUFS5			COX6C		
			COX4I1		

Down
Up

B

Gene ID	Description	Vitreous (FC)	p-value	Retina (FC)
MRPL13	39S mitochondrial ribosomal protein L13	-1.43	<0.0001	NC
MRPL39	39S mitochondrial ribosomal protein L39	-1.37	<0.0001	ND
MRPL47	39S mitochondrial ribosomal protein L47	-1.43	<0.0001	ND
MRPL20	39S mitochondrial ribosomal protein L20	-1.43	<0.0001	ND
MRPL28	39S mitochondrial ribosomal protein L28	-1.35	<0.0001	ND
MRPL3	39S mitochondrial ribosomal protein L3	-1.3	<0.0001	NC
MRPL50	39S mitochondrial ribosomal protein L50	-1.37	<0.0001	NC
MRPS23	39S mitochondrial ribosomal protein L23	1.37	<0.0001	ND

Figure 6.5. Down regulation of ETC proteins and mitochondrial ribosomal proteins in glaucoma (A) A schematic diagram representing the overall down regulation of proteins associated with the electron transport chain (ETC) complexes of the mitochondria in glaucoma condition. (B) A table representing the down regulation of 7 mitochondrial ribosomal proteins in vitreous, which were not detected (ND) or not significantly altered (NC) in the retina (p- value ≤ 0.05).

6.3.5 Activation of classical complement and coagulation cascades

In agreement with previous studies in glaucoma (Doudevski et al., 2014, Williams et al., 2016, Lauwen et al., 2017) and AD (Inoue et al., 2013, McGeer et al., 1989, Hong et al., 2016), the activation of classical complement pathway in glaucoma patient samples was also observed in this study. We quantified majority of key proteins associated with classical complement pathway, such as C1q, C1s, C1r, C4a, C4b, C3, C5, C6, C7, C8a, C8b, C8g

and C9, as up-regulated in glaucoma condition for both vitreous and retinal tissues when compared to the controls. Supporting these findings, two membrane attack complex (MAC) assembly endogenous inhibitors, vitronectin and clusterin, were also found to be upregulated in glaucoma (Figure 6.6A, B). The expression of these inhibitory proteins was further validated using western blotting (Figure 6.6C). The coagulation cascade exhibited a similar expression pattern, where the majority of proteins involved such as F2, F3, A2M, PLG, KNG1, CFB, F9, F10, FGG, KLB1, PROC were up-regulated in glaucoma. However, higher expression of these proteins was observed in vitreous samples compared to that of the retina. Additionally, F9, F10, FGG, KLKB1 and PROC were exclusive to the vitreous tissue (Figure 6.6A).

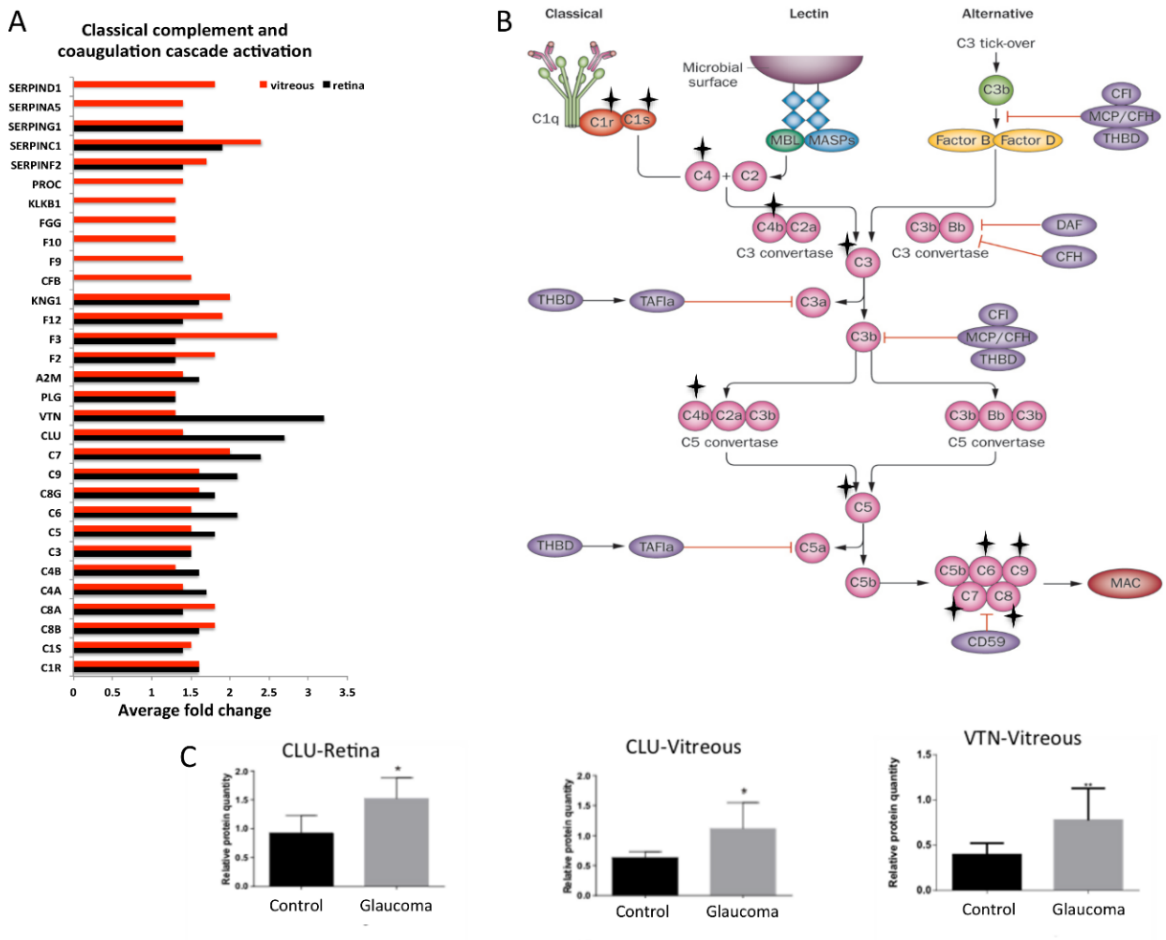

Figure 6.6. Activation of complement (classical) and coagulation cascades (A) A bar graph representing the comparison of the relative abundance of proteins involved in complement and coagulation cascade. The x-axis represent the average fold changes (p-value ≤ 0.05 and ≥ 1.3-fold change, n=10). (B) A schematic diagram showing the details of the three pathways activating the complement cascade (classical, lectin and alternative), of which our quantitative proteomics data supports the activation of the classical pathway in both Western blotting analysis measuring the protein level of CLU (retina and vitreous, n = 10) and VTN in vitreous (n = 10) of glaucoma and control samples. GAPDH was used as the loading control. The bar graphs indicate average densitometry measurements (ImageJ software) (n = 10, average ± sd, *, p-value < 0.05). Black bars represent control, while the light grey bars represent glaucoma. The copy right of the basic complement pathway image belongs to Noris, Mescia, & Remuzzi, Nat. Rev Neprh. 2012.

6.3.6 A) Induction of cholesterol metabolism and transport proteins

Defects in cholesterol transport and metabolism have been reported in several neurodegenerative diseases (Liu et al., 2010) including glaucoma (Fourgeux et al., 2009), AD (Puglielli et al., 2003, Cutler et al., 2004, Martins et al., 2009), Huntington's (Valenza

et al., 2005, Valenza et al., 2010), and Parkinson's disease (Huang et al., 2015). Apolipoproteins are lipid transport and redistribution vesicles in the CNS and other tissues (Martins et al., 2009). Recent genetic studies highlighted the importance of apolipoprotein gene polymorphisms as key elements and risk factors for a number of neurological diseases including AD (Van Cauwenberghe et al., 2015, Saykin et al., 2015). This study identified 12 members of apolipoproteins as upregulated in glaucoma compared to samples from control subjects. Of these, five members (APOA1, APOA4, APOC1, APOC3, APOH) were identified in both vitreous and retinal tissues, however a greater abundance related differences were observed in the vitreous. Four other members were specific to the retina (APOB, APOE, APOL1, APOM) and three were detected uniquely in the vitreous (APOA2, APOL2 and APOC2). Interestingly, of the 12 identified apolipoproteins, eight have previously been reported to be associated with neuropathological progression in AD (Song et al., 2012, Zhou et al., 2014, Liu et al., 2013, Caramelli et al., 1999, Elliott et al., 2010, Khoonsari et al., 2016) (Figure 6.7A).

6.3.6 B) Reduced expression of glutathione S-transferase proteins

This study identified three distinct groups of Glutathione-S-Transferases (GSTs): GSTM1, GSTM2, GSTM3 and GSTM5 from the mu family, GSTT1 and GSTT2 from the theta family, and two microsomal GSTs, MGST1 and MGST2. Interestingly, all eight GSTs were identified as down-regulated in glaucoma eyes compared to the control samples (Figure 6.7B). Five of these GSTs were quantified in both retina and vitreous, with the extent of regulation consistently greater in the vitreous, while the other three (MGST1, MGST3 and GSTM2) were distinctly affected in the vitreous (Figure 6.7B).

6.3.6 C) Up-regulation of proteins associated with RNA processing

Defects in RNA splicing occur in several age related neurodegenerative conditions and are reported previously in glaucoma (Jain et al., 2014) and AD (Tollervey et al., 2011, Bai et al., 2013). Accordingly, we identified 29 protein associated with mRNA processing as significantly up regulated in vitreous along with SRSF9 and HNRNPM proteins, which were upregulated in both the retina and vitreous. From this network, 8 members of the serine/arginine-rich splicing factors (SR proteins) were found, which are involved in alternative mRNA splicing *via* the spliceosome, including; SRSF1, SRSF2, SRSF3, SRSF4, SRSF7, SRSF9, SRSF10 and SRSF11. Additionally, 5 members of hnRNPs complexes (Heterogeneous nuclear ribonucleoproteins) HNRNPC, HNRNPH3, HNRNPF, HNRNPM, HNRNPU and 7 members of small nuclear ribonucleoproteins (SNRA, SNRPD2, SNRPD3, SNRPE, SNRP70 and EFTUD2) were upregulated exclusively in the vitreous tissue.

6.3.6 D) Down regulation of Crystallins

Crystallins are known as dominant structural proteins of the lens and are classified into 3 main families, alpha, beta and gamma (Andley, 2007). Due to their significant homology and characteristic similarities with heat shock proteins and chaperones, they are known to play a role in enhancing cellular resistance to ageing induced apoptotic cell death. We identified 11 members of crystallin family as significantly down-regulated exclusively in the vitreous samples. Crystallins were the most differentially expressed proteins in our dataset (up to 18-fold down regulation in glaucoma condition compared to control). The Reactome pathway analysis revealed that crystallins are clustered with proteins associated with cholesterol transport and apoptosis. Of these 12 proteins, 7 belonged to the beta

(CRYBA1, CRYBA2, CRYBB2, CRYBA4, CRYBB1, and CRYBB3), 2 to alpha (CRYAA, CRYAB) and 3 to the gamma family (CRYGB, CRYGS, and CRYGD). The protein expression of CRYBB3 and CRYBB2 were validated using western blotting approach (Figure 6.7C and D).

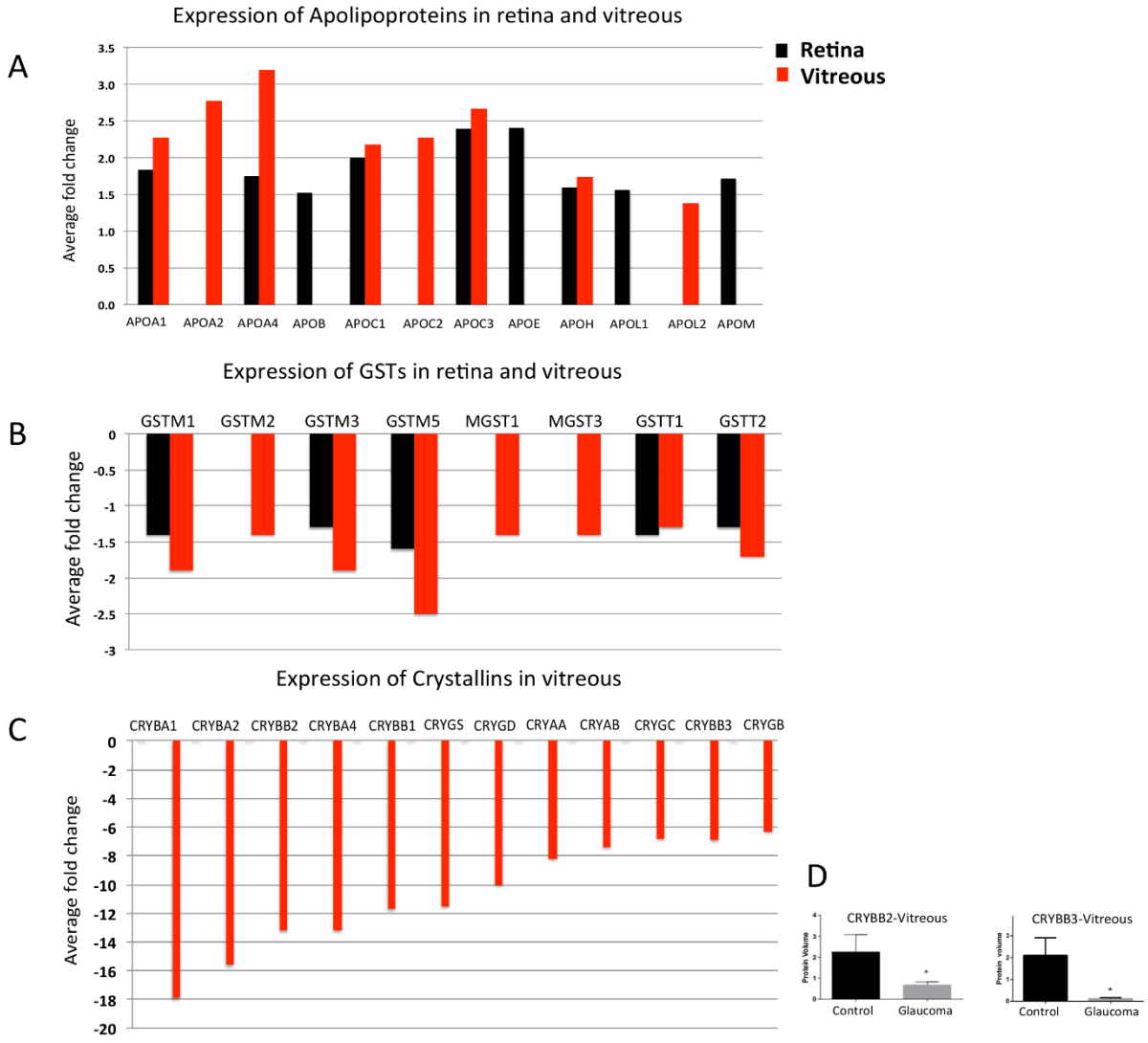

Figure 6.7. Upregulation of Apolipoproteins and down regulation of Crystallin and GSTs in glaucoma (A) A bar graph representing the expression pattern of 12 differentially expressed Apolipoproteins identified in retina and/or vitreous (p-value ≤ 0.05 and ≥ 1.3-fold change, n = 10). (B) A bar graph representing the relative abundance of eight differentially expressed GSTs identified in retina and/or vitreous (p- value ≤ 0.05 and ≤ 0.77 -fold change, n = 10). (C) A bar graph representing the relative abundance of 12 differentially expressed crystallin proteins identified in vitreous (p- value ≤ 0.05 and ≤ 0.77 -fold change, n=10) (D) Western blotting analysis for measuring the relative protein expression level of CRYBB2 and CRYBB3 in vitreous (n= 10) of glaucoma and control samples. GAPDH was used as the loading control. The bar graphs indicate average densitometry measurements (ImageJ software) (n = 10, average ± SD, *, p-value < 0.05). Black bars represent control, while the light grey bars represent glaucoma.

6.3.7 Confirmation of proteomics data (selected AD associated markers) using an ECL assay

To support our quantitative MS results and provide further evidence for the molecular association of glaucoma with other neurodegenerative diseases, specifically AD, we selectively examined expression changes of proteins that are widely reported to be affected in AD, using a quantitative ECL based assay. ECL assay was carried out on ten known AD biomarkers (A2M, B2M, Clusterin, TNC, FVII, Adiponectin, CRP, SAA, ICAM-1 and VCAM-1), which were identified in our proteomics datasets. The association of these markers with AD is extensively reported in the literature (Varma et al., 2017, Doecke et al., 2012, Yu and Tan, 2012, O'Bryant et al., 2016, O'Bryant et al., 2011, Ewers et al., 2010). The up regulation of A2M, Clusterin, SAA, ICAM-1 VCAM-1 and down regulation of TNC in both tissues was detected, consistent with the proteomics experiments. B2M remained unchanged in vitreous and was up regulated in the retina, while MS analysis showed that both of these markers were up regulated. Similarly, TNC and FVII were up regulated in vitreous and down regulated or unchanged in retina using ECL, but remained unchanged or were not detected in either tissue using proteomics (Figure 6.8). This may be attributed to differences in the capture affinity of the detection antibodies used in ECL, potential for cross-reactivity, buffers and other reagents that are used in these assays. Together both these approaches demonstrate that six of these ten markers were similarly affected in the disease condition.

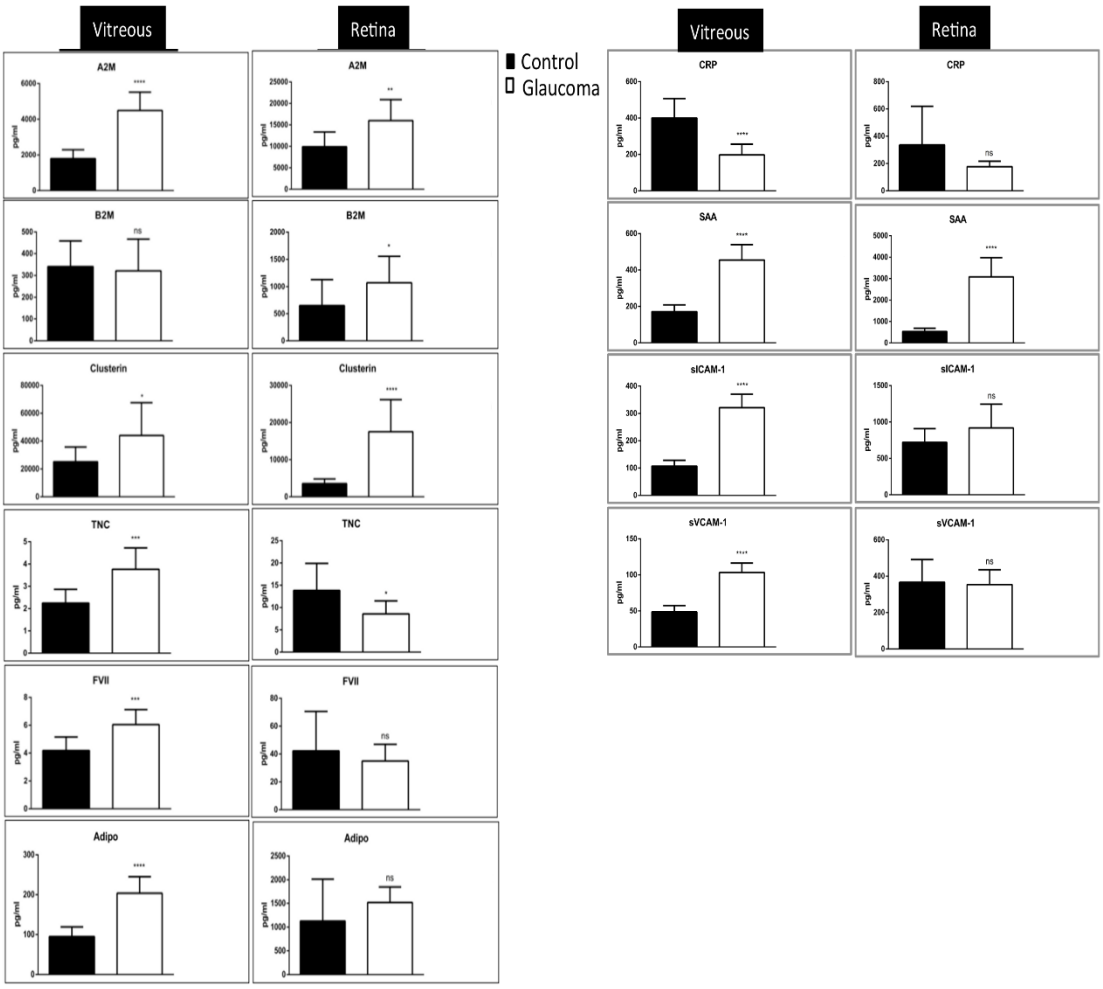

Figure 6.8. ECL analysis of AD associated markers. ECL analysis of selected proteins (SAA, CRP, sVCAM1, sICAM1, A2M, B2M, FVII, TNC), which are known as AD biomarkers in the literature and also identified in the proteomics data of this study. All samples (n = 10 control and n = 10 glaucoma) were assayed in duplicate via a multiplex biomarker assay platform using ECL on the SECTOR Imager 2400A from Meso Scale Discovery.

6.4 Discussion

This study used a combination of multiplexed mass spectrometry-based proteomics (TMT labelling), functional protein network and pathways analyses, ECL analysis, and western blotting to delineate global and specific proteomics changes in human retinal and vitreous glaucoma tissues. Only a limited number of proteomics studies have been performed on

human glaucoma tissues (Funke et al., 2016, Tezel et al., 2010). For instance, Funke *et al* (Funke et al., 2016) has previously reported identifying 600 proteins from human retinal tissues, of which about 10% showed proteome alterations in the glaucomatous tissues. In the current study, our approach analysed both retinal and vitreous tissue proteomes to a significant depth of about 5000 proteins, providing the first comprehensive elucidation of proteome changes in the these tissues from glaucoma patients. We report differential regulation of 122 proteins in retinal and vitreous tissues, which overlap with functional networks associated with neurodegenerative conditions of CNS with a particular focus on AD pathology. We believe that the elucidation of the complex proteome alterations occurring in the vitreous and retinas of glaucoma subjects will serve as a key source for the identification of glaucoma specific biological targets for diagnostic biomarkers, disease prevention, and therapeutic strategies. Our in-depth computational analysis highlights several unique biochemical pathways that are also known to be impaired in AD conditions. The proteomics overlap highlighting similarities and differences between glaucoma and AD will further help to elucidate converging pathological mechanisms underlying AD and various other neurodegenerative disorders.

More specifically, our data analysis revealed that a significant proportion of annotated proteins belonged to categories related to neuronal components and neurological disorders. Pathway enrichment analysis followed by examining functional networks supported the notion that pathways linked to cellular energy regulation, complement pathway activation, antioxidant defence mechanisms and acute phase response signalling were predominantly affected. Our findings also implicate impairment in mitochondrial machinery, cholesterol metabolism, inflammatory responses, regulation of cytoskeletal proteins, receptor mediated endocytosis and retinoid nuclear receptor alterations in glaucoma conditions. Interestingly, we observed significant downregulation of several crystallin proteins in the

vitreous of glaucoma subjects. Crystallins are a class of heat shock protein which are suggested to protect neurons by suppressing signals linked to stress mediated apoptosis; therefore, reduced crystallin levels in glaucoma vitreous could make the retinal neurons more vulnerable to cytotoxic injury and cell death. Downregulation of various crystallin proteins and mRNA has previously been reported in a rat model of experimental glaucoma (Piri et al., 2006, Anders et al., 2017).

Several *in vivo* and *in vitro* studies have demonstrated the potential neuroprotective role of crystallins (β-crystallin B2) in survival of injured retinal ganglion cells in rat(Böhm et al., 2012) and axonal regeneration in the injured optic nerve and photo receptors in animal experimental model (Böhm et al., 2015). Interestingly the most recent retinal proteomics study of the experimental glaucoma model (Anders et al., 2017) reported down regulation of several crystalline proteins 3 week after IOP elevation, however, their expression trend was reversed after 7^{th} week. Furthermore the authors showed that an intravitreal injection of β-crystallin B2 during the IOP elevation is responsible for increasing the retinal ganglion cell survival and protecting against the loss of the retinal nerve fiber layer and optic nerve injury (Anders et al., 2017).

Conversely, while AD brains show increased αB-crystallin expression, changes in retinal expression of various crystallins in AD remains unclear (Renkawek et al., 1994).

Proteome characterization of the retina and vitreous tissues, which are primarily associated with glaucoma disease process, represent the first step towards enhancing our molecular understanding of this complex neurodegenerative disorder and explain the development of specific features of the disease. Functional network analysis of the differentially regulated proteins in glaucoma may hold the key to pathognomonic processes associated with other CNS neurodegenerative disorders that have increasingly been shown to affect molecular,

anatomical and functional networks in the retina. We also validated our proteomics findings using highly sensitive electro-chemiluminescence assay on MSD platform (O'Bryant et al., 2016) to evaluate protein expression of selected candidate markers such as clusterin, vitronectin and crystallins (B2 and B3). Consistent with mass spectrometry findings, we observed that A2M, B2M, Clusterin, TNC, FVII, Adiponectin, CRP, SAA, ICAM-1 and VCAM-1 were differentially affected in the retinas and vitreous of glaucoma subjects. Importantly, of these A2M, B2M, Clusterin, TNC, FVII, Adiponectin represent metabolic markers that are modulated in AD (O'Bryant et al., 2016). Altered expression of AD associated vascular markers like CRP, SAA, ICAM-1 and VCAM-1 also correlated well with our proteomics analysis. These observations support the hypothesis that glaucoma is associated with both neuronal and vascular stress.

The biochemical interactions identified in several signalling networks elucidated in this study could lead to neurodegeneration through cell apoptosis. The impact of altered metabolic and biochemical function on complex biomolecules can lead to conformational alterations and covalent modifications. It is difficult to determine whether proteome alterations in glaucoma are a consequence or cause of the disease. Our analysis highlighted a significant decrease in proteins associated with regulating glutathione metabolism that directly modulates oxidative stress response, which may reflect an attempt, by the retinal and vitreous tissues to neutralize the increased oxidative stress associated with glaucoma pathogenesis. Similarly, we observed a down regulation of proteins involved in mitochondrial function and ATP generation, which may suggest an inability of the retinal tissue to meet the energy requirements leading to shifting of equilibrium to pro-apoptotic pathways. Increased expression of some of the components of complex 1 in vitreous may represent a compensatory effect or efflux of these proteins from dying retinal cells.

Apart from oxidative stress, our study suggests complement cascade involvement in glaucoma. The complement pathway not only plays a critical role in the inflammatory response, but is also involved in synaptic development and pruning. Defective synaptic elimination has been associated with limited refinement of the retinogeniculate pathway. Preferential over-expression of several components of the complement pathway were identified in glaucoma samples. Our study provides a highly inclusive data set regarding alterations in complement proteins. Together with previous observations, our findings corroborate the reported upregulation of C1q complement protein in glaucoma (Stasi et al., 2006). C1q along with synaptic markers such as PSD95 has been implicated in early glaucoma pathogenesis, suggesting complement activation in synaptic regulation in glaucoma. Increased C1q expression was also reported in neurons in AD animal models (Fonseca et al., 2011). Differential effects on complement pathways is known in other neurodegenerative disorders and amyloid β accumulation in particular is an activator of complement pathway (Salminen et al., 2009).

Aβ deposits are well known to accumulate in the retinas in both AD and glaucoma conditions (Gupta et al., 2014, Gupta et al., 2016). Similarly, plaque formation in AD is influenced by cholesterol, chronic oxidative stress, complement activation and neuroinflammation. The inflammatory responses, such as the activation of complement pathways play a fundamental role in synaptic development and pruning, cell death and ultimately in pathophysiology of numerous neurodegenerative diseases, including glaucoma (Stephan et al., 2012, Dunkelberger and Song, 2010). The complement system is activated by three separate pathways; the classical, alternative and lectin (Noris et al., 2012). However, among the three pathways, the classical pathway has been shown to be predominantly affected in both AD (McGeer et al., 1989) and glaucoma (Williams et al., 2016). The classical complement pathway is comprised of more than 20 proteins,

comprising several serine proteinases linked as an amplifying cascade. There is evidence for the bidirectional cross-talk between the complement and coagulation cascades (Levi et al., 2004, Levi and van der Poll, 2005). Since some complement proteins act as substrates for coagulation factors, enhanced levels of coagulation cascade proteins could potentially promote the complement cascade activation. Alternatively, complement activation might also lead to coagulation and fibrin deposition (Cortes-Canteli et al., 2012).

We identified for the first time a direct link of apolipoprotein expression in glaucoma. Our study found significant upregulation of various apolipoproteins in the retinas and vitreous of glaucoma subjects. Apo A-I plays a crucial role in cholesterol transport and metabolism and we observed increased Apo A-I concentrations in glaucoma samples. The regulatory effects of Apo-A1 on reverse cholesterol transport pathway have also been suggested in AD. ApoE4 changes were primarily localised to the retina and no overexpression of ApoE4 was identified in the vitreous. Importantly the *APOE* allele variant is a significant risk factor for sporadic type of late onset AD (Liu et al., 2013). The *APOE* allele is involved in moderating Aβ proteolysis and clearance, and is associated with both glaucoma and AD effects on the retina (Gupta et al., 2016, Gupta et al., 2016). This study establishes the changes in expression of various members of the apolipoprotein family, indicating significant alterations in apolipoprotein metabolism. It is thus highly likely that apolipoproteins may form potential biomarkers to predict the effects of glaucoma in the future.

Increased ROS production underlies oxidative damage to macromolecules in the cells, including lipids, proteins and nucleic acids. These changes have been directly associated with aging and neurodegeneration (Lin and Beal, 2006). Association between the production of oxidant/free radical species, dysfunction of the antioxidant system, and the onset and progression of neurodegenerative diseases has been increasingly well established

(Barnham et al., 2004, MatÉs et al., 1999). For instance, glutathione (GSH), a thiol-containing tripeptide, and GSH-related enzymes (GSTs) are important endogenous antioxidant components that are involved in mediating protection of cells against oxidative stress by neutralising highly reactive free radical species (Marí et al., 2009). GSTs catalyse the conjugation of reduced GSH to xenobiotic compounds, which are less reactive and more soluble, and hence facilitate clearance from the body. GSH synthetases regulate the GSH system in both cytoplasm and endoplasmic reticulum and dysregulation of the system is linked with neurodegeneration (Generally, 1997). GST has also been described as a glaucoma associated stress marker, and increased serum GST immunoreactivity was reported in glaucoma patients. Furthermore, polymorphisms of selected GSTs such as GSTM1 and GSTT1 were shown to be associated with the onset and development of glaucoma (Jansson et al., 2003, Ünal et al., 2007), cataract (Çelįk et al., 2014, Qi et al., 2015), PD (Wang and Wang, 2014, Perez-Pastene et al., 2007) and AD (Wang et al., 2016a).

A limitation of our approach is that we analysed whole retinal tissues, and thus cannot distinguish the individual contribution of distinct cell types that comprise the retina. This may lead to changes in proteins in the inner retinal region, which are particularly affected in glaucoma to be masked, or lead to significantly diminished fold alterations. Future studies may use techniques like laser dissection microscopy in the unfixed tissues to identify region and layer specific proteomics changes in the retina. Immunostaining of the retinal sections with selected markers will further help to elucidate the layer/region specific protein expression differences in the retina under glaucoma conditions. The protein expression changes in vitreous may similarly be caused by efflux of proteins from retinas or other ocular tissues and may not reflect *bona fide* vitreous proteome alterations. Further, although a great deal of reproducibility was observed between the samples suggesting

differential regulation of proteins in the disease state, detailed information from the post-mortem donor samples including the drug treatments etc. will help for in-depth analysis of the data. Nevertheless, this study enables us to understand the complex nature of disease-associated pathology in retinal and vitreous tissues although it does not suggest whether it is a cause or effect of the chronic disease condition. Furthermore, the downregulation of several proteins in the retina may be caused by loss of neuronal cells in glaucoma leading to reduced protein quantity from particular retinal cells. This may reflect reduced expression at the tissue level and not at individual neuronal levels.

Overall, very few studies have tried to substantiate the molecular similarities and differences between open angle glaucoma and more generalised CNS neurodegenerative disorders such as AD. The comprehensive profile of the eye proteome changes identified in this study provides novel insights into the pathobiology of glaucoma. Similarities and differences between various proteins in glaucoma and other neurodegenerative conditions may lead to the development of novel drug targets and disease specific biomarker identification. Our results provide a significant advancement towards a better understanding of the mechanistic basis of glaucoma and its association with other neurodegenerative diseases.

CHAPTER 7

CONCLUSION AND FUTURE PERSPECTIVES

Glaucoma is a degenerative optic neuropathy affecting 80 million individuals by 2020 worldwide (Quigley and Broman, 2006). Glaucoma is mainly manifested as alterations of optic disc with progressive degeneration of retinal ganglion cells (RGCs) contributing to visual field loss. High intraocular pressure (IOP) is considered as the main risk factor of glaucoma. Unfortunately, a significant number of patients show disease progression despite treating with IOP lowering drugs. So, RGC degeneration cannot be prevented only by reducing eye pressure. There is need for development of more novel strategies targeting retinal neuroprotection. Within this context, this PhD project aimed to assess the potential neuroprotective effect of RXR activation by its agonist bexarotene both *in vitro* studies as well as *in vivo* in the acute and chronic glaucoma models. Retinoid X receptors (RXRs) are ligand-dependent transcription factors that belong to the nuclear receptor (NR) superfamily. RXRs have three different isoforms (α, β, and γ) and can form both homo- and heterodimers with other nuclear receptors. Numerous studies have linked RXR modulation with neuroprotection. This thesis was mainly focused to elucidate the role of bexarotene as RXR modulator in glaucoma pathology.

In the first part of this work (chapter 3), we observed concentration-dependent decrease in cell viability using the trypan blue vital dye exclusion assay. Higher concentrations of drug induces cytotoxicity and cell death (Figure 3.1). We demonstrated RXR expression modulation by using different bexarotene concentrations ranging from 0.001-10μM using western blotting and immunofluorescence approaches. Result of both methods showed that drug treatment leads to upregulation of expression of all the three RXR isoforms with maximum expression of RXRα and γ isoform at 0.1 μM and RXRβ isoform at 1 μM (Figure 3.3). We further identified an increased RXR expression in the mice brains treated with bexarotene in comparison to control mice brain tissues (Figure 3.4). As previous studies have shown that bexarotene modulates the AD pathology in mouse models, we also

observed reduced levels of RXR expression in APP/PS1 mouse model (Figures 3.5 and 3.6) as well as in Aβ treated SH-SY5Y cells (Figure 3.7). The result of *in-vitro* studies proved that optimum concentrations of bexarotene significantly alleviate loss of RXR expression caused by Aβ treatment. Aβ has been shown to induce ER stress response which further results in apoptosis. We observed that optimum concentrations of bexarotene (0.1 and 1 μM) protects against Aβ-induced ER stress and apoptosis (Figure 3.8). We also observed that high concentration of bexarotene (5 and 10 μM) upregulates ER stress and BAD activation in neuroblastoma cells (Figure 3.9) which were moderated by pharmacological modulation of TrkB receptor (Figure 3.10).

In the second part of this work, we investigated potential neuroprotective effects of activation of RXR receptors in animal models of glaucoma (Chapter 4). Systemic treatment with bexarotene promoted upregulation of RXR expression in different retinal layers confirmed by both immunofluorescence and immunoblotting (Figures 4.1, 4.2 and 4.3). As ER stress is associated with retinal ganglion cell death so further we investigated the expression of ER stress protein markers p-PERK and GADD 153 in retinal sections. We observed that RXR activation inhibits retinal ER stress and related apoptosis in both acute as well as chronic glaucomatous stress (Figures 4.5, 4.6, 4.7 and 4.8). RXR activation by bexarotene also reduced Aβ accumulation in glaucoma eyes (Figure 4.9). The significant increase in amplitude of pSTR (Figure 4.10) and preservation of ganglion layer cells (Figures 4.11 and 4.12) with bexarotene treated animals reflects that bexarotene treatment maintained inner retinal functional and structural integrity. These results showed that RXR activation exerts neuroprotective effects in mice in preventing loss of retinal ganglion cells (RGCs) under both acute and chronic experimental glaucoma conditions. Docking studies have also validated binding of natural and synthetic retinoids with RXRs. High and stable binding affinity of bexarotene to RXR α and β receptors was observed but weak binding

with RXR γ was predicted by molecular modelling studies which indicated that bexarotene has higher potential to activate RXR receptors (Chapter 5).Proteomics data from human retinal lysates revealed activation of LXR/RXR and FXR/RXR activation pathways in glaucoma confirming that these pathways could serve as possible targets for glaucomatous therapeutic benefits (Chapter 6). To our knowledge, no previous studies have been published which target RXR receptors in glaucoma treatment. In fact, modulation of RXR receptors has been described to be one of the most promising neuroprotective strategies in various neurodegenerative disorders. Therefore altogether this work shows that RXR activation by bexarotene is neuroprotective to RGCs and can be used in the treatment of glaucoma.

This thesis involved *in vitro, in vivo* and *in silico* approaches to understand the effects of RXR agonist on the RXR receptors and protective effects of RXR activation in glaucoma. The results from this thesis support the hypothesis that RXR activation can be neuroprotective to RGCs in preventing apoptosis and cell death. Bexarotene, a RXR agonist may have great potential for future therapeutic management of glaucoma.

Future perspectives:

1. To further elucidate molecular mechanisms of RXR activation which provides neuroprotection. Our studies suggest that RXR activation can serve as potential target in the treatment of glaucoma. A more detailed study using preclinical and clinical trials and additional experiments are needed to evaluate the involvement of RXR activation-mediated neuroprotection in glaucoma.
2. The role of TrkB agonist is well known in providing neuroprotection, and *in vitro* studies confirmed TrkB signalling along with RXR modulation provides an

additional drug target to minimize endoplasmic reticulum (ER) stress response and apoptosis. Further *in vivo* studies are needed to investigate the mechanism on how TrkB/RXR signalling cross-talk in glaucoma and potentially in other retinal diseases.

3. Future work with RXR knock down studies in adult mice will provide greater understanding of RXR involvement in retinal morphology and visual function.
4. In the present study, oral route of drug (bexarotene) administration was used. Possible further work in future can lead to topical application of the drug e.g. eye drops.
5. Our study showed that treatment with RXR agonist induces significant suppression of ER stress and apoptosis in retina. Future studies will be required to understand the other mechanisms of RXR-mediated neuroprotection in retina which will help to understand the therapeutic benefits of the drug.
6. Further sequence analysis can be carried out using a combination of bioinformatics tools such as BLAST, PolyPhen, CUPSAT and CLUSTALW/X for a comprehensive knowledge on the expression profile of these RXR receptors in the eye.
7. As RXRs are involved in histone acetylation and chromatin condensation processes and several of the histone deacteylase inhibitors have a protective effect on RGCs. Future experiments can be conducted to detect any pathological changes in the RXR receptors that would reflect in abnormal deacetylation of histone proteins in glaucoma.
8. This study can be further extended in the development of a sustained release (extended release) of bexarotene by incorporating it in polymer, polyamidoamine (PAMAM) dendrimer. Dendrimer hydrogel (DH) formulation can be made from

PAMAM from generation- G2.0 to G3.0. The delivery and RGC protective action of bexarotene/ its derivatives can be studied for the ocular drug delivery system.

References

ABDULL, M. M., CHANDLER, C. & GILBERT, C. 2016. Glaucoma, "the silent thief of sight": patients' perspectives and health seeking behaviour in Bauchi, northern Nigeria. *BMC Ophthalmology,* 16**,** 44.

AGARWAL, R., GUPTA, S. K., AGARWAL, P., SAXENA, R. & AGRAWAL, S. S. 2009. Current concepts in the pathophysiology of glaucoma. *Indian Journal of Ophthalmology,* 57**,** 257-266.

AGORASTOS, A., SKEVAS, C., MATTHAEI, M., OTTE, C., KLEMM, M., RICHARD, G. & HUBER, C. G. 2013. Depression, anxiety, and disturbed sleep in glaucoma. *J Neuropsychiatry Clin Neurosci,* 25**,** 205-13.

AHUJA, H. S., SZANTO, A., NAGY, L. & DAVIES, P. J. 2003. The retinoid X receptor and its ligands: versatile regulators of metabolic function, cell differentiation and cell death. *J Biol Regul Homeost Agents,* 17**,** 29-45.

AIHARA, M., LINDSEY, J. D. & WEINREB, R. N. 2003. Experimental mouse ocular hypertension: establishment of the model. *Invest Ophthalmol Vis Sci,* 44**,** 4314-20.

ALLEN, J. W., ELDADAH, B. A., HUANG, X., KNOBLACH, S. M. & FADEN, A. I. 2001. Multiple caspases are involved in beta-amyloid-induced neuronal apoptosis. *J Neurosci Res,* 65**,** 45-53.

ALLENBY, G., BOCQUEL, M. T., SAUNDERS, M., KAZMER, S., SPECK, J., ROSENBERGER, M., LOVEY, A., KASTNER, P., GRIPPO, J. F., CHAMBON, P. & ET AL. 1993. Retinoic acid receptors and retinoid X receptors: interactions with endogenous retinoic acids. *Proc Natl Acad Sci U S A,* 90**,** 30-4.

ALTANGEREL, U., SPAETH, G. L. & RHEE, D. J. 2003. Visual function, disability, and psychological impact of glaucoma. *Curr Opin Ophthalmol,* 14**,** 100-5.

ALTUCCI, L. & GRONEMEYER, H. 2001. The promise of retinoids to fight against cancer. *Nature Reviews Cancer,* 1**,** 181.

ALTUCCI, L., LEIBOWITZ, M. D., OGILVIE, K. M., DE LERA, A. R. & GRONEMEYER, H. 2007. RAR and RXR modulation in cancer and metabolic disease. *Nat Rev Drug Discov,* 6**,** 793-810.

ALVAREZ, A. R., SANDOVAL, P. C., LEAL, N. R., CASTRO, P. U. & KOSIK, K. S. 2004. Activation of the neuronal c-Abl tyrosine kinase by amyloid-β-peptide and reactive oxygen species. *Neurobiology of Disease,* 17**,** 326-336.

ANDERS, F., TEISTER, J., LIU, A., FUNKE, S., GRUS, F. H., THANOS, S., VON PEIN, H. D., PFEIFFER, N. & PROKOSCH, V. 2017. Intravitreal injection of β-crystallin B2 improves retinal ganglion cell survival in an experimental animal model of glaucoma. *PLOS ONE,* 12**,** e0175451.

ANDLEY, U. P. 2007. Crystallins in the eye: function and pathology. *Progress in retinal and eye research,* 26**,** 78-98.

ANG, G. S. & EKE, T. 2007. Lifetime visual prognosis for patients with primary open-angle glaucoma. *Eye (Lond),* 21**,** 604-8.

ANHOLT, R. R. & CARBONE, M. A. 2013. A molecular mechanism for glaucoma: endoplasmic reticulum stress and the unfolded protein response. *Trends Mol Med,* 19**,** 586-93.

ARANDA, A. & PASCUAL, A. 2001. Nuclear Hormone Receptors and Gene Expression. *Physiological Reviews,* 81**,** 1269.

ARNOLD, A. C. 2005. Evolving management of optic neuritis and multiple sclerosis. *Am J Ophthalmol,* 139**,** 1101-8.

AWAI, M., KOGA, T., INOMATA, Y., OYADOMARI, S., GOTOH, T., MORI, M. & TANIHARA, H. 2006. NMDA-induced retinal injury is mediated by an endoplasmic reticulum stress-related protein, CHOP/GADD153. *J Neurochem,* 96**,** 43-52.

AYALA-PEÑA, V. B., PILOTTI, F., VOLONTÉ, Y., ROTSTEIN, N. P., POLITI, L. E. & GERMAN, O. L. 2016. Protective effects of retinoid x receptors on retina pigment epithelium cells. *Biochimica et Biophysica Acta (BBA) - Molecular Cell Research,* 1863**,** 1134-1145.

BACHMEIER, C., BEAULIEU-ABDELAHAD, D., CRAWFORD, F., MULLAN, M. & PARIS, D. 2013a. Stimulation of the retinoid X receptor facilitates beta-amyloid clearance across the blood-brain barrier. *J Mol Neurosci,* 49**,** 270-6.

BAI, B., HALES, C. M., CHEN, P.-C., GOZAL, Y., DAMMER, E. B., FRITZ, J. J., WANG, X., XIA, Q., DUONG, D. M. & STREET, C. 2013. U1 small nuclear ribonucleoprotein complex and RNA splicing alterations in Alzheimer's disease. *Proceedings of the National Academy of Sciences,* 110**,** 16562-16567.

BARNEDA-ZAHONERO, B. & PARRA, M. 2012. Histone deacetylases and cancer. *Mol Oncol,* 6**,** 579-89.

BARNHAM, K. J., MASTERS, C. L. & BUSH, A. I. 2004. Neurodegenerative diseases and oxidative stress. *Nature reviews Drug discovery,* 3**,** 205-214.

BARSONY, J. & PRUFER, K. 2002. Vitamin D receptor and retinoid X receptor interactions in motion. *Vitam Horm,* 65**,** 345-76.

BASCONI, J. E. & SHIRTS, M. R. 2013. Effects of Temperature Control Algorithms on Transport Properties and Kinetics in Molecular Dynamics Simulations. *J Chem Theory Comput,* 9**,** 2887-99.

BAYER, A. U., FERRARI, F. & ERB, C. 2002. High occurrence rate of glaucoma among patients with Alzheimer's disease. *Eur Neurol,* 47**,** 165-8.

BERNARDI, P., SCORRANO, L., COLONNA, R., PETRONILLI, V. & DI LISA, F. 1999. Mitochondria and cell death. *European Journal of Biochemistry,* 264**,** 687-701.

BERRODIN, T. J., MARKS, M. S., OZATO, K., LINNEY, E. & LAZAR, M. A. 1992. Heterodimerization among thyroid hormone receptor, retinoic acid receptor, retinoid X receptor, chicken ovalbumin upstream promoter transcription factor, and an endogenous liver protein. *Molecular Endocrinology,* 6**,** 1468-1478.

BERTOLOTTI, A., ZHANG, Y., HENDERSHOT, L. M., HARDING, H. P. & RON, D. 2000. Dynamic interaction of BiP and ER stress transducers in the unfolded-protein response. *Nat Cell Biol,* 2**,** 326-32.

BOEHM-CAGAN, A. & MICHAELSON, D. M. 2014. Reversal of apoE4-driven brain pathology and behavioral deficits by bexarotene. *J Neurosci,* 34**,** 7293-301.

BOEHM, M. F., ZHANG, L., ZHI, L., MCCLURG, M. R., BERGER, E., WAGONER, M., MAIS, D. E., SUTO, C. M., DAVIES, J. A., HEYMAN, R. A. & ET AL. 1995. Design and synthesis of potent retinoid X receptor selective ligands that induce apoptosis in leukemia cells. *J Med Chem,* 38**,** 3146-55.

BOGNER, B., BOYE, S. L., MIN, S. H., PETERSON, J. J., RUAN, Q., ZHANG, Z., REITSAMER, H. A., HAUSWIRTH, W. W. & BOYE, S. E. 2015. Capsid Mutated Adeno-Associated Virus Delivered to the Anterior Chamber Results in Efficient Transduction of Trabecular Meshwork in Mouse and Rat. *PLOS ONE,* 10**,** e0128759.

BÖHM, M. R. R., PFROMMER, S., CHIWITT, C., BRÜCKNER, M., MELKONYAN, H. & THANOS, S. 2012. Crystallin-β-b2-Overexpressing NPCs Support the Survival of Injured Retinal Ganglion Cells and Photoreceptors in RatsCrystallin-β-b2-Overexpressing NPCs. *Investigative Ophthalmology & Visual Science,* 53**,** 8265-8279.

BÖHM, M. R. R., PROKOSCH, V., BRÜCKNER, M., PFROMMER, S., MELKONYAN, H. & THANOS, S. 2015. βB2-Crystallin Promotes Axonal Regeneration in the Injured Optic Nerve in Adult Rats. *Cell Transplantation,* 24**,** 1829-1844.

BOMBEN, V., HOLTH, J., REED, J., CRAMER, P., LANDRETH, G. & NOEBELS, J. 2014. Bexarotene reduces network excitability in models of Alzheimer's disease and epilepsy. *Neurobiology of Aging,* 35**,** 2091-2095.

BOURGUET, W., RUFF, M., CHAMBON, P., GRONEMEYER, H. & MORAS, D. 1995. Crystal structure of the ligand-binding domain of the human nuclear receptor RXR-alpha. *Nature,* 375**,** 377-82.

BOURNE, R. R. A. 2006. Worldwide glaucoma through the looking glass. *The British Journal of Ophthalmology,* 90**,** 253-254.

BRANCATO, R., CARASSA, R. & TRABUCCHI, G. 1991. Diode laser compared with argon laser for trabeculoplasty. *Am J Ophthalmol,* 112**,** 50-5.

BRAZDA, P., KRIEGER, J., DANIEL, B., JONAS, D., SZEKERES, T., LANGOWSKI, J., TOTH, K., NAGY, L. & VAMOSI, G. 2014. Ligand binding shifts highly mobile retinoid X receptor to the chromatin-bound state in a coactivator-dependent manner, as revealed by single-cell imaging. *Mol Cell Biol,* 34**,** 1234-45.

BUCHI, E. R., LAM, T. T., SUVAIZDIS, I. & TSO, M. O. 1994. Injuries induced by diffuse photodynamic action in retina and choroid of albino rats. Morphologic study of an experimental model. *Retina,* 14**,** 370-8.

BUDGIN, J. B., RICHARDSON, S. K., NEWTON, S. B., WYSOCKA, M., ZAKI, M. H., BENOIT, B. & ROOK, A. H. 2005. Biological effects of bexarotene in cutaneous T-cell lymphoma. *Arch Dermatol,* 141**,** 315-21.

BUI, B. V., HU, R. G., ACOSTA, M. L., DONALDSON, P., VINGRYS, A. J. & KALLONIATIS, M. 2009. Glutamate metabolic pathways and retinal function. *J Neurochem,* 111**,** 589-99.

CALFON, M., ZENG, H., URANO, F., TILL, J. H., HUBBARD, S. R., HARDING, H. P., CLARK, S. G. & RON, D. 2002. IRE1 couples endoplasmic reticulum load to secretory capacity by processing the XBP-1 mRNA. *Nature,* 415**,** 92-6.

CANCINO, G. I., TOLEDO, E. M., LEAL, N. R., HERNANDEZ, D. E., YÉVENES, L. F., INESTROSA, N. C. & ALVAREZ, A. R. 2008. STI571 prevents apoptosis, tau phosphorylation and behavioural impairments induced by Alzheimer's β-amyloid deposits. *Brain,* 131**,** 2425-2442.

CARAMELLI, P., NITRINI, R., MARANHAO, R., LOURENCO, A. C. G., DAMASCENO, M. C., VINAGRE, C. & CARAMELLI, B. 1999. Increased apolipoprotein B serum concentration in Alzheimer's disease. *Acta neurologica scandinavica,* 100**,** 61-63.

CASSON, R. J. 2006. Possible role of excitotoxicity in the pathogenesis of glaucoma. *Clinical & Experimental Ophthalmology,* 34**,** 54-63.

CAZORLA, M., JOUVENCEAU, A., ROSE, C., GUILLOUX, J. P., PILON, C., DRANOVSKY, A. & PREMONT, J. 2010. Cyclotraxin-B, the first highly potent and selective TrkB inhibitor, has anxiolytic properties in mice. *PLoS One,* 5**,** e9777.

ÇELĮK, S. K., ARAS, N., YILDIRIM, Ö., TURAN, F., GÖRÜR, A., YILDIRIM, H. & TAMER, L. 2014. Glutathione S-transferase GSTM 1, null genotype may be associated with susceptibility to age-related cataract. *Advances in clinical and experimental medicine: official organ Wroclaw Medical University,* 24**,** 113-119.

CERTO, M., ENDO, Y., OHTA, K., SAKURADA, S., BAGETTA, G. & AMANTEA, D. 2015. Activation of RXR/PPARgamma underlies neuroprotection by bexarotene in ischemic stroke. *Pharmacol Res,* 102**,** 298-307.

CHEN, G., FAN, Z., WANG, X., MA, C., BOWER, K. A., SHI, X., KE, Z. J. & LUO, J. 2007. Brain-derived neurotrophic factor suppresses tunicamycin-induced upregulation of CHOP in neurons. *J Neurosci Res,* 85**,** 1674-84.

CHENG, L., SAPIEHA, P., KITTLEROVA, P., HAUSWIRTH, W. W. & DI POLO, A. 2002. TrkB gene transfer protects retinal ganglion cells from axotomy-induced death in vivo. *J Neurosci,* 22**,** 3977-86.

CHEON, E. W., PARK, C. H., KANG, S. S., CHO, G. J., YOO, J. M., SONG, J. K. & CHOI, W. S. 2003. Change in endothelial nitric oxide synthase in the rat retina following transient ischemia. *Neuroreport,* 14**,** 329-33.

CHIANG, M. Y., MISNER, D., KEMPERMANN, G., SCHIKORSKI, T., GIGUERE, V., SUCOV, H. M., GAGE, F. H., STEVENS, C. F. & EVANS, R. M. 1998. An essential role for retinoid receptors RARbeta and RXRgamma in long-term potentiation and depression. *Neuron,* 21**,** 1353-61.

CHIBA, H., CLIFFORD, J., METZGER, D. & CHAMBON, P. 1997. Specific and Redundant Functions of Retinoid X Receptor/Retinoic Acid Receptor Heterodimers in Differentiation, Proliferation, and Apoptosis of F9 Embryonal Carcinoma Cells. *The Journal of Cell Biology,* 139**,** 735-747.

CHICK, J. M., MUNGER, S. C., SIMECEK, P., HUTTLIN, E. L., CHOI, K., GATTI, D. M., RAGHUPATHY, N., SVENSON, K. L., CHURCHILL, G. A. & GYGI, S. P. 2016. Defining the consequences of genetic variation on a proteome-wide scale. *Nature,* 534**,** 500-505.

CHITRANSHI, N., GUPTA, S., TRIPATHI, P. K. & SETH, P. K. 2013. New molecular scaffolds for the design of Alzheimer's acetylcholinesterase inhibitors identified using ligand- and receptor-based virtual screening. *Medicinal Chemistry Research,* 22**,** 2328-2345.

CHITRANSHI, N., GUPTA, V., DHEER, Y., GUPTA, V., VANDER WALL, R. & GRAHAM, S. 2016. Molecular determinants and interaction data of cyclic peptide inhibitor with the extracellular domain of TrkB receptor. *Data Brief,* 6**,** 776-82.

CHITRANSHI, N., GUPTA, V., KUMAR, S. & GRAHAM, S. L. 2015. Exploring the Molecular Interactions of 7,8-Dihydroxyflavone and Its Derivatives with TrkB and VEGFR2 Proteins. *International Journal of Molecular Sciences,* 16**,** 21087-21108.

CHIU, K., LAM, T. T., YING LI, W. W., CAPRIOLI, J. & KWONG KWONG, J. M. 2005. Calpain and N-methyl-d-aspartate (NMDA)-induced excitotoxicity in rat retinas. *Brain Res,* 1046**,** 207-15.

CHUNG, A. C. & COONEY, A. J. 2003. The varied roles of nuclear receptors during vertebrate embryonic development. *Nuclear Receptor Signaling,* 1**,** e007.

CLAUDEL, T., LEIBOWITZ, M. D., FIÉVET, C., TAILLEUX, A., WAGNER, B., REPA, J. J., TORPIER, G., LOBACCARO, J.-M., PATERNITI, J. R., MANGELSDORF, D. J., HEYMAN, R. A. & AUWERX, J. 2001. Reduction of atherosclerosis in apolipoprotein E knockout mice by activation of the retinoid X receptor. *Proceedings of the National Academy of Sciences,* 98**,** 2610.

COLEMAN, A. L., STONE, K., EWING, S. K., NEVITT, M., CUMMINGS, S., CAULEY, J. A., ENSRUD, K. E., HARRIS, E. L., HOCHBERG, M. C. & MANGIONE, C. M. 2004. Higher risk of multiple falls among elderly women who lose visual acuity. *Ophthalmology,* 111**,** 857-62.

CORNEJO, V. H. & HETZ, C. 2013. The unfolded protein response in Alzheimer's disease. *Semin Immunopathol,* 35**,** 277-92.

CORTES-CANTELI, M., ZAMOLODCHIKOV, D., AHN, H. J., STRICKLAND, S. & NORRIS, E. H. 2012. Fibrinogen and altered hemostasis in Alzheimer's disease. *Journal of Alzheimer's Disease,* 32**,** 599-608.

COSGROVE, M. S., BOEKE, J. D. & WOLBERGER, C. 2004. Regulated nucleosome mobility and the histone code. *Nat Struct Mol Biol,* 11**,** 1037-43.

COSTARIDES, A. P., RILEY, M. V. & GREEN, K. 1991. Roles of Catalase and the Glutathione Redox Cycle in the Regulation of Anterior-Chamber Hydrogen Peroxide. *Ophthalmic Research,* 23**,** 284-294.

CRAMER, P. E., CIRRITO, J. R., WESSON, D. W., DANIEL LEE, C. Y., KARLO, J. C., ZINN, A. E., CASALI, B. T., RESTIVO, J. L., GOEBEL, W. D., JAMES, M. J., BRUNDEN, K. R., WILSON, D. A. & LANDRETH, G. E. 2012. ApoE-Directed Therapeutics Rapidly Clear β-Amyloid and Reverse Deficits in AD Mouse Models. *Science (New York, N.Y.),* 335**,** 1503-1506.

CRAWFORD, M. L., HARWERTH, R. S., SMITH, E. L., 3RD, SHEN, F. & CARTER-DAWSON, L. 2000. Glaucoma in primates: cytochrome oxidase reactivity in parvo- and magnocellular pathways. *Invest Ophthalmol Vis Sci,* 41**,** 1791-802.

CRUNKHORN, S. 2012. Neurodegenerative disease: RXR agonist reverses Alzheimer's disease. *Nat Rev Drug Discov,* 11**,** 271.

CUMMINGS, J. L., ZHONG, K., KINNEY, J. W., HEANEY, C., MOLL-TUDLA, J., JOSHI, A., PONTECORVO, M., DEVOUS, M., TANG, A. & BENA, J. 2016. Double-blind, placebo-controlled, proof-of-concept trial of bexarotene Xin moderate Alzheimer's disease. *Alzheimers Res Ther,* 8**,** 4.

CUTLER, R. G., KELLY, J., STORIE, K., PEDERSEN, W. A., TAMMARA, A., HATANPAA, K., TRONCOSO, J. C. & MATTSON, M. P. 2004. Involvement of oxidative stress-induced abnormalities in ceramide and cholesterol metabolism in brain aging and Alzheimer's disease. *Proceedings of the National Academy of Sciences,* 101**,** 2070-2075.

CVEKL, A. & TAMM, E. R. 2004. Anterior eye development and ocular mesenchyme: new insights from mouse models and human diseases. *Bioessays,* 26**,** 374-86.

CVEKL, A. & WANG, W.-L. 2009. Retinoic acid signaling in mammalian eye development. *Experimental eye research,* 89**,** 280-291.
DAS, A., GARNER, D. P., DEL RE, A. M., WOODWARD, J. J., KUMAR, D. M., AGARWAL, N., BANIK, N. L. & RAY, S. K. 2006. Calpeptin provides functional neuroprotection to rat retinal ganglion cells following Ca2+ influx. *Brain Research,* 1084**,** 146-157.
DASGUPTA, S., HOHMAN, T. C. & CARPER, D. 1992. Hypertonic stress induces αB-crystallin expression. *Experimental Eye Research,* 54**,** 461-470.
DAWSON, M. I. & XIA, Z. 2012. The retinoid X receptors and their ligands. *Biochim Biophys Acta,* 1821**,** 21-56.
DELLA SANTINA, L., INMAN, D. M., LUPIEN, C. B., HORNER, P. J. & WONG, R. O. L. 2013. Differential Progression of Structural and Functional Alterations in Distinct Retinal Ganglion Cell Types in a Mouse Model of Glaucoma. *The Journal of Neuroscience,* 33**,** 17444-17457.
DEVI, L. & OHNO, M. 2012. 7,8-dihydroxyflavone, a small-molecule TrkB agonist, reverses memory deficits and BACE1 elevation in a mouse model of Alzheimer's disease. *Neuropsychopharmacology,* 37**,** 434-44.
DILSIZ, N., SAHABOGLU, A., YILDIZ, M. Z. & REICHENBACH, A. 2006. Protective effects of various antioxidants during ischemia-reperfusion in the rat retina. *Graefes Arch Clin Exp Ophthalmol,* 244**,** 627-33.
DING, W., YANG, L., ZHANG, M. & GU, Y. 2012. Reactive oxygen species-mediated endoplasmic reticulum stress contributes to aldosterone-induced apoptosis in tubular epithelial cells. *Biochem Biophys Res Commun,* 418**,** 451-6.
DING, Y., QIAO, A., WANG, Z., GOODWIN, J. S., LEE, E. S., BLOCK, M. L., ALLSBROOK, M., MCDONALD, M. P. & FAN, G. H. 2008. Retinoic acid attenuates beta-amyloid deposition and rescues memory deficits in an Alzheimer's disease transgenic mouse model. *J Neurosci,* 28**,** 11622-34.
DOECKE, J. D., LAWS, S. M., FAUX, N. G., WILSON, W., BURNHAM, S. C., LAM, C.-P., MONDAL, A., BEDO, J., BUSH, A. I. & BROWN, B. 2012. Blood-based protein biomarkers for diagnosis of Alzheimer disease. *Archives of neurology,* 69**,** 1318-1325.
DOH, S. H., KIM, J. H., LEE, K. M., PARK, H. Y. & PARK, C. K. 2010. Retinal ganglion cell death induced by endoplasmic reticulum stress in a chronic glaucoma model. *Brain Research,* 1308**,** 158-166.
DOUDEVSKI, I., ROSTAGNO, A., COWMAN, M., LIEBMANN, J., RITCH, R. & GHISO, J. 2014. Clusterin and Complement Activation in Exfoliation Glaucoma. *Investigative Ophthalmology & Visual Science,* 55**,** 2491-2499.
DUGGER, B. N., SERRANO, G. E., SUE, L. I., WALKER, D. G., ADLER, C. H., SHILL, H. A., SABBAGH, M. N., CAVINESS, J. N., HIDALGO, J., SAXON-LABELLE, M., CHIAROLANZA, G., MARINER, M., HENRY-WATSON, J., BEACH, T. G. & THE ARIZONA PARKINSON'S DISEASE, C. 2012. Presence of Striatal Amyloid Plaques in Parkinson's Disease Dementia Predicts Concomitant Alzheimer's Disease: Usefulness for Amyloid Imaging. *Journal of Parkinson's disease,* 2**,** 57-65.
DUNDAS, J., OUYANG, Z., TSENG, J., BINKOWSKI, A., TURPAZ, Y. & LIANG, J. 2006. CASTp: computed atlas of surface topography of proteins with structural and topographical mapping of functionally annotated residues. *Nucleic Acids Res,* 34**,** W116-8.
DUNKELBERGER, J. R. & SONG, W.-C. 2010. Complement and its role in innate and adaptive immune responses. *Cell research,* 20**,** 34-50.
EDSJO, A., LAVENIUS, E., NILSSON, H., HOEHNER, J. C., SIMONSSON, P., CULP, L. A., MARTINSSON, T., LARSSON, C. & PAHLMAN, S. 2003. Expression of trkB in human neuroblastoma in relation to MYCN expression and retinoic acid treatment. *Lab Invest,* 83**,** 813-23.
EGEA, P. F., MITSCHLER, A. & MORAS, D. 2002. Molecular recognition of agonist ligands by RXRs. *Mol Endocrinol,* 16**,** 987-97.

ELIAS, J. E. & GYGI, S. P. 2010. Target-Decoy Search Strategy for Mass Spectrometry-Based Proteomics. *In:* HUBBARD, S. J. & JONES, A. R. (eds.) *Proteome Bioinformatics.* Totowa, NJ: Humana Press.

ELLIOTT, D. A., WEICKERT, C. S. & GARNER, B. 2010. Apolipoproteins in the brain: implications for neurological and psychiatric disorders. *Clinical lipidology,* 5**,** 555-573.

ENG, J. K., MCCORMACK, A. L. & YATES, J. R. 1994. An approach to correlate tandem mass spectral data of peptides with amino acid sequences in a protein database. *Journal of the American Society for Mass Spectrometry,* 5**,** 976-989.

EPIS, R., MARCELLO, E., GARDONI, F. & DI LUCA, M. 2012. Alpha, beta-and gamma-secretases in Alzheimer's disease. *Front Biosci (Schol Ed),* 4**,** 1126-50.

EPPING, M. T., WANG, L., PLUMB, J. A., LIEB, M., GRONEMEYER, H., BROWN, R. & BERNARDS, R. 2007. A functional genetic screen identifies retinoic acid signaling as a target of histone deacetylase inhibitors. *Proc Natl Acad Sci U S A,* 104**,** 17777-82.

ETCHAMENDY, N., ENDERLIN, V., MARIGHETTO, A., PALLET, V., HIGUERET, P. & JAFFARD, R. 2003. Vitamin A deficiency and relational memory deficit in adult mice: relationships with changes in brain retinoid signalling. *Behav Brain Res,* 145**,** 37-49.

EWERS, M., MIELKE, M. M. & HAMPEL, H. 2010. Blood-based biomarkers of microvascular pathology in Alzheimer's disease. *Experimental gerontology,* 45**,** 75-79.

FAROL, L. T. & HYMES, K. B. 2004. Bexarotene: a clinical review. *Expert Rev Anticancer Ther,* 4**,** 180-8.

FEDOROV, S. N., IOFFE, D. I. & RONKINA, T. I. 1982. [Glaucoma surgery--deep sclerectomy]. *Vestn Oftalmol***,** 6-10.

FENG, D. F., CHEN, E. T., LI, X. Y., LIU, Y. & WANG, Y. 2010. Standardizing optic nerve crushes with an aneurysm clip. *Neurol Res,* 32**,** 476-81.

FENG, L., CHEN, H., SUYEOKA, G. & LIU, X. 2013. A Laser-induced Mouse Model of Chronic Ocular Hypertension to Characterize Visual Defects. *Journal of Visualized Experiments : JoVE***,** 50440.

FERRARA, F. F., FAZI, F., BIANCHINI, A., PADULA, F., GELMETTI, V., MINUCCI, S., MANCINI, M., PELICCI, P. G., LO COCO, F. & NERVI, C. 2001. Histone deacetylase-targeted treatment restores retinoic acid signaling and differentiation in acute myeloid leukemia. *Cancer Res,* 61**,** 2-7.

FITZ, N. F., CRONICAN, A. A., LEFTEROV, I. & KOLDAMOVA, R. 2013. Comment on "ApoE-directed therapeutics rapidly clear beta-amyloid and reverse deficits in AD mouse models". *Science,* 340**,** 924-c.

FONSECA, A. C., FERREIRO, E., OLIVEIRA, C. R., CARDOSO, S. M. & PEREIRA, C. F. 2013. Activation of the endoplasmic reticulum stress response by the amyloid-beta 1-40 peptide in brain endothelial cells. *Biochim Biophys Acta,* 1832**,** 2191-203.

FONSECA, M. I., CHU, S.-H., BERCI, A. M., BENOIT, M. E., PETERS, D. G., KIMURA, Y. & TENNER, A. J. 2011. Contribution of complement activation pathways to neuropathology differs among mouse models of Alzheimer's disease. *Journal of neuroinflammation,* 8**,** 4.

FORMAN, B. M., UMESONO, K., CHEN, J. & EVANS, R. M. 1995. Unique response pathways are established by allosteric interactions among nuclear hormone receptors. *Cell,* 81**,** 541-50.

FOSTER, P. J., BUHRMANN, R., QUIGLEY, H. A. & JOHNSON, G. J. 2002. The definition and classification of glaucoma in prevalence surveys. *British Journal of Ophthalmology,* 86**,** 238.

FOURGEUX, C., MARTINE, L., BJÖRKHEM, I., DICZFALUSY, U., JOFFRE, C., ACAR, N., CREUZOT-GARCHER, C., BRON, A. & BRETILLON, L. 2009. Primary open-angle glaucoma: association with cholesterol 24S-hydroxylase (CYP46A1) gene polymorphism and plasma 24-hydroxycholesterol levels. *Investigative ophthalmology & visual science,* 50**,** 5712-5717.

FRANCIS, B. A., SEE, R. F., RAO, N. A., MINCKLER, D. S. & BAERVELDT, G. 2006. Ab interno trabeculectomy: development of a novel device (Trabectome) and surgery for open-angle glaucoma. *J Glaucoma,* 15**,** 68-73.

FRANKFORT, B. J., KHAN, A. K., TSE, D. Y., CHUNG, I., PANG, J.-J., YANG, Z., GROSS, R. L. & WU, S. M. 2013. Elevated Intraocular Pressure Causes Inner Retinal Dysfunction Before Cell Loss in a Mouse Model of Experimental Glaucoma. *Investigative Ophthalmology & Visual Science,* 54**,** 762-770.

FROST, S., MARTINS, R. N. & KANAGASINGAM, Y. 2010. Ocular biomarkers for early detection of Alzheimer's disease. *Journal of Alzheimer's Disease,* 22**,** 1-16.

FU, C. T. & SRETAVAN, D. 2010. Laser-Induced Ocular Hypertension in Albino CD-1 Mice. *Investigative Ophthalmology & Visual Science,* 51**,** 980-990.

FU, Q. L., LI, X., YIP, H. K., SHAO, Z., WU, W., MI, S. & SO, K. F. 2009. Combined effect of brain-derived neurotrophic factor and LINGO-1 fusion protein on long-term survival of retinal ganglion cells in chronic glaucoma. *Neuroscience,* 162**,** 375-82.

FUNKE, S., PERUMAL, N., BECK, S., GABEL-SCHEURICH, S., SCHMELTER, C., TEISTER, J., GERBIG, C., GRAMLICH, O. W., PFEIFFER, N. & GRUS, F. H. 2016. Glaucoma related Proteomic Alterations in Human Retina Samples. *Scientific Reports,* 6**,** 29759.

GAMPE, R. T., JR., MONTANA, V. G., LAMBERT, M. H., MILLER, A. B., BLEDSOE, R. K., MILBURN, M. V., KLIEWER, S. A., WILLSON, T. M. & XU, H. E. 2000. Asymmetry in the PPARgamma/RXRalpha crystal structure reveals the molecular basis of heterodimerization among nuclear receptors. *Mol Cell,* 5**,** 545-55.

GENERALLY, G. S. H. 1997. Multiple roles of glutathione in the central nervous system. *Biol. Chem,* 378**,** 793-802.

GERMAIN, P., CHAMBON, P., EICHELE, G., EVANS, R. M., LAZAR, M. A., LEID, M., DE LERA, A. R., LOTAN, R., MANGELSDORF, D. J. & GRONEMEYER, H. 2006. International union of pharmacology. LXIII. Retinoid X receptors. *Pharmacological Reviews,* 58**,** 760-772.

GERMAN, O. L., MONACO, S., AGNOLAZZA, D. L., ROTSTEIN, N. P. & POLITI, L. E. 2013. Retinoid X receptor activation is essential for docosahexaenoic acid protection of retina photoreceptors. *J Lipid Res,* 54**,** 2236-46.

GERVAIS, F. G., XU, D., ROBERTSON, G. S., VAILLANCOURT, J. P., ZHU, Y., HUANG, J., LEBLANC, A., SMITH, D., RIGBY, M., SHEARMAN, M. S., CLARKE, E. E., ZHENG, H., VAN DER PLOEG, L. H., RUFFOLO, S. C., THORNBERRY, N. A., XANTHOUDAKIS, S., ZAMBONI, R. J., ROY, S. & NICHOLSON, D. W. 1999. Involvement of caspases in proteolytic cleavage of Alzheimer's amyloid-beta precursor protein and amyloidogenic A beta peptide formation. *Cell,* 97**,** 395-406.

GHARAGHANI, S., KHAYAMIAN, T. & EBRAHIMI, M. 2013. Molecular dynamics simulation study and molecular docking descriptors in structure-based QSAR on acetylcholinesterase (AChE) inhibitors. *SAR QSAR Environ Res,* 24**,** 773-94.

GHISO, J. A., DOUDEVSKI, I., RITCH, R. & ROSTAGNO, A. A. 2013. Alzheimer's Disease and Glaucoma: Mechanistic Similarities and Differences. *Journal of glaucoma,* 22**,** S36-S38.

GIANNACCARE, G., BAGNIS, A., GIZZI, C., VAGGE, A., FRESINA, M., DEL NOCE, C., SEBASTIANI, S., DORMI, A., TRAVERSO, C. E. & CAMPOS, E. 2016. EyeOP1 as a novel non-invasive surgical treatment of glaucoma: an Italian multicenter study. *Acta Ophthalmologica,* 94**,** n/a-n/a.

GINTY, D. D. & SEGAL, R. A. 2002. Retrograde neurotrophin signaling: Trk-ing along the axon. *Curr Opin Neurobiol,* 12**,** 268-74.

GNIADECKI, R., ASSAF, C., BAGOT, M., DUMMER, R., DUVIC, M., KNOBLER, R., RANKI, A., SCHWANDT, P. & WHITTAKER, S. 2007. The optimal use of bexarotene in cutaneous T-cell lymphoma. *Br J Dermatol,* 157**,** 433-40.

GOLDBLUM, D., KIPFER-KAUER, A., SARRA, G. M., WOLF, S. & FRUEH, B. E. 2007. Distribution of amyloid precursor protein and amyloid-beta immunoreactivity in DBA/2J glaucomatous mouse retinas. *Invest Ophthalmol Vis Sci,* 48**,** 5085-90.

GOLDSWORTHY, M. R. & VALLENCE, A.-M. 2013. The Role of β-Amyloid in Alzheimer's Disease-Related Neurodegeneration. *The Journal of Neuroscience,* 33**,** 12910-12911.

GOODMAN, A. B. 2006. Retinoid receptors, transporters, and metabolizers as therapeutic targets in late onset Alzheimer disease. *J Cell Physiol,* 209**,** 598-603.

GORLACH, A., KLAPPA, P. & KIETZMANN, T. 2006. The endoplasmic reticulum: folding, calcium homeostasis, signaling, and redox control. *Antioxid Redox Signal,* 8**,** 1391-418.
GOULD, D. B., SMITH, R. S. & JOHN, S. W. 2004. Anterior segment development relevant to glaucoma. *Int J Dev Biol,* 48**,** 1015-29.
GREEN, D. R. & REED, J. C. 1998. Mitochondria and apoptosis. *Science,* 281**,** 1309.
GRIESHABER, M. C., PIENAAR, A., OLIVIER, J. & STEGMANN, R. 2010. Canaloplasty for primary open-angle glaucoma: long-term outcome. *Br J Ophthalmol,* 94**,** 1478-82.
GUAN, B., ZHANG, C. & NING, J. 2017. Genetic algorithm with a crossover elitist preservation mechanism for protein-ligand docking. *AMB Express,* 7**,** 174.
GUETTE-FERNANDEZ, J. R., MELENDEZ, E., MALDONADO-ROJAS, W., ORTEGA-ZUNIGA, C., OLIVERO-VERBEL, J. & PARES-MATOS, E. I. 2017. A molecular docking study of the interactions between human transferrin and seven metallocene dichlorides. *J Mol Graph Model,* 75**,** 250-265.
GUO, L., MOSS, S. E., ALEXANDER, R. A., ALI, R. R., FITZKE, F. W. & CORDEIRO, M. F. 2005. Retinal ganglion cell apoptosis in glaucoma is related to intraocular pressure and IOP-induced effects on extracellular matrix. *Investigative ophthalmology & visual science,* 46**,** 175-182.
GUO, L., SALT, T. E., LUONG, V., WOOD, N., CHEUNG, W., MAASS, A., FERRARI, G., RUSSO-MARIE, F., SILLITO, A. M., CHEETHAM, M. E., MOSS, S. E., FITZKE, F. W. & CORDEIRO, M. F. 2007. Targeting amyloid-β in glaucoma treatment. *Proceedings of the National Academy of Sciences of the United States of America,* 104**,** 13444-13449.
GUO, L., SALT, T. E., MAASS, A., LUONG, V., MOSS, S. E., FITZKE, F. W. & CORDEIRO, M. F. 2006. Assessment of neuroprotective effects of glutamate modulation on glaucoma-related retinal ganglion cell apoptosis in vivo. *Invest Ophthalmol Vis Sci,* 47**,** 626-33.
GUPTA, N., ANG, L. C., DE TILLY, L. N., BIDAISEE, L. & YÜCEL, Y. H. 2006. Human glaucoma and neural degeneration in intracranial optic nerve, lateral geniculate nucleus, and visual cortex. *The British Journal of Ophthalmology,* 90**,** 674-678.
GUPTA, V., CHITRANSHI, N., YOU, Y., GUPTA, V., KLISTORNER, A. & GRAHAM, S. 2014. Brain derived neurotrophic factor is involved in the regulation of glycogen synthase kinase 3beta (GSK3beta) signalling. *Biochem Biophys Res Commun,* 454**,** 381-386.
GUPTA, V., GUPTA, V. B., CHITRANSHI, N., GANGODA, S., VANDER WALL, R., ABBASI, M., GOLZAN, M., DHEER, Y., SHAH, T. & AVOLIO, A. 2016a. One protein, multiple pathologies: multifaceted involvement of amyloid β in neurodegenerative disorders of the brain and retina. *Cellular and Molecular Life Sciences,* 73**,** 4279-4297.
GUPTA, V., GUPTA, V. B., CHITRANSHI, N., GANGODA, S., VANDER WALL, R., ABBASI, M., GOLZAN, M., DHEER, Y., SHAH, T., AVOLIO, A., CHUNG, R., MARTINS, R. & GRAHAM, S. 2016. One protein, multiple pathologies: multifaceted involvement of amyloid beta in neurodegenerative disorders of the brain and retina. *Cell Mol Life Sci,* 73**,** 4279-4297.
GUPTA, V. B., LAWS, S. M., VILLEMAGNE, V. L., AMES, D., BUSH, A. I., ELLIS, K. A., LUI, J. K., MASTERS, C., ROWE, C. C., SZOEKE, C., TADDEI, K., MARTINS, R. N. & GROUP, A. R. 2011. Plasma apolipoprotein E and Alzheimer disease risk: the AIBL study of aging. *Neurology,* 76**,** 1091-8.
GUPTA, V. K., CHITRANSHI, N., GUPTA, V. B., GOLZAN, M., DHEER, Y., VANDER WALL, R., GEORGEVSKY, D., KING, A. E., VICKERS, J. C. & CHUNG, R. 2016. Amyloid β accumulation and inner retinal degenerative changes in Alzheimer's disease transgenic mouse. *Neuroscience letters,* 623**,** 52-56.
GUPTA, V. K., YOU, Y., GUPTA, V. B., KLISTORNER, A. & GRAHAM, S. L. 2013. TrkB Receptor Signalling: Implications in Neurodegenerative, Psychiatric and Proliferative Disorders. *Int J Mol Sci,* 14**,** 10122-42.
GUPTA, V. K., YOU, Y., LI, J. C., KLISTORNER, A. & GRAHAM, S. L. 2013. Protective effects of 7,8-dihydroxyflavone on retinal ganglion and RGC-5 cells against excitotoxic and oxidative stress. *J Mol Neurosci,* 49**,** 96-104.

HARADA, T., HARADA, C., NAKAMURA, K., QUAH, H. M., OKUMURA, A., NAMEKATA, K., SAEKI, T., AIHARA, M., YOSHIDA, H., MITANI, A. & TANAKA, K. 2007. The potential role of glutamate transporters in the pathogenesis of normal tension glaucoma. *J Clin Invest,* 117**,** 1763-70.

HARDING, H. P., ZHANG, Y. & RON, D. 1999. Protein translation and folding are coupled by an endoplasmic-reticulum-resident kinase. *Nature,* 397**,** 271-4.

HAYMES, S. A., LEBLANC, R. P., NICOLELA, M. T., CHIASSON, L. A. & CHAUHAN, B. C. 2007. Risk of falls and motor vehicle collisions in glaucoma. *Invest Ophthalmol Vis Sci,* 48**,** 1149-55.

HAZE, K., OKADA, T., YOSHIDA, H., YANAGI, H., YURA, T., NEGISHI, M. & MORI, K. 2001. Identification of the G13 (cAMP-response-element-binding protein-related protein) gene product related to activating transcription factor 6 as a transcriptional activator of the mammalian unfolded protein response. *Biochem J,* 355**,** 19-28.

HEIJL, A., LESKE, M. C., BENGTSSON, B., HYMAN, L., BENGTSSON, B. & HUSSEIN, M. 2002. Reduction of intraocular pressure and glaucoma progression: results from the Early Manifest Glaucoma Trial. *Archives of ophthalmology,* 120**,** 1268-1279.

HELMER, C., MALET, F., ROUGIER, M. B., SCHWEITZER, C., COLIN, J., DELYFER, M. N., KOROBELNIK, J. F., BARBERGER-GATEAU, P., DARTIGUES, J. F. & DELCOURT, C. 2013. Is there a link between open-angle glaucoma and dementia? The Three-City-Alienor cohort. *Ann Neurol,* 74**,** 171-9.

HESS, B. 2008. P-LINCS: A Parallel Linear Constraint Solver for Molecular Simulation. *J Chem Theory Comput,* 4**,** 116-22.

HEYMAN, R. A., MANGELSDORF, D. J., DYCK, J. A., STEIN, R. B., EICHELE, G., EVANS, R. M. & THALLER, C. 1992. 9-cis retinoic acid is a high affinity ligand for the retinoid X receptor. *Cell,* 68**,** 397-406.

HINTON, D. R., SADUN, A. A., BLANKS, J. C. & MILLER, C. A. 1986. Optic-nerve degeneration in Alzheimer's disease. *N Engl J Med,* 315**,** 485-7.

HO, Y. S., YANG, X., LAU, J. C., HUNG, C. H., WUWONGSE, S., ZHANG, Q., WANG, J., BAUM, L., SO, K. F. & CHANG, R. C. 2012. Endoplasmic reticulum stress induces tau pathology and forms a vicious cycle: implication in Alzheimer's disease pathogenesis. *J Alzheimers Dis,* 28**,** 839-54.

HOLMES, C., BOCHE, D., WILKINSON, D., YADEGARFAR, G., HOPKINS, V., BAYER, A., JONES, R. W., BULLOCK, R., LOVE, S., NEAL, J. W., ZOTOVA, E. & NICOLL, J. A. 2008. Long-term effects of Abeta42 immunisation in Alzheimer's disease: follow-up of a randomised, placebo-controlled phase I trial. *Lancet,* 372**,** 216-23.

HONG, S., BEJA-GLASSER, V. F., NFONOYIM, B. M., FROUIN, A., LI, S., RAMAKRISHNAN, S., MERRY, K. M., SHI, Q., ROSENTHAL, A. & BARRES, B. A. 2016. Complement and microglia mediate early synapse loss in Alzheimer mouse models. *Science,* 352**,** 712-716.

HONG, S., IIZUKA, Y., KIM, C. Y. & SEONG, G. J. 2012. Isolation of primary mouse retinal ganglion cells using immunopanning-magnetic separation. *Molecular Vision,* 18**,** 2922-2930.

HOWELL, S. R., SHIRLEY, M. A., GRESE, T. A., NEEL, D. A., WELLS, K. E. & ULM, E. H. 2001. Bexarotene Metabolism in Rat, Dog, and Human, Synthesis of Oxidative Metabolites, and in Vitro Activity at Retinoid Receptors. *Drug Metabolism and Disposition,* 29**,** 990-998.

HSIEH, J., NAKASHIMA, K., KUWABARA, T., MEJIA, E. & GAGE, F. H. 2004. Histone deacetylase inhibition-mediated neuronal differentiation of multipotent adult neural progenitor cells. *Proceedings of the National Academy of Sciences of the United States of America,* 101**,** 16659.

HUANG, X., ALONSO, A., GUO, X., UMBACH, D. M., LICHTENSTEIN, M. L., BALLANTYNE, C. M., MAILMAN, R. B., MOSLEY, T. H. & CHEN, H. 2015. Statins, plasma cholesterol, and risk of Parkinson's disease: a prospective study. *Movement Disorders,* 30**,** 552-559.

HUNG, C.-W., CHEN, Y.-C., HSIEH, W.-L., CHIOU, S.-H. & KAO, C.-L. 2010. Ageing and neurodegenerative diseases. *Ageing Research Reviews,* 9**,** S36-S46.

HUTTLIN, E. L., TING, L., BRUCKNER, R. J., GEBREAB, F., GYGI, M. P., SZPYT, J., TAM, S., ZARRAGA, G., COLBY, G. & BALTIER, K. 2015. The BioPlex network: a systematic exploration of the human interactome. *Cell,* 162**,** 425-440.

HUUSKONEN, M. T., LOPPI, S., DHUNGANA, H., KEKSA-GOLDSTEINE, V., LEMARCHANT, S., KORHONEN, P., WOJCIECHOWSKI, S., POLLARI, E., VALONEN, P., KOPONEN, J., TAKASHIMA, A., LANDRETH, G., GOLDSTEINS, G., MALM, T., KOISTINAHO, J. & KANNINEN, K. M. 2016. Bexarotene targets autophagy and is protective against thromboembolic stroke in aged mice with tauopathy. *Scientific Reports,* 6**,** 33176.

INOUE, T., KAWAJI, T. & TANIHARA, H. 2013. Elevated Levels of Multiple Biomarkers of Alzheimer's Disease in the Aqueous Humor of Eyes With Open-Angle GlaucomaAlzheimer's Disease and OAG. *Investigative ophthalmology & visual science,* 54**,** 5353-5358.

JAIN, A., WORDINGER, R. J., YORIO, T. & CLARK, A. F. 2014. Role of the alternatively spliced glucocorticoid receptor isoform GRβ in steroid responsiveness and glaucoma. *Journal of Ocular Pharmacology and Therapeutics,* 30**,** 121-127.

JAIN, A. N. 2007. Surflex-Dock 2.1: robust performance from ligand energetic modeling, ring flexibility, and knowledge-based search. *J Comput Aided Mol Des,* 21**,** 281-306.

JANAKIRAM, N. B., MOHAMMED, A., QIAN, L., CHOI, C. I., STEELE, V. E. & RAO, C. V. 2012. Chemopreventive effects of RXR-selective rexinoid bexarotene on intestinal neoplasia of Apc(Min/+) mice. *Neoplasia,* 14**,** 159-68.

JANSSEN, J. J., KUHLMANN, E. D., VAN VUGT, A. H., WINKENS, H. J., JANSSEN, B. P., DEUTMAN, A. F. & DRIESSEN, C. A. 1999. Retinoic acid receptors and retinoid X receptors in the mature retina: subtype determination and cellular distribution. *Curr Eye Res,* 19**,** 338-47.

JANSSON, M., RADA, A., TOMIC, L., LARSSON, L.-I. & WADELIUS, C. 2003. Analysis of the Glutathione S-transferase M1 gene using pyrosequencing and multiplex PCR–no evidence of association to glaucoma. *Experimental eye research,* 77**,** 239-243.

JEE, B., KUMAR, S., YADAV, R., SINGH, Y., KUMAR, A. & SHARMA, N. 2017. Ursolic acid and carvacrol may be potential inhibitors of dormancy protein small heat shock protein16.3 of Mycobacterium tuberculosis. *J Biomol Struct Dyn***,** 1-10.

JERONIMO-SANTOS, A., VAZ, S. H., PARREIRA, S., RAPAZ-LERIAS, S., CAETANO, A. P., BUEE-SCHERRER, V., CASTREN, E., VALENTE, C. A., BLUM, D., SEBASTIAO, A. M. & DIOGENES, M. J. 2015. Dysregulation of TrkB Receptors and BDNF Function by Amyloid-beta Peptide is Mediated by Calpain. *Cereb Cortex,* 25**,** 3107-21.

JIANG, S.-M., ZENG, L.-P., ZENG, J.-H., TANG, L., CHEN, X.-M. & WEI, X. 2015. β-III-Tubulin: a reliable marker for retinal ganglion cell labeling in experimental models of glaucoma. *International Journal of Ophthalmology,* 8**,** 643-652.

JING, G., WANG, J. J. & ZHANG, S. X. 2012. ER stress and apoptosis: a new mechanism for retinal cell death. *Exp Diabetes Res,* 2012**,** 589589.

KASTNER, P., GRONDONA, J. M., MARK, M., GANSMULLER, A., LEMEUR, M., DECIMO, D., VONESCH, J.-L., DOLLÉ, P. & CHAMBON, P. 1994. Genetic analysis of RXRα developmental function: Convergence of RXR and RAR signaling pathways in heart and eye morphogenesis. *Cell,* 78**,** 987-1003.

KASTNER, P., MARK, M., LEID, M., GANSMULLER, A., CHIN, W., GRONDONA, J. M., DECIMO, D., KREZEL, W., DIERICH, A. & CHAMBON, P. 1996. Abnormal spermatogenesis in RXR beta mutant mice. *Genes Dev,* 10**,** 80-92.

KAWAHARA, K., SUENOBU, M., OHTSUKA, H., KUNIYASU, A., SUGIMOTO, Y., NAKAGOMI, M., FUKASAWA, H., SHUDO, K. & NAKAYAMA, H. 2014. Cooperative therapeutic action of retinoic acid receptor and retinoid x receptor agonists in a mouse model of Alzheimer's disease. *J Alzheimers Dis,* 42**,** 587-605.

KHOONSARI, P. E., HÄGGMARK, A., LÖNNBERG, M., MIKUS, M., KILANDER, L., LANNFELT, L., BERGQUIST, J., INGELSSON, M., NILSSON, P. & KULTIMA, K. 2016. Analysis of the Cerebrospinal Fluid Proteome in Alzheimer's Disease. *PloS one,* 11**,** e0150672.

KIM, H. Y., EGBERT, P. R. & SINGH, K. 2008. Long-term comparison of primary trabeculectomy with 5-fluorouracil versus mitomycin C in West Africa. *J Glaucoma,* 17**,** 578-83.

KINGMAN, S. 2004. Glaucoma is second leading cause of blindness globally. *Bull World Health Organ,* 82**,** 887-8.

KLIEWER, S. A., UMESONO, K., MANGELSDORF, D. J. & EVANS, R. M. 1992. Retinoid X receptor interacts with nuclear receptors in retinoic acid, thyroid hormone and vitamin D3 signalling. 355**,** 446.

KOLLURI, S. K., CORR, M., JAMES, S. Y., BERNASCONI, M., LU, D., LIU, W., COTTAM, H. B., LEONI, L. M., CARSON, D. A. & ZHANG, X.-K. 2005. The R-enantiomer of the nonsteroidal antiinflammatory drug etodolac binds retinoid X receptor and induces tumor-selective apoptosis. *Proceedings of the National Academy of Sciences of the United States of America,* 102**,** 2525-2530.

KORONYO-HAMAOUI, M., KORONYO, Y., LJUBIMOV, A. V., MILLER, C. A., KO, M. K., BLACK, K. L., SCHWARTZ, M. & FARKAS, D. L. 2011. Identification of amyloid plaques in retinas from Alzheimer's patients and noninvasive in vivo optical imaging of retinal plaques in a mouse model. *Neuroimage,* 54 Suppl 1**,** S204-17.

KORTUEM, K., GEIGER, L. K. & LEVIN, L. A. 2000. Differential susceptibility of retinal ganglion cells to reactive oxygen species. *Invest Ophthalmol Vis Sci,* 41**,** 3176-82.

KOTANI, H., TANABE, H., MIZUKAMI, H., MAKISHIMA, M. & INOUE, M. 2010. Identification of a Naturally Occurring Rexinoid, Honokiol, That Activates the Retinoid X Receptor. *Journal of Natural Products,* 73**,** 1332-1336.

KREZEL, W., DUPÉ, V., MARK, M., DIERICH, A., KASTNER, P. & CHAMBON, P. 1996. RXR gamma null mice are apparently normal and compound RXR alpha +/-/RXR beta -/-/RXR gamma -/- mutant mice are viable. *Proceedings of the National Academy of Sciences of the United States of America,* 93**,** 9010-9014.

KRISTIAN, T. & SIESJO, B. K. 1998. Calcium in ischemic cell death. *Stroke,* 29**,** 705-18.

KULAK, N. A., PICHLER, G., PARON, I., NAGARAJ, N. & MANN, M. 2014. Minimal, encapsulated proteomic-sample processing applied to copy-number estimation in eukaryotic cells. *Nature methods,* 11**,** 319-324.

KUNTZ, M., CANDELA, P., SAINT-POL, J., LAMARTINIERE, Y., BOUCAU, M. C., SEVIN, E., FENART, L. & GOSSELET, F. 2015. Bexarotene Promotes Cholesterol Efflux and Restricts Apical-to-Basolateral Transport of Amyloid-beta Peptides in an In Vitro Model of the Human Blood-Brain Barrier. *J Alzheimers Dis,* 48**,** 849-62.

KUO, M. H. & ALLIS, C. D. 1998. Roles of histone acetyltransferases and deacetylases in gene regulation. *Bioessays,* 20**,** 615-26.

KUROKAWA, R., DIRENZO, J., BOEHM, M., SUGARMAN, J., GLOSS, B., ROSENFELD, M. G., HEYMAN, R. A. & GLASS, C. K. 1994. Regulation of retinoid signalling by receptor polarity and allosteric control of ligand binding. *Nature,* 371**,** 528.

LAABICH, A., LI, G. & COOPER, N. G. 2001. Characterization of apoptosis-genes associated with NMDA mediated cell death in the adult rat retina. *Brain Res Mol Brain Res,* 91**,** 34-42.

LACLAIR, K. D., MANAYE, K. F., LEE, D. L., ALLARD, J. S., SAVONENKO, A. V., TRONCOSO, J. C. & WONG, P. C. 2013. Treatment with bexarotene, a compound that increases apolipoprotein-E, provides no cognitive benefit in mutant APP/PS1 mice. *Mol Neurodegener,* 8**,** 18.

LALLOYER, F., FIEVET, C., LESTAVEL, S., TORPIER, G., VAN DER VEEN, J., TOUCHE, V., BULTEL, S., YOUS, S., KUIPERS, F., PAUMELLE, R., FRUCHART, J. C., STAELS, B. & TAILLEUX, A. 2006. The RXR agonist bexarotene improves cholesterol homeostasis and inhibits atherosclerosis progression in a mouse model of mixed dyslipidemia. *Arterioscler Thromb Vasc Biol,* 26**,** 2731-7.

LANE, M. A. & BAILEY, S. J. 2005. Role of retinoid signalling in the adult brain. *Prog Neurobiol,* 75**,** 275-93.

LAUWEN, S., DE JONG, E. K., LEFEBER, D. J. & DEN HOLLANDER, A. I. 2017. Omics Biomarkers in OphthalmologyOmics Biomarkers in Ophthalmology. *Investigative Ophthalmology & Visual Science,* 58**,** BIO88-BIO98.

LE MAIRE, A., GRIMALDI, M., ROECKLIN, D., DAGNINO, S., VIVAT-HANNAH, V., BALAGUER, P. & BOURGUET, W. 2009. Activation of RXR-PPAR heterodimers by organotin environmental endocrine disruptors. *EMBO Reports,* 10**,** 367-373.

LEE, S. E., KOO, Y. D., LEE, J. S., KWAK, S. H., JUNG, H. S., CHO, Y. M., PARK, Y. J., CHUNG, S. S. & PARK, K. S. 2015. Retinoid X Receptor α Overexpression Alleviates Mitochondrial Dysfunction-induced Insulin Resistance through Transcriptional Regulation of Insulin Receptor Substrate 1. *Molecules and Cells,* 38**,** 356-361.

LEFEBVRE, P., BENOMAR, Y. & STAELS, B. 2010. Retinoid X receptors: common heterodimerization partners with distinct functions. *Trends in Endocrinology & Metabolism,* 21**,** 676-683.

LEFFLER, C. T., SCHWARTZ, S. G., HADI, T. M., SALMAN, A. & VASUKI, V. 2015. The early history of glaucoma: the glaucous eye (800 BC to 1050 AD). *Clin Ophthalmol,* 9**,** 207-15.

LENGQVIST, J., MATA DE URQUIZA, A., BERGMAN, A. C., WILLSON, T. M., SJOVALL, J., PERLMANN, T. & GRIFFITHS, W. J. 2004. Polyunsaturated fatty acids including docosahexaenoic and arachidonic acid bind to the retinoid X receptor alpha ligand-binding domain. *Mol Cell Proteomics,* 3**,** 692-703.

LESKE, M. C., HEIJL, A., HYMAN, L., BENGTSSON, B. & KOMAROFF, E. 2004. Factors for progression and glaucoma treatment: the Early Manifest Glaucoma Trial. *Curr Opin Ophthalmol,* 15**,** 102-6.

LEVI, M. & VAN DER POLL, T. 2005. Two-way interactions between inflammation and coagulation. *Trends in cardiovascular medicine,* 15**,** 254-259.

LEVI, M., VAN DER POLL, T. & BÜLLER, H. R. 2004. Bidirectional relation between inflammation and coagulation. *Circulation,* 109**,** 2698-2704.

LEWIS, R. A., VON WOLFF, K., TETZ, M., KORBER, N., KEARNEY, J. R., SHINGLETON, B. & SAMUELSON, T. W. 2007. Canaloplasty: circumferential viscodilation and tensioning of Schlemm's canal using a flexible microcatheter for the treatment of open-angle glaucoma in adults: interim clinical study analysis. *J Cataract Refract Surg,* 33**,** 1217-26.

LI, R., YANG, L., LINDHOLM, K., KONISHI, Y., YUE, X., HAMPEL, H., ZHANG, D. & SHEN, Y. 2004. Tumor necrosis factor death receptor signaling cascade is required for amyloid-beta protein-induced neuron death. *J Neurosci,* 24**,** 1760-71.

LI, Y., ROTH, S., LASER, M., MA, J.-X. & CROSSON, C. E. 2003. Retinal Preconditioning and the Induction of Heat-Shock Protein 27. *Investigative Ophthalmology & Visual Science,* 44**,** 1299-1304.

LIAO, Y., FUNG, T. S., HUANG, M., FANG, S. G., ZHONG, Y. & LIU, D. X. 2013. Upregulation of CHOP/GADD153 during Coronavirus Infectious Bronchitis Virus Infection Modulates Apoptosis by Restricting Activation of the Extracellular Signal-Regulated Kinase Pathway. *J Virol,* 87**,** 8124-34.

LIBBY, R. T., ANDERSON, M. G., PANG, I. H., ROBINSON, Z. H., SAVINOVA, O. V., COSMA, I. M., SNOW, A., WILSON, L. A., SMITH, R. S., CLARK, A. F. & JOHN, S. W. 2005. Inherited glaucoma in DBA/2J mice: pertinent disease features for studying the neurodegeneration. *Vis Neurosci,* 22**,** 637-48.

LICHTENTHALER, S. F. 2012. Alpha-secretase cleavage of the amyloid precursor protein: proteolysis regulated by signaling pathways and protein trafficking. *Curr Alzheimer Res,* 9**,** 165-77.

LIN, M. T. & BEAL, M. F. 2006. Mitochondrial dysfunction and oxidative stress in neurodegenerative diseases. *Nature,* 443**,** 787-795.

LINDEN, R. 2000. The anti-death league: associative control of apoptosis in developing retinal tissue. *Brain Research Reviews,* 32**,** 146-158.

LINDQUIST, S. & CRAIG, E. A. 1988. The Heat-Shock Proteins. *Annual Review of Genetics,* 22**,** 631-677.

LIU, C.-C., KANEKIYO, T., XU, H. & BU, G. 2013. Apolipoprotein E and Alzheimer disease: risk, mechanisms and therapy. *Nature Reviews Neurology,* 9**,** 106-118.
LIU, J.-P., TANG, Y., ZHOU, S., TOH, B. H., MCLEAN, C. & LI, H. 2010. Cholesterol involvement in the pathogenesis of neurodegenerative diseases. *Molecular and Cellular Neuroscience,* 43**,** 33-42.
LIU, K., ZOU, C. & QIN, B. 2017. The association between nuclear receptors and ocular diseases. *Oncotarget,* 8**,** 27603-27615.
LIU, Y. & ALLINGHAM, R. R. 2011. Molecular genetics in glaucoma. *Exp Eye Res,* 93**,** 331-9.
LONDON, A., BENHAR, I. & SCHWARTZ, M. 2013. The retina as a window to the brain—from eye research to CNS disorders. *Nature Reviews Neurology,* 9**,** 44-53.
LU, Y., LI, Z., ZHANG, X., MING, B., JIA, J., WANG, R. & MA, D. 2010. Retinal nerve fiber layer structure abnormalities in early Alzheimer's disease: evidence in optical coherence tomography. *Neuroscience letters,* 480**,** 69-72.
LUCARELLI, E., KAPLAN, D. R. & THIELE, C. J. 1995. Selective regulation of TrkA and TrkB receptors by retinoic acid and interferon-gamma in human neuroblastoma cell lines. *J Biol Chem,* 270**,** 24725-31.
LUCAS, D. R. & NEWHOUSE, J. P. 1957. The toxic effect of sodium L-glutamate on the inner layers of the retina. *AMA Arch Ophthalmol,* 58**,** 193-201.
MA, R., ZHANG, J., LIU, X., YUE, S., ZHAO, Q. & XU, Y. 2016. 7,8-DHF Treatment Induces Cyr61 Expression to Suppress Hypoxia Induced ER Stress in HK-2 Cells. *Biomed Res Int,* 2016**,** 5029797.
MANDREKAR-COLUCCI, S. & LANDRETH, G. E. 2011. Nuclear receptors as therapeutic targets for Alzheimer's disease. *Expert Opin Ther Targets,* 15**,** 1085-97.
MANGELSDORF, D. J., BORGMEYER, U., HEYMAN, R. A., ZHOU, J. Y., ONG, E. S., ORO, A. E., KAKIZUKA, A. & EVANS, R. M. 1992. Characterization of three RXR genes that mediate the action of 9-cis retinoic acid. *Genes Dev,* 6**,** 329-44.
MANGELSDORF, D. J., ONG, E. S., DYCK, J. A. & EVANS, R. M. 1990. Nuclear receptor that identifies a novel retinoic acid response pathway. 345**,** 224.
MANGELSDORF, D. J., THUMMEL, C., BEATO, M., HERRLICH, P., SCHÜTZ, G., UMESONO, K., BLUMBERG, B., KASTNER, P., MARK, M., CHAMBON, P. & EVANS, R. M. 1995. The nuclear receptor superfamily: The second decade. *Cell,* 83**,** 835-839.
MANGIALASCHE, F., SOLOMON, A., WINBLAD, B., MECOCCI, P. & KIVIPELTO, M. 2010. Alzheimer's disease: clinical trials and drug development. *Lancet Neurol,* 9**,** 702-16.
MARCELO, R. & SARAGOVI, H. U. 2005. Glaucoma: Validated and Facile In Vivo Experimental Models of a Chronic Neurodegenerative Disease for Drug Development. *Current Medicinal Chemistry - Central Nervous System Agents,* 5**,** 43-49.
MARÍ, M., MORALES, A., COLELL, A., GARCÍA-RUIZ, C. & FERNÁNDEZ-CHECA, J. C. 2009. Mitochondrial glutathione, a key survival antioxidant. *Antioxidants & redox signaling,* 11**,** 2685-2700.
MARIANI, M. M., MALM, T., LAMB, R., JAY, T. R., NEILSON, L., CASALI, B., MEDARAMETLA, L. & LANDRETH, G. E. 2017. Neuronally-directed effects of RXR activation in a mouse model of Alzheimer's disease. *Sci Rep,* 7**,** 42270.
MARTIN, L. J. 2010. Mitochondrial and cell death mechanisms in neurodegenerative diseases. *Pharmaceuticals,* 3**,** 839-915.
MARTINS, I. J., BERGER, T., SHARMAN, M. J., VERDILE, G., FULLER, S. J. & MARTINS, R. N. 2009. Cholesterol metabolism and transport in the pathogenesis of Alzheimer's disease. *Journal of neurochemistry,* 111**,** 1275-1308.
MARTONAK, R., LAIO, A. & PARRINELLO, M. 2003. Predicting crystal structures: the Parrinello-Rahman method revisited. *Phys Rev Lett,* 90**,** 075503.
MATÉS, J. M., PÉREZ-GÓMEZ, C. & DE CASTRO, I. N. 1999. Antioxidant enzymes and human diseases. *Clinical biochemistry,* 32**,** 595-603.

MATÍAS-GUIU, J. A., OREJA-GUEVARA, C., CABRERA-MARTÍN, M. N., MORENO-RAMOS, T., CARRERAS, J. L. & MATÍAS-GUIU, J. 2016. Amyloid Proteins and Their Role in Multiple Sclerosis. Considerations in the Use of Amyloid-PET Imaging. *Frontiers in Neurology,* 7**,** 53.

MATSUMOTO, K., WADA, R. K., YAMASHIRO, J. M., KAPLAN, D. R. & THIELE, C. J. 1995. Expression of brain-derived neurotrophic factor and p145TrkB affects survival, differentiation, and invasiveness of human neuroblastoma cells. *Cancer Res,* 55**,** 1798-806.

MCALISTER, G. C., HUTTLIN, E. L., HAAS, W., TING, L., JEDRYCHOWSKI, M. P., ROGERS, J. C., KUHN, K., PIKE, I., GROTHE, R. A. & BLETHROW, J. D. 2012. Increasing the multiplexing capacity of TMTs using reporter ion isotopologues with isobaric masses. *Analytical chemistry,* 84**,** 7469-7478.

MCALISTER, G. C., NUSINOW, D. P., JEDRYCHOWSKI, M. P., WÜHR, M., HUTTLIN, E. L., ERICKSON, B. K., RAD, R., HAAS, W. & GYGI, S. P. 2014. MultiNotch MS3 enables accurate, sensitive, and multiplexed detection of differential expression across cancer cell line proteomes. *Analytical chemistry,* 86**,** 7150-7158.

MCFARLAND, K., SPALDING, T. A., HUBBARD, D., MA, J. N., OLSSON, R. & BURSTEIN, E. S. 2013. Low dose bexarotene treatment rescues dopamine neurons and restores behavioral function in models of Parkinson's disease. *ACS Chem Neurosci,* 4**,** 1430-8.

MCGEER, P. L., AKIYAMA, H., ITAGAKI, S. & MCGEER, E. G. 1989. Activation of the classical complement pathway in brain tissue of Alzheimer patients. *Neuroscience Letters,* 107**,** 341-346.

MCGWIN, G., JR., OWSLEY, C. & BALL, K. 1998. Identifying crash involvement among older drivers: agreement between self-report and state records. *Accid Anal Prev,* 30**,** 781-91.

MCKINNON, S. J. 2003. Glaucoma: ocular Alzheimer's disease? *Front Biosci,* 8**,** s1140-56.

MCKINNON, S. J., LEHMAN, D. M., KERRIGAN-BAUMRIND, L. A., MERGES, C. A., PEASE, M. E., KERRIGAN, D. F., RANSOM, N. L., TAHZIB, N. G., REITSAMER, H. A., LEVKOVITCH-VERBIN, H., QUIGLEY, H. A. & ZACK, D. J. 2002. Caspase activation and amyloid precursor protein cleavage in rat ocular hypertension. *Invest Ophthalmol Vis Sci,* 43**,** 1077-87.

MENIKARACHCHI, L. C., HAMDALLA, M. A., HILL, D. W. & GRANT, D. F. 2013. Chemical structure identification in metabolomics: computational modeling of experimental features. *Comput Struct Biotechnol J,* 5**,** e201302005.

MINGAUD, F., MORMEDE, C., ETCHAMENDY, N., MONS, N., NIEDERGANG, B., WIETRZYCH, M., PALLET, V., JAFFARD, R., KREZEL, W., HIGUERET, P. & MARIGHETTO, A. 2008. Retinoid hyposignaling contributes to aging-related decline in hippocampal function in short-term/working memory organization and long-term declarative memory encoding in mice. *J Neurosci,* 28**,** 279-91.

MINICHIELLO, L. 2009. TrkB signalling pathways in LTP and learning. *Nat Rev Neurosci,* 10**,** 850-60.

MIRZAEI, M., PASCOVICI, D., WU, J. X., CHICK, J., WU, Y., COOKE, B., HAYNES, P. & MOLLOY, M. P. 2017. TMT One-Stop Shop: From Reliable Sample Preparation to Computational Analysis Platform. *In:* KEERTHIKUMAR, S. & MATHIVANAN, S. (eds.) *Proteome Bioinformatics.* New York, NY: Springer New York.

MOITESSIER, N., HENRY, C., MAIGRET, B. & CHAPLEUR, Y. 2004. Combining pharmacophore search, automated docking, and molecular dynamics simulations as a novel strategy for flexible docking. Proof of concept: docking of arginine-glycine-aspartic acid-like compounds into the alphavbeta3 binding site. *J Med Chem,* 47**,** 4178-87.

MONEMI, S., SPAETH, G., DASILVA, A., POPINCHALK, S., ILITCHEV, E., LIEBMANN, J., RITCH, R., HEON, E., CRICK, R. P., CHILD, A. & SARFARAZI, M. 2005. Identification of a novel adult-onset primary open-angle glaucoma (POAG) gene on 5q22.1. *Hum Mol Genet,* 14**,** 725-33.

MOREIRA, P. I., CARVALHO, C., ZHU, X., SMITH, M. A. & PERRY, G. 2010. Mitochondrial dysfunction is a trigger of Alzheimer's disease pathophysiology. *Biochimica et Biophysica Acta (BBA)-Molecular Basis of Disease,* 1802**,** 2-10.

MORENO, M. C., MARCOS, H. J. A., OSCAR CROXATTO, J., SANDE, P. H., CAMPANELLI, J., JALIFFA, C. O., BENOZZI, J. & ROSENSTEIN, R. E. 2005. A new experimental model of glaucoma in

rats through intracameral injections of hyaluronic acid. *Experimental Eye Research,* 81**,** 71-80.

MORI, K., MA, W., GETHING, M. J. & SAMBROOK, J. 1993. A transmembrane protein with a cdc2+/CDC28-related kinase activity is required for signaling from the ER to the nucleus. *Cell,* 74**,** 743-56.

MORI, M., GHYSELINCK, N. B., CHAMBON, P. & MARK, M. 2001. Systematic immunolocalization of retinoid receptors in developing and adult mouse eyes. *Invest Ophthalmol Vis Sci,* 42**,** 1312-8.

MORI, M., METZGER, D., PICAUD, S., HINDELANG, C., SIMONUTTI, M., SAHEL, J., CHAMBON, P. & MARK, M. 2004. Retinal dystrophy resulting from ablation of RXR alpha in the mouse retinal pigment epithelium. *Am J Pathol,* 164**,** 701-10.

MORIMOTO, R. I. 1998. Regulation of the heat shock transcriptional response: cross talk between a family of heat shock factors, molecular chaperones, and negative regulators. *Genes Dev,* 12**,** 3788-96.

MORISHIMA, Y., GOTOH, Y., ZIEG, J., BARRETT, T., TAKANO, H., FLAVELL, R., DAVIS, R. J., SHIRASAKI, Y. & GREENBERG, M. E. 2001. Beta-amyloid induces neuronal apoptosis via a mechanism that involves the c-Jun N-terminal kinase pathway and the induction of Fas ligand. *J Neurosci,* 21**,** 7551-60.

MORRIS, G. M., GREEN, L. G., RADIC, Z., TAYLOR, P., SHARPLESS, K. B., OLSON, A. J. & GRYNSZPAN, F. 2013. Automated docking with protein flexibility in the design of femtomolar "click chemistry" inhibitors of acetylcholinesterase. *J Chem Inf Model,* 53**,** 898-906.

MORRIS, G. M., HUEY, R. & OLSON, A. J. 2008. Using AutoDock for ligand-receptor docking. *Curr Protoc Bioinformatics,* Chapter 8**,** Unit 8 14.

MORRISON, J. C., MOORE, C. G., DEPPMEIER, L. M., GOLD, B. G., MESHUL, C. K. & JOHNSON, E. C. 1997. A rat model of chronic pressure-induced optic nerve damage. *Exp Eye Res,* 64**,** 85-96.

MOUNIER, A., GEORGIEV, D., NAM, K. N., FITZ, N. F., CASTRANIO, E. L., WOLFE, C. M., CRONICAN, A. A., SCHUG, J., LEFTEROV, I. & KOLDAMOVA, R. 2015. Bexarotene-Activated Retinoid X Receptors Regulate Neuronal Differentiation and Dendritic Complexity. *J Neurosci,* 35**,** 11862-76.

MURPHY, M. P. & LEVINE, H. 2010. Alzheimer's Disease and the β-Amyloid Peptide. *Journal of Alzheimer's disease : JAD,* 19**,** 311.

NA, C. H., JEON, S. H., ZHANG, G., OLSON, G. L. & CHAE, C. B. 2007. Inhibition of amyloid beta-peptide production by blockage of beta-secretase cleavage site of amyloid precursor protein. *J Neurochem,* 101**,** 1583-95.

NAGAHARA, A. H., MERRILL, D. A., COPPOLA, G., TSUKADA, S., SCHROEDER, B. E., SHAKED, G. M., WANG, L., BLESCH, A., KIM, A., CONNER, J. M., ROCKENSTEIN, E., CHAO, M. V., KOO, E. H., GESCHWIND, D., MASLIAH, E., CHIBA, A. A. & TUSZYNSKI, M. H. 2009. Neuroprotective effects of brain-derived neurotrophic factor in rodent and primate models of Alzheimer's disease. *Nat Med,* 15**,** 331-7.

NAKAMURA, O., MORITOH, S., SATO, K., MAEKAWA, S., MURAYAMA, N., HIMORI, N., OMODAKA, K., SOGON, T. & NAKAZAWA, T. 2017. Bilberry extract administration prevents retinal ganglion cell death in mice via the regulation of chaperone molecules under conditions of endoplasmic reticulum stress. *Clin Ophthalmol,* 11**,** 1825-1834.

NAM, K. N., MOUNIER, A., FITZ, N. F., WOLFE, C., SCHUG, J., LEFTEROV, I. & KOLDAMOVA, R. 2016. RXR controlled regulatory networks identified in mouse brain counteract deleterious effects of Aβ oligomers. *Scientific Reports,* 6**,** 24048.

NATRAJAN, M. S., DE LA FUENTE, A. G., CRAWFORD, A. H., LINEHAN, E., NUNEZ, V., JOHNSON, K. R., WU, T., FITZGERALD, D. C., RICOTE, M., BIELEKOVA, B. & FRANKLIN, R. J. 2015. Retinoid X receptor activation reverses age-related deficiencies in myelin debris phagocytosis and remyelination. *Brain,* 138**,** 3581-97.

NEUFELD, A. H., DAS, S., VORA, S., GACHIE, E., KAWAI, S., MANNING, P. T. & CONNOR, J. R. 2002. A prodrug of a selective inhibitor of inducible nitric oxide synthase is neuroprotective in the rat model of glaucoma. *J Glaucoma,* 11**,** 221-5.

NEUFELD, A. H. & LIU, B. 2003. Glaucomatous optic neuropathy: when glia misbehave. *Neuroscientist,* 9**,** 485-95.

NG, D. T., WATOWICH, S. S. & LAMB, R. A. 1992. Analysis in vivo of GRP78-BiP/substrate interactions and their role in induction of the GRP78-BiP gene. *Mol Biol Cell,* 3**,** 143-55.

NGUYEN, N., LEE, S. B., LEE, Y. S., LEE, K. H. & AHN, J. Y. 2009. Neuroprotection by NGF and BDNF against neurotoxin-exerted apoptotic death in neural stem cells are mediated through Trk receptors, activating PI3-kinase and MAPK pathways. *Neurochem Res,* 34**,** 942-51.

NICHAMIN, L. D. 2009. Glaukos iStent(®) Trabecular Micro-Bypass. *Middle East African Journal of Ophthalmology,* 16**,** 138-140.

NICKELLS, R. W. 1999. Apoptosis of retinal ganglion cells in glaucoma: an update of the molecular pathways involved in cell death. *Surv Ophthalmol,* 43 Suppl 1**,** S151-61.

NITA, M. & GRZYBOWSKI, A. 2016. The Role of the Reactive Oxygen Species and Oxidative Stress in the Pathomechanism of the Age-Related Ocular Diseases and Other Pathologies of the Anterior and Posterior Eye Segments in Adults. *Oxidative Medicine and Cellular Longevity,* 2016**,** 3164734.

NJIE-MBYE, Y. F., CHITNIS, M., OPERE, C. & OHIA, S. 2013. Lipid peroxidation: pathophysiological and pharmacological implications in the eye. *Frontiers in Physiology,* 4.

NORIS, M., MESCIA, F. & REMUZZI, G. 2012. STEC-HUS, atypical HUS and TTP are all diseases of complement activation. *Nature Reviews Nephrology,* 8**,** 622-633.

O'BRYANT, S. E., LISTA, S., RISSMAN, R. A., EDWARDS, M., ZHANG, F., HALL, J., ZETTERBERG, H., LOVESTONE, S., GUPTA, V. & GRAFF-RADFORD, N. 2016. Comparing biological markers of Alzheimer's disease across blood fraction and platforms: Comparing apples to oranges. *Alzheimer's & Dementia: Diagnosis, Assessment & Disease Monitoring,* 3**,** 27-34.

O'BRYANT, S. E., XIAO, G., BARBER, R., HUEBINGER, R., WILHELMSEN, K., EDWARDS, M., GRAFF-RADFORD, N., DOODY, R., DIAZ-ARRASTIA, R., TEXAS ALZHEIMER'S, R. & CARE, C. 2011. A blood-based screening tool for Alzheimer's disease that spans serum and plasma: findings from TARC and ADNI. *PloS one,* 6**,** e28092.

OHLSSON, M., MATTSSON, P. & SVENSSON, M. 2004. A temporal study of axonal degeneration and glial scar formation following a standardized crush injury of the optic nerve in the adult rat. *Restor Neurol Neurosci,* 22**,** 1-10.

OMAR, R. & PAPPOLLA, M. 1993. Oxygen free radicals as inducers of heat shock protein synthesis in cultured human neuroblastoma cells: Relevance to neurodegenerative disease. *European Archives of Psychiatry and Clinical Neuroscience,* 242**,** 262-267.

OPPENHEIM, R. W. 1991. Cell death during development of the nervous system. *Annu Rev Neurosci,* 14**,** 453-501.

OSBORNE, N. N. 2008. Pathogenesis of ganglion "cell death" in glaucoma and neuroprotection: focus on ganglion cell axonal mitochondria. *Prog Brain Res,* 173**,** 339-52.

OSBORNE, N. N. 2010. Mitochondria: their role in ganglion cell death and survival in primary open angle glaucoma. *Experimental eye research,* 90**,** 750-757.

OSBORNE, N. N., CHIDLOW, G. & WOOD, J. P. 2006. Glutamate excitotoxicity in glaucoma: truth or fiction? By AJ Lotery. *Eye (Lond),* 20**,** 1392-4.

OWSLEY, C. & MCGWIN, G., JR. 2004. Depression and the 25-item National Eye Institute Visual Function Questionnaire in older adults. *Ophthalmology,* 111**,** 2259-64.

OYADOMARI, S. & MORI, M. 2003. Roles of CHOP//GADD153 in endoplasmic reticulum stress. *Cell Death Differ,* 11**,** 381-389.

PASCHEN, W. & FRANDSEN, A. 2001. Endoplasmic reticulum dysfunction--a common denominator for cell injury in acute and degenerative diseases of the brain? *J Neurochem,* 79**,** 719-25.

PASCHEN, W. & MENGESDORF, T. 2005. Endoplasmic reticulum stress response and neurodegeneration. *Cell Calcium,* 38**,** 409-15.

PENG, S., WUU, J., MUFSON, E. J. & FAHNESTOCK, M. 2005. Precursor form of brain-derived neurotrophic factor and mature brain-derived neurotrophic factor are decreased in the pre-clinical stages of Alzheimer's disease. *J Neurochem,* 93**,** 1412-21.

PEREZ-PASTENE, C., GRAUMANN, R., DÍAZ-GREZ, F., MIRANDA, M., VENEGAS, P., GODOY, O. T., LAYSON, L., VILLAGRA, R., MATAMALA, J. M. & HERRERA, L. 2007. Association of GST M1 null polymorphism with Parkinson's disease in a Chilean population with a strong Amerindian genetic component. *Neuroscience letters,* 418**,** 181-185.

PÉREZ, E., BOURGUET, W., GRONEMEYER, H. & DE LERA, A. R. 2012. Modulation of RXR function through ligand design. *Biochimica et Biophysica Acta (BBA) - Molecular and Cell Biology of Lipids,* 1821**,** 57-69.

PERRY, T. L., GODIN, D. V. & HANSEN, S. 1982. Parkinson's disease: a disorder due to nigral glutathione deficiency? *Neurosci Lett,* 33**,** 305-10.

PETERS, J. C., BHATTACHARYA, S., CLARK, A. F. & ZODE, G. S. 2015. Increased Endoplasmic Reticulum Stress in Human Glaucomatous Trabecular Meshwork Cells and Tissues. *Invest Ophthalmol Vis Sci,* 56**,** 3860-8.

PETTERSEN, E. F., GODDARD, T. D., HUANG, C. C., COUCH, G. S., GREENBLATT, D. M., MENG, E. C. & FERRIN, T. E. 2004. UCSF Chimera--a visualization system for exploratory research and analysis. *J Comput Chem,* 25**,** 1605-12.

PIRI, N., KWONG, J. M. K., GU, L. & CAPRIOLI, J. 2016. Heat shock proteins in the retina: Focus on HSP70 and alpha crystallins in ganglion cell survival. *Progress in Retinal and Eye Research,* 52**,** 22-46.

PIRI, N., SONG, M., KWONG, J. M. K. & CAPRIOLI, J. 2006. Expression of Crystallin Genes Is Downregulated in Experimental Glaucoma. *Investigative Ophthalmology & Visual Science,* 47**,** 1825-1825.

POLYMEROPOULOS, M. H., LAVEDAN, C., LEROY, E., IDE, S. E., DEHEJIA, A., DUTRA, A., PIKE, B., ROOT, H., RUBENSTEIN, J., BOYER, R., STENROOS, E. S., CHANDRASEKHARAPPA, S., ATHANASSIADOU, A., PAPAPETROPOULOS, T., JOHNSON, W. G., LAZZARINI, A. M., DUVOISIN, R. C., DI IORIO, G., GOLBE, L. I. & NUSSBAUM, R. L. 1997. Mutation in the alpha-synuclein gene identified in families with Parkinson's disease. *Science,* 276**,** 2045-7.

PRICE, A. R., XU, G., SIEMIENSKI, Z. B., SMITHSON, L. A., BORCHELT, D. R., GOLDE, T. E. & FELSENSTEIN, K. M. 2013. Comment on "ApoE-directed therapeutics rapidly clear beta-amyloid and reverse deficits in AD mouse models". *Science,* 340**,** 924-d.

PRICE, R. D., MILNE, S. A., SHARKEY, J. & MATSUOKA, N. 2007. Advances in small molecules promoting neurotrophic function. *Pharmacology & therapeutics,* 115**,** 292-306.

PUGLIELLI, L., TANZI, R. E. & KOVACS, D. M. 2003. Alzheimer's disease: the cholesterol connection. *Nature neuroscience,* 6**,** 345-351.

QI, R., GU, Z. & ZHOU, L. 2015. The effect of GSTT1, GSTM1 and GSTP1 gene polymorphisms on the susceptibility of age-related cataract in Chinese Han population. *International journal of clinical and experimental medicine,* 8**,** 19448.

QU, L. & TANG, X. 2010. Bexarotene: a promising anticancer agent. *Cancer Chemotherapy and Pharmacology,* 65**,** 201-205.

QUIGLEY, H. A. & BROMAN, A. T. 2006. The number of people with glaucoma worldwide in 2010 and 2020. *The British Journal of Ophthalmology,* 90**,** 262-267.

RADHAKRISHNAN, O. K., PAHUJA, K., PATEL, K. & CHANDNA, S. 2014. OLOGEN(®) implant in the management of glaucoma in an unusual case of Axenfeld–Rieger syndrome. *Oman Journal of Ophthalmology,* 7**,** 90-92.

RAJALA, A., GUPTA, V. K., ANDERSON, R. E. & RAJALA, R. V. 2013. Light activation of the insulin receptor regulates mitochondrial hexokinase. A possible mechanism of retinal neuroprotection. *Mitochondrion,* 13**,** 566-76.

RAO, R. V., ELLERBY, H. M. & BREDESEN, D. E. 2004. Coupling endoplasmic reticulum stress to the cell death program. *Cell Death Differ,* 11**,** 372-80.

RASTINEJAD, F., OLLENDORFF, V. & POLIKARPOV, I. 2015. Nuclear receptor full-length architectures: confronting myth and illusion with high resolution. *Trends Biochem Sci,* 40**,** 16-24.
RENAUD, J. P., ROCHEL, N., RUFF, M., VIVAT, V., CHAMBON, P., GRONEMEYER, H. & MORAS, D. 1995. Crystal structure of the RAR-gamma ligand-binding domain bound to all-trans retinoic acid. *Nature,* 378**,** 681-9.
RENKAWEK, K., VOORTER, C. E., BOSMAN, G. J., VAN WORKUM, F. P. & DE JONG, W. W. 1994. Expression of alpha B-crystallin in Alzheimer's disease. *Acta Neuropathol,* 87**,** 155-60.
REZAIE, T., CHILD, A., HITCHINGS, R., BRICE, G., MILLER, L., COCA-PRADOS, M., HEON, E., KRUPIN, T., RITCH, R., KREUTZER, D., CRICK, R. P. & SARFARAZI, M. 2002. Adult-onset primary open-angle glaucoma caused by mutations in optineurin. *Science,* 295**,** 1077-9.
RIANCHO, J., RUIZ-SOTO, M., BERCIANO, M. T., BERCIANO, J. & LAFARGA, M. 2015. Neuroprotective Effect of Bexarotene in the SOD1(G93A) Mouse Model of Amyotrophic Lateral Sclerosis. *Front Cell Neurosci,* 9**,** 250.
ROBERSON, E. D., SCEARCE-LEVIE, K., PALOP, J. J., YAN, F., CHENG, I. H., WU, T., GERSTEIN, H., YU, G.-Q. & MUCKE, L. 2007. Reducing endogenous tau ameliorates amyloid ß-induced deficits in an Alzheimer's disease mouse model. *Science,* 316**,** 750-754.
RON, D. & WALTER, P. 2007. Signal integration in the endoplasmic reticulum unfolded protein response. *Nat Rev Mol Cell Biol,* 8**,** 519-29.
ROSENBLUM, W. I. 2014. Why Alzheimer trials fail: removing soluble oligomeric beta amyloid is essential, inconsistent, and difficult. *Neurobiol Aging,* 35**,** 969-74.
ROTH, A. D., RAMIREZ, G., ALARCON, R. & VON BERNHARDI, R. 2005. Oligodendrocytes damage in Alzheimer's disease: beta amyloid toxicity and inflammation. *Biol Res,* 38**,** 381-7.
RÖTIG, A. 2011. Human diseases with impaired mitochondrial protein synthesis. *Biochimica et Biophysica Acta (BBA)-Bioenergetics,* 1807**,** 1198-1205.
ROZPĘDEK, W., NOWAK, A., PYTEL, D., LEWKO, D., DIEHL, J. A. & MAJSTEREK, I. 2016. The role of the Amyloid Precursor Protein mutations and PERK-dependent signaling pathways in the pathogenesis of Alzheimer's disease. *Folia Biologica et Oecologica.*
RUDNICKA, A. R., MT-ISA, S., OWEN, C. G., COOK, D. G. & ASHBY, D. 2006. Variations in primary open-angle glaucoma prevalence by age, gender, and race: a Bayesian meta-analysis. *Invest Ophthalmol Vis Sci,* 47**,** 4254-61.
RÜHL, R., KRZYŻOSIAK, A., NIEWIADOMSKA-CIMICKA, A., ROCHEL, N., SZELES, L., VAZ, B., WIETRZYCH-SCHINDLER, M., ÁLVAREZ, S., SZKLENAR, M., NAGY, L., DE LERA, A. R. & KRĘŻEL, W. 2015. 9-cis-13,14-Dihydroretinoic Acid Is an Endogenous Retinoid Acting as RXR Ligand in Mice. *PLOS Genetics,* 11**,** e1005213.
RUIZ-EDERRA, J. & VERKMAN, A. S. 2006. Mouse model of sustained elevation in intraocular pressure produced by episcleral vein occlusion. *Exp Eye Res,* 82**,** 879-84.
SADUN, A. A. & BASSI, C. J. 1990. Optic nerve damage in Alzheimer's disease. *Ophthalmology,* 97**,** 9-17.
SALMINEN, A., OJALA, J., KAUPPINEN, A., KAARNIRANTA, K. & SUURONEN, T. 2009. Inflammation in Alzheimer's disease: amyloid-beta oligomers trigger innate immunity defence via pattern recognition receptors. *Prog Neurobiol,* 87**,** 181-94.
SAMSEL, P. A., KISISWA, L., ERICHSEN, J. T., CROSS, S. D. & MORGAN, J. E. 2011. A novel method for the induction of experimental glaucoma using magnetic microspheres. *Invest Ophthalmol Vis Sci,* 52**,** 1671-5.
SAPPINGTON, R. M., CARLSON, B. J., CRISH, S. D. & CALKINS, D. J. 2010. The microbead occlusion model: a paradigm for induced ocular hypertension in rats and mice. *Invest Ophthalmol Vis Sci,* 51**,** 207-16.
SARKISIAN, S. R. 2009. The ex-press mini glaucoma shunt: technique and experience. *Middle East Afr J Ophthalmol,* 16**,** 134-7.
SARTUCCI, F., BORGHETTI, D., BOCCI, T., MURRI, L., ORSINI, P., PORCIATTI, V., ORIGLIA, N. & DOMENICI, L. 2010. Dysfunction of the magnocellular stream in Alzheimer's disease

evaluated by pattern electroretinograms and visual evoked potentials. *Brain Res Bull,* 82**,** 169-76.
SAYKIN, A. J., SHEN, L., YAO, X., KIM, S., NHO, K., RISACHER, S. L., RAMANAN, V. K., FOROUD, T. M., FABER, K. M. & SARWAR, N. 2015. Genetic studies of quantitative MCI and AD phenotypes in ADNI: Progress, opportunities, and plans. *Alzheimer's & Dementia,* 11**,** 792-814.
SCHEIFE, R. T., SCHUMOCK, G. T., BURSTEIN, A., GOTTWALD, M. D. & LUER, M. S. 2000. Impact of Parkinson's disease and its pharmacologic treatment on quality of life and economic outcomes. *American Journal of Health-System Pharmacy,* 57**,** 953.
SCHMITT, H. M., SCHLAMP, C. L. & NICKELLS, R. W. 2016. Role of HDACs in optic nerve damage-induced nuclear atrophy of retinal ganglion cells. *Neuroscience letters,* 625**,** 11-15.
SCHREINER, W., KARCH, R., KNAPP, B. & ILIEVA, N. 2012. Relaxation estimation of RMSD in molecular dynamics immunosimulations. *Comput Math Methods Med,* 2012**,** 173521.
SCHRODER, M. & KAUFMAN, R. J. 2005a. ER stress and the unfolded protein response. *Mutat Res,* 569**,** 29-63.
SCHRODER, M. & KAUFMAN, R. J. 2005b. The mammalian unfolded protein response. *Annu Rev Biochem,* 74**,** 739-89.
SERRE, V., ROZANSKA, A., BEINAT, M., CHRETIEN, D., BODDAERT, N., MUNNICH, A., RÖTIG, A. & CHRZANOWSKA-LIGHTOWLERS, Z. M. 2013. Mutations in mitochondrial ribosomal protein MRPL12 leads to growth retardation, neurological deterioration and mitochondrial translation deficiency. *Biochimica et Biophysica Acta (BBA)-Molecular Basis of Disease,* 1832**,** 1304-1312.
SHIMAZAWA, M., INOKUCHI, Y., ITO, Y., MURATA, H., AIHARA, M., MIURA, M., ARAIE, M. & HARA, H. 2007. Involvement of ER stress in retinal cell death. *Mol Vis,* 13**,** 578-87.
SHINDLER, K. S., GUAN, Y., VENTURA, E., BENNETT, J. & ROSTAMI, A. 2006. Retinal ganglion cell loss induced by acute optic neuritis in a relapsing model of multiple sclerosis. *Mult Scler,* 12**,** 526-32.
SIDDIQUI, N., KOZLOV, G., D'ORSO, I., TREMPE, J. F. & GEHRING, K. 2003. Solution structure of the C-terminal domain from poly(A)-binding protein in Trypanosoma cruzi: a vegetal PABC domain. *Protein Sci,* 12**,** 1925-33.
SIVAK, J. M. 2013. The aging eye: common degenerative mechanisms between the Alzheimer's brain and retinal disease. *Invest Ophthalmol Vis Sci,* 54**,** 871-80.
.
SONG, F., POLJAK, A., CRAWFORD, J., KOCHAN, N. A., WEN, W., CAMERON, B., LUX, O., BRODATY, H., MATHER, K. & SMYTHE, G. A. 2012. Plasma apolipoprotein levels are associated with cognitive status and decline in a community cohort of older individuals. *PloS one,* 7**,** e34078.
SOUZA, J. M., GIASSON, B. I., LEE, V. M. & ISCHIROPOULOS, H. 2000. Chaperone-like activity of synucleins. *FEBS Lett,* 474**,** 116-9.
SOWDEN, J. C. 2007. Molecular and developmental mechanisms of anterior segment dysgenesis. *Eye (Lond),* 21**,** 1310-8.
SPAETH, G., WALT, J. & KEENER, J. 2006. Evaluation of quality of life for patients with glaucoma. *Am J Ophthalmol,* 141**,** S3-14.
STASI, K., NAGEL, D., YANG, X., WANG, R.-F., REN, L., PODOS, S. M., MITTAG, T. & DANIAS, J. 2006. Complement component 1Q (C1Q) upregulation in retina of murine, primate, and human glaucomatous eyes. *Investigative ophthalmology & visual science,* 47**,** 1024-1029.
STEGMANN, R., PIENAAR, A. & MILLER, D. 1999. Viscocanalostomy for open-angle glaucoma in black African patients. *J Cataract Refract Surg,* 25**,** 316-22.
STEPHAN, A. H., BARRES, B. A. & STEVENS, B. 2012. The complement system: an unexpected role in synaptic pruning during development and disease. *Annual review of neuroscience,* 35**,** 369-389.
STONE, E. M., FINGERT, J. H., ALWARD, W. L., NGUYEN, T. D., POLANSKY, J. R., SUNDEN, S. L., NISHIMURA, D., CLARK, A. F., NYSTUEN, A., NICHOLS, B. E., MACKEY, D. A., RITCH, R.,

KALENAK, J. W., CRAVEN, E. R. & SHEFFIELD, V. C. 1997. Identification of a gene that causes primary open angle glaucoma. *Science,* 275**,** 668-70.
STROBER, W. 2015. Trypan Blue Exclusion Test of Cell Viability. *Curr Protoc Immunol,* 111**,** A3 B 1-3.
SUCHER, N. J., LIPTON, S. A. & DREYER, E. B. 1997. Molecular basis of glutamate toxicity in retinal ganglion cells. *Vision Research,* 37**,** 3483-3493.
SUN, M. H., CHEN, K. J., TSAO, Y. P., KAO, L. Y., HAN, W. H., LIN, K. K. & PANG, J. H. 2011. Down-regulation of matrix metalloproteinase-9 by pyrrolidine dithiocarbamate prevented retinal ganglion cell death after transection of optic nerve in rats. *Curr Eye Res,* 36**,** 1053-63.
SURGUCHEVA, I., WEISMAN, A. D., GOLDBERG, J. L., SHNYRA, A. & SURGUCHOV, A. 2008. Gamma-synuclein as a marker of retinal ganglion cells. *Mol Vis,* 14**,** 1540-8.
SVENSSON, S., OSTBERG, T., JACOBSSON, M., NORSTROM, C., STEFANSSON, K., HALLEN, D., JOHANSSON, I. C., ZACHRISSON, K., OGG, D. & JENDEBERG, L. 2003. Crystal structure of the heterodimeric complex of LXRalpha and RXRbeta ligand-binding domains in a fully agonistic conformation. *EMBO J,* 22**,** 4625-33.
SZANTO, A., NARKAR, V., SHEN, Q., URAY, I. P., DAVIES, P. J. A. & NAGY, L. 2004. Retinoid X receptors: X-ploring their (patho)physiological functions. *Cell Death And Differentiation,* 11**,** S126.
SZEGEZDI, E., LOGUE, S. E., GORMAN, A. M. & SAMALI, A. 2006. Mediators of endoplasmic reticulum stress-induced apoptosis. *EMBO Reports,* 7**,** 880-885.
TABAS, I. & RON, D. 2011. Integrating the mechanisms of apoptosis induced by endoplasmic reticulum stress. *Nature cell biology,* 13**,** 184-190.
TACHIBANA, M., SHINOHARA, M., YAMAZAKI, Y., LIU, C. C., ROGERS, J., BU, G. & KANEKIYO, T. 2016. Rescuing effects of RXR agonist bexarotene on aging-related synapse loss depend on neuronal LRP1. *Exp Neurol,* 277**,** 1-9.
TAI, L. M., KOSTER, K. P., LUO, J., LEE, S. H., WANG, Y. T., COLLINS, N. C., BEN AISSA, M., THATCHER, G. R. & LADU, M. J. 2014. Amyloid-beta pathology and APOE genotype modulate retinoid X receptor agonist activity in vivo. *J Biol Chem,* 289**,** 30538-55.
TAKAHASHI, K., NIIDOME, T., AKAIKE, A., KIHARA, T. & SUGIMOTO, H. 2009. Amyloid precursor protein promotes endoplasmic reticulum stress-induced cell death via C/EBP homologous protein-mediated pathway. *J Neurochem,* 109**,** 1324-37.
TAKEDA, H., KITAOKA, Y., HAYASHI, Y., KUMAI, T., MUNEMASA, Y., FUJINO, H., KOBAYASHI, S. & UENO, S. 2007. Calcium/calmodulin-dependent protein kinase II regulates the phosphorylation of CREB in NMDA-induced retinal neurotoxicity. *Brain Res,* 1184**,** 306-15.
TAMM, E. R. 2009. The trabecular meshwork outflow pathways: structural and functional aspects. *Exp Eye Res,* 88**,** 648-55.
TAMURA, H., KAWAKAMI, H., KANAMOTO, T., KATO, T., YOKOYAMA, T., SASAKI, K., IZUMI, Y., MATSUMOTO, M. & MISHIMA, H. K. 2006. High frequency of open-angle glaucoma in Japanese patients with Alzheimer's disease. *J Neurol Sci,* 246**,** 79-83.
TANITO, M., KAIDZU, S., TAKAI, Y. & OHIRA, A. 2012. Status of Systemic Oxidative Stresses in Patients with Primary Open-Angle Glaucoma and Pseudoexfoliation Syndrome. *PLoS ONE,* 7**,** e49680.
TANITO, M., KAIDZU, S., TAKAI, Y. & OHIRA, A. 2015. Correlation between Systemic Oxidative Stress and Intraocular Pressure Level. *PLoS One,* 10**,** e0133582.
TESSEUR, I., LO, A. C., ROBERFROID, A., DIETVORST, S., VAN BROECK, B., BORGERS, M., GIJSEN, H., MOECHARS, D., MERCKEN, M., KEMP, J., D'HOOGE, R. & DE STROOPER, B. 2013. Comment on "ApoE-directed therapeutics rapidly clear beta-amyloid and reverse deficits in AD mouse models". *Science,* 340**,** 924-e.
TEZEL, G., YANG, X., LUO, C., KAIN, A. D., POWELL, D. W., KUEHN, M. H. & KAPLAN, H. J. 2010. Oxidative Stress and the Regulation of Complement Activation in Human Glaucoma. *Investigative Ophthalmology & Visual Science,* 51**,** 5071-5082.

THAM, Y.-C., LI, X., WONG, T. Y., QUIGLEY, H. A., AUNG, T. & CHENG, C.-Y. 2014. Global Prevalence of Glaucoma and Projections of Glaucoma Burden through 2040: A Systematic Review and Meta-Analysis. *Ophthalmology,* 121**,** 2081-2090.

THOMAS, M., SUKHAI, M. A. & KAMEL-REID, S. 2012. An emerging role for retinoid X receptor alpha in malignant hematopoiesis. *Leuk Res,* 36**,** 1075-81.

THORESON, W. B. & WITKOVSKY, P. 1999. Glutamate receptors and circuits in the vertebrate retina. *Prog Retin Eye Res,* 18**,** 765-810.

TODD, D. J., LEE, A. H. & GLIMCHER, L. H. 2008. The endoplasmic reticulum stress response in immunity and autoimmunity. *Nat Rev Immunol,* 8**,** 663-74.

TOLLERVEY, J. R., WANG, Z., HORTOBÁGYI, T., WITTEN, J. T., ZARNACK, K., KAYIKCI, M., CLARK, T. A., SCHWEITZER, A. C., ROT, G. & CURK, T. 2011. Analysis of alternative splicing associated with aging and neurodegeneration in the human brain. *Genome research,* 21**,** 1572-1582.

TOUSI, B. 2015. The emerging role of bexarotene in the treatment of Alzheimer's disease: current evidence. *Neuropsychiatr Dis Treat,* 11**,** 311-5.

TRAPP, B. D. & NAVE, K. A. 2008. Multiple sclerosis: an immune or neurodegenerative disorder? *Annu Rev Neurosci,* 31**,** 247-69.

TSAI, C. S., RITCH, R., SCHWARTZ, B., LEE, S. S., MILLER, N. R., CHI, T. & HSIEH, F. Y. 1991. Optic nerve head and nerve fiber layer in Alzheimer's disease. *Arch Ophthalmol,* 109**,** 199-204.

TSUJI, M., SHUDO, K. & KAGECHIKA, H. 2015. Docking simulations suggest that all-trans retinoic acid could bind to retinoid X receptors. *J Comput Aided Mol Des,* 29**,** 975-88.

TSURUMA, K., SHIMAZAKI, H., NAKASHIMA, K., YAMAUCHI, M., SUGITANI, S., SHIMAZAWA, M., IINUMA, M. & HARA, H. 2012. Annatto prevents retinal degeneration induced by endoplasmic reticulum stress in vitro and in vivo. *Mol Nutr Food Res,* 56**,** 713-24.

TZEKOV, R., STEIN, L. & KAUSHAL, S. 2011. Protein Misfolding and Retinal Degeneration. *Cold Spring Harbor Perspectives in Biology,* 3**,** a007492.

ULRICH, J. D., BURCHETT, J. M., RESTIVO, J. L., SCHULER, D. R., VERGHESE, P. B., MAHAN, T. E., LANDRETH, G. E., CASTELLANO, J. M., JIANG, H., CIRRITO, J. R. & HOLTZMAN, D. M. 2013. In vivo measurement of apolipoprotein E from the brain interstitial fluid using microdialysis. *Mol Neurodegener,* 8**,** 13.

ÜNAL, M., GÜVEN, M., DEVRANOĞLU, K., ÖZAYDıN, A., BATAR, B., TAMÇELIK, N., GÖRGÜN, E. E., UÇAR, D. & SARıCı, A. 2007. Glutathione S transferase M1 and T1 genetic polymorphisms are related to the risk of primary open-angle glaucoma: a study in a Turkish population. *British journal of ophthalmology,* 91**,** 527-530.

VALENZA, M., LEONI, V., KARASINSKA, J. M., PETRICCA, L., FAN, J., CARROLL, J., POULADI, M. A., FOSSALE, E., NGUYEN, H. P. & RIESS, O. 2010. Cholesterol defect is marked across multiple rodent models of Huntington's disease and is manifest in astrocytes. *Journal of Neuroscience,* 30**,** 10844-10850.

VALENZA, M., RIGAMONTI, D., GOFFREDO, D., ZUCCATO, C., FENU, S., JAMOT, L., STRAND, A., TARDITI, A., WOODMAN, B. & RACCHI, M. 2005. Dysfunction of the cholesterol biosynthetic pathway in Huntington's disease. *Journal of Neuroscience,* 25**,** 9932-9939.

VAN CAUWENBERGHE, C., VAN BROECKHOVEN, C. & SLEEGERS, K. 2015. The genetic landscape of Alzheimer disease: clinical implications and perspectives. *Genetics in Medicine,* 18**,** 421-430.

VARMA, R., LEE, P. P., GOLDBERG, I. & KOTAK, S. 2011. An Assessment of the Health and Economic Burdens of Glaucoma. *American journal of ophthalmology,* 152**,** 515-522.

VARMA, V. R., VARMA, S., AN, Y., HOHMAN, T. J., SEDDIGHI, S., CASANOVA, R., BERI, A., DAMMER, E. B., SEYFRIED, N. T. & PLETNIKOVA, O. 2017. Alpha-2 macroglobulin in Alzheimer's disease: a marker of neuronal injury through the RCAN1 pathway. *Molecular psychiatry,* 22**,** 13-23.

VAZ, B. & DE LERA, A. R. 2012. Advances in drug design with RXR modulators. *Expert Opin Drug Discov,* 7**,** 1003-16.

VEERARAGHAVALU, K., ZHANG, C., MILLER, S., HEFENDEHL, J. K., RAJAPAKSHA, T. W., ULRICH, J., JUCKER, M., HOLTZMAN, D. M., TANZI, R. E., VASSAR, R. & SISODIA, S. S. 2013. Comment on "ApoE-directed therapeutics rapidly clear beta-amyloid and reverse deficits in AD mouse models". *Science,* 340**,** 924-f.

VICKERS, J. C., HOF, P. R., SCHUMER, R. A., WANG, R. F., PODOS, S. M. & MORRISON, J. H. 1997. Magnocellular and parvocellular visual pathways are both affected in a macaque monkey model of glaucoma. *Aust N Z J Ophthalmol,* 25**,** 239-43.

VIET, M. H. & LI, M. S. 2012. Amyloid peptide Abeta40 inhibits aggregation of Abeta42: evidence from molecular dynamics simulations. *J Chem Phys,* 136**,** 245105.

VORWERK, C. K., LIPTON, S. A., ZURAKOWSKI, D., HYMAN, B. T., SABEL, B. A. & DREYER, E. B. 1996. Chronic low-dose glutamate is toxic to retinal ganglion cells. Toxicity blocked by memantine. *Invest Ophthalmol Vis Sci,* 37**,** 1618-24.

WANG, L., HARA, K., VAN BAAREN, J. M., PRICE, J. C., BEECHAM, G. W., GALLINS, P. J., WHITEHEAD, P. L., WANG, G., LU, C., SLIFER, M. A., ZUCHNER, S., MARTIN, E. R., MASH, D., HAINES, J. L., PERICAK-VANCE, M. A. & GILBERT, J. R. 2012. Vitamin D receptor and Alzheimer's disease: a genetic and functional study. *Neurobiol Aging,* 33**,** 1844 e1-9.

WANG, M., LI, Y., LIN, L., SONG, G. & DENG, T. 2016a. GSTM1 null genotype and GSTP1 ILE105Val polymorphism are associated with alzheimer's disease: A meta-analysis. *Molecular neurobiology,* 53**,** 1355-1364.

WANG, S. K. & CHANG, R. T. 2014. An emerging treatment option for glaucoma: Rho kinase inhibitors. *Clinical Ophthalmology (Auckland, N.Z.),* 8**,** 883-890.

WANG, T. & WANG, B. 2014. Association between glutathione S-transferase M1/glutathione S-transferase T1 polymorphisms and Parkinson's disease: a meta-analysis. *Journal of the neurological sciences,* 338**,** 65-70.

WANG, X. Z., LAWSON, B., BREWER, J. W., ZINSZNER, H., SANJAY, A., MI, L. J., BOORSTEIN, R., KREIBICH, G., HENDERSHOT, L. M. & RON, D. 1996. Signals from the stressed endoplasmic reticulum induce C/EBP-homologous protein (CHOP/GADD153). *Mol Cell Biol,* 16**,** 4273-80.

WANG, Z., SUN, H., YAO, X., LI, D., XU, L., LI, Y., TIAN, S. & HOU, T. 2016b. Comprehensive evaluation of ten docking programs on a diverse set of protein-ligand complexes: the prediction accuracy of sampling power and scoring power. *Phys Chem Chem Phys,* 18**,** 12964-75.

WEINREB, R. N., AUNG, T. & MEDEIROS, F. A. 2014. The pathophysiology and treatment of glaucoma: a review. *Jama,* 311**,** 1901-1911.

WESSEL, D. & FLÜGGE, U. I. 1984. A method for the quantitative recovery of protein in dilute solution in the presence of detergents and lipids. *Analytical biochemistry,* 138**,** 141-143.

WIENS, M., BATEL, R., KORZHEV, M. & MÜLLER, W. E. G. 2003. Retinoid X receptor and retinoic acid response in the marine sponge <em>Suberites domuncula</em&gt. *Journal of Experimental Biology,* 206**,** 3261.

WIETRZYCH, M., MEZIANE, H., SUTTER, A., GHYSELINCK, N., CHAPMAN, P. F., CHAMBON, P. & KREZEL, W. 2005. Working memory deficits in retinoid X receptor gamma-deficient mice. *Learn Mem,* 12**,** 318-26.

WILLIAMS, P. A., TRIBBLE, J. R., PEPPER, K. W., CROSS, S. D., MORGAN, B. P., MORGAN, J. E., JOHN, S. W. M. & HOWELL, G. R. 2016. Inhibition of the classical pathway of the complement cascade prevents early dendritic and synaptic degeneration in glaucoma. *Molecular neurodegeneration,* 11**,** 26.

WOLF, G. 2006. Is 9-cis-retinoic acid the endogenous ligand for the retinoic acid-X receptor? *Nutr Rev,* 64**,** 532-8.

WOOD, J. M., BLACK, A. A., MALLON, K., THOMAS, R. & OWSLEY, C. 2016. Glaucoma and Driving: On-Road Driving Characteristics. *PLOS ONE,* 11**,** e0158318.

WU, C. H., HUNG, T. H., CHEN, C. C., KE, C. H., LEE, C. Y., WANG, P. Y. & CHEN, S. F. 2014. Post-injury treatment with 7,8-dihydroxyflavone, a TrkB receptor agonist, protects against experimental traumatic brain injury via PI3K/Akt signaling. *PLoS One,* 9**,** e113397.

WU, Z., LIN, C., CROWTHER, M., MAK, H., YU, M. & LEUNG, C. K. 2017. Impact of Rates of Change of Lamina Cribrosa and Optic Nerve Head Surface Depths on Visual Field Progression in Glaucoma. *Invest Ophthalmol Vis Sci,* 58**,** 1825-1833.

YAMADA, S. & KAKUTA, H. 2014. Retinoid X receptor ligands: a patent review (2007 - 2013). *Expert Opin Ther Pat,* 24**,** 443-52.

YAN, Q., ZHANG, J., LIU, H., BABU-KHAN, S., VASSAR, R., BIERE, A. L., CITRON, M. & LANDRETH, G. 2003. Anti-inflammatory drug therapy alters beta-amyloid processing and deposition in an animal model of Alzheimer's disease. *J Neurosci,* 23**,** 7504-9.

YANG, L., LI, S., MIAO, L., HUANG, H., LIANG, F., TENG, X., XU, L., WANG, Q., XIAO, W., RIDDER, W. H., 3RD, FERGUSON, T. A., CHEN, D. F., KAUFMAN, R. J. & HU, Y. 2016. Rescue of Glaucomatous Neurodegeneration by Differentially Modulating Neuronal Endoplasmic Reticulum Stress Molecules. *J Neurosci,* 36**,** 5891-903.

YANG, X., LUO, C., CAI, J., POWELL, D. W., YU, D., KUEHN, M. H. & TEZEL, G. 2011. Neurodegenerative and inflammatory pathway components linked to TNF-alpha/TNFR1 signaling in the glaucomatous human retina. *Invest Ophthalmol Vis Sci,* 52**,** 8442-54.

YASUDA, M., TANAKA, Y., RYU, M., TSUDA, S. & NAKAZAWA, T. 2014. RNA sequence reveals mouse retinal transcriptome changes early after axonal injury. *PLoS One,* 9**,** e93258.

YEN, W. C. & LAMPH, W. W. 2005. The selective retinoid X receptor agonist bexarotene (LGD1069, Targretin) prevents and overcomes multidrug resistance in advanced breast carcinoma. *Mol Cancer Ther,* 4**,** 824-34.

YILDIRIM, O., ATES, N. A., ERCAN, B., MUSLU, N., UNLU, A., TAMER, L., ATIK, U. & KANIK, A. 2005. Role of oxidative stress enzymes in open-angle glaucoma. *Eye (Lond),* 19**,** 580-3.

YORIO, T., KRISHNAMOORTHY, R. & PRASANNA, G. 2002. Endothelin: is it a contributor to glaucoma pathophysiology? *J Glaucoma,* 11**,** 259-70.

YOSHIDA, H., HAZE, K., YANAGI, H., YURA, T. & MORI, K. 1998. Identification of the cis-acting endoplasmic reticulum stress response element responsible for transcriptional induction of mammalian glucose-regulated proteins. Involvement of basic leucine zipper transcription factors. *J Biol Chem,* 273**,** 33741-9.

YOU, Y., KLISTORNER, A., THIE, J. & GRAHAM, S. L. 2011. Latency delay of visual evoked potential is a real measurement of demyelination in a rat model of optic neuritis. *Invest Ophthalmol Vis Sci,* 52**,** 6911-8.

YU, J.-T. & TAN, L. 2012. The role of clusterin in Alzheimer's disease: pathways, pathogenesis, and therapy. *Molecular neurobiology,* 45**,** 314-326.

YU, S., TANABE, T. & YOSHIMURA, N. 2006. A rat model of glaucoma induced by episcleral vein ligation. *Exp Eye Res,* 83**,** 758-70.

YU, W. & MILLER, R. F. 1996. The mechanism by which NBQX enhances NMDA currents in retinal ganglion cells. *Brain Res,* 709**,** 184-96.

YUCEL, Y. H., ZHANG, Q., GUPTA, N., KAUFMAN, P. L. & WEINREB, R. N. 2000. Loss of neurons in magnocellular and parvocellular layers of the lateral geniculate nucleus in glaucoma. *Arch Ophthalmol,* 118**,** 378-84.

YÜCEL, Y. H., ZHANG, Q., WEINREB, R. N., KAUFMAN, P. L. & GUPTA, N. 2003. Effects of retinal ganglion cell loss on magno-, parvo-, koniocellular pathways in the lateral geniculate nucleus and visual cortex in glaucoma. *Progress in Retinal and Eye Research,* 22**,** 465-481.

ZHANG, C., HAZARIKA, P., NI, X., WEIDNER, D. A. & DUVIC, M. 2002. Induction of apoptosis by bexarotene in cutaneous T-cell lymphoma cells: relevance to mechanism of therapeutic action. *Clin Cancer Res,* 8**,** 1234-40.

ZHANG, K. & KAUFMAN, R. J. 2006. Protein folding in the endoplasmic reticulum and the unfolded protein response. *Handb Exp Pharmacol***,** 69-91.

ZHANG, Q., PAN, J., ZHANG, J., LIU, P., CHEN, R., CHEN, D. R., LUBET, R., WANG, Y. & YOU, M. 2011. Aerosolized bexarotene inhibits lung tumorigenesis without increasing plasma triglyceride and cholesterol levels in mice. *Cancer Prev Res (Phila),* 4**,** 270-6.

ZHANG, Z., LIU, X., SCHROEDER, J. P., CHAN, C. B., SONG, M., YU, S. P., WEINSHENKER, D. & YE, K. 2014. 7,8-dihydroxyflavone prevents synaptic loss and memory deficits in a mouse model of Alzheimer's disease. *Neuropsychopharmacology,* 39**,** 638-50.

ZHOU, H., LIU, W., SU, Y., WEI, Z., LIU, J., KOLLURI, S. K., WU, H., CAO, Y., CHEN, J., WU, Y., YAN, T., CAO, X., GAO, W., MOLOTKOV, A., JIANG, F., LI, W.-G., LIN, B., ZHANG, H.-P., YU, J., LUO, S.-P., ZENG, J.-Z., DUESTER, G., HUANG, P.-Q. & ZHANG, X.-K. 2010. NSAID Sulindac and Its Analogs Bind RXRα and Inhibit RXRα-dependent AKT Signaling. *Cancer cell,* 17**,** 560-573.

ZHOU, Q., ZHAO, F., LV, Z.-P., ZHENG, C.-G., ZHENG, W.-D., SUN, L., WANG, N.-N., PANG, S., DE ANDRADE, F. M. & FU, M. 2014. Association between APOC1 Polymorphism and Alzheimer's Disease: A Case-Control Study and Meta-Analysis. *PloS one,* 9**,** e87017.

ZHOU, Y., PERNET, V., HAUSWIRTH, W. W. & DI POLO, A. 2005. Activation of the extracellular signal-regulated kinase 1/2 pathway by AAV gene transfer protects retinal ganglion cells in glaucoma. *Mol Ther,* 12**,** 402-12.

ZINSZNER, H., KURODA, M., WANG, X., BATCHVAROVA, N., LIGHTFOOT, R. T., REMOTTI, H., STEVENS, J. L. & RON, D. 1998. CHOP is implicated in programmed cell death in response to impaired function of the endoplasmic reticulum. *Genes Dev,* 12**,** 982-95.

ZODE, G. S., KUEHN, M. H., NISHIMURA, D. Y., SEARBY, C. C., MOHAN, K., GROZDANIC, S. D., BUGGE, K., ANDERSON, M. G., CLARK, A. F., STONE, E. M. & SHEFFIELD, V. C. 2011. Reduction of ER stress via a chemical chaperone prevents disease phenotypes in a mouse model of primary open angle glaucoma. *The Journal of Clinical Investigation,* 121**,** 3542-3553.

ZODE, G. S., SHARMA, A. B., LIN, X., SEARBY, C. C., BUGGE, K., KIM, G. H., CLARK, A. F. & SHEFFIELD, V. C. 2014a. Ocular-specific ER stress reduction rescues glaucoma in murine glucocorticoid-induced glaucoma. *J Clin Invest,* 124**,** 1956-65.